The benefits of combining geometric attributes from Labyrinth and Piano key weirs

Shenaaz Hoosen

A dissertation submitted to the Faculty of Engineering and the Built Environment, University of the Witwatersrand, Johannesburg, in fulfilment of requirements for the degree of Master of Science in Engineering

Johannesburg, 2017

DECLARATION

I declare that this dissertation is my own unaided work. It is being submitted to the degree of Master of Science to the University of the Witwatersrand, Johannesburg. It has not been submitted before for any degree or examination to any other University.

(Signature of candidate)

--------- day of ------------ , -----------

(day) (month) (year)

ABSTRACT

South Africa is a water scarce country and dams play a large role in the infrastructure of our country by providing water for many purposes. With the growth of the country, new dams are needed and existing dams require rehabilitation. Often, increasing a spillways capacity forms part of the rehabilitation required at dams. Therefore, one of the main aims of this study is to look at an option for increasing a spillways discharge capacity. The labyrinth and Piano key weirs (PKW) were investigated together with a combination of the two spillway types. Different geometric attributes were combined and varied to develop a new design that would assist in improving discharge capacity while reducing the cost, producing an economically viable option. Thirty five physical models were built and tested in this regard. Comparison was made with the standard PKW design in terms of discharge capacity, hydraulic efficiency, length ratio (L/W) and cost related to concrete volume required. It was concluded that efficiency, discharge capacity and cost can be improved with this new combined design however more geometric variations need to be studied to ascertain these results.

To my husband and my family

For their support, encouragement, inspiration and patience during this study.

Acknowledgements

I wish to express my appreciation to the following organisations and persons who made this project possible:

a) Prof. C.S. James for his patience, guidance, support and criticism throughout this study. It has been an honour and privilege to work with him.
b) The entire staff from the hydraulics laboratory of the Department of Water and Sanitation (DWS). Particularly Patrick and Johannes who have taken much time in assisting with the construction of the physical models.
c) Mr Pieter Mynhardt for his assistance with the quality control as well as the construction of the physical models.
d) Mr Kobus van Deventer for his contribution and continuous advice, support and guidance from a professional perspective.
e) God almighty for giving me the strength and courage to complete my studies.

TABLE OF CONTENTS

List of tables

List of figures

List of symbols

B - Base width/ transversal length

C - Constant representative of discharge coefficient

$C_{measured}$ - Measured value of constant representative of discharge coefficient

$C_{predicted}$ - Predicted value of constant representative of discharge coefficient

C_d - Discharge coefficient for standard linear weir equation

C_d' - Discharge coefficient defined in this study for PKW and combined designs

C_d'$_{measured}$ - Predicted value of discharge coefficient defined in this study for PKW and combined designs

C_d'$_{predicted}$ - Predicted value of discharge coefficient defined in this study for PKW and combined designs

C_p - Discharge coefficient of PKW

C_s - Discharge coefficient of sharp crested weir

D - Outside apex width

DWS - Department of Water and Sanitation

FSL - Full supply level

g - Gravitational acceleration

h - Upstream water level

H_o - Design head

H_T - Total upstream head

L - Weir crest length

l_c - Centreline length of sidewall

m - Metre

N - Number of cycles

P	-	Weir height
PKW	-	Piano key weir
P_{in}	-	Inlet channel height
P_m	-	Maximum height of PKW walls
P_{out}	-	Outlet channel height
Q	-	Discharge
q	-	Unit discharge
q_d	-	Downstream crest specific discharge
Q_p	-	Discharge of PKW
Q_s	-	Discharge of sharp crested weir
q_s	-	Side crest specific discharge
q_u	-	Upstream crest specific discharge
s	-	Second
t_w	-	Wall thickness
v	-	Velocity
$\frac{v^2}{2g}$	-	Energy head
W	-	Overall spillway width
W_{in}	-	Width of inlet channel
$W_{in\ Effective}$	-	Effective width of inlet channel
W_{out}	-	Width of outlet channel
W_u	-	PKW unit width
α	-	Sidewall angle
α’	-	Inlet channel width proportion

1 INTRODUCTION

There are over 1000 registered dams in South Africa. Many of these dams are getting older and require rehabilitation. With the increasing demands for additional reservoir storage, increased floods and the continuous need for dam safety and operation, many of the existing spillways are undersized and in need of replacement. Reservoir spillways generally use overflow weirs, gated or non – gated, as the flow control structure.

In order to ensure the safety of such dams, rehabilitation is a necessity. There are many types of rehabilitation work that can be done. These include repairing of concrete, relining and repairing water passages as well as the rehabilitation of gates. However, structural stability is not the only means of ensuring dam safety. A dam also requires hydrological safety and that means having adequate spillway capacity.

The discharge relationship for a linear weir is as follows:

$$Q = C_d \frac{2}{3}\sqrt{2g} L H_T^{\frac{3}{2}} \tag{1.1}$$

Where: Q – discharge (m^3/s)

C_d – Discharge coefficient

g – Gravitational acceleration (m/s^2)

L – Weir crest length (m)

H_T – Total upstream Head ($h + \frac{v^2}{2g}$) (m)

v – Velocity

h – Upstream water level

In general, there are three identified ways for increasing discharge capacity, these are: (1) increasing the length (L) of the spillway; (2) lowering the spillway crest elevation; and/or (3) increasing the spillway width (W). The length of the spillway refers to the developed crest wall length (see Fig. 1.1) and the width is the total width of the spillway. Increasing L of a linear spillway, and consequently increasing the discharge channel width, can often become impractical due to the dam geometry or economic reasons. For this reason, the labyrinth and Piano key weirs (PKW's) were investigated as a means to raise existing dam spillways and increase capacity. These non-linear weirs can increase the L of the spillway for a fixed channel width and can be used to improve a spillways discharge capacity.

The main difference between these two spillways lies in their geometry (e.g. sidewall angle (α)). The labyrinth spillway generally has a horizontal floor with a trapezoidal plan layout whereas the PKW has sloping floors, with a reduced base width(B), and a rectangular plan layout (Fig. 1.1).

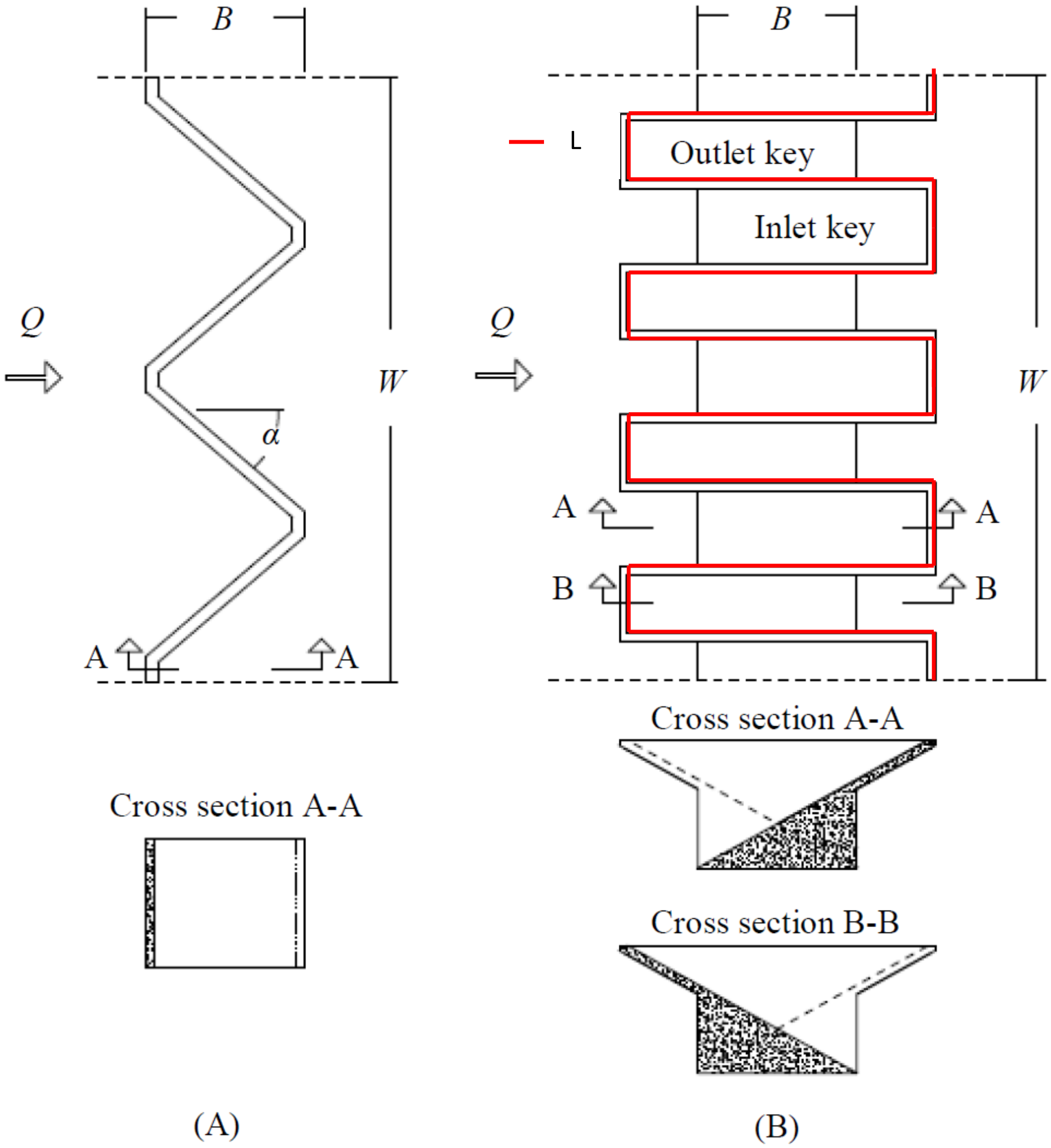

Figure 1.1: General trapezoidal labyrinth (A) and standard PKW (B) geometries

The objectives of this study are to investigate the advantages and disadvantages of a combined labyrinth and PKW design for increased discharge capacity. These designs are compared to standard PKW layouts through a systematic variation of geometric parameters. This study aims to provide a more innovative arrangement by combining geometric attributes of both labyrinth and

PKW designs. The hydraulic and economic aspects of such a design are also considered and discussed.

2 BACKGROUND

Labyrinth spillways have been a preferred option for increasing spillway capacity, but a need for a more economic and efficient spillway design arose in the new millennium. As a result, the French led a study that developed the piano key weir (PKW) (Lempérière & Ouamane, 2003). These are both non-linear spillways.

Labyrinth and piano key weirs (PKW) have become an effective means of raising existing dams to increase spillway capacity and reservoir storage. In doing so, these type of weirs also improve discharge capacity of the spillway and improve its hydraulic efficiency. This hydraulic efficiency refers to the ability of a hydraulic structure to conduct water with minimum energy loss whilst spillway capacity is the capability of a spillway, determined by its dimensions, crest level and hydraulic characteristics to dispose of water at any specific level. The efficiency of the spillway in this study is quantified by the C_d' – value which is directly linked to the geometry of the spillway and the effect it has in reducing the energy losses.

Spillways are structures constructed to provide safe release of flood waters from a dam to a downstream area. Overflow spillways can be controlled or uncontrolled for flow over a gravity dam section. A controlled spillway is provided with gates which can be raised or lowered. Water can be stored even above the spillway crest level by keeping these gates closed. Flow remains in contact with a spillway surface from the crest of the dam to the vicinity of its base.

One of the most commonly applied equations for computing discharge of overflow weirs was developed by James B. Francis (Horton, 1907). This equation is often aptly referred to as the "weir equation" presented as Eq. (1.1) previously.

Deducing from the weir head-discharge relationship indicated by Eq.(1.1)it is shown that, increasing the spillway capacity is dependent on the total crest length (L) and total up-stream head (H_T). The non-linear spillways serve a purpose of increasing the spillway length. They are generally used to improve existing spillway performance by replacing the most efficient of the conventionally used linear spillways i.e. Uncontrolled Ogee spillways. One of the main reasons for choosing a non-linear spillway for an existing dam is that the additional spillway capacity can be obtained and the full supply level (FSL) can be raised even with the limited length of the existing spillway (Anderson, 2011).

PKW's and labyrinth spillways have the advantage that no operation is necessary and there is no risk of an uncontrolled release of reservoir storage due to misoperation (Paxson et al., 2012).

In order to have a better understanding of the subject, previous works on ways to increase spillway capacity are analysed and summarised. This study will focus on labyrinth weirs and piano key weirs as the two main alternatives to increase spillway capacity.

2.1 Labyrinth weirs

Weirs have been implemented in canals, streams, rivers, ponds and reservoirs. There are many different types of weirs and therefore different weir geometries. The labyrinth weir is a non-linear weir that is folded in plan view (Crookston, 2010) (Fig. 2.1). Labyrinth weirs are well suited for spillway rehabilitation where aging infrastructure, dam safety concerns, freeboard limitations, and revised and larger probable maximum flows have required increased spillway capacity.

According to Lempérière (2011) labyrinth weirs have been used to increase discharge at weirs for over 50 years. Their layout is generally conceived as vertical walls upon a flat base with a trapezoidal layout in plan as captured by Crookston (2010) (Fig.2.1).

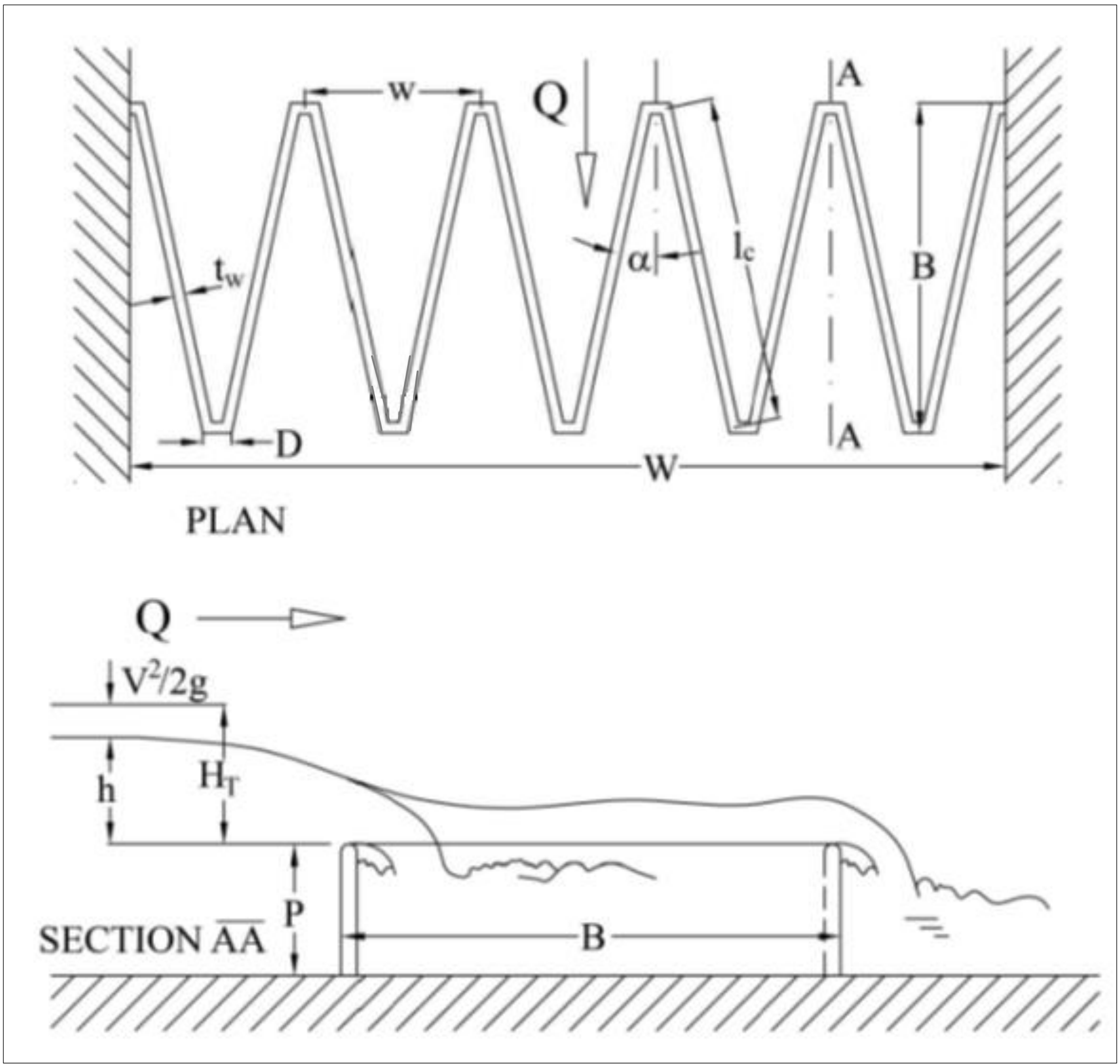

Figure 2.1: Typical Labyrinth layout showing the main geometric parameters (Crookston, 2010)

The folded length of the labyrinth spillway provides a longer total effective weir crest length for a given spillway overall width (W), see Fig.2.2. The total length of the labyrinth weir is typically 3-5 times the spillway width and its capacity varies with head. The capacity is typically twice that of a standard weir. They are used to increase outlet capacity for a specific spillway crest elevation and length or increase storage by raising the crest and maintaining spillway capacity (Tullis et al., 1995).

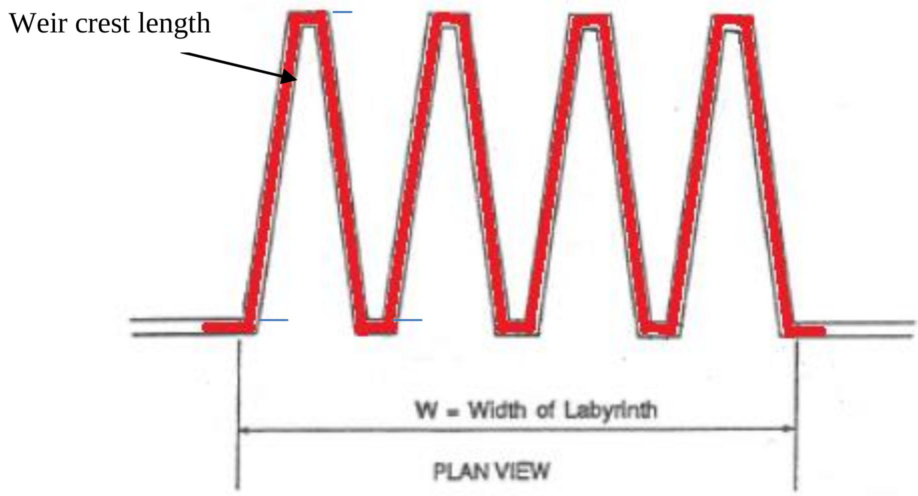

Figure 2.2: Plan layout showing increases crest length of a typical labyrinth weir (Tullis et al., 1995)

Labyrinth weirs can pass large flows at relatively low heads. They are primarily used as spillways for dams where the spillway width is restricted. They are sensitive to a reservoirs approach flow conditions due to their geometry and large discharge capacities. Flow over a labyrinth weir is very complex as it is three dimensional and influenced by many parameters. Therefore laboratory tests are needed to empirically determine the influence of the various parameters on the discharge capacity (Schleiss, 2011).

2.1.1 Discharge over a labyrinth spillway

The capacity of a labyrinth spillway is a function of the total head (H_T), the effective crest length (L) and the discharge coefficient (C_d). The discharge over a labyrinth spillway is calculated using the standard linear equation (Eq. (1.1)).

The discharge coefficient (C_d) is dependent on the total head (H_T), weir height (P), wall thickness (t_w), crest shape, apex configuration and the sidewall angles (α) (Fig. 2.1). Data as well as a procedure for designing labyrinth weirs for angles between 6^0 and 35^0 and for a range of heads was presented by Tullis et al. (1995) in a study on the design of labyrinth spillways. The solution was presented in a spreadsheet format that automatically calculated the dimensions for the labyrinth weir. For these designs, Tullis et al. (1995) adopted the general equation of linear weirs (Eq. (1.1)) for the design of labyrinth weirs. Even though this design procedure is fairly accurate; it is still recommended that a model study be conducted to verify the capacity and performance of a design. The model study can assist in evaluating factors like aeration effects and unusual flow conditions not included in the design procedure.

Since labyrinth weirs typically consist of a sequence of linear weirs folded in a zigzag fashion producing a longer crest length, the discharge (Q) capacity of this weir is directly proportional to the weir length (L) (see Eq. (1.1)). Even though the labyrinth weir discharge coefficient (C_d) values are lower than linear weir C_d values, its increased L (length) more than compensates, increasing Q by 3-4 times (Anderson & Tullis, 2012).

Labyrinth weirs maintain a more constant upstream depth and require less freeboard than linear weirs. They can satisfy increased flood routing requirements and increase reservoir storage under base flow conditions compared to linear weir structures. Labyrinth weirs have also been found to be effective flow aeration control structures, energy dissipaters, and drop structures (Crookston, 2010).

It must be noted that the discharge over a labyrinth weir increasing directly proportional to the crest length is only the case for labyrinth spillways operating under low heads, as the upstream head increases, the flow pattern passes through four basic phases namely fully aerated, partially aerated, transitional and suppressed (Schleiss, 2011).

In the *fully aerated phase*, the flow falls freely over the entire length of the labyrinth crest. For this phase, the thickness of the nappe and depth of tail water have no influence on the discharge capacity of the labyrinth spillway.

As the head increases, the flow becomes *partially aerated* due to converging of opposing nappes and higher tail water depths. Aeration becomes difficult due to the onset of nappe interference and results in a lowered discharge coefficient.

Further increase in the upstream head and tail water depth results in the nappe becoming suppressed at various locations. This condition is the beginning of the *transitional phase*. This phase can easily be identified as a slope change in the discharge coefficient curve.

Finally, if the flow forms a solid and non-aerated nappe, it is in the *suppressed phase* and no air is drawn under the nappe. According to Schleiss (2011) complete submergence occurs if the head above the crest is greater than the height of the labyrinth weir. In this phase, efficiency decreases rapidly approaching that of a linear crest. This is due to the water level being so high that it evades the labyrinth weir and flows directly over the weir as if it is a linear weir.

2.1.2 Geometry of a labyrinth spillway

The geometry of the labyrinth spillway has a significant impact on its discharge capacity. Different geometric parameters influence the discharge coefficient and can either improve or reduce the discharge coefficient. Many studies have looked into the geometric parameters and configurations of the labyrinth spillway to improve its design. Some of these studies are discussed further.

The study by Crookston (2010) listed a large number of possible geometric configurations of labyrinth weirs; though, there are three general classifications based upon cycle shape: triangular, trapezoidal or rectangular (see Fig.2.3). Triangular and trapezoidal configurations are more efficient based on their unit discharge per metre length along the crest.

According to Schleiss (2011), the crest of the weir may have different shapes (see Fig. 2.4):

- Sharp or narrow crest (SH);
- Flat crest (Flat);
- Quarter round crest (QR);
- Half round crest (HR); and
- Ogee crest (Ogee).

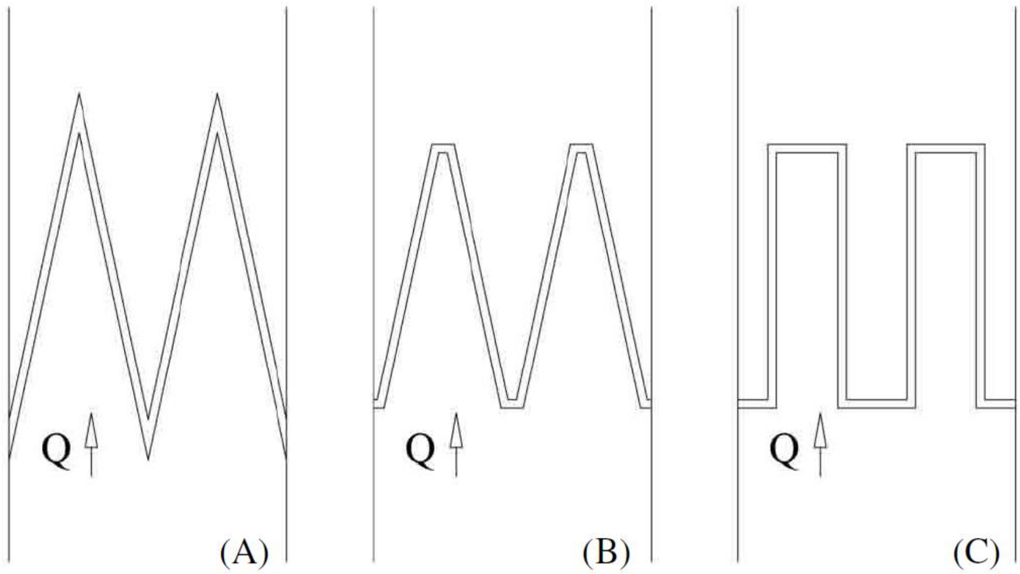

Figure 2.3: General classifications of labyrinth weir; (A) Triangular, (B) Trapezoidal, and (C) Rectangular (Crookston, 2010)

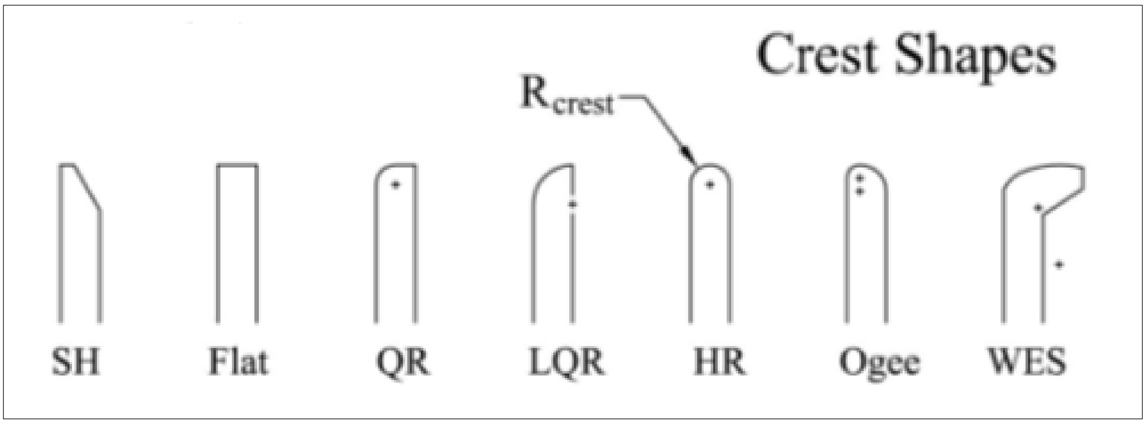

Figure 2.4: Labyrinth weir crest shapes (Crookston, 2010)

Crookston & Tullis (2013) presented a method for the hydraulic design and analysis of labyrinth weirs looking at labyrinth weirs with quarter and half round crest shapes for sidewall angles ranging from 6^o to 35^o. Results were based on physical modelling. Recommendations were made regarding specific important geometric parameters associated with the labyrinth weir design. These parameters include:

- Thickness of the weir wall at the crest (t_w);
- Head water ratio (H_T/P);
- Centreline length of sidewall (l_c);
- Outside apex width (D);
- Cycle width ratio (W/P); and
- Relative thickness ratio (P/t_w)

This study concluded the importance of the headwater ratio relative to crest shape. It was found that an increase in efficiency provided by a half round crest shape compared to a quarter round crest shape is more significant for $H_T/P \leq 0.4$.

Crookston (2010) also did an in-depth study on ways to improve labyrinth weir design and analyses techniques using physical modelling data sets and previous studies by compiling published design methodologies and labyrinth weir information. This study also included a method for the hydraulic design and analyses of labyrinth weirs. The cycle efficiency and parameters affecting flow performance were discussed and a standard geometric design was presented for arced labyrinth weirs. Cycle efficiency (also known as flow efficiency) was developed as a simple method for optimising a labyrinth weir design. Cycle efficiency represents the discharge per cycle of spillway and was used as a tool for examining the discharge capacity of different labyrinth weir geometries. It was introduced to aid in sidewall angle (α) selection. Different labyrinth weir orientations were also discussed as well as nappe aeration conditions for trapezoidal labyrinth weirs on a horizontal apron with quarter and half round crests. In the standard discharge equation (Eq. (1.1)) for a labyrinth weir, the flow was calculated using the total head (H_T) and the centreline length (l_c) of the weir as the characteristic length (L).

2.1.3 Nappe aeration, nappe stability and submergence

It must also be noted that nappe aeration and nappe stability should not be overlooked in the hydraulic and structural design of labyrinth weirs (Crookston, 2010).

Nappe aeration refers to the presence or absence of an air cavity behind the nappe. The behaviour of the nappe and the air cavity behind the nappe influences the discharge coefficient and aid in the selection of a crest shape. In the study by Crookston (2010) four different aeration conditions were observed during the testing: clinging, aerated, partially aerated and drowned. The aeration condition is influenced by the crest shape, H_T, the depth and turbulence of the flow behind the nappe, the momentum and trajectory of the flow passing over the crest and the pressure behind the nappe. As H_T increases, the nappe will transition from clinging to aerated, to partially aerated, and finally to drowned.

Nappe aeration condition can account for changes in C_d; a clinging nappe is more efficient than an aerated, partially aerated, or drowned nappe. This is due to the sub-atmospheric pressures that develop on the downstream face of the weir.

Nappe aeration conditions are a function of crest shape, velocity head, turbulence and tail water elevation adjacent to the labyrinth sidewalls. Venting the nappe to the atmosphere can stabilize the pressures behind the nappe and may aid in stabilising an unstable or oscillating nappe and may decrease vibrations and noise.

Crookston (2010) refined the definition of nappe interference for the reason that nappe interaction can produce a turbulent collision region or a region of local submergence depending on H_T.

In 2007 Tullis et al. conducted a study on head-discharge relationships for submerged labyrinth weirs. Weir submergence occurs when the tail water surpasses the weir crest elevation, causing an increase in the upstream driving head for a given discharge. Therefore for a given discharge over the weir a higher upstream head is required to pass the flow under submerged conditions. The most familiar relationship for predicting submerged weir head-discharge relationships is that of Villemonte (1974) for sharp crested linear weirs and had also been applied to submerged labyrinth weirs. This study shows the limited accuracy of using this relationship to describe labyrinth weir submergence. Alternative methods developed in the study using dimensionless submerged head parameters to predict submerged linear and labyrinth weir head-discharge relationships. The dimensionless submerged head relationships developed in this study show that the submergence does not begin until the tail water exceeds the crest.

As effective as labyrinth weirs are in increasing discharge and weir length, one of the main drawbacks of this structure is the need for large space as the base area it requires is not easily found on existing gravity dams (Lempérière, 2011). Piano key weirs (PKW) overcome this limitation with their sloping floors and overhangs that help reduce the base area requirement.

2.2 Piano key weirs

In the scope of dam rehabilitation to manage increasing floods or to increase water storage, the piano key weir (PKW) can be a good solution for concrete dams. The PKW can be a cost effective solution for new dams with low space or with limited reservoir section available to release a large design discharge (Machiels et al., 2012b).

After 2000, the piano key weir (PKW) was introduced as an evolution to the traditional labyrinth weir. Piano key weirs are a new type of weir, showing very good flood release capacities as well as strong economic and structural benefits (Machiels et al., 2009). These benefits include a reduced cost for construction and easy use for dams with smaller base widths available. The conception of this weir came about when the need for an optimal shape of weir which possesses a high performance and low cost came about (Ouamane & Lempérière, 2006).

The aim of the PKW is to increase discharge capacities and reduce upstream water levels in reservoirs. The PKW is ideal for installation on top of dam spillway structures as their footprint space requirement is relatively small in comparison to their developed weir length (L) (Oertel, 2015). Their inclined floors also help improve the hydraulic efficiency for relatively small discharges. They can be constructed of concrete, either cast in-situ or precast.

PKW’s can be used either on new dams or on existing dams. They can be used in many instances, as follows: (Lempérière & Vigny, 2007)

- Increasing storage of reservoirs with free flow spillway;
- Increasing the safety of dams; and
- On rivers as well as canals.

2.2.1 Discharge of a Piano Key Weir

In 2011, Lempérière proposed a new cost efficient design for the piano key weir. The study mentions that the most favourable design for the PKW is based upon two principles:

- The layout of the walls has a rectangular shape similar to piano keys; and

- The walls orthogonal to the flow are inclined. This is hydraulically favourable especially for large discharges and it also allows the base width of the structure to be reduced, allowing it to be used on most spillways and gravity dams.

The proposed cost efficient design has an upstream and downstream overhang of the same length. The L/W ratio is close to 5. The dimensions of the PKW are based on P_m (maximum height of the labyrinth walls). With the upstream head over the weir crest, h, between $0.4P_m$ and $2P_m$, the discharge per metre of spillway according to Lempérière (2011) is close to:

$$q = 4.3h\sqrt{P_m} \tag{2.1}$$

Where: q – Unit discharge over the weir ($\frac{Q}{W}$) ($m^3/s/m$);

h – H_T

P_m – Maximum height of the PKW walls (m)

4.3 – Coefficient representative of discharge inclusive of $\sqrt{2g}$

In this study Lempérière did not state clearly the thickness of the walls in this cost efficient design and therefore, this value had to be assumed in studies that followed. Also, Lempérière indicated that to improve the hydraulic efficiency when design conditions do not limit the height of the weir, it is more economical to increase P_m and keep the same dimensional properties. This study also looked at the construction of such structures and indicated that the cost is generally proportional to P_m(Lempérière, 2011).

The hydraulic behaviour of PKW's is different from the conventional labyrinth weirs. In the PKW, the flow is divided into 2 parts. One comes from the inlet channel of the PKW, overflowing the channel as a thin sheet and the second comes from the outlet channel, flowing as a jet toward the bottom of the channel (Leite Ribeiro et al., 2012a).

2.2.2 Geometry of a Piano Key Weir (PKW) and its effects on the discharge

Just like the labyrinth weirs, the geometry of the PKW also plays an important role in the discharge capacity and the value of the discharge coefficient. The different parameters influence the hydraulic efficiency of the weir and studies have looked at ways to improve this. Many studies have tried to capture the most important geometric variations having the largest impact on the discharge coefficient and discharge capacity. These studies have been on going as one of the main challenges when designing this type of structure is the geometry and the sensitivity and influence these geometric parameters have on the performance of the weir. Some of these studies are discussed as follows:

The geometry of the PKW based on preliminary studies of physical models by Ouamane & Lempérière (2006) is as follows:

- A rectangular shape of the channels, similar to the shape of piano keys;
- A tilted apron of the upstream and downstream channels which favours the use of overhangs;
- A reduced length of the base due to overhangs;
- A reduced width of the elements due to the rectangular form; and
- A reduced surface of the side walls.

This configuration is defined by the height (H), the width of the upstream (W_{in}) and downstream (W_{out}) channels, the length of the overhangs, the ratio of L/W (developed plan length to the overall spillway width), number of cycles (N) forming the weir, and the vertical aspect ratio (W/P_m) (see Figs (2.5 –2.7)) (Ouamane & Lempérière, 2006).

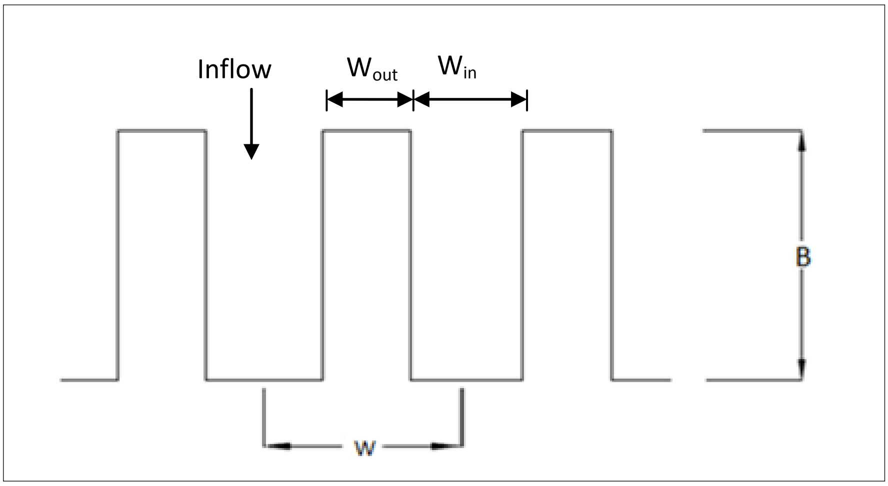

Figure 2.5: Plan layout of typical piano key weir

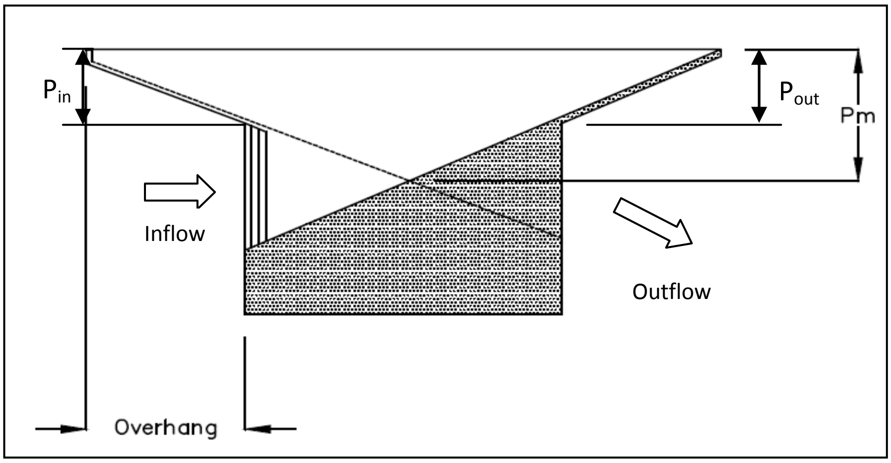

Figure 2.6: Side view of a piano key weir showing overhangs

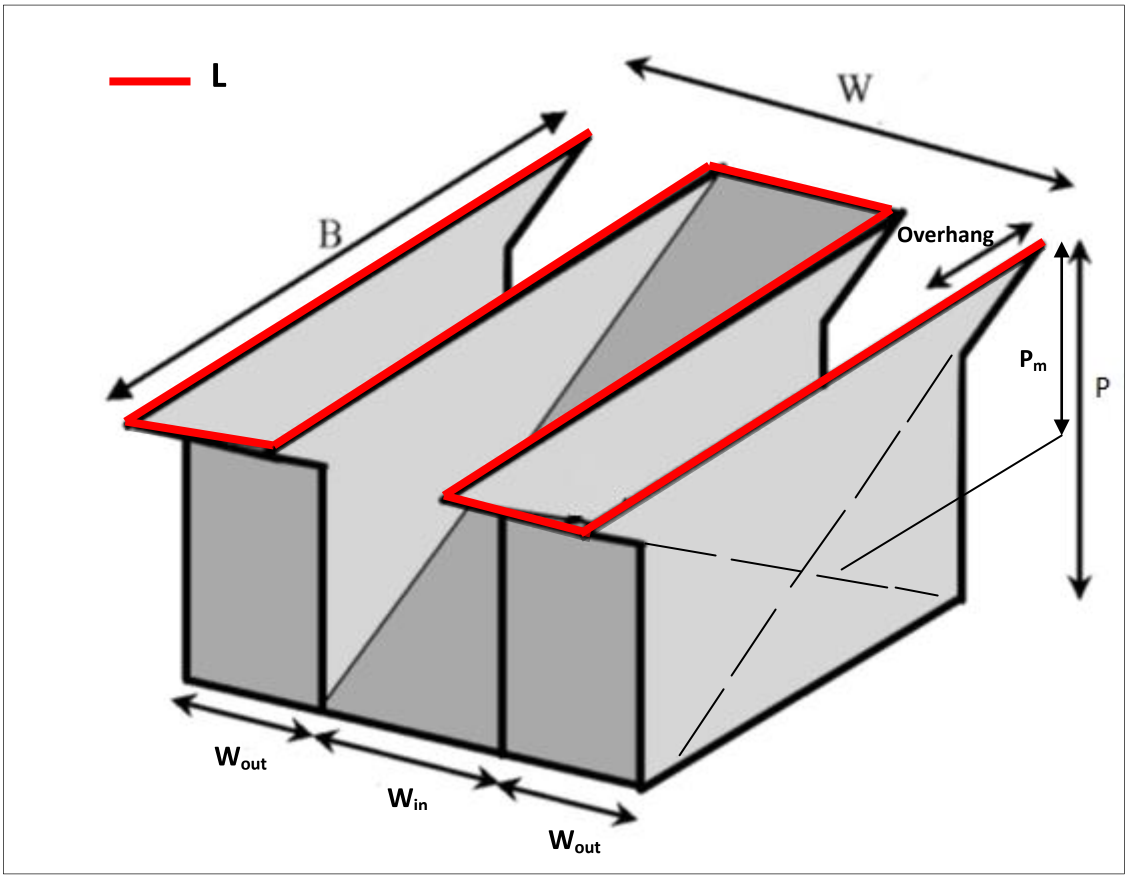

Figure 2.7: Geometric parameters of PKW

In addition to the basic configuration of the PKW, some optional features can be developed as follows: (Schleiss, 2011)

- Parapet walls: placed on the crest of the PKW and transform its upper part to a rectangular labyrinth;

- Width of inlet and outlet keys: a higher inlet to outlet ratio results in better hydraulic performance; and
- Sidewall angle: a sidewall angle narrowing the inlet and widening the outlet channel is likely to improve the discharge capacity.

In the study by Ouamane & Lempérière (2006) many geometrical aspects for this new weir shape were considered. Other studies that looked at these aspects were the studies conducted by Pfister & Schleiss (2013a), Anderson (2011) and Machiels et al. (2012b).From these studies the importance of the inlet and outlet channel heights (P_{in} and P_{out}) as well as the overhang lengths, different W_{in}/W_{out} ratios and the sensitivity of the PKW discharge efficiency to the W_{in}/W_{out} ratio were mentioned. Anderson (2011) and Machiels et al. (2012b) found the optimal range of W_{in}/W_{out} to be between 1.25 and 1.5. Machiels et al. (2012b) also looked at defining the main geometric parameters that for new dams, high weir geometries have to be preferred (P/W=1.25) whilst for rehabilitation projects lower geometries (P/W=0.5) give the best compromise between hydraulics and economic interests.

Other geometries and modifications that were made to test the discharge efficiency were: using a parapet wall, installing fillets underneath the upstream overhangs and replacing a flat topped crest with a half round crest. Anderson (2011) also tested the influence of sloping floors and overhangs on the discharge efficiency and compared the discharge efficiency of the PKW with a trapezoidal labyrinth weir. The overhangs resulted in a measurable increase in discharge efficiency while the sloped floors had a less significant influence on the weir discharge efficiency. The fillets under the upstream overhang increased the discharge efficiency as well as the parapet walls whilst the change in crest shapes resulted in significant gains in discharge efficiency at low heads. A study by Machiels et al. (2012) found similar conclusions regarding the overhangs, indicating that symmetric overhangs are favoured for making the structure self – equilibrated and favouring the use of precast elements.

Lempérière (2011) made geometric recommendations for an efficient PKW design, however, some geometric parameters in the recommended design were not specified like that of the crest shape, wall thickness and shape of weir beneath the upstream overhang etc. Also, the discharge relationship (Eq. (2.1)) proposed by Lempérière (2011) is not generally applicable to all PKW's but rather it's specifically applicable to the geometry specified by Lempérière (2011). Anderson's (2011) study also noted a lack of information from this study.

Erpicum et al. (2014) investigated these main geometric parameters influencing the weir hydraulic efficiency. Experimental data was gathered to show how the weir height (P), channel widths (W_{in} and W_{out}), and overhangs influence for a given crest length, the weir discharge capacity.

Comparison was made with the theoretical rating curve of a standard linear weir. This analysis highlighted how the channel widths and overhang length ratios influence the weir efficiency significantly but less than the weir height.

There are four different types of PKW's noted in literature. The different PKW's are classified according to the presence or absence of overhangs. Type A has equal up-and downstream overhangs, type B and C include only up-or downstream overhangs and type D has no overhangs (Fig.2.8) (Pfister & Schleiss, 2013b).

A study by Kabiri-Samani & Javaheri (2012)on the discharge coefficients for free and submerged flow over Piano Key weirs (PKW) looked at the four types of PKW's and derived empirical formulae for the discharge coefficient of each of these. The results from this study showed that the upstream overhang increases the inlet flow area and wetted perimeter, resulting in reduced inlet velocities, flow contraction and energy loss. Therefore, decreasing the upstream channel width results in increased local submergence of the upstream channel and a decrease in the discharge efficiency.

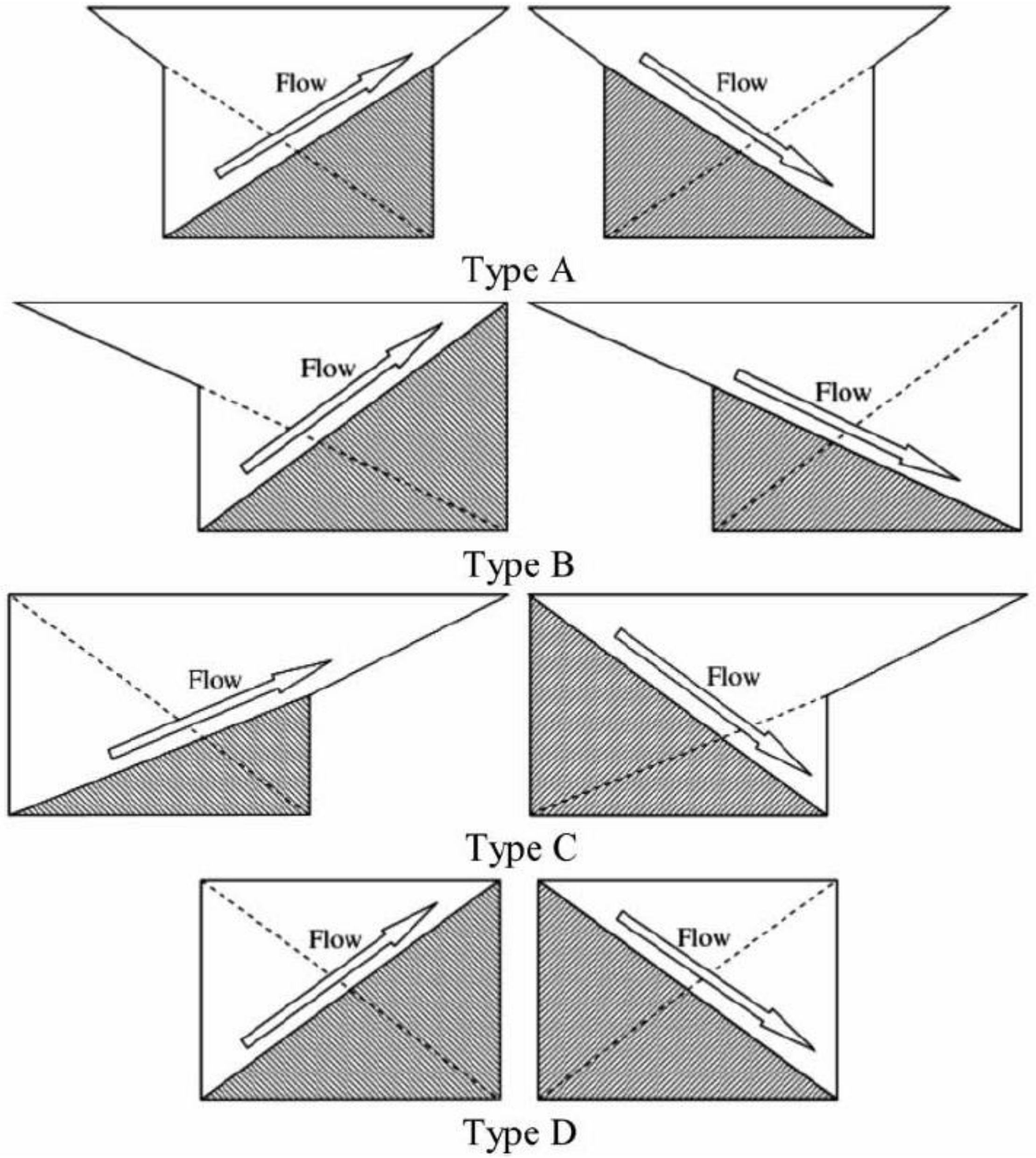

Figure 2.8: Different types of piano key weirs (Kabiri-Samani & Javaheri, 2012)

In a study by Leite Ribeiro et al. (2012b) several A-type PKW's were setup and model studies were conducted in which relevant parameters were systematically varied. Taking into account former studies, a general design equations relating to the head-discharge ratio was derived and expressed as a discharge increase ratio as follows:

$$r = \frac{Q_p}{Q_s} = \frac{C_p L \sqrt{2g} H^{3/2}}{C_s W \sqrt{2g} H^{3/2}} \approx f\left(\frac{L}{W}\right) \tag{2.2}$$

Where: r – discharge increase ratio

Q_p – Discharge of the PKW (m^3/s)

Q_s – Discharge of the sharp crested weir (m^3/s)

C_p – discharge coefficient of the PKW

C_s – Discharge coefficient of the sharp crested weir

L – Developed crest length

W –Width (m)

g – Gravitational acceleration (m^2/s)

H_T – Total approach flow head (m)

This ratio was mainly a function of the flow head (H_T), developed crest length (L), inlet key height (P_{in}) and width (W). Case study model tests were analysed to provide a design approach if reservoir approach is considered.

In another study, Pfister & Schleiss (2013) looked at different PKW configurations to determine the rating curve of A-type PKW's. A comparison with previous studies by Kabiri-Samani & Javaheri (2012), Leite Ribeiro et al. (2012b) and Machiels et al. (2012b)was done as well using a chosen prototype case study. It was found that the main parameters affecting the rating curve are the crest length (L) and weir height (P). The secondary geometrical parameters have a small but negligible effect.

An experimental study by Machiels et al. (2009) looked at the physics of the flows on the PKW to determine the limitations of this type of weir. This was achieved by exploiting a large scale experimental model of a PKW in a wide range of discharges. In addition to this, the study also looked at the influence of the different geometrical parameters on the discharge capacity of the PKW. In parallel to the experimental tests, numerical modelling was also performed to help define the most important geometrical parameters of the weir.

The aim of another study by Machiels et al. (2011) was to determine the flow features along the weir depending on the upstream head. These flow conditions are characterised in terms of specific discharge, velocity, pressure, water level and streamlines along the weir. This study showed that the PKW configuration is up to three times more efficient than the ogee crest weir based on the discharge coefficient (C_d). It also highlighted the effects of wall thickness (t_w) and weir shape on the discharge capacity.

Lempérière & Ouamane (2003) found that the piano key weir (PKW) can increase the specific discharge (Q/W) fourfold or more compared to a standard linear weir. Two solutions/ variations of the PKW were tested. Solution A had similar upstream and downstream overhangs. This solution favours the use of precast concrete elements. Solution B had only an upstream overhang. Savings in this design are approximately 10% higher than solution A and the structural loads are less for high flows. However, solution B does not favour the use of precast elements. Solution B is more appropriate for new dams where high specific flows will be favoured and for very large existing spillways. In this study, Lempérière & Ouamane (2003) also mention the use of PKW's results in a considerably aerated flow; this reduces the risk of downstream erosion and cavitation. The study concluded that PKW's are simple solutions that are safe and easy to operate as well as efficient.

Later, Machiels et al. (2012a) developed a method for the preliminary design of PKW's. This design is based on the project constraints and an extrapolation of existing experimental results from a reference scale model. The elements necessary to the design method are characterised in project elements and reference model elements. The project elements are the hydraulic and geometric specificities of the project (discharge, maximum head and available width) whilst the reference model requires a release capacity curve as well as geometric characteristics of the tested model. The release capacity curve is the specific discharge plotted against different geometrical parameters to show the influence on release capacity (see Fig. 2.9). The method can be summarized as follows:

- Choosing a reference model – regarding the reference model, a release capacity curve is necessary as well as geometric characteristics of the model;
- Scaling the geometric and hydraulic characteristics of the reference model corresponding to different number of PKW units – based on the project elements, different efficient designs may exist. The first step of the method aims at defining these possibilities as a function of the number of PKW units in the structure, by scaling the geometric and hydraulic parameters of the reference model;
- Isolating the designs enabled to respond to the project constraints – this is done by drawing the head/discharge curves for different numbers of PKW units and limiting these curves to head and discharge values under the design head and over the design discharge so different designs may respond to the project constraints ;
- Optimising the designs based on structural, economical or hydraulic criteria – based on the project engineer's interests (this clearly defines the final design).

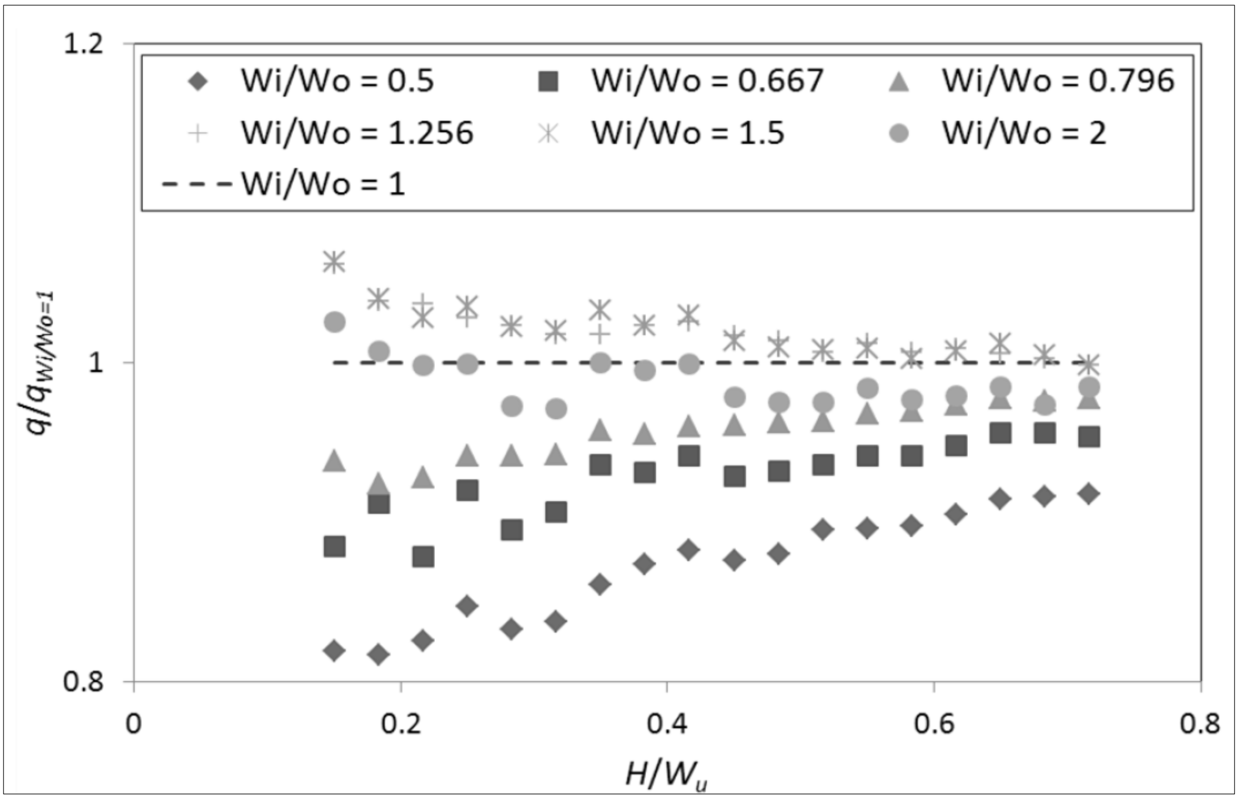

Figure 2.9: Example of various curves showing the comparison of specific discharges provided by PKW's with various W_{in}/W_{out} ratios for P/W_u = 0.5 (Machiels et al., 2012b)

In order to improve the efficiency of the PKW design, another experimental study on the influence of the main geometric parameters was performed. Thirty one configurations were tested for a variety of discharges. The results show the influence of weir height, channel discharges and overhang lengths on the discharge capacity and flow characteristics. An analytical formulation was developed to predict the discharge capacity of the weir as a function of its geometry (see Eq. (2.3)). This formulation shows an accuracy of 10% in comparison to the experimental results of this study and other sources (Machiels et al., 2014).

$$q = q_u \frac{W_{out}}{W_u} + q_d \frac{W_{in}}{W_u} + q_s \frac{2B}{W_u} \tag{2.3}$$

Where: q –specific/unit discharge (m^2/s)

q_u - Upstream crest specific discharge (m^2/s)

W_{out} – Outlet channel width (m)

W_u – PKW unit width (m)

q_d – Downstream crest specific discharge (m^2/s)

W_{in} – Inlet channel width (m)

q_s – Side crest specific discharge (m^2/s)

B – Side crest length (m)

The three specific discharges were computed using the standard weir equation (Eq. (1.1)) and considering specific formulations of the discharge coefficient. For the up – and downstream crests, the discharge coefficients were calculated using the SIA formulation for sharp – crested weirs (Swiss Society of Engineers and Architects , 1926). For the up – and downstream constant discharge coefficient terms were modified to take into account the weir inclination over the vertical. For the side crest, a correction term was added to take into account the flow inertia in the inlet key direction.

The accuracy of this design method is therefore directly linked to the experimental tests accuracy and the number of available results for the reference model. Figures 2.10 and 2.11 show the comparison between the specific discharges computed with the analytical formulation proposed in this study and the experimental results from this study and other sources. This method was applied to the preliminary design of a PKW to show how to optimise the design regarding the project engineer's interests.

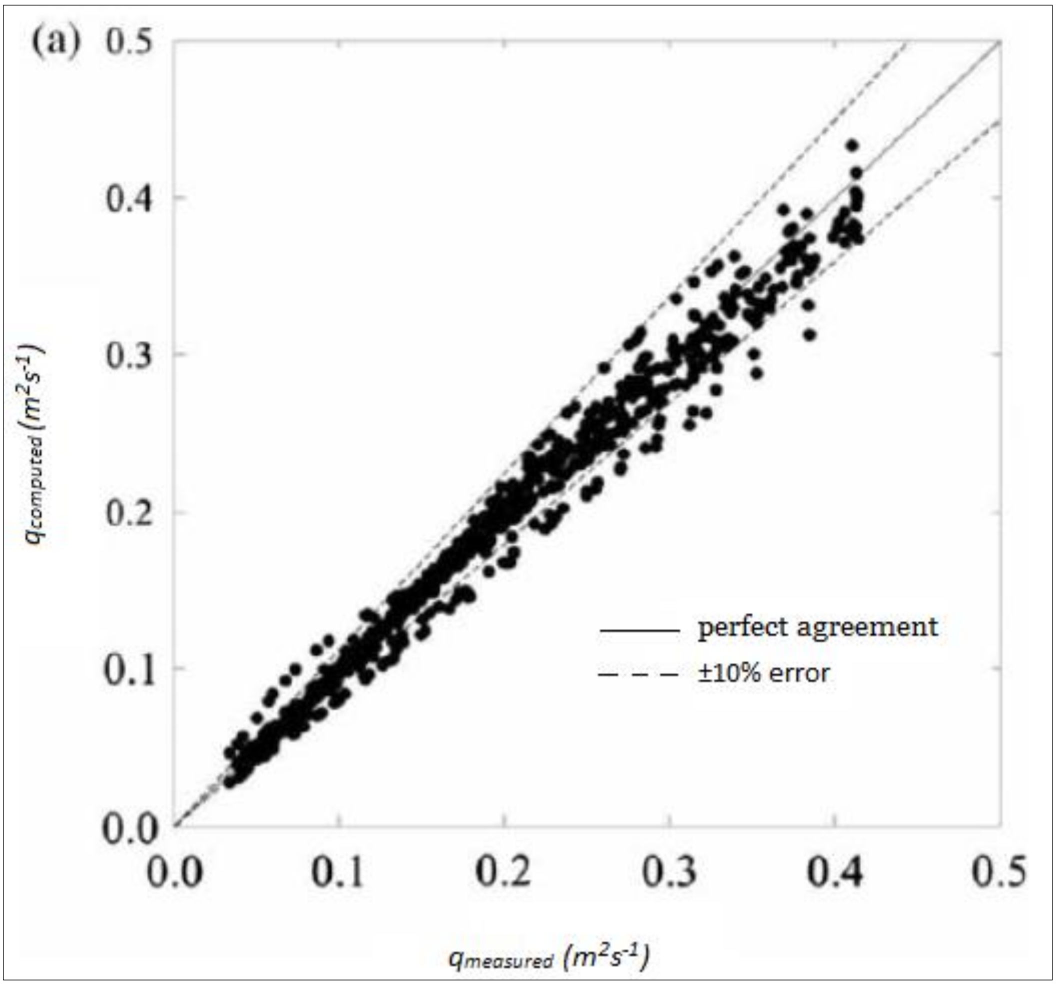

Figure 2.10: Comparison between specific discharges computed with analytical formulation proposed in the study by Machiels et al (2014) and the experimental results from this study (Machiels et al., 2014)

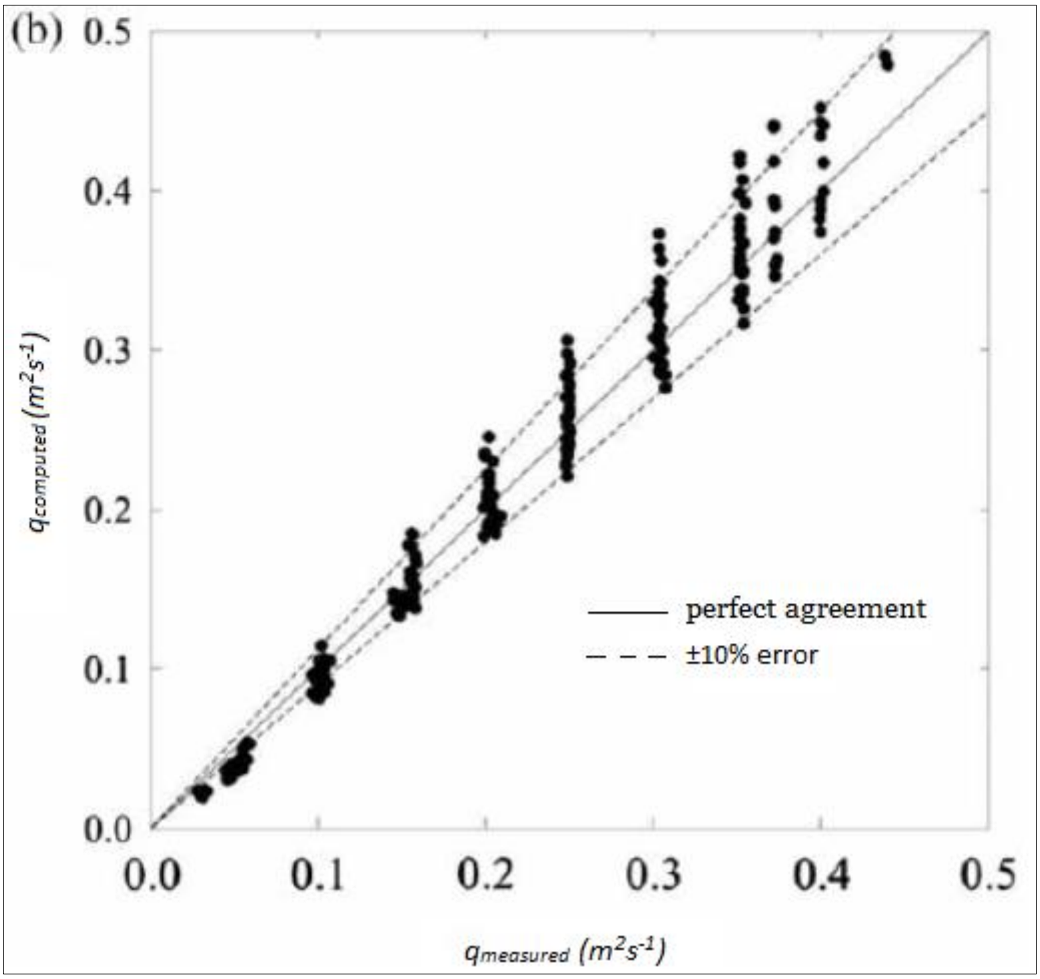

Figure 2.11: Comparison between specific discharges computed with analytical formulation proposed in the study by Machiels et al (2014) and the experimental results from other sources (Machiels et al., 2014)

A study conducted by Lade et al. (2015) tested the discharge capacity of two PKW's with different side crest geometries (see Figs 2.12 -2.14). One had a sloping side crest and the other a triangular side crest. The results indicated that at low discharges these modifications did not exhibit remarkable improvement in discharge coefficient as compared to the regular PKW, but can have greater efficiency at higher discharges. According to Lade et al. (2015), at higher discharge, the improvised models went under submergence and showed remarkable discharge efficiency.

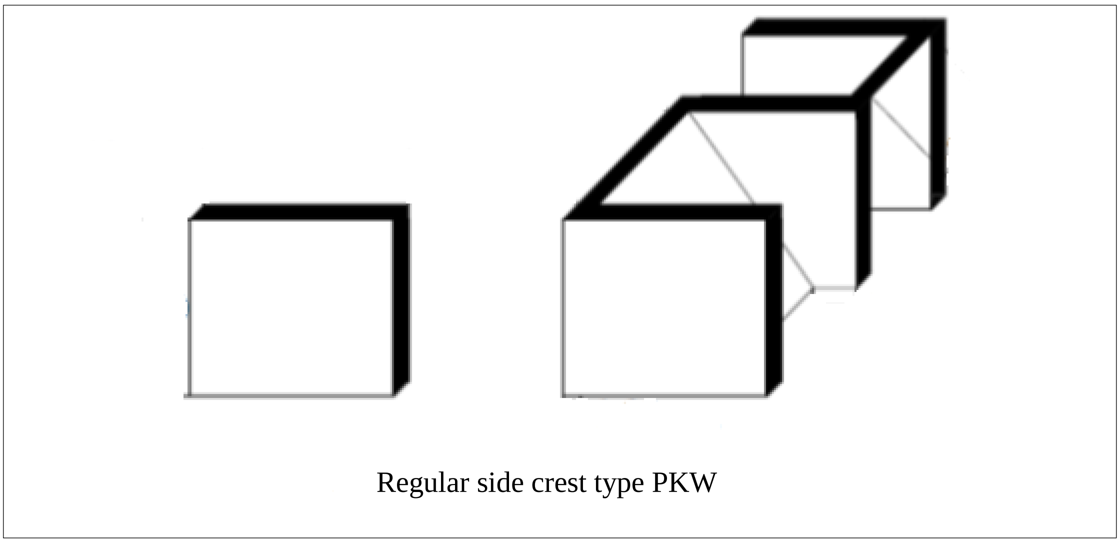

Figure 2.12: Regular side crest type PKW (Lade et al., 2015)

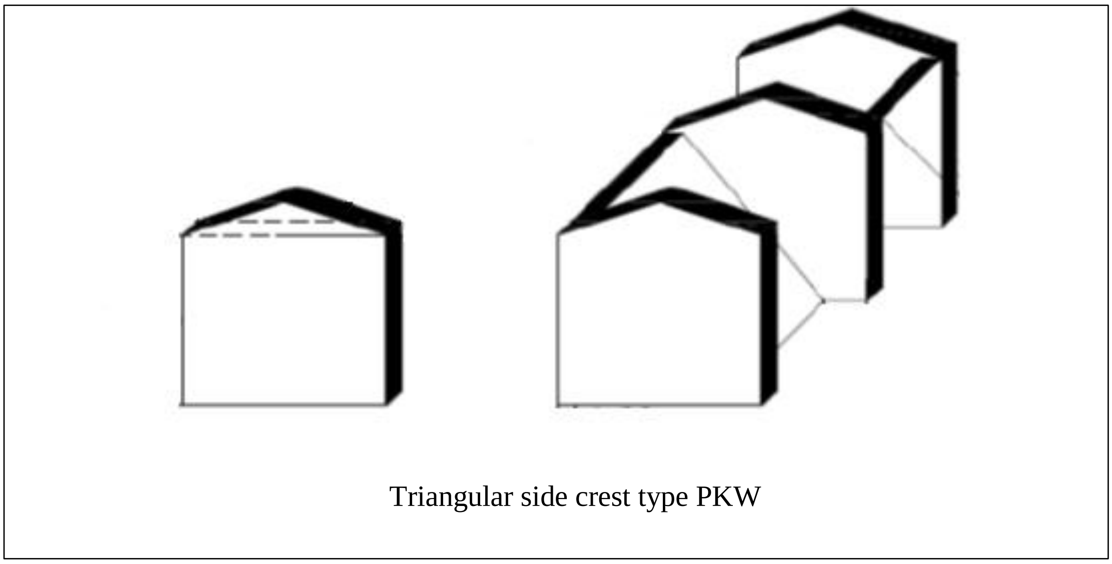

Figure 2.13: Triangular side crest type PKW (Lade et al., 2015)

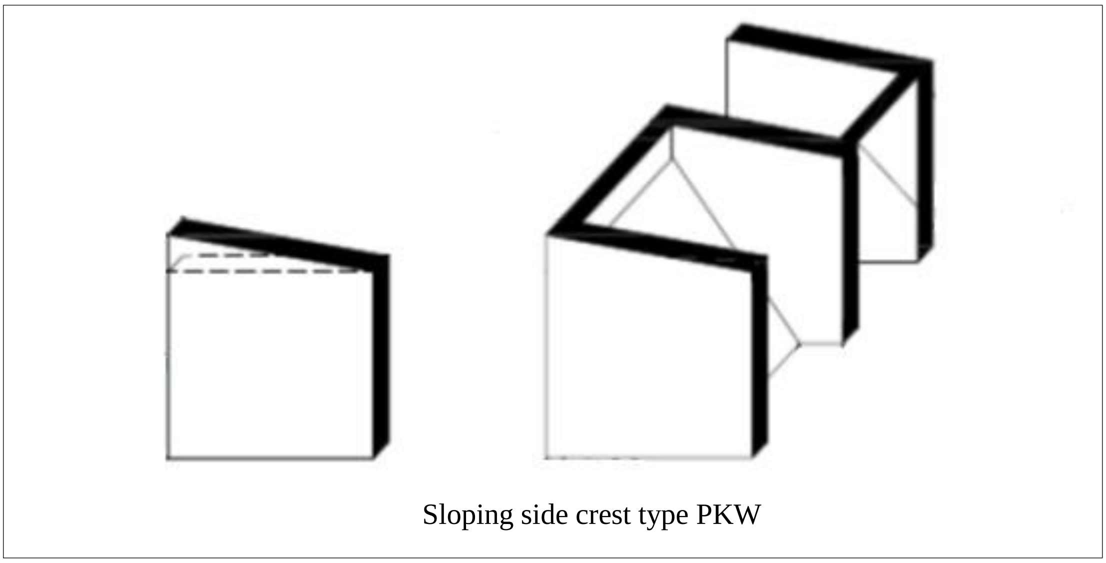

Figure 2.14: Sloping side crest type PKW (Lade et al., 2015)

Oertel (2015) analysed the discharge coefficients of different PKW structures. This study focused on the comparison of discharge coefficients for PKW with and without geometric adaptations at the downstream end of the top of the structure. In this study, geometric variations such as triangular and semi-circle expansions were fixed at the downstream crest end (Fig. 2.15). The results indicated that these expansions decrease the efficiency of the PKW for small discharges.

Figure 2.15: Sketches of Laboratory-scale PKW model (Left:Regualar PKW; Middle: Triangular expansion at downstream of PKW; Right: Semi-circle expansion at downstream end of PKW), flow direction left to right (Oertel, 2015)

Khassaf & Al-Baghdadi (2015) did an experimental study on non-rectangular piano key weir (PKW) discharge coefficient. They tested the effects of side wall angle and side wall inclination angle on the discharge coefficient and achieved the head-discharge relationship for each model. They concluded that changing these angles to as much as 10^0 had a negative impact whilst changing around 5^0 can increase capacity with appropriate changes to the inlet and outlet key width ratios. It must be noted that these tests were performed on structures with very thin walls more appropriate to steel plate structures.

Although the higher efficiency of the Piano Key weir (PKW) has already been demonstrated, its optimal geometry is still poorly defined. To improve the design of the complex geometry of this structure, the use of parapet walls has been tested. These parapet walls are vertical extensions placed over the weir crest. The study by Machiels et al. (2013) investigated the effect of parapet walls to increase weir height while reducing bottom slopes and keeping the weir height constant. The main influence of the parapet wall on the PKW crest is an increase in the total PKW height. Increasing the total weir height has been shown to increase the discharge capacity; however the discharge capacity does not increase when a parapet wall is placed on the PKW that already has an optimal weir height. Similarly, the discharge capacity does not change for a PKW having the same total height with or without a parapet wall. The height of the PKW also has to be limited to maintain the interest of overhang use, limiting the head losses at the inlet entrance. Therefore, due to the practical design of a PKW based on project constraints, it was found that it is more convenient and cost effective to use standard PK weir without parapet walls.

In another study regarding parapet walls, Pfister et al. (2012) looked at the Piano Key weirs as efficient spillway structures. The hydraulic behaviour of PKW's were analysed and the parameters considered were the number of units and the presence of parapet walls. The results showed that for identical normal approach conditions, the number of PKW units does not affect the specific discharge of the PKW unit. The parapet walls on the inlet channels were not effective; however, the presence of the parapet wall on the outlet channel slightly improves the efficiency of the PKW (see Fig 2.16).

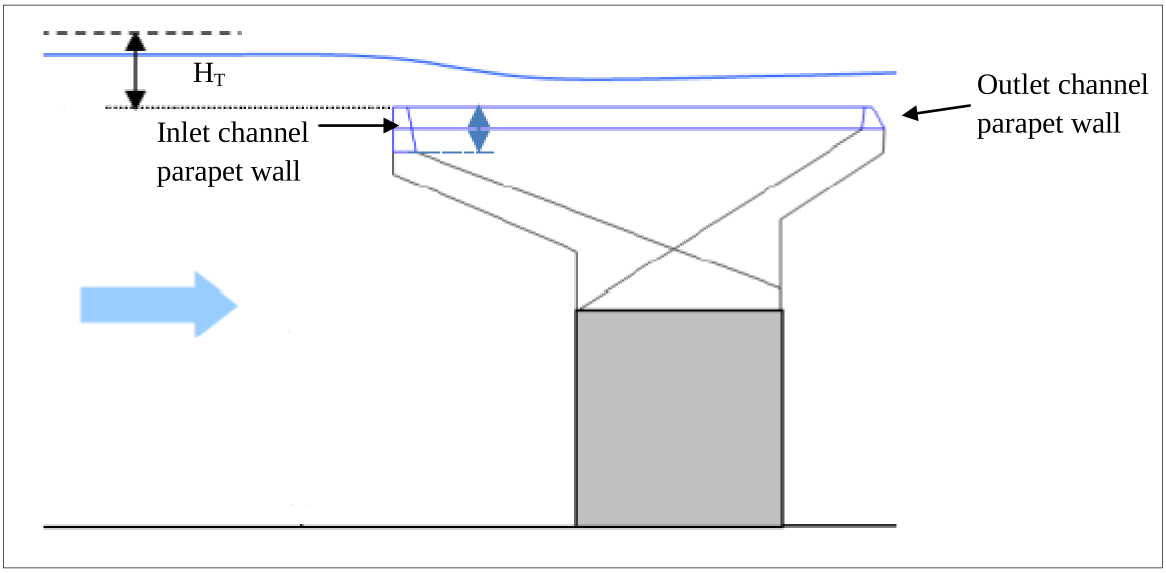

Figure 2.16: Side view of PKW showing difference in inlet and outlet channel parapet walls

Anderson (2011) also looked at parapet walls as a modificaton in the geometry of the PKW. The findings in this study indicated that the parapet wall improves the discharge efficiency of the weir.

The PKW offers many geometrical options, especially the use of side wall angles which would result in a converging inlet key. Another consideration not yet featured would be to incline the sidewall slightly which would enlarge the width of the inlet key (Schleiss, 2011).

2.2.3 PKW Application

PKW's can be applied to dams as well as open channels and in order to understand the different applications, Anderson & Tullis, (2012) looked at reservoir and channel applications of the PKW. Using a scale physical model, the hydraulic efficiency of a PKW design was tested with varying approach flow depths, upstream apron slopes and abutment details. In general, it was found that discharge efficiency increased with increasing approach flow depth, steeper approach aprons, and improved abutment geometries that reduced the effects of flow separation.

2.2.4 Rehabilitation projects using Piano Key Weirs

As in many countries, some dams in France have spillway capacities which are small compared to updated design floods. Therefore improving spillway discharge capacity has become a significant issue. Costs associated with projects to increase spillway capacity can be significant since: (Leite Ribeiro et al., 2009)

- The modification of the spillways has an important impact on the dam structure by removing significant amounts of concrete or the addition of new loads to existing structures;
- The energy dissipating structures are significant; and
- The energy production can be reduced during construction works.

Some rehabilitation projects where PKW's have been considered to increase the capacity of the existing spillway system are: (Leite Ribeiro et al., 2009)

- Golours Dam (France);
- St Marc Dam (France);
- Les Gloriettes Dam (France); and
- Etroit Dam (France)

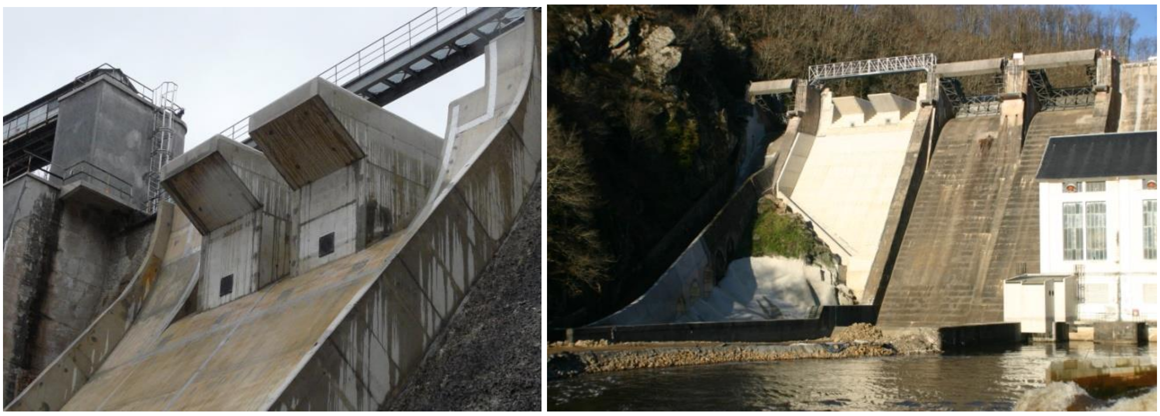

Figure 2.17: Etriot and St. Marc Dams in France(Anon., 2016)

Figure 2.18: Les Gloriettes Dam in France (Anon., n.d.)

Figure 2.19: Goulors dam in France (Anon., n.d.)

Layouts of the abovementioned dams with tested PKW's were summarised with regards to their geometrical characteristics. Experimental data of the physical modelling tests on the PKW's mentioned above show the influence of each specific parameter on the hydraulic capacity of the weir. From the analysis of the PKW shapes it was found that for increasing head, the absolute capacity increases. At low heads the PKW behaves like a sharp crested weir with the total crest length (L) used and at high heads its behaviour is close to that of broad crested weirs of width W (Leite Ribeiro et al., 2009).

2.3 Comparison of labyrinth and piano key weirs

Both labyrinth and piano key weirs (PKW) have proven to improve a spillways discharge capacity. These weirs have been known to increase a spillways effective crest length due to their folded shape. From the standard linear equation (Eq. (1.1)), it is clear that Q is proportional to L, therefore an increase in L will result in higher discharges over the spillway. C_d is also improved due to reduced energy losses from the geometry of PKW spillways making the flow lines smoother over the spillway crest. These geometric changes mainly come from the roundings associated with the standard PKW design. However, it is unknown as to which of these is the most efficient hydraulically and economically. Many studies have concluded and favoured the use of the piano key weir (PKW) for various reasons whilst other studies maintain that even with the improved design of the PKW, the labyrinth weir is still favoured under certain circumstances. Lempérière (2011) and Schleiss (2011) have made recommendations and conclusions based in favour of the PKW, indicating that it can result in hydraulic efficiency gains and improved discharge coefficient (C_d). Other studies by Anderson (2011) and Leite Ribeiro et al. (2012a) have indictaed that the labyrinth spillway is still more efficient per crest length based on the changes in lateral length (B), width (W) and sidewall angle aswell as the hydraulic head. The studies that follow compare both of these spillway types based on experimental data.

The piano key weir (PKW) represents a particular type or development of the labyrinth weir. Different from the labyrinth weirs, the structural footprint of PKW's is relatively short in the stream wise direction allowing for the installation on top of existing gravity dams. Their inclined floors (in comparison to the vertical arrangement of the labyrinth weirs) improve the hydraulic efficiency for relatively small discharges (Pfister & Schleiss, 2013a).

Comparing the PKW with a corresponding rectangular labyrinth weir reveals the PKW has a significantly better discharge efficiency when looking at the discharge coefficient. This is also the case if considering trapezoidal labyrinth weirs for comparison. According to Schleiss (2011) the gain in efficiency of a PKW can reach up to 20%. The PKW can also result in considerable construction cost savings compared to the traditional labyrinths.

In a study by Anderson & Tullis (2012)a comparison between the PKW and rectangular labyrinth weir hydraulics was made. The study was conducted to get a better understanding of the effects of PKW geometry on discharge efficiency. In this study, the hydraulic efficiency of the recommended PKW design was compared with geometrically comparable rectangular labyrinth weirs with and without sloping floors. The study concluded that the PKW with Lempérière's recommended design produced higher discharge efficiencies than all the rectangular labyrinth weirs. The rectangular labyrinth weir without sloping floors matched the PKW's performance at H_T/P <0.15. Rectangular labyrinths had sloping floors at the inlet and outlet channels, these floors resulted in a slight decrease in discharge efficiency for H_T/P< 0.60 and modest increase in discharge efficiency for H_T/P > 0.60.

Comparing PKW's to the traditional labyrinth weir, Anderson (2011) found that in general, trapezoidal labyrinth weirs are more discharge efficient per crest length than PKW's. If restrictions on lateral length (B) and Width (W) exist then PKW's produce the highest discharge efficiency due to the increased weir length produced by the PKW geometry. If W is not restricted, increasing W of a trapezoidal labyrinth weir can result in an increase in discharge efficiency, relative to a PKW. If B is not restricted, trapezoidal labyrinth weirs with small sidewall angles produce an increase in discharge efficiency compared to a PKW with the same W.

Even though it is said to improve hydraulic capacity, a study by Leite Ribeiro et al. (2012a)that looked at the discharge capacity of PKW's found that the PKW is very efficient at low heads but with increasing hydraulic head the discharge efficiency decreases quickly.

In order to develop a better understanding of the effects of the PKW geometry on discharge efficiency, Anderson & Tullis (2013) tested nine scale models including Lempérière's (2011) recommended design. The effects of the weir geometry or modifications on the weir performance were partially isolated; varying the inlet – to – outlet channel ratio, raising the crest via a parapet wall, rounding the upstream apex walls and varying the crest type. The head – discharge efficiency of the trapezoidal labyrinth and PK weirs with respect to footprint restrictions and crest length were compared (Anderson & Tullis, 2013).

The objectives of the study conducted by Anderson & Tullis (2013) were as follows:

- To evaluate the design and head – discharge relationship recommended by Lempérière(2011);
- To investigate the sensitivity of the PKW with respect to W_{in}/W_{out};
- To evaluate the effects of other PKW geometric design variations; and
- To compare the discharge efficiencies of PKW and trapezoidal labyrinth weirs.

The conclusions of this study indicated that using the water level (h) as the upstream characteristic head parameter, correlates well with the Lempérière (2011) specific weir design in a channel application. It was less applicable to PKW geometries where the head-discharge relationships were less linear. The optimal range of W_{in}/W_{out} is between 1.25 and 1.50 for maximising discharge efficiency. The noses installed on the upstream apex, the parapet wall and improved crest shapes all increased the discharge efficiency of the design. It was also concluded that in general, trapezoidal labyrinth weirs have higher discharge efficiencies per crest length than PKW's.

Karaeren (2014) compared linear, labyrinth and piano key weirs (PKW) to increase discharge capacity of existing spillways for a given head. The main goal of this study was to investigate some practical methods used in increasing the spillway capacity of dams. In this study, labyrinth and piano key weir (PKW) types were selected as the two effective methods in achieving an increased spillway capacity. Design procedures of these two weirs were outlined and each one was applied in five different existing projects. Comparisons were made with the linear weirs and different geometric parameters were also studied to see their effect on the discharge capacity. These parameters were as follows:

- Different labyrinth angles (for greater discharge capacity, lower angles should be used);
- Different number of labyrinth cycles (as number of cycles decrease, effective length and discharge capacity increase);
- Different H_T/P ratios for labyrinth weirs (as H_T/P decrease, C_d increases and effective length decrease);
- H_T/P ratios for PKW's (increase in discharge with longer crest length but the advantage is lost with increasing upstream head);
- Different W_{in}/W_{out} ratios for PKW's (demonstrated that W_{in}/W_{out} =1.25 is the most efficient).

Using a labyrinth spillway instead of a standard spillway can increase the crest length by about five times. Therefore, the discharge capacity of a labyrinth spillway can be twice as much as that of a standard spillway (Karaeren, 2014).

Similar to the labyrinth weirs, PKW's are designed to increase discharge capacity. This feature will be lost if the upstream head increases. When the head increases, the discharge coefficient of a PKW is more sensitive than a labyrinth weir. Therefore, they are designed for moderate heads to avoid any reduction in the discharge capacity (Karaeren, 2014).

The conclusions obtained in this study were as follows: (Karaeren, 2014)

- When the ratio of H_T/P increases in labyrinth spillways, C_d starts to decrease and the benefits gained by using the labyrinth spillway is lost.
- When labyrinth angle (α) increases, discharge coefficient increases and the effective length (L) decreases;

- As the number of cycles (N) decreases, effective length (L) and discharge capacity increase;
- PKW's are more effective than labyrinth weirs at low heads as the advantage of longer crests is lost with increasing upstream head ;
- The W_{in}/W_{out} = 1.25 geometry is the most efficient of the 3 geometries tested;
- Labyrinth weirs with small sidewall angle (α) ensure more discharge capacity; and
- PKW's are an economic and cost effective way to increase spillway capacity.

In a study by Lempérière et al. (2013) it was noted that the traditional labyrinths may also be adapted and improved. This can be done as follows:

- The shape of the layout may be optimised; and
- The inlet may be wider than the outlet.

Such optimisations may be preferred and overhangs avoided.

2.3.1 Cost comparison

Paxson et al. (2012) comparatively assessed the potential application of a PKW where a labyrinth weir or other type of control structure was constructed. Using the Tullis et al. (1995) method, a two cycle labyrinth weir with a 12^0 sidewall angle (α) was selected for comparison with a four key PKW with similar head discharge characteristics. The weir height (P) was the same for both weirs. The upstream to downstream footprint for the PKW was stated to be less than that of the labyrinth weir. In this study, the concrete volumes for the PKW and labyrinth weirs were estimated based on typical weir dimensions and are presented in Tables 2.1 and 2.2.

Table 2.1: PK weir concrete volumes (Paxson et al., 2012)

Element	Type of concrete	Volume (cubic yards)
Base	Mass	195
Weir walls	Reinforced	55
Overhangs	Reinforced	20
Training walls	Reinforced	130
Slab	Reinforced	40
Total	Reinforced	245
Total	All	440

Table 2.2: Labyrinth weir reinforced concrete volumes (Paxson et al., 2012)

Element	Volume (cubic yards)
Weir	195
Slab	260
Training walls	240
Total	695

From Tables2.1 and 2.2 it can be seen that the PKW requires 40% less concrete volume with similar head-discharge characteristics. This is due to the significantly reduced upstream to downstream footprint of both the foundation and weir. Moreover, the assumed unit costs and resulting estimated costs are presented in Table 2.3 for each of these structures. These results indicate that the estimated cost of the PK weir is 20% - 40% less than that of the labyrinth weir with similar hydraulic capacity.

Table 2.3: Cost estimates for PK weir and Labyrinth weir (Paxson et al., 2012)

Structure	Element type	Unit cost (per cubic yard)	Concrete cost
PKW	Base/mass	$600	$117,000
	Weir and overhangs/Reinforced	$1000	$75,000
	Slab and training walls/Reinforced	$800	$136,000
	Total	N/A	$328,000
Labyrinth weir	Slabs/Reinforced	$700	$182,000
	Weir and training walls/Reinforced	$800	$348,000
	Total	N/A	$530,000

The PKW development achieved a considerable increase in discharge compared to straight weirs and the labyrinth weir. This increased discharge is achieved by using a considerable amount of additional concrete, reflected by the increased length ratio (L/W).

The objective of this study is to combine the geometric attributes from both labyrinth and PKW's to achieve an optimum increase in discharge capacity. The study aims to provide a more innovative arrangement in order to reduce the amount of concrete used reflected by a lower length ratio (L/W). This new option will aim to provide an efficient and economical solution for new and existing dams. The methodology used to achieve this is explained in detail in Chapter 3.

3 METHODOLOGY

As discussed in Chapter 2, this chapter covers the details of the optimal design that this study is aimed at producing. This optimal design takes geometric attributes from both labyrinth and PKW's. In Chapter 1, a major part of the discussion covered the geometric parameters of PKW's and labyrinth spillways that improved the discharge capacity and the value of the discharge coefficient. Many geometric parameters were mentioned and much work has been completed showing the effects of these parameters. This study aims at using just a few of those parameters and varying them with a combined design of PKW and labyrinth to see the hydraulic effects and economic benefit of such a design.

Some of the main geometric parameters mentioned earlier were the height of the weir (P), wall thickness (t_w), transversal length (B), overall width (W), inlet and outlet channel widths (W_{in} and W_{out}), crest shape, maximum height of the PKW walls (P_m) and the effective crest length (L) of the weir (see Figs. 2.4, 2.6 &2.7).

This study covers a range of layouts in systematic variation of parameters: W/P_m, B/P_m and upstream inlet width (W_{in}). The P_m value works as a pivot point for the footprint of the structure and also defines most of the geometry of the structure according to the optimal design proposed by Lempérière (2011).

Thirty five physical models were built and tested at the Pretoria West Hydraulics Laboratory of the DWS (Department of Water and Sanitation) (Table 3.1). The designs were set up based on the hypothesis that W and B values are limiting factors in designing PKW's and labyrinth weirs. Particularly because the B value is limiting structurally due to the overhangs and the W value is limiting because of the standard jointing found in dams and the limiting width of some spillways. The designs were chosen assuming that there was potential for tapering a PKW walls and that this taper would result in a combined PKW and labyrinth weir. The taper of each model set was varied with a limitation on the taper becoming completely triangular (see Fig. 3.1), this was done by keeping the effective inlet width constant for all models. Therefore, the approach was to have three sets of models, each model set having an established W ratio and within each model set, three B values varied for the established W value. Within these model sets, the potential for taper was tested by having standard PKW designs as well as tapered designs for the established W and varying B values.

The ultimate aim for having these different model sets was to have a table with the different W and B values and using these values, a designer could decide on whether to use a tapered design or a PKW based on costs, C_d and the limitation of W and B.

The first two models were large scale models (L1 and L2) of PKW layout that were built in order to test the sensitivity of the PKW design to the wall thickness (t_w). These models had singular and double wall thickness, i.e. P_m= 6t_w and P_m= 12t_w, with t_w = 36 mm and t_w = 18 mm resulting in a constant P_m = 216 mm.

The remaining thirty three models had a wall thickness (t_w) of 18 mm with P_m = 8t_w, resulting in a P_m value of 144 mm. These were built in three sets of eleven models each with each set having a different total width (W) and three transversal lengths (B). Fifteen of these models reflected PKW's with a rectangular wall layout. These models are referred to as models A1 – A5, B1 – B5 and C1 – C5 in Table2.1. Of these fifteen models, six were tested for varying inlet widths (W_{in} (PKW)) (see Fig. 3.1), i.e. models A2, A4, B2, B4, C2 and C4, while the rest were kept within the limits of Lempérière's (2011) design where W_{in}(PKW)/W = 0.556. Eighteen of the models were combined labyrinth and PKW designs. These designs had tapered walls and were also tested for varying inlet widths (W_{in} (combined)), i.e. models A6 – A11, B6 – B11 and C6 – C11, while maintaining an effective inlet width ratio of $W_{in\ effective}$/W = 0.556 (see Fig. 3.1). The taper for the combined design models was also varied and is referred to as the inlet channel width proportion (α') in Table 3.1; this denotes the proportion by which the models inlet channel is widened from the standard rectangular form of the PKW to the tapered trapezoidal plan layout of the combined design. This was done to compare how wider inlet widths affected the discharge capacity of the weir. Therefor α' is directly linked to the W_{in}/W ratio.

The L/W ratios for all the models ranged between 2.5 and 6.0 with quarter round crest shapes. All thirty five models were tested for cases with and without roundings under the upstream overhang (Fig. 4.4).

In the cases for the combined design, the taper of the walls was limited due to the wall thickness and a constraint on the shape not becoming completely triangular (see Fig.3.1). The sectional view of the combined design remained the same as that of the standard PKW (see Fig. 2.6 in Chapter 2) and the plan view resembled that of a trapezoidal labyrinth weir.

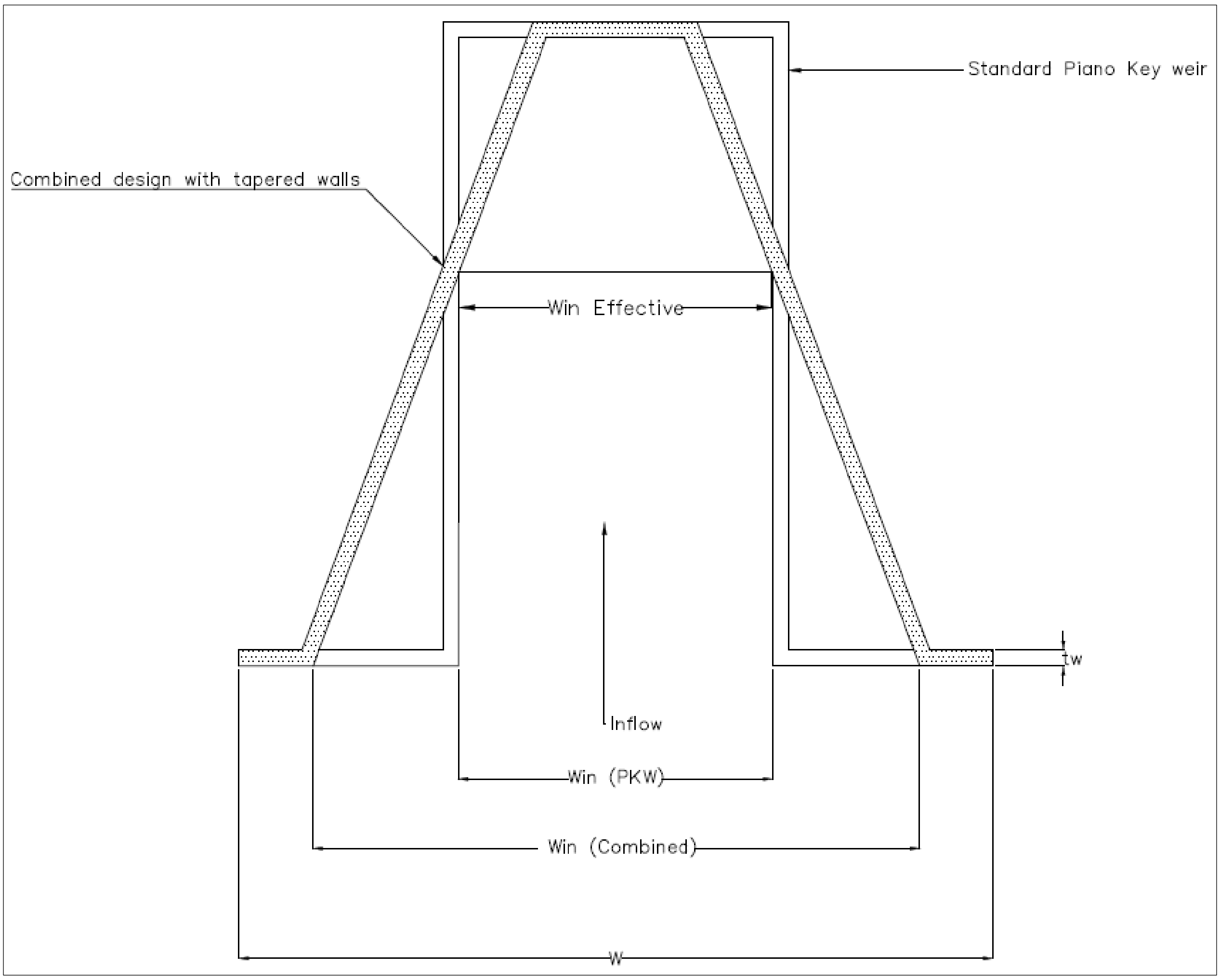

Figure 3.1: Parameters for standard PKW with rectangular walls and combined design with tapered walls

Head - discharge data were collected for each model configuration and plotted to compare the discharge capacity. The discharge coefficient (C_d'), for each model was also calculated according to Eq. 5.5and plotted to see how the coefficient varied for the different H_T/P_m values. C_d' data were collected for $0.5<H_T/P_m<1.0$ with higher values where required for increased data points.

3.1 Further modelling details

Table 3.1 represents the parameters of the different models that were built for the rectangular wall PKW's and the tapered wall combined design.

Table 3.1: Summary of models that were built and tested

Model	P_m (mm)	W/P_m	B (mm)	B/P_m	W_{in} (mm)	W (mm)	W_{in}/W	Inlet channel width proportion (α’)	t_w (mm)	L/W	Type
Large scale models											
L1	216	1.80	779	3.60	216	389	0.56	1.00	18	5.00	PKW
L2	216	1.80	779	3.60	216	389	0.55	1.00	36	5.00	PKW
Model set A											
A1	144	1.80	432	3.00	144	259	0.56	1.00	18	4.34	PKW
A2	144	1.80	518	3.60	130	259	0.50	1.00	18	5.00	PKW
A3	144	1.80	518	3.60	144	259	0.56	1.00	18	5.00	PKW
A4	144	1.80	518	3.60	162	259	0.62	1.00	18	5.00	PKW
A5	144	1.80	605	4.20	144	259	0.56	1.00	18	5.67	PKW
A6	144	1.80	432	3.00	173	259	0.67	1.20	18	4.13	Combined
A7	144	1.80	518	3.60	173	259	0.67	1.20	18	4.79	Combined
A8	144	1.80	605	4.20	173	259	0.67	1.20	18	5.46	Combined
A9	144	1.80	432	3.00	209	259	0.81	1.45	18	3.90	Combined
A10	144	1.80	518	3.60	209	259	0.81	1.45	18	4.54	Combined
A11	144	1.80	605	4.20	209	259	0.81	1.45	18	5.21	Combined
Model set B											
B1	144	2.40	432	3.00	192	346	0.56	1.00	18	3.50	PKW
B2	144	2.40	518	3.60	173	346	0.50	1.00	18	3.99	PKW
B3	144	2.40	518	3.60	192	346	0.56	1.00	18	3.99	PKW
B4	144	2.40	518	3.60	216	346	0.62	1.00	18	3.99	PKW
B5	144	2.40	605	4.20	192	346	0.56	1.00	18	4.50	PKW
B6	144	2.40	432	3.00	259	346	0.75	1.35	18	3.16	Combined
B7	144	2.40	518	3.60	259	346	0.75	1.35	18	3.65	Combined
B8	144	2.40	605	4.20	259	346	0.75	1.35	18	4.14	Combined
B9	144	2.40	432	3.00	298	346	0.86	1.55	18	2.98	Combined
B10	144	2.40	518	3.60	298	346	0.86	1.55	18	3.46	Combined
B11	144	2.40	605	4.20	298	346	0.86	1.55	18	3.95	Combined
Model set C											
C1	144	3.00	432	3.00	240	432	0.56	1.00	18	3.00	PKW

C2	144	3.00	518	3.60	216	432	0.50	1.00	18	3.40	PKW
C3	144	3.00	518	3.60	240	432	0.56	1.00	18	3.40	PKW
C4	144	3.00	518	3.60	270	432	0.62	1.00	18	3.40	PKW
C5	144	3.00	605	4.20	240	432	0.56	1.00	18	3.80	PKW
C6	144	3.00	432	3.00	348	432	0.81	1.45	18	2.58	Combined
C7	144	3.00	518	3.60	348	432	0.81	1.45	18	2.97	Combined
C8	144	3.00	605	4.20	348	432	0.81	1.45	18	3.36	Combined
C9	144	3.00	432	3.00	384	432	0.89	1.60	18	2.47	Combined
C10	144	3.00	518	3.60	384	432	0.89	1.60	18	2.84	Combined
C11	144	3.00	605	4.20	384	432	0.89	1.60	18	3.23	Combined

The inlet channel width proportion is explained as follows:

Figure 3.1 shows the W_{in} for a PKW and a combined design. The inlet channel width proportion refers to the opening or widening of W_{in}. If the inlet channel width proportion is 1 it means that there is 0% widening and the design has parallel walls. If the inlet channel width proportion is 1.20 or 1.45 it means that W_{in} is made wider by 20% or 45% respectively (see Figs. 3.2 &3.3).

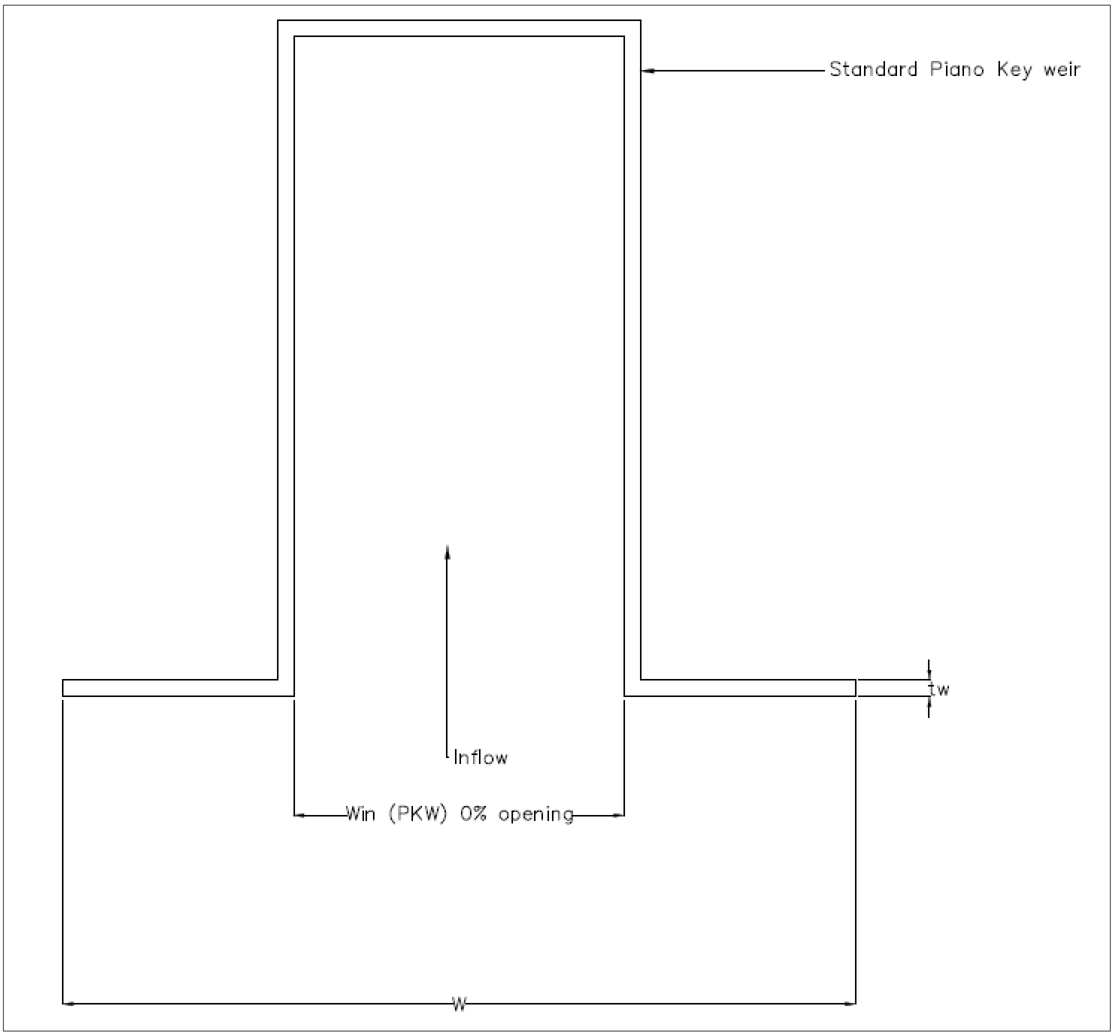

Figure 3.2: Inlet channel width proportion shown for PKW with 0% opening of W_{in}

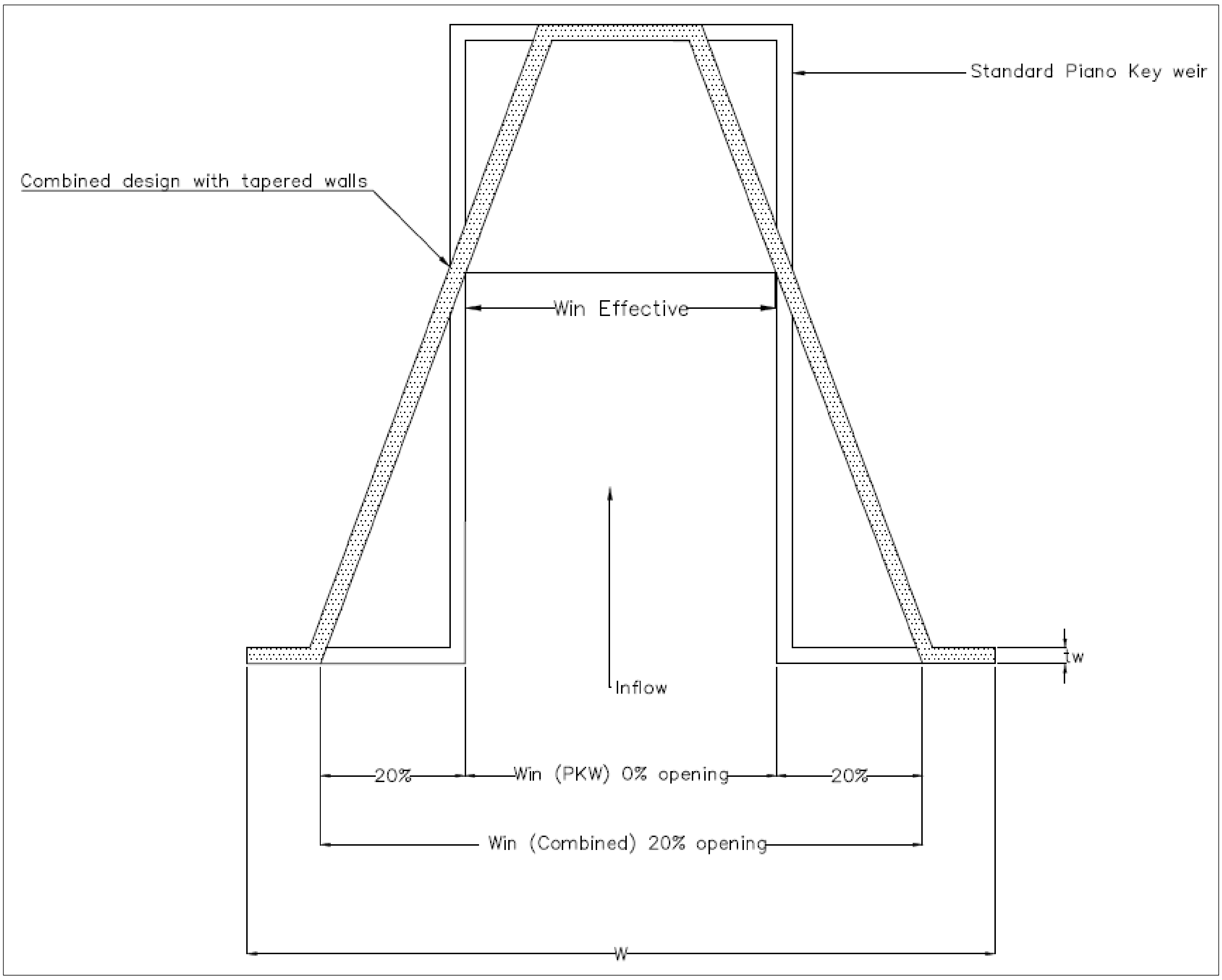

Figure 3.3: Inlet channel width proportion shown for a combined design with 20% opening of W_{in}

4 EXPERIMENTAL SETUP AND PROCEDURE

4.1 Test facility and experimental setup

One facility within the hydraulics laboratory was used for the physical modelling. This facility was in the form of a rectangular flume 2.5m in length, 1.3m in depth with varying widths (389 mm, 259 mm, 346 mm and 432 mm) based on the models that were tested. Water enters the flume through a headbox followed by a baffle wall (to improve approach flow uniformity). Two stilling wells were hydraulically connected to the flume and equipped with point gauges which were used to measure the upstream water surface elevations (H) at a distance of 0.5m from the side of the flume (see Fig. 4.2). Two were used in order to check for accuracy in the readings that were taken.

Figure 4.1: Stilling wells installed just next to flume to measure water surface elevations in flume

The water supply at the hydraulics laboratory is pumped through a series of pipes to the supply line of the flume with a flow capacity of approximately 140 l/s. The flow meters were calibrated for the flume using a standard crump weir in the flume to obtain a flow calibration factor of approximately 1.12. This factor is multiplied by the observed flow reading (Q) to get more accurate results.

An adjustable base was installed in the flume to facilitate easy installation, levelling and removal of each weir (Fig. 4.3). Weirs were attached to the base using screws and sealed off using silicon and other sealants. An overview of the weir setup is shown in Fig. 4.2.

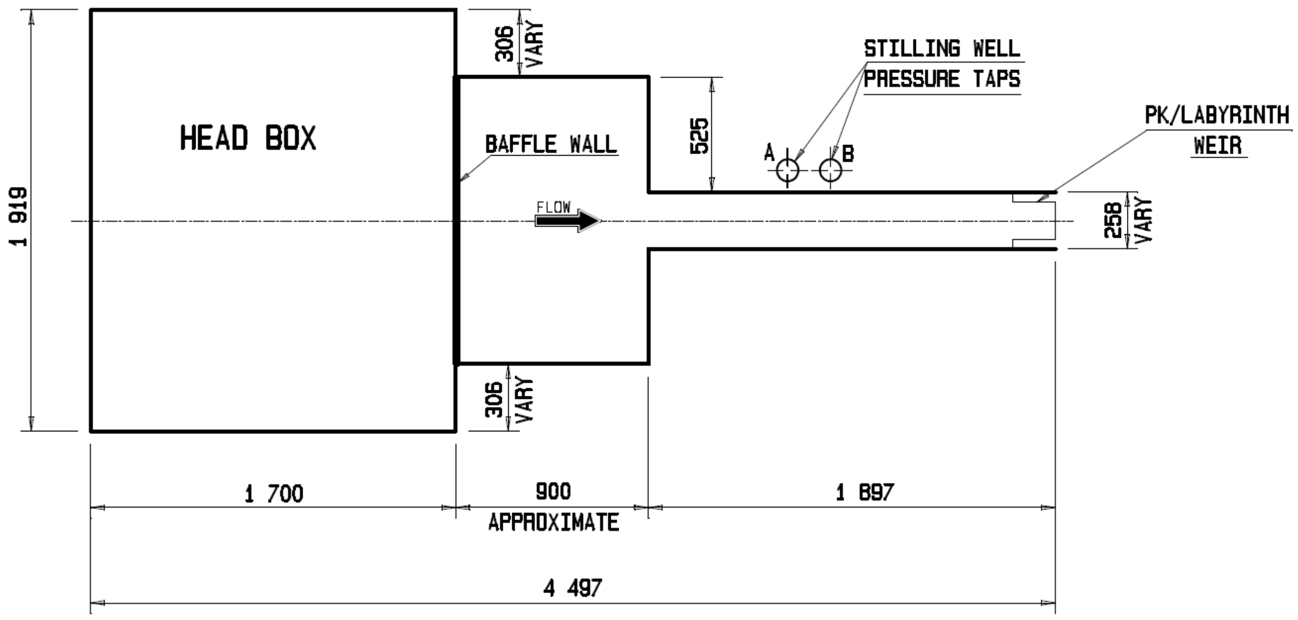

Figure 4.2: Testing facility plan layout (measurements in mm)

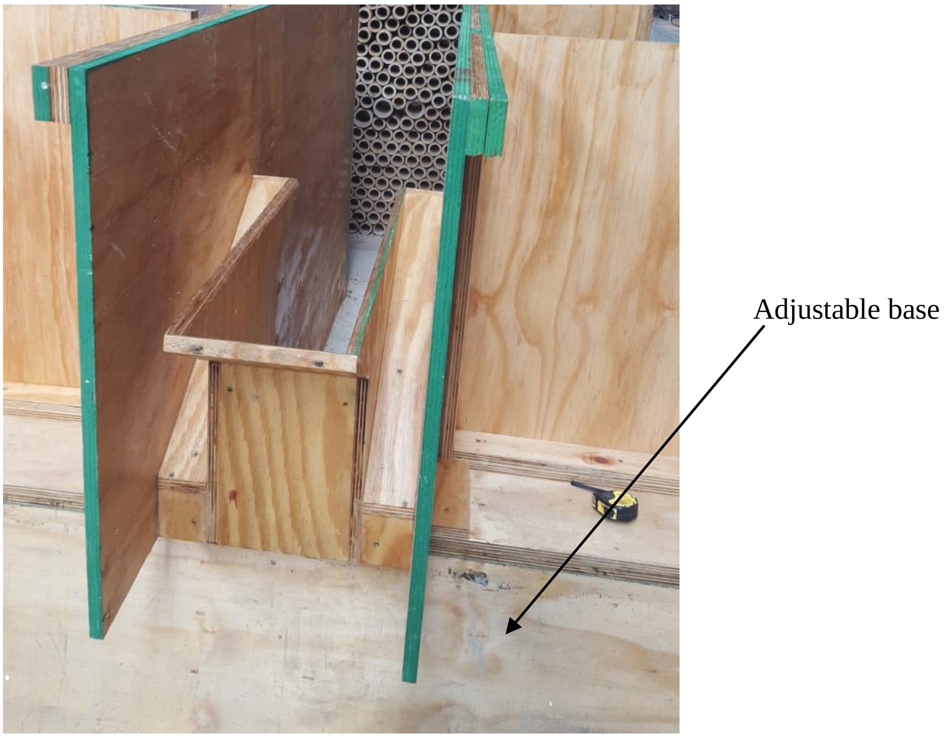

Figure 4.3: Front view of testing facility showing adjustable base

4.2 Physical models

Data from thirty five laboratory – scale PKW and combined weir models were measured and analysed in this study (two large scale models and thirty three parametric models). Standard and non-standard PKW designs were tested along with new geometric layouts of combined trapezoidal labyrinth and PKW designs. These models had different geometric configurations in terms of W_{in}/W_{out} ratios, Lateral/transversal length (B) and weir shape.

All thirty five laboratory scale weirs were fabricated using 18 mm thick wooden planks. Only one cycle of each model was built featuring a quarter round crest shape. This was taken as a conservative approach. These models were tested with and without roundings which were installed under the upstream overhang. These roundings were not built –in as suggested by Lempérière (2011), but rather built separately and added on as shown in Fig. 4.4. All model features were fabricated using wood and various tools with roundings being milled on a machine.

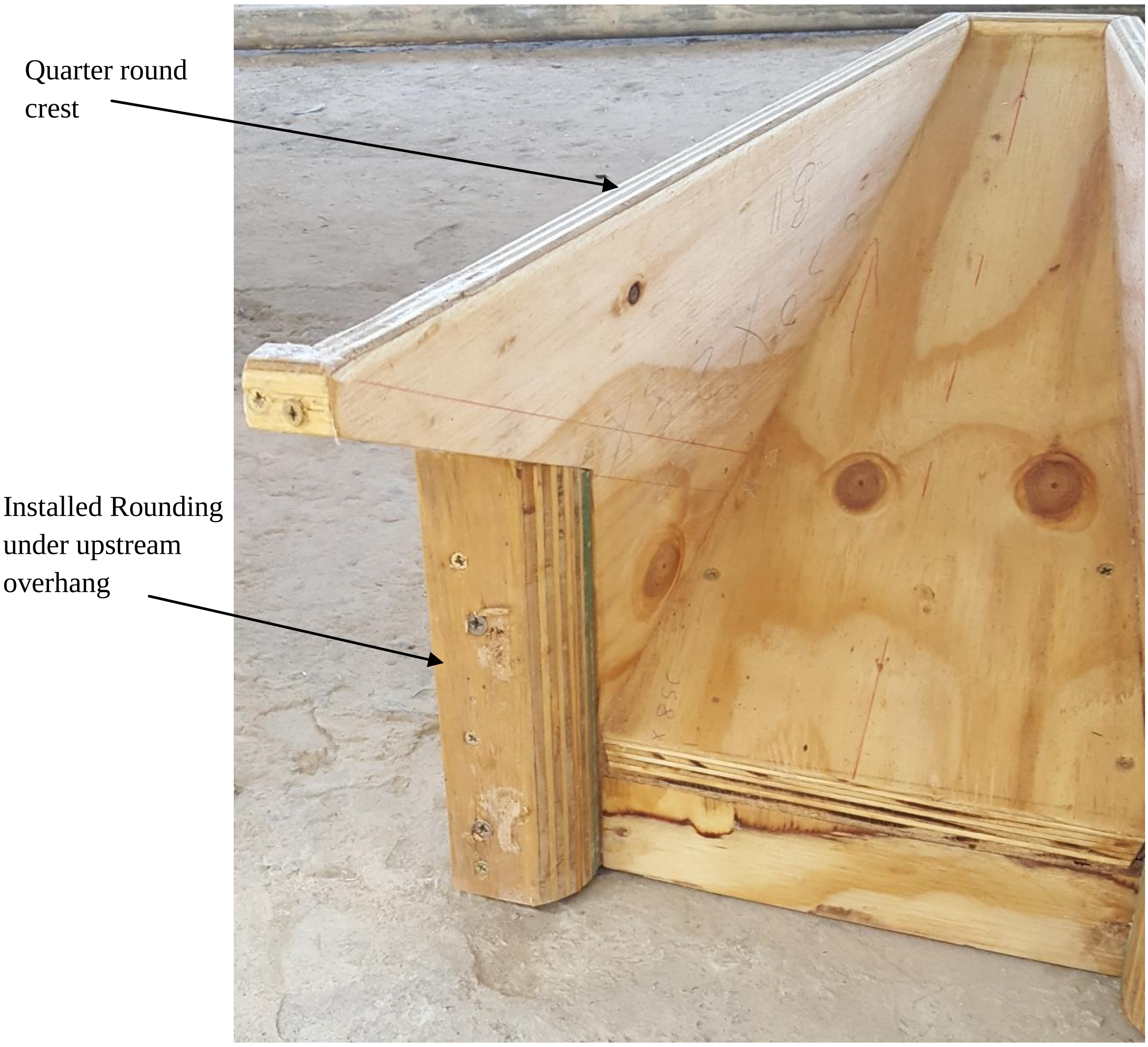

Figure 4.4: Roundings under upstream overhang

4.3 Testing procedure

After construction of each model, the as-built weir dimensions were measured to ensure that they complied with the design. The weirs were then installed in the flume and sealed off. After the sealant had dried, a leak test was performed to ensure that all joints were watertight. A survey was then conducted to ensure the crest elevation reference level. This was done by measuring reference levels at approximately 6 different locations on the weir crest as well as the relative levels of each stilling well and the channel of the flume. A zero reading was taken on the point gauge of the stilling well before any water was filled in it and the flume was empty. This value was then added to the difference in reference levels of the stilling wells and the weir crest to get the zero point of each stilling well and the relative crest elevation.

All models were tested for flows ranging between 100 l/s and 20 l/s. Data were collected manually measuring the H value in the stilling wells point gauge after the water level was allowed to stabilize for approximately 5-7 minutes. A minimum of three point gauge readings were taken consecutively for each flow rate to ensure that stable steady state flow conditions upstream of the weir were achieved; if the three readings were not in agreement with each other, the flow was allowed to stabilize for a longer period of time (longer stabilization times were required for higher flow rates). Data were collected for each model in two sets, one for the model with roundings under the upstream overhang and the other for the model without roundings under the upstream overhang. An excel spreadsheet was then used to calculate H_T, q, C and C_d' using the equations from Chapter 5.

5 COMPARISON OF EQUATIONS FOR LINEAR AND NON-LINEAR SPILLWAYS

In order to compare linear and non-linear spillways, it is important to compare the equations for the two different spillway types. Eq. (5.1) represents the unit discharge of the standard linear weir equation.

$$q = C_d \frac{2}{3} \sqrt{2g} H_T^{\frac{3}{2}} \tag{5.1}$$

Where: q – Unit discharge ($\frac{Q}{L}$) ($m^3/s/m$)

Eq. (5.2) represents the unit discharge of a PKW. For the purpose of this study the total head (H_T) was used when calculating q for the PKW.

$$q = C\sqrt{P_m} H_T \tag{5.2}$$

Where: q – unit flow ($\frac{Q}{W}$) ($m^3/s/m$)

C – Constant representative of discharge coefficient = 4.3

The form of Eq. (5.2) ($q \propto H_T$) is different from the standard weir equation (Eq. (5.1)) ($q \propto H_T^{1.5}$). In Eq. (5.2), the constant (C = 4.3), which is representative of a discharge coefficient inclusive of $\sqrt{2g}$, remains constant as opposed to the varying discharge coefficient (C_d) of the standard weir equation(Eq. (5.1)).

In order to change the C value in Eq. (5.2) so that it is dimensionless like the C_d value in Eq. 5.1, Eq. 5.3 was derived.

$$q = C_d' \sqrt{2g} \sqrt{P_m} H_T \tag{5.3}$$

The C – value in Eq. (5.2) then becomes:

$$C = C_d' \sqrt{2g} \tag{5.4}$$

Therefore if C = 4.3, C_d’ = 0.97, which is a dimensionless variant that does not stay constant for varying P_m and H_T values. The calculation of discharge coefficient (C_d’) in this study made use of Eq. 5.2 in its dimensionless form and is simplified as follows:

$$C_d{}' = \frac{q}{\sqrt{2g}\sqrt{P_m}H_T} \tag{5.5}$$

Since $H_T = h + \frac{v^2}{2g}$; the equation then becomes:

$$C_d{}' = \frac{q}{\sqrt{2g}\sqrt{P_m}\,(h + \frac{v^2}{2g})} \tag{5.6}$$

Eq. (5.5) gives the opportunity to calculate different C_d' values based on different H_T and P_m measurements.

Calculation of the discharge coefficient (C_d) from the standard weir equation can be manipulated as follows:

$$C_d = \frac{3q}{2\sqrt{2g}H_T^{\frac{3}{2}}} \tag{5.7}$$

From Eq.'s (5.5) and (5.7) it can be seen that in order to change or improve on the discharge coefficient for both the standard linear weir and the PKW, the value of H_T is important.

A reduction in H_T will result in higher C_d' values for the PKW. One method for reducing the H_T value is to lower the velocities in order to get a reduction in energy head ($\frac{v^2}{2g}$). The combined design proposed in this study aimed at achieving this. The P_m value also plays an important role in calculating C_d' for the PKW.

In Chapter 1, many geometric parameters were mentioned which have an effect on the discharge coefficient (C_d') of the PKW. As a result of the study at hand the discharge coefficient (C_d') of a PKW or combined PKW and labyrinth spillway has shown to be a function of the following parameters:

$$C_d' = f\ (\frac{B}{P_m};\frac{W}{P_m};\frac{L}{W};\frac{H_T}{P_m};\frac{W_{in}}{W};\alpha') \tag{5.8}$$

In this study, Eq. (5.6) was used for the calculation of C_d'. This was done using measured H_T values and known P_m values. The value of C = 4.3, recommended by Lempérière (2011), was based on a specific geometry and therefore could not be used for the changes in geometry of the physical models in this study. Using Eq. (5.6) gave a more constant C_d' compared to the standard linear equation that produces large variations in the discharge coefficient (C_d). The main difference for this resides in the power function of the H_T value. In the standard linear equation $H_T^{1.5}$ is used whereas in the new equation developed by Lempérière (2011), H_T is used. Many previous studies on PKW's and labyrinths have used the standard weir equation with $H_T^{1.5}$ and the results when compared to those from this study show that for the non – linear spillways Lempérière's (2011) equation (Eq. (5.2)) is more appropriate. The reason for using the equation with $H_T$instead of $H_T^{1.5}$ is because with the water flowing over the non – linear spillway, as the h (water level) drops, C_d' tends to become more constant and H_T moves away from $H_T^{1.5}$ to H_T. The difference is velocity change, as the water starts to flow better over the spillway.

Chapter 6 discusses these results in more detail.

6 EXPERIMENTAL RESULTS

6.1 Large scale models

Many studies have indicated the geometrical parameters and dimensions required for an optimal design of PKW's and labyrinths; however most studies have not mentioned the wall thickness (t_w) required for such optimal designs.

In the initial tests conducted for this study, two large scale models were built and tested in order to determine how the wall thickness of the model affects its discharge capacity and discharge coefficient (C_d') (Eq. (5.6)). The details of these models are shown in Table 3.1 in Chapter 3.

Both these models were tested with and without roundings under the upstream overhang. Results show that the upstream rounding does improve the discharge coefficient (C_d') and that the thickness of the walls does affect the discharge coefficient and hydraulic efficiency of the weir. C_d' data were determined for $0.5< H_T/P_m<1.0$.

The results from these tests are shown in Figs 6.1 and 6.2. Figure6.1 shows the discharge coefficient for various H_T/P_m values. C_d' becomes constant as the H_T/P_m value increases. This is due to the equation that was used to calculate C_d' as explained in Chapter 5. These graphs will look different to those presented in previous studies due to the difference in the equations used (see Fig.6.2). Figure6.2 shows the C_d vs H_T/P_m curve for the same data presented in Fig. 6.1 using Eq. (5.7). This was done for comparison purposes to show how the different equations used can affect the results. The results show a parabolic trend between C_d and H_T/P_m compared to the results of in Fig. 6.1 that uses Eq. (5.2) and follow a linear trend.

In a study by Tullis et al. (1995), the results for a labyrinth spillway with different sidewall angles (α) showed a similar trend to that in Fig. 6.2. Fig 6.3 shows these results and indicates that Eq. (5.7) was used to calculate C_d.

The difference in the discharge coefficient (C_d') with and without roundings is about 0.1. This shows that for the PKW design the roundings don't have a very significant effect but they do bring about a small improvement and an increase in the C_d' value.

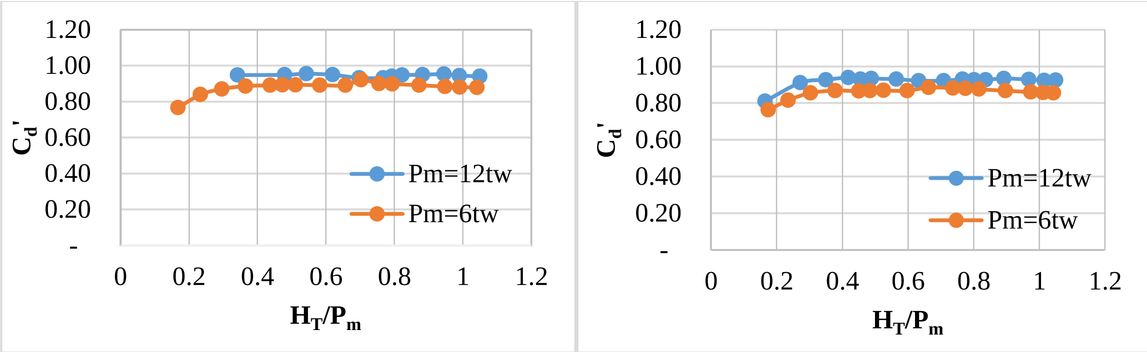

Figure 6.1: C_d' vs H_T/P_m for large scale models with roundings (left) and without roundings (right)

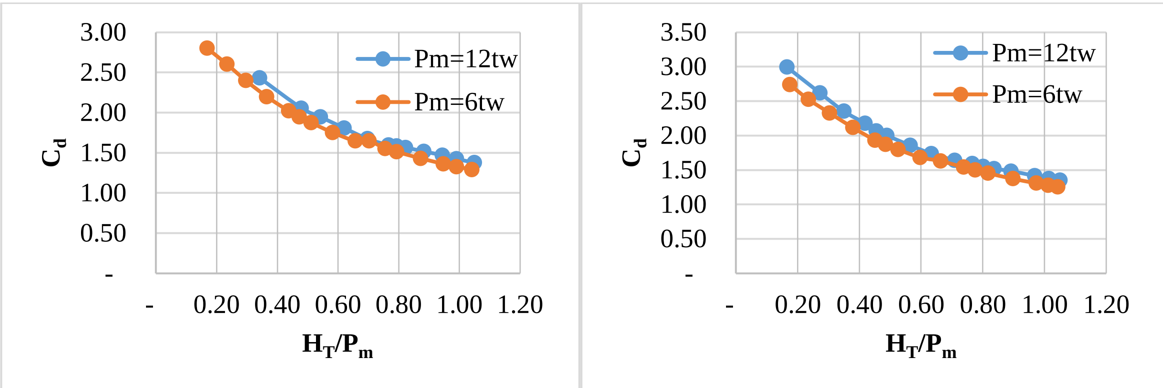

Figure 6.2: C_d vs H_T/P_m for large scale models with roundings (left) and without roundings(right) using Eq.(5.7)

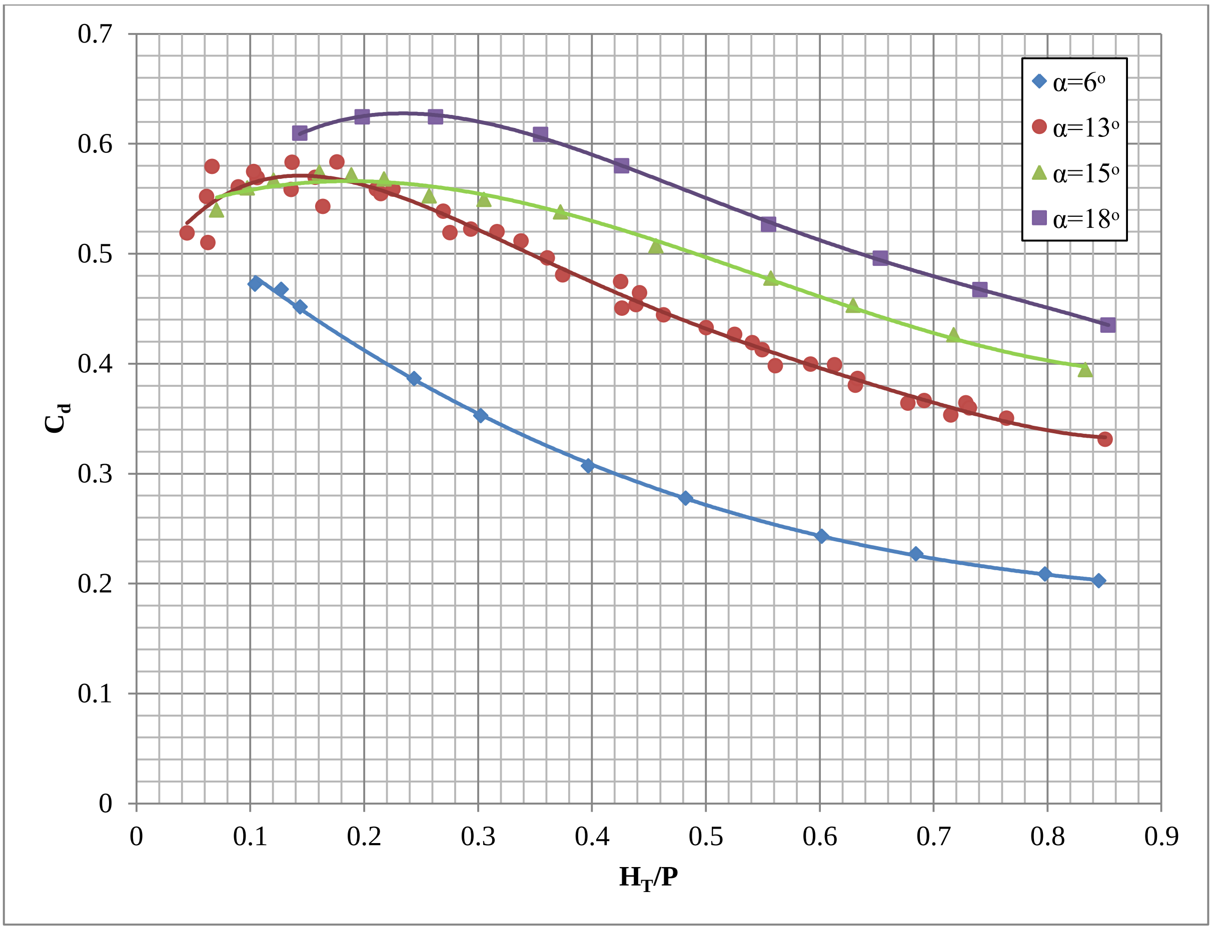

Figure 6.3: C_d vs H_T/P Results from Tullis et al (1995).

Figure6.4 shows the discharge rating curve for the two models. These indicate the discharge capacity of the weirs and show the hydraulic efficiency. This is shown in getting a higher unit flow (q) at a lower head (H_T). Looking at Fig. 6.4, if a unit flow rate of 0.4 $m^3/s/m$ is considered, this gives a total head (H_T) of 0.200 for the case where P_m =12t_w and 0.225 for the case where P_m = 6t_w. The percentage difference in H_T over the range of q is5% between P_m = 6t_w and P_m = 12t_w. The difference between the models with and without roundings is small. The percentage difference in $H_T$between the models with and without roundings is 1% over the range of q.

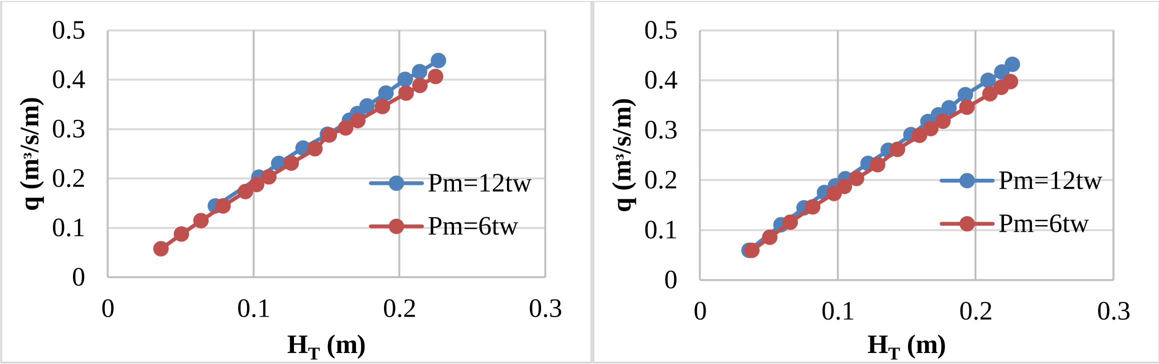

Figure 6.4: q vs H_T for large scale models with roundings (left) and without roundings (right)

From these results it is shown that the thickness of the walls can be an important geometric feature when designing PKW type spillways. Therefore, for the models that followed, a thickness (t_w) where $P_m = 8t_w$ was chosen as it lies between $6t_w$ and $12t_w$. Since P_m was kept constant for the following thirty three models, t_w stayed constant with a value of 18mm.

6.2 C_d' vs H_T/P_m

With the results from the large models displaying the importance of the wall thickness, a thickness of $t_w=P_m/8$ ($P_m=8t_w$) was then chosen for the model tests that followed. The following thirty three models were split into three sets of eleven models each as indicated in Chapter 3. Each set had a constant W/P_m ratio with different B/P_m, W_{in}/W and α' values. For models with the new combined design, the α' value determined the W_{in}/W value. C_d' data were calculated for $0.5<H_T/P_m<1.0$ and higher values were required for increased data points. The discharge coefficient (C_d') was calculated using Eq. (5.5). Data were collected for all models with and without roundings under the upstream overhang as mentioned in Chapter 3.

For the purpose of this study, the coefficient of discharge (C_d') was used as a measure of efficiency and calculated using Eq. (5.5). Each model set result has a few curves showing the variations in geometry. Each model has a particular α' value, W_{in}/W, B/P_mratio and W/P_m ratio. The figures in the following sections will comprise of different curves. These curves are representative of these changing parameters in each model.

6.2.1 Model set A

The first set of model data (models A1, A6 and A9) had a constant $W/P_m$and B/P_m values with varying W_{in}/W and α' values (see Table 3.1 in Chapter 3). The results from these model tests with and without roundings under the upstream overhang are shown in Figs. 6.5 and 6.6.

It can be seen from Figs. 6.5 and 6.6 that the maximum C_d' value for these models lies in the region where H_T/P_m is between 0.5 and 1. The variation in C_d' becomes smaller and more constant as H_T/P_m increases. The C_d' values for these three models lie in the region between 0.80 and 1.00 with model A1 exhibiting the highest C_d' value of 0.89 (no roundings) and 0.88 (with roundings).Model A1is a PKW design with α' = 1.00, B/P_m = 3.00 and W_{in}/W = 0.56. Model A9 shows the lowest C_d' values and is a combined design with α' = 1.45, B/P_m = 3.00 and W_{in}/W = 0.81.The difference between models A1 and A9 is that one is tapered while other is not, the α' and W_{in}/W ratios are different.

Model A6 sits in between A1 and A9 having the same B/P_m and W/P_m ratios but different α' and therefore different W_{in}/W ratios. Model A6 is also tapered. The C_d' values of models A6 and A9 are closer at low values of H_T/P_m

This experimental data set demonstrates how C_d' does not depend very strongly on H_T/P_m except at very small values. The vertical shift between each model of the experimental dataset is based on the changing α' and W_{in}/W parameters. The C_d' value changes based on these changes in geometry. This demonstrates the effect the various geometric parameters have on C_d'.

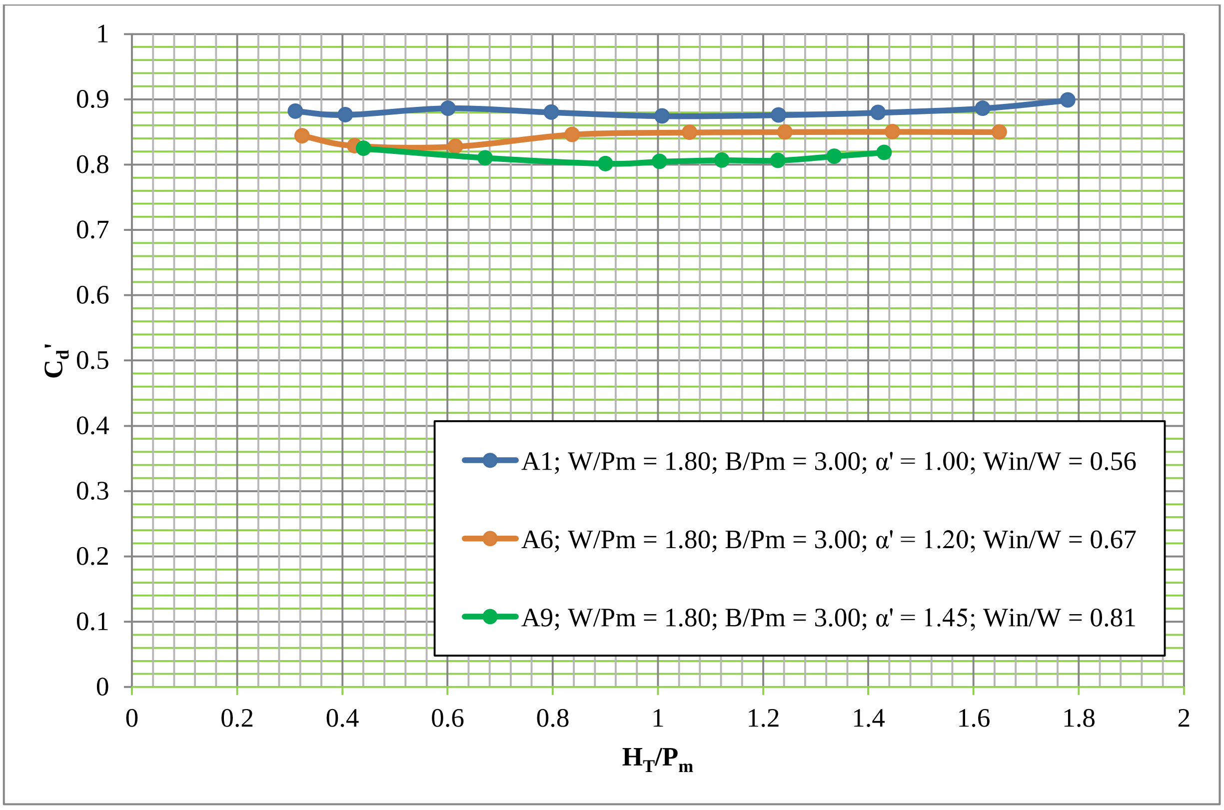

Figure 6.5: C_d'vs H_T/P_m for Models A1, A6 and A9 with roundings

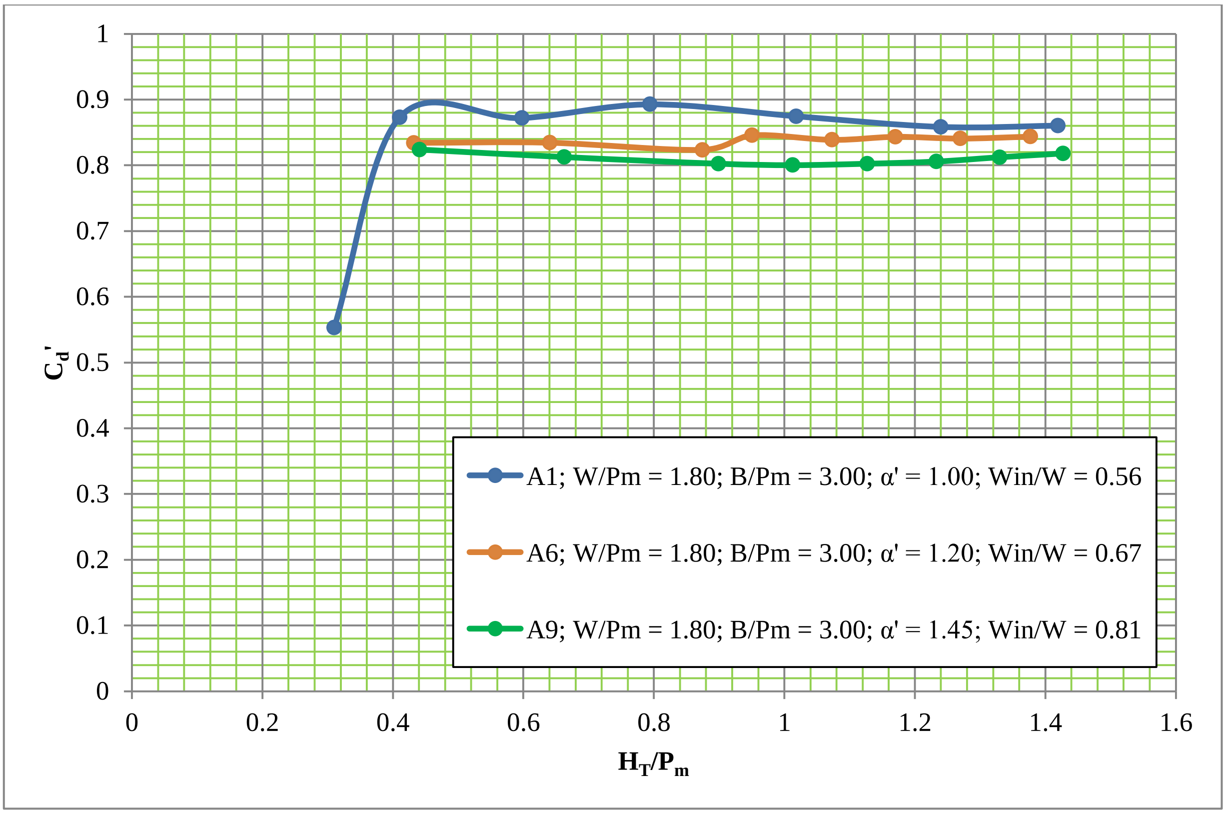

Figure 6.6: C_d' vs H_T/P_m for Models A1, A6 and A9 with no roundings

In a second set of results, with Models A2, A3, A4, A7 and A10, the B/Pm and W/Pm values were again constant with varying α' and W_{in}/W ratios. Similar to Figs 6.5 and 6.6, the results are shown in Figs 6.7 and 6.8.

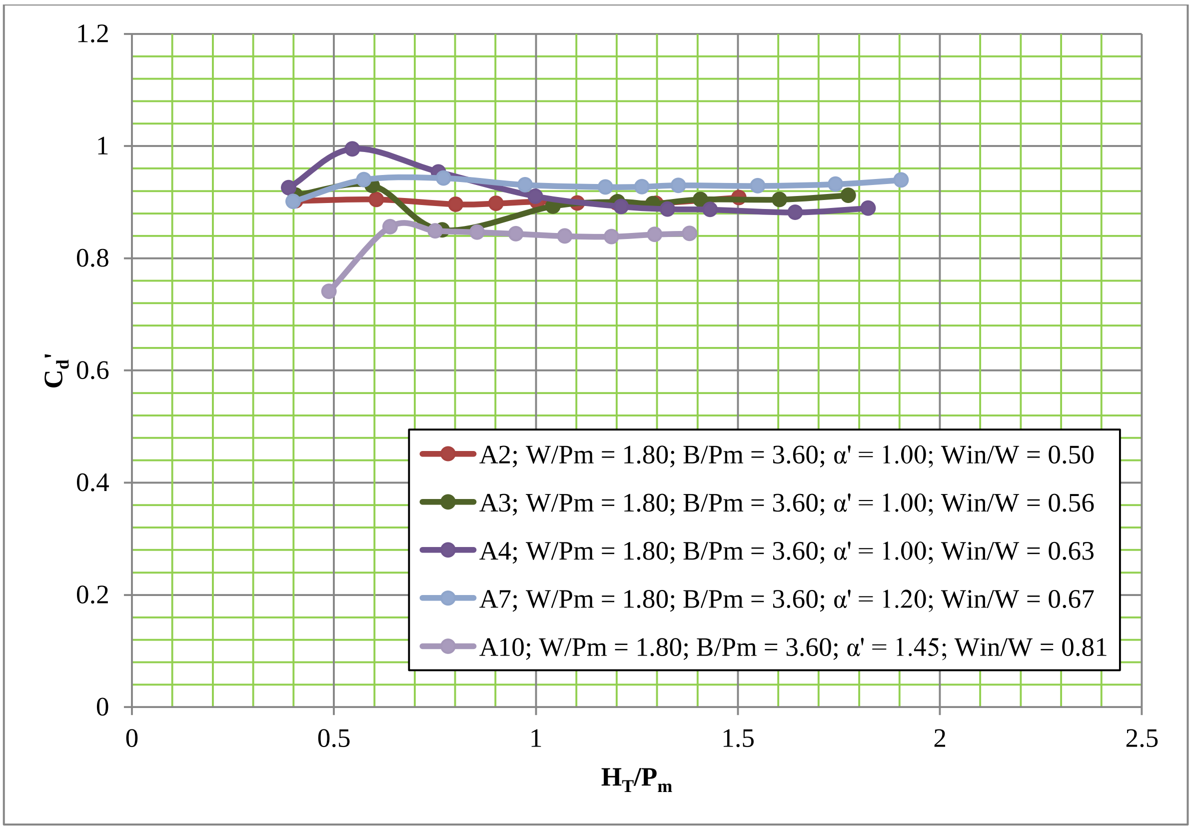

Figure 6.7: C_d' vs H_T/P_m for Models A2, A3, A4, A7 and A10 with roundings

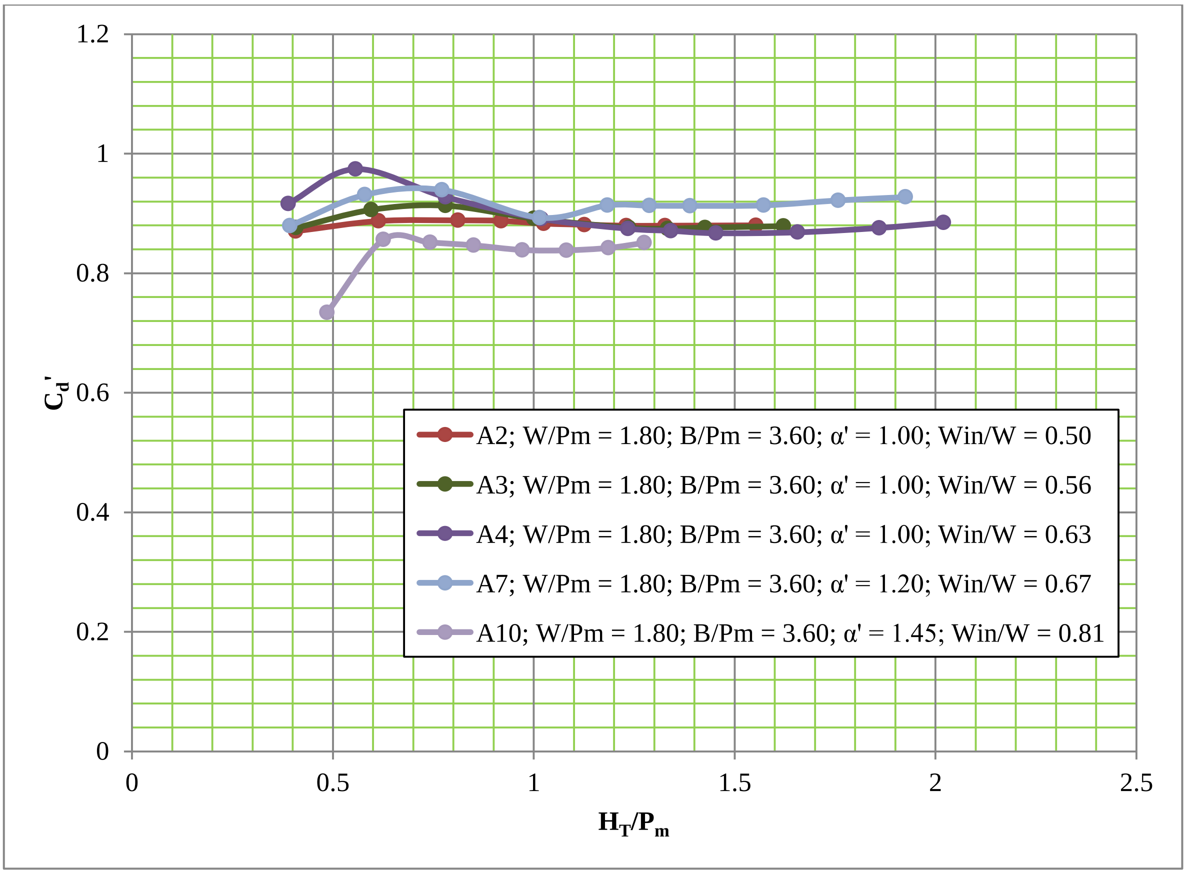

Figure 6.8: C_d' vs H_T/P_m for Models A2, A3, A4, A7 and A10 with no roundings

In Figs 6.7 and 6.8, Model A4 Exhibits the highest C_d' values with and without roundings at H_T/P_m = 0.55. Model A4 is a PKW design and has a α' value of 1.00 and a Win/W ratio of 0.63. This model has a wider inlet. At higher H_T/P_m values, it appears that model A7 displays the highest C_d' values of 0.93 (with roundings) and 0.92 (no roundings).

Model A3 was based on the optimal design recommended by Lempérière (2011). The maximum C_d'value achieved with this design was 0.93 (with roundings). This is different from the value attained by Lempérière (2011) of 0.97. This is possibly due to the fact that the roundings in this study were placed differently to that of Lempérière's (2011) design.

Model A10 shows the lowest C_d' values ranging between 0.84 and 0.85 for models with and without roundings. This is a combined design with α' = 1.45 and W_{in}/W = 0.81.

There are sudden descents in the graphs of models A3 and A7 in Figs 6.7 and 6.8 respectively. This can be due to experimental error during the testing of these models which is also an important factor to consider when doing physical modelling.

The last set of results are for models A5, A8 and A11. These results are shown in Figs 6.9 and 6.10. Figures 6.9 and 6.10 show the results with and without roundings respectively. It can be seen that models A5, A8 and A11 have C_d' values in close proximity at low values of H_T/P_m with greater deviation in these values at higher values of H_T/P_m. Model A8 has the highest C_d' value of 1.00 (with roundings) and 0.98 (without roundings). Model A8 is a combined design with W/P_m = 1.80, B/P_m = 4.20 and α' = 1.20.

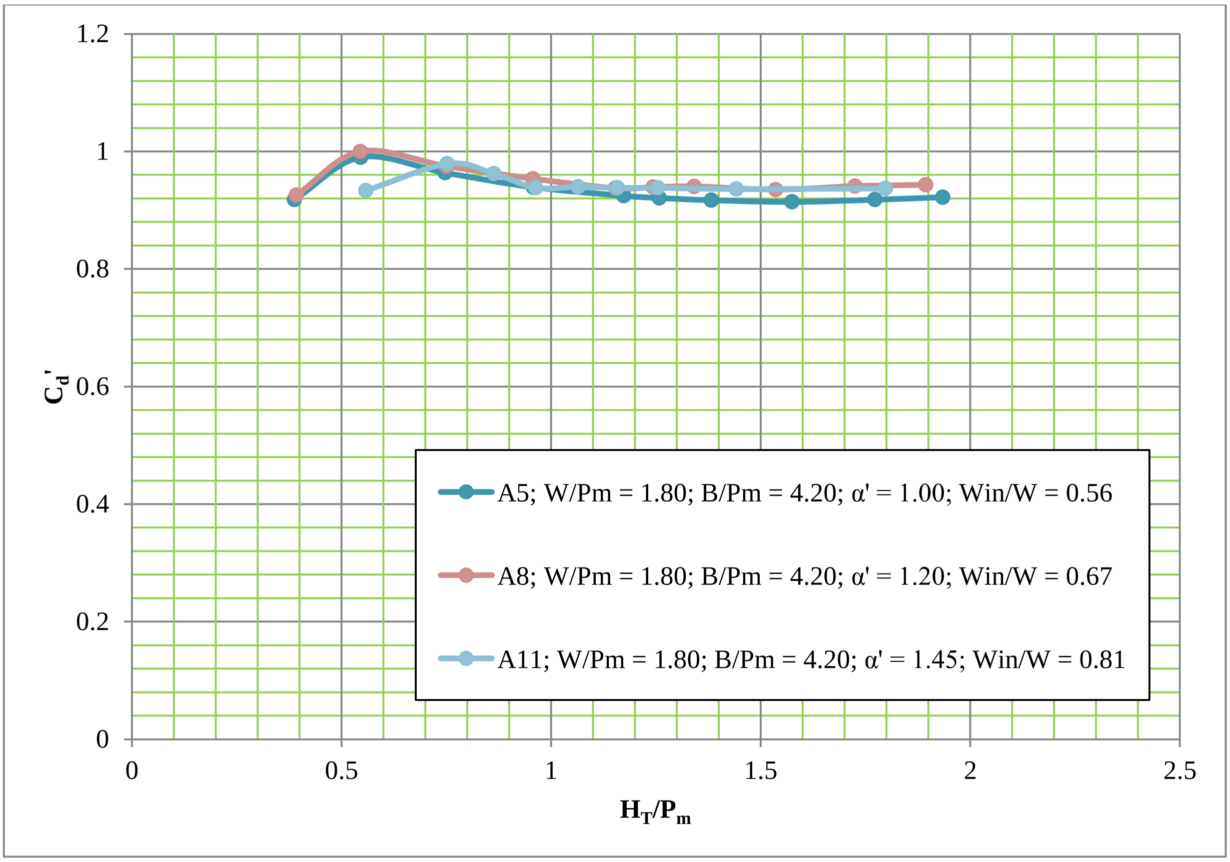

Figure 6.9: C_d' vs H_T/P_m for Models A5, A8 and A11 with roundings

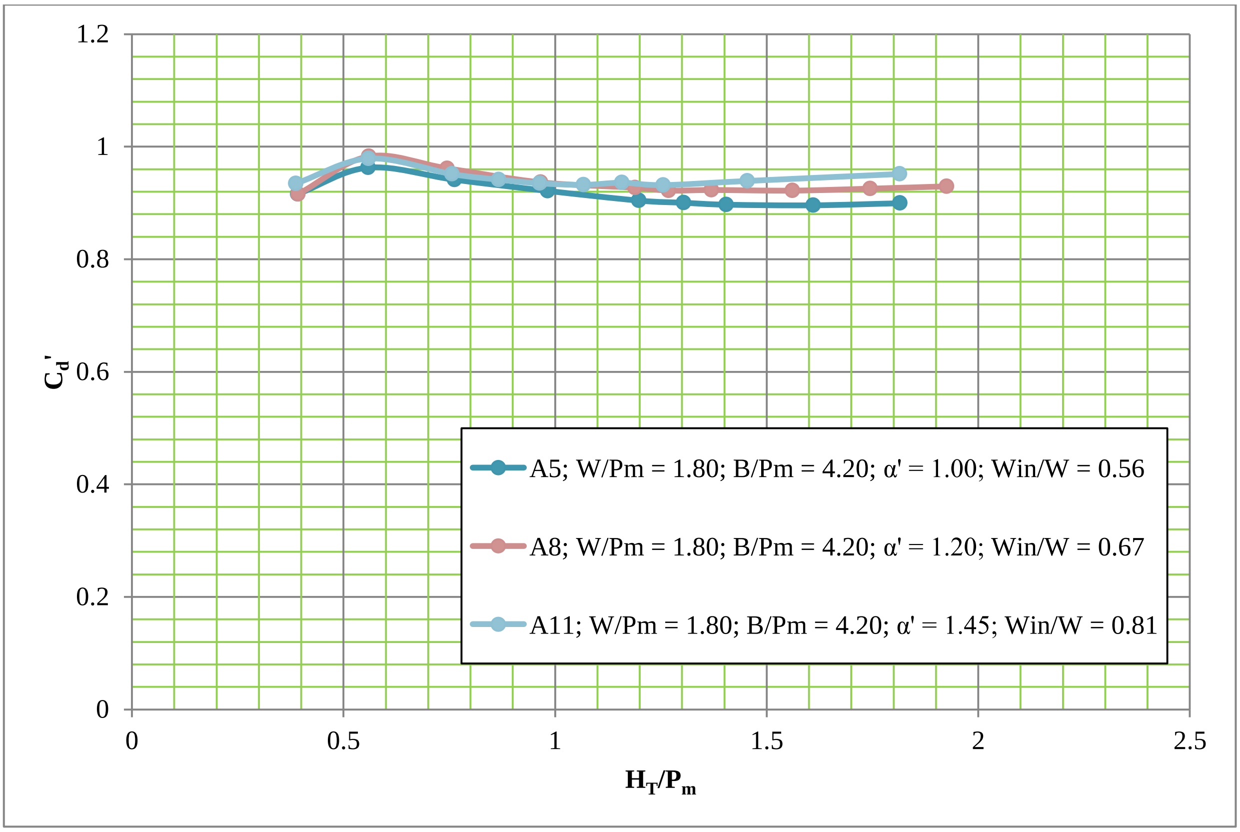

Figure 6.10: C_d' vs H_T/P_m for Models A5, A8 and A11 with no roundings

From the results of Figs 6.5 – 6.10 it can be seen that as B/Pm increases, the combined designs display higher C_d' values. However, it is only for models with low percentages of taper, i.e. α' = 1.20. This shows that changes in geometry do have an effect of C_d' and that there is potential for tapering. Where W/P_m is constant, increasing B/P_m would require a combined design as opposed to a standard PKW design.

6.2.2 Model set B

Model set B (B1-B11) had a constant but higher W/P_m value than model set A with varying B/P_m, α' and W_{in}/W values. The results from these tests are shown in Figs. 6.11 and 6.16.

Figures 6.11 and 6.12 show flatter curves than those in Figs. 6.5 and 6.6. There is less variation in the discharge coefficient(C_d') for models B1, B6 and B9. The C_d' value is constant in the H_T/P_m region between 0.50 and 1.00. The C_d' values for this model set lie in the region of 0.70 and 0.95. The model with the highest C_d' value is B1 with a value of 0.83 (no roundings) and 0.84(with roundings), this is a PKW design with parallel walls where α' = 1.00, B/P_m = 3.00 and W_{in}/W = 0.62. Model B9 has the lowest C_d' values, this is a combined design with α' = 1.55, B/P_m =3.00 and W_{in}/W = 0.86.

Results from models B1, B6 and B9in comparison with model set A show that increasing the overall channel width (W), resulting in a higher W/P_m ratio, can result in a more constant C_d', particularly for $0.5<H_T/P_m<1.0$ (see Figs.6.11 & 6.12).

The same conclusions can be made for Models B1, B6 and B9 as that of Models A1, A6 and A9 regarding the vertical shift between each model in the dataset. It can also be seen that C_d' does not depend strongly on H_T/P_m except at small values.

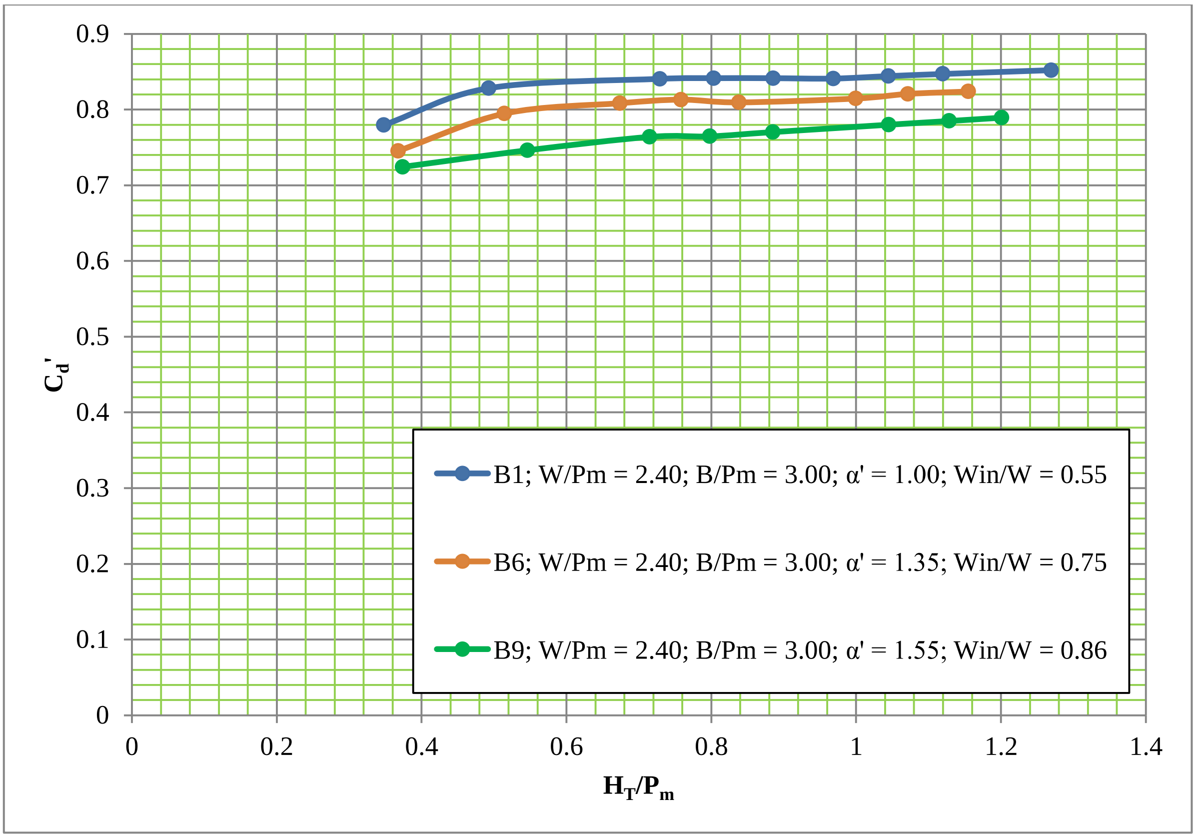

Figure 6.11: C_d' vs H_T/P_m for Models B1, B6 and B9 with roundings

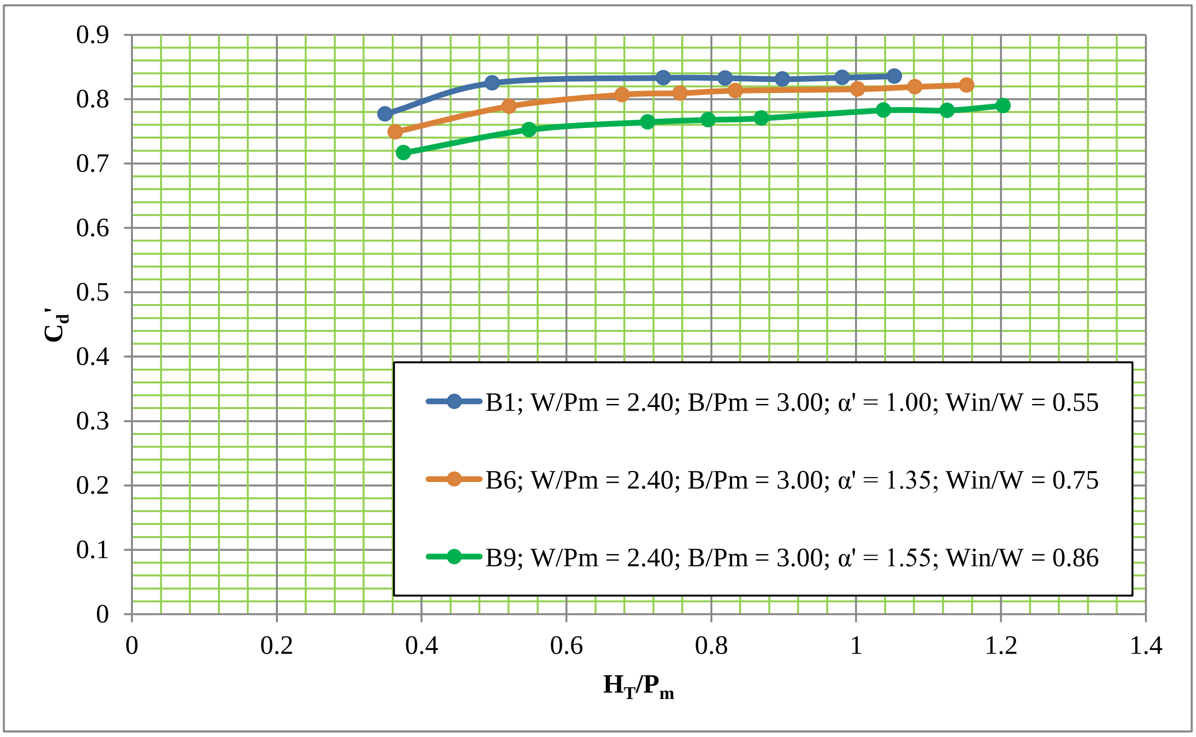

Figure 6.12: C_d' vs H_T/P_m for Models B1, B6 and B9 with no roundings

The second set of results comprises models B2, B3, B4, B7 and B10. These results are depicted in Figs 6.13 and 6.14. Once more it can be seen that model set B have much flatter curves that model set A. This could be due to the increase in W/P_m. From Figs 6.13 and 6.14, the C_d' values lie in the region between 0.75 and 1.00 with model B4 shows the highest C_d' value of 0.95 (with roundings) and 0.94 (with no roundings). This is a PKW design although it has a wider inlet channel than the standard designs.

At higher values of H_T/P_m, it seems the Cd' values get closer. Model B7 gets closer to the values of model B4 at H_T/P_m values greater than 1.2. Model B7 has a higher α' value of 1.35 than model A7.

Model B10, similar to Model A10 depicts the lowest Cd' values compare to the other models with the same W/P_m and B/P_m values. The only difference is the α' value of 1.55 and in turn the W_{in}/W ratio of 0.86.

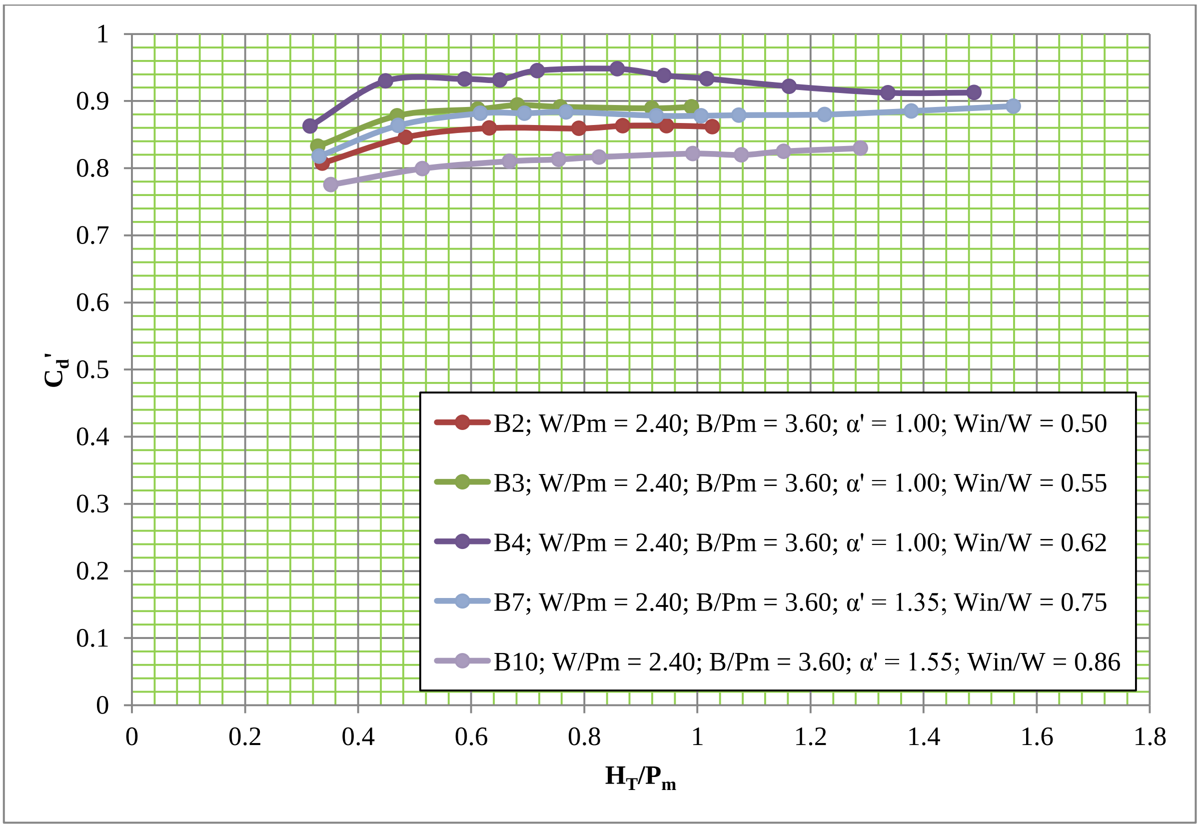

Figure 6.13: C_d' vs H_T/P_m for Models B2, B3, B4, B7 and B10 with roundings

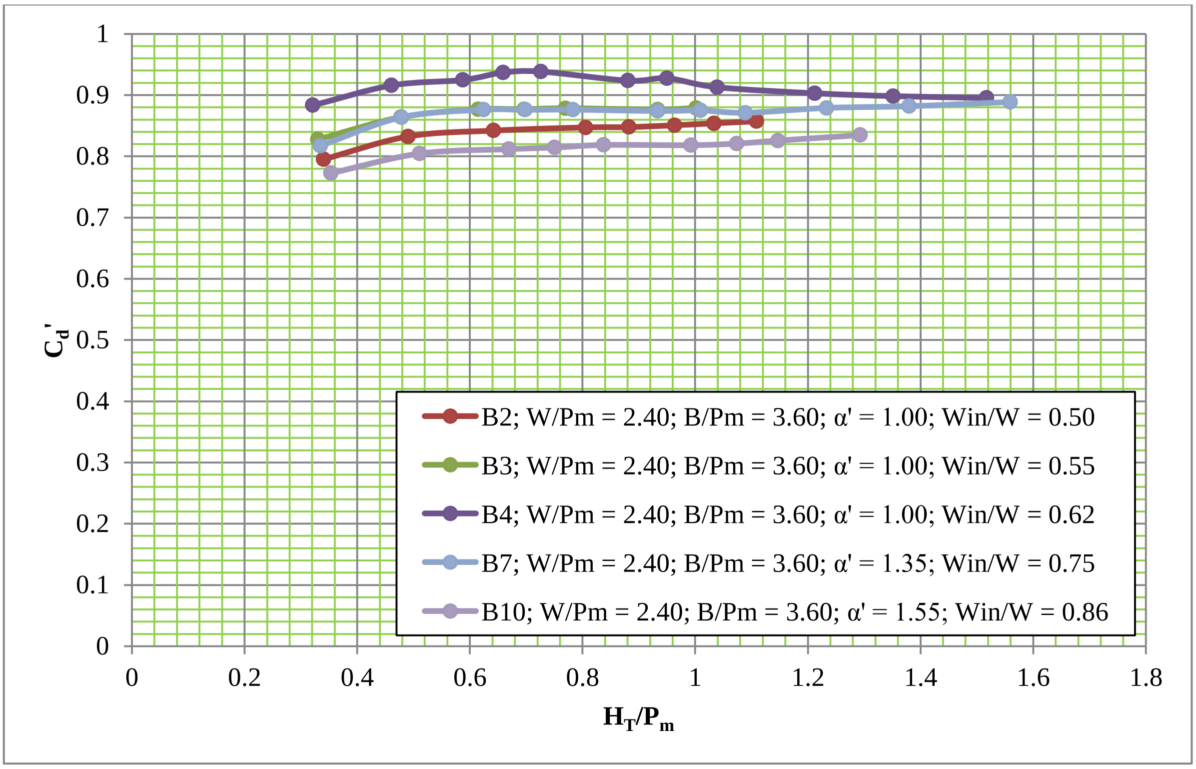

Figure 6.14: C_d' vs H_T/P_m for Models B2, B3, B4, B7 and B10 with no roundings

The last set of results is for models B5, B8 and B11 and are shown in Figs 6.15 and 6.16. From Figs 6.15 and 6.16 it can be seen that the results for models B5 and B8 are almost the same with a slight variance from H_T/P_m =1.00 for the models with roundings. Model B5 is a PKW design and model B8 is a combined design with α' = 1.35. This shows that for a W/P_m value of 2.40 and a B/P_m value of 4.20, either a PKW or a combined design with a higher α' value can give the same C_d' values.

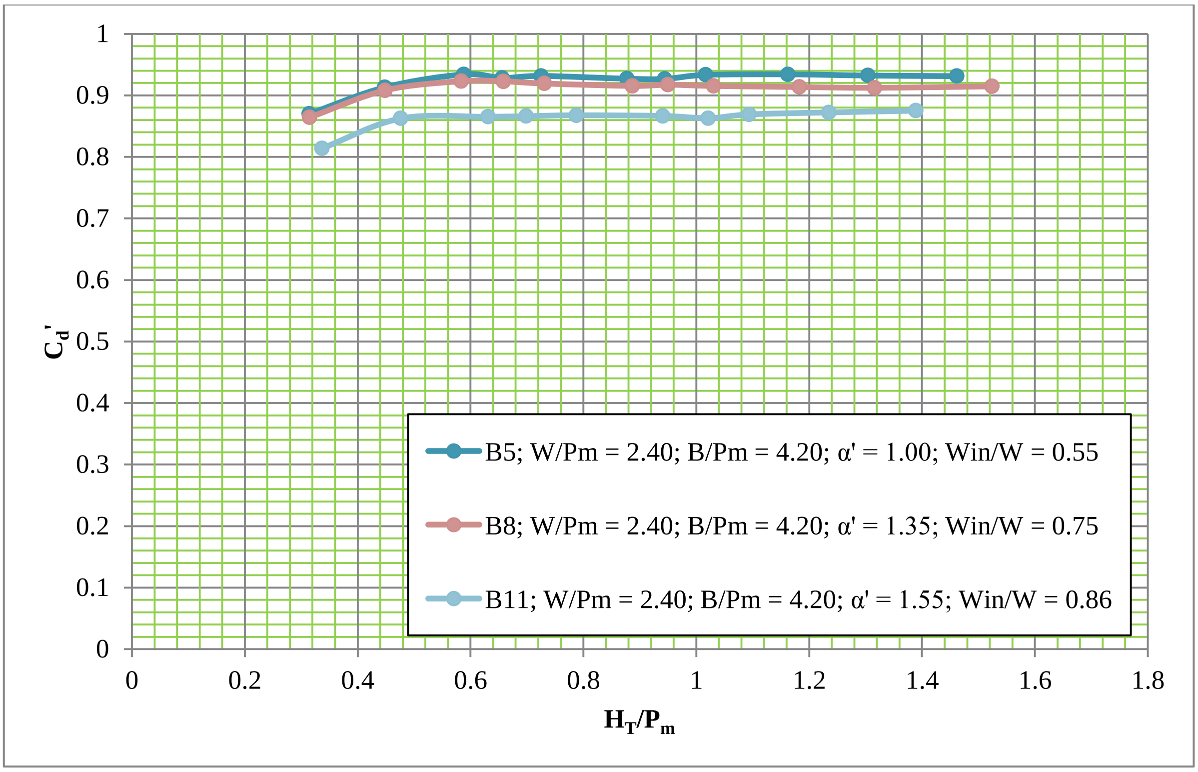

Figure 6.15: C_d' vs H_T/P_m for Models B5, B8, and B11 with roundings

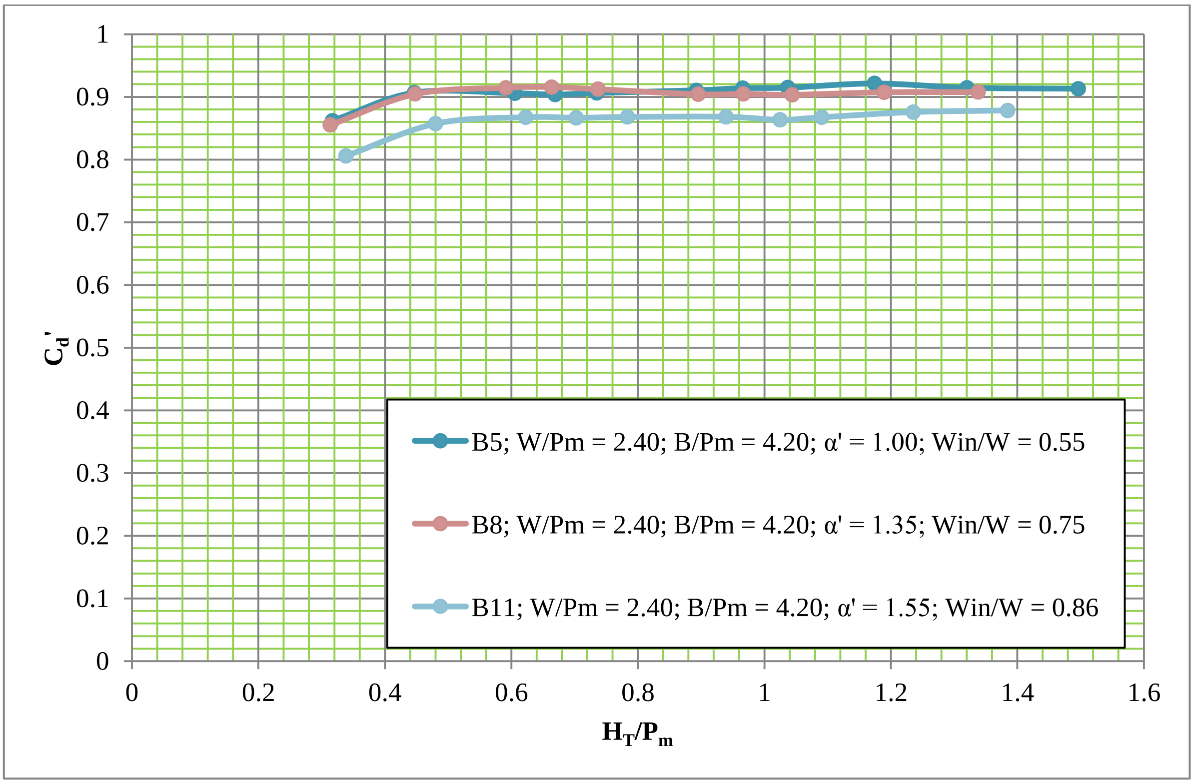

Figure 6.16: C_d' vs H_T/P_m for Models B5, B8 and B11 with no roundings

Just as model set A showed that for higher B/P_m values and constant W/P_m values, the potential for taper and hence the combined design increases, so does model set B. In model set B the experimental error is less, the graphs are smoother and flatter and with a higher W/P_m value it shows that higher B/P_m values can result in the same results for both PKW and combined designs.

6.2.3 Model set C

Model set C also had a higher W/P_m ratio than both Model sets A and B that was kept constant with varying B/P_m, α' and W_{in}/W values. The results are shown in Figs.6.17- 6.22.

Figures 6.17 and 6.18 show that the data exhibit an upward trend for the models with wider overall width (W), indicating that C_d' has not become constant as quickly as in model sets A and B (see Figs. 6.5 & 6.11). As H_T/P_m increases, so does C_d' even though the variation in C_d' remains small. The range of C_d' for the various H_T/P_m values is greater as is spans between 0.60 and 0.90. Model C1, just like models A1 and B1 shows the highest discharge coefficient compared to models C6 and C9 with the highest C_d' value of 0.85 with and without roundings. Model C1 is a PKW design with W/P_m = 3.00, B/P_m = 3.00 and α' = 1.00.

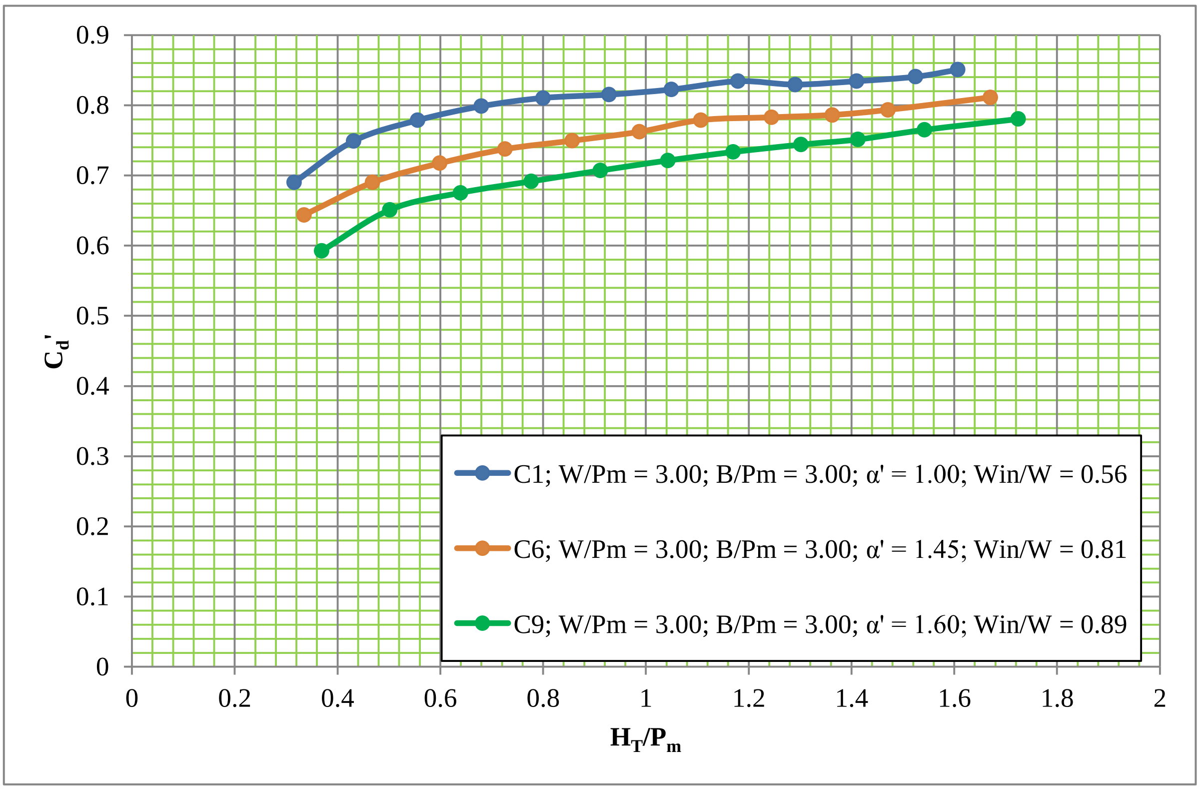

Figure 6.17: C_d' vs H_T/P_m for Models C1, C6 and C9 with roundings

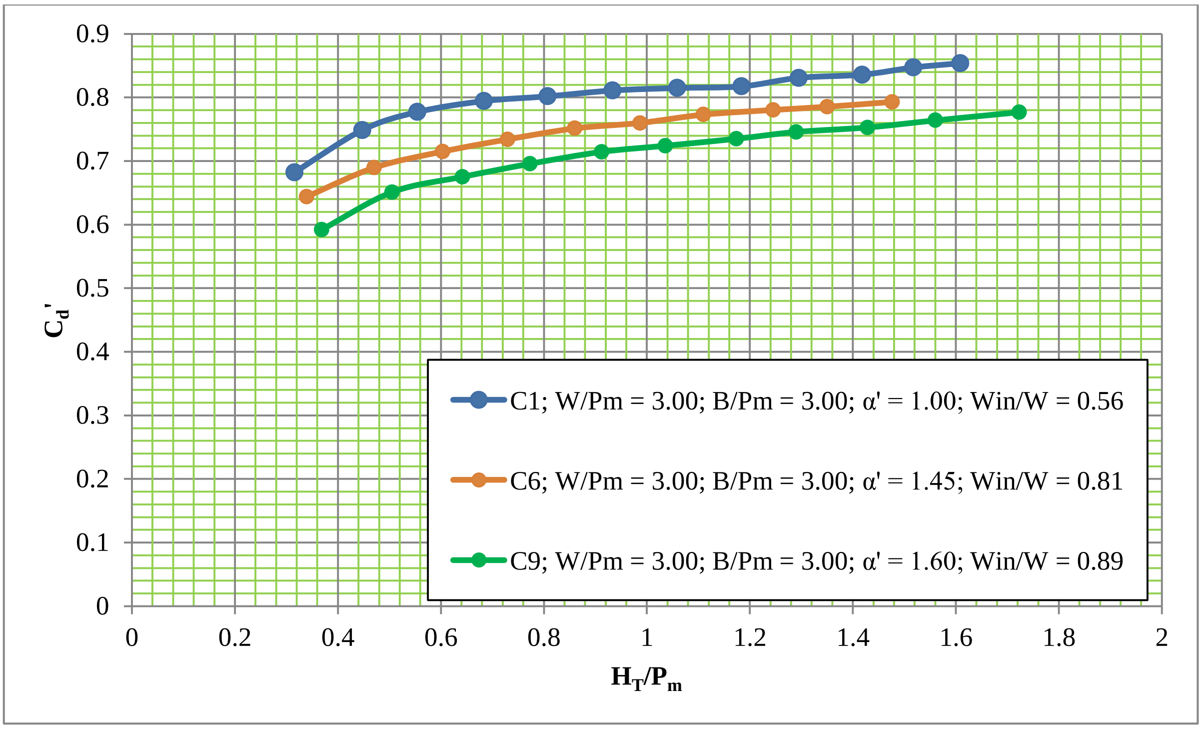

Figure 6.18: C_d' vs H_T/P_m for Models C1, C6 and C9 with no rounding

The second set of data is for models C2, C3, C4, C7 and C10 shown in Figs 6.19 and 6.20. These models all have a B/P_m value of 3.00, W/P_m value of 3.00 and varying α' and W_{in}/W values.

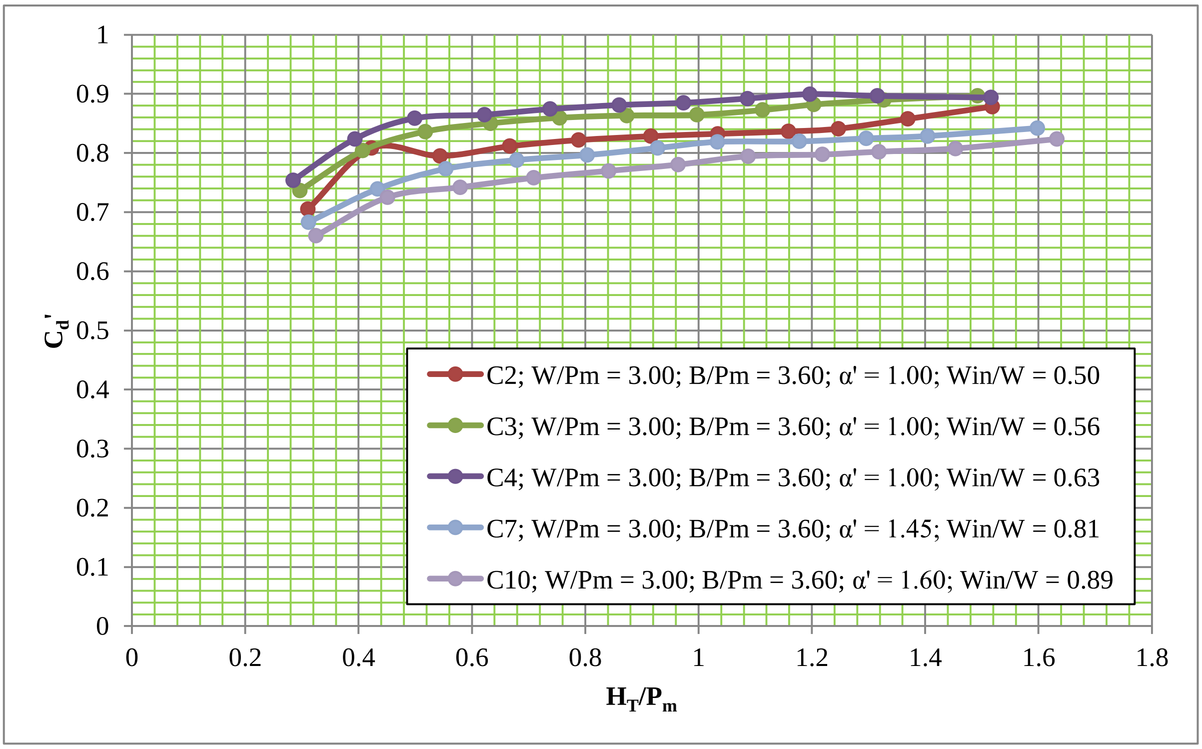

Figure 6.19: C_d' vs H_T/P_m for Models C2, C3, C4, C7 and C10 with rounding

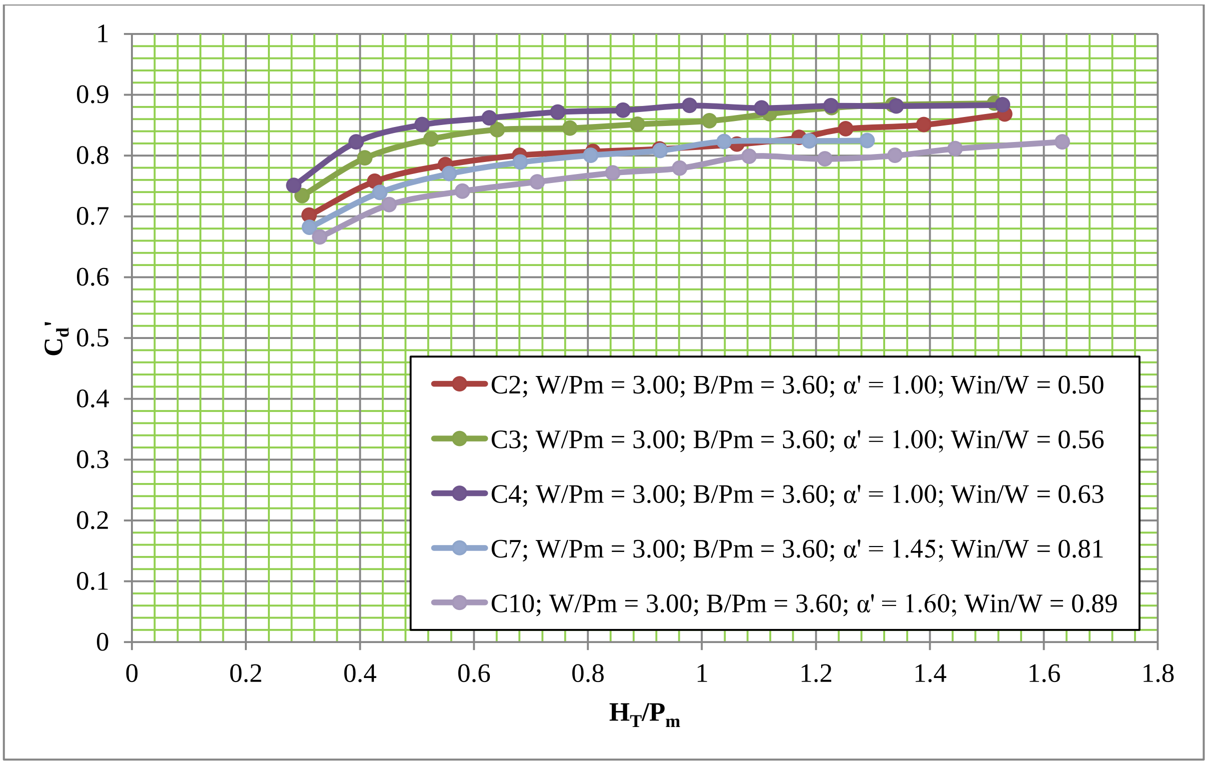

Figure 6.20: C_d' vs H_T/P_m for Models C2, C3, C4, C7 and C10 with no rounding

Figures 6.19 and 6.20 show that for higher B/Pm values the curves get closer and flatter. Model C4 shows the highest C_d' values of 0.90 (with roundings) and 0.88 (with no roundings). Model C4 is a PKW design with a wider inlet. Model C10 shows the lowest C_d' values, this model is tapered and has a α' value of 1.60.

The last set of data is for models C5, C8 and C11. This is shown in Figs 6.21 and 6.22.

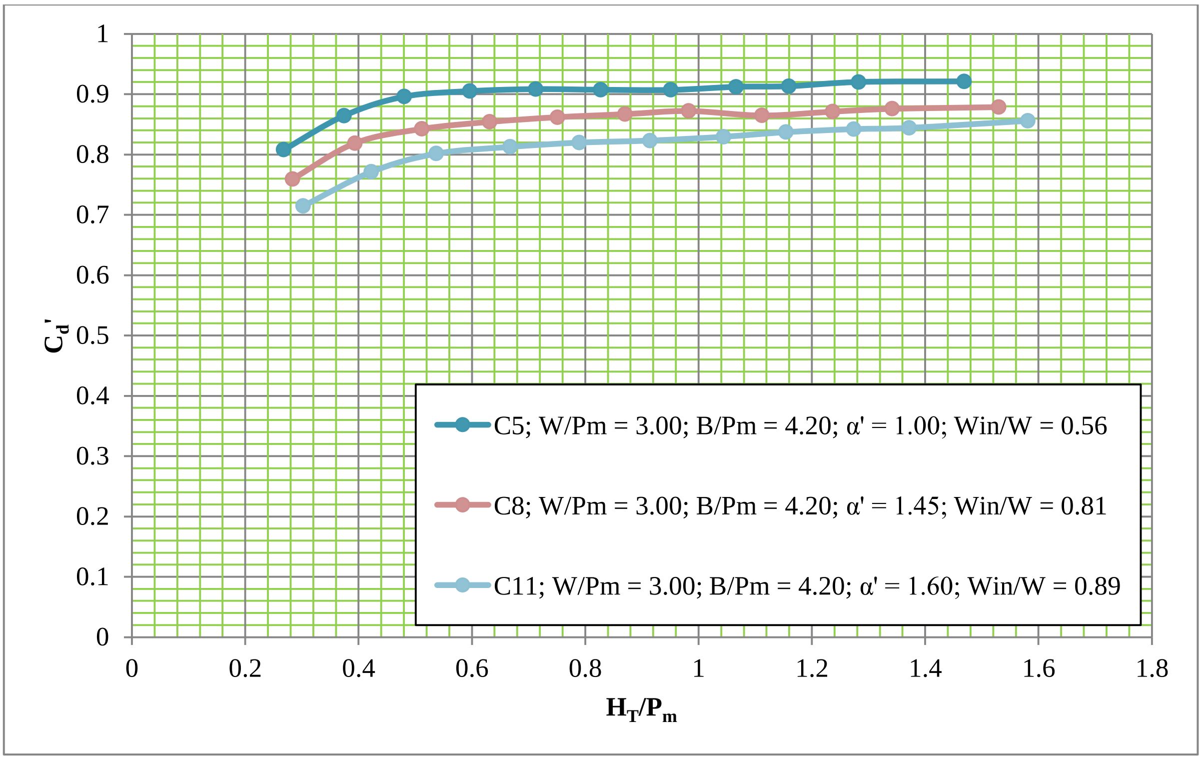

Figure 6.21: C_d' vs H_T/P_m for Models C5, C8 and C11 with rounding

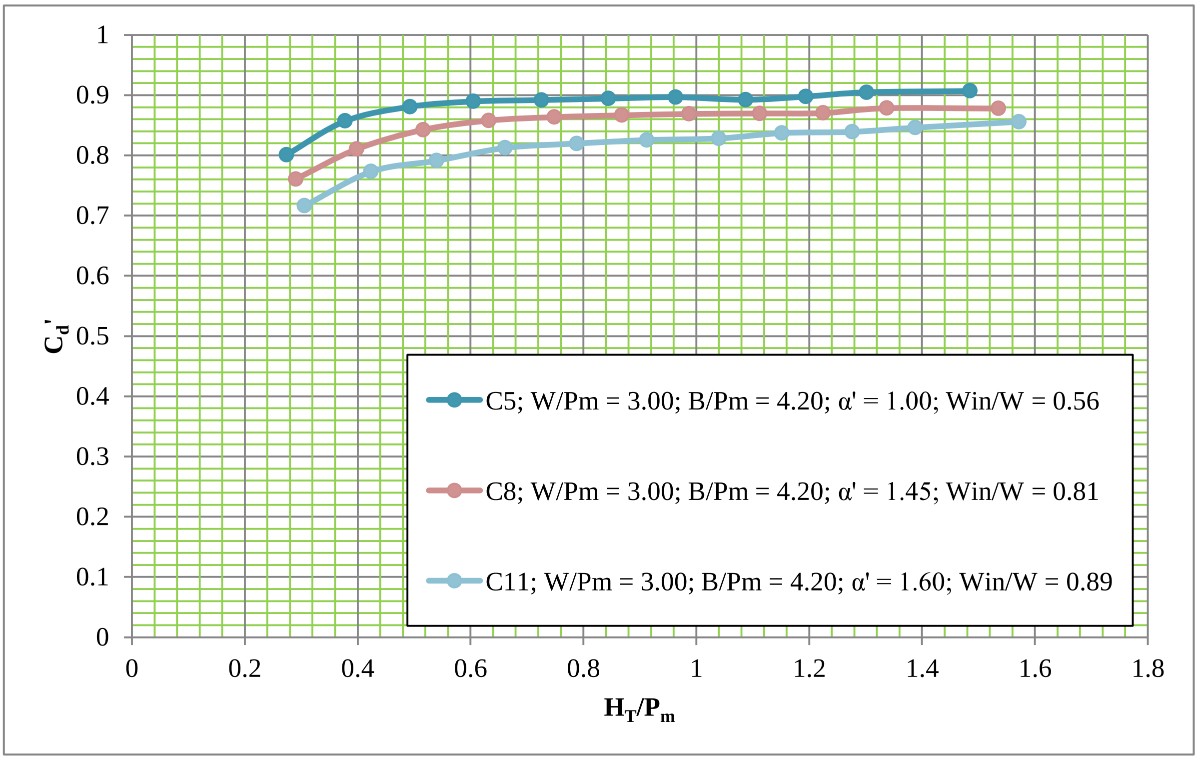

Figure 6.22: C_d' vs H_T/P_m for Models C5, C8 and C11 with no rounding

Figures 6.21 and 6.22 show how the curves flatten out as B/P_m increases. These models have the same W/P_m and B/P_m values with different α' and W_{in}/W ratios. In this experimental dataset, model C5 exhibited the highest C_d' values of 0.90 (no roundings) and 0.92 (with roundings). Model C5 is a PKW design with parallel walls (α' = 1.00), B/P_m = 4.20 and W_{in}/W = 0.56. Model C11 had the lowest C_d' values and is a combined design with α' = 1.60, B/P_m = 4.20 and W_{in}/W =0.89.

There is a greater variance in the C_d' values showing a bigger vertical shift in the data of Figs 6.21 and 6.22. This shows that having greater W/P_m and B/P_m values could result in lower C_d' values. It also indicates that having too large a taper may have a negative impact on the C_d' value.

The results from model set C indicate that wider overall channel widths (W) could result in the C_d' becoming constant at higher H_T/P_m values. Although, models with longer transversal lengths (B) and smaller inlet widths (W_{in}/W) reached a constant C_d' value faster than others (i.e. C5). The results have also shown that working with larger W and B values could result in lowered C_d' values. Wider tapering can also result in lowered C_d' values which indicate that tapering has limitation.

6.2.4 Comparison of model sets A, B and C

Figures 6.5 – 6.22 have reflected the results of model sets A to C with and without roundings under the upstream overhang. From all the data presented, it can be seen that the roundings have a very small effect, especially on the models with a combined design. Having a trapezoidal labyrinth type plan layout can be effectively used to avoid the intricate roundings associated with the standard PKW design. The average percentage difference in H_T/P_m between models with and without roundings over the range of C_d' is 1.07%. The average percentage difference in C_d' over the range of H_T/P_m is 1.00%.

From the data presented on C_d' vs H_T/P_m, it can be seen that for $0.5<H_T/P_m<1.0$, the C_d' values are more constant. For all three datasets it is also evident that the H_T/P_m does not have a very strong effect on C_d' except at low values. The vertical displacements between the models of each data set can be attached to the changing B/P_m, α' and W_{in}/W ratios. These geometric variations result in the change in C_d' for each model. In each dataset, it is evident that the models with higher B/P_m, lower W_{in}/W and lower α' ratios exhibit higher C_d' values. This is possibly due to the larger flow area found with the higher B/P_m values and lower α' values.

Figures 6.23 and 6.24 shows the comparison of models A1, B1 and C1 with and without roundings respectively. These models all have the same B/P_m, α' and W_{in}/W ratios with varying W/P_m values. Keeping all other variables constant, this gives an indication of how W/P_m affects C_d'. From these results it can be seen that having a lower W/P_m ratio results in higher C_d' values. Model B1 gets to a constant C_d' before Models A1 and C1 and remains constant for $0.5<H_T/P_m<1$.

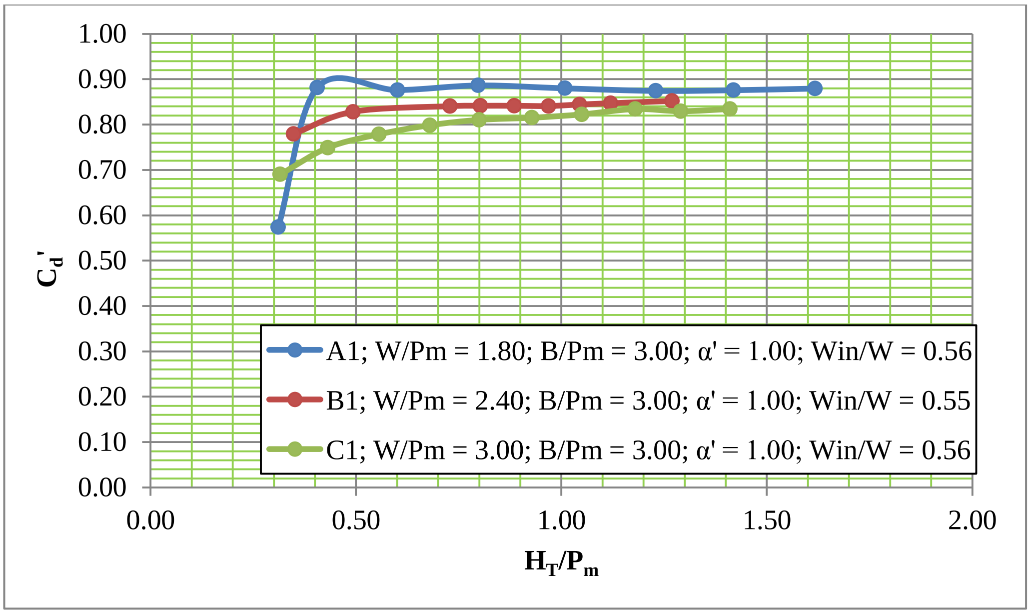

Figure 6.23: Comparison of Models A1, B1 and C1 for C_d' vs H_T/P_m with roundings

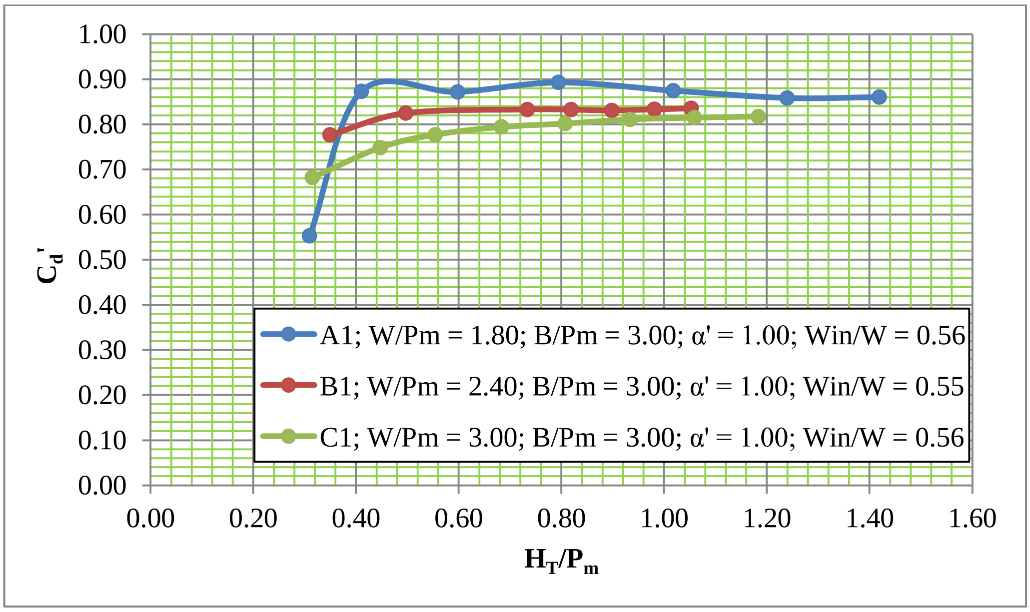

Figure 6.24: Comparison of Models A1, B1 and C1 for C_d' vs H_T/P_m with no roundings

From Figs 6.23 and 6.24 it can be seen that when B/P_m is constant, the models with lower W/P_m values have the highest C_d' values. This is true even when B/P_m in increased. Although at H_T/P_m>1, the C_d' values for models with higher W/P_m values come closer to those with lower values. This is true for all the models with varying W/P_m values and constant B/P_m values.

6.3 Head – discharge relationships

Discharge rating curves were generated for all model sets with q (unit flow) ($m^3/s/m$) as a function of H_T(m). All results were compared with Eq. (2.1), differences in the measured data and the Eq.

(2.1) predicted data indicate how close the different geometric variations of the study come to the optimal design.

As discussed in Chapter 5, the standard weir head – discharge relationship (Eq. (5.1)) is typically parabolic in nature ($q \propto H_T^{1.5}$), the head – discharge relationship predicted by Eq. (2.1) and verified by the experimental data is linear. Differences between the measured data and the (Eq. (2.1)) predicted data, using C=4.3, is due to the change in geometric features of the models in this study. These geometric features refer to the inlet channel width proportion (α’) and variousW and B values of each model (Table 3.1).

Figures 6.25 – 6.28 show that as the cycle width (W) increases, the experimental data shifts away from the predicted curve of Eq. (2.1). As W increases, models with a lower inlet channel width proportion (α’) are shown to have a higher discharge capacity. In Fig. 6.25 model A11 is the highest with α’=1.45, Fig. 6.26 shows model B8 as the highest with α’=1.35 and Fig. 6.27 shows model C5 as the highest with α’=1.00.

As established in the previous section, the roundings have little effect on the results, particularly those of the combined labyrinth and PKW design, and are therefore not shown in this section. The results with roundings can be found in Appendix A.

6.3.1 Model set A

The rating curves for model set A are shown in Figs6.25 – 6.27. When compared with Eq. (2.1), in Fig 6.25, model A1 (W/P_m =1.80, B/P_m = 3.00, α’ = 1.00 and W_{in}/W = 0.56) has the closest fit and is the most linear in shape. Models A6 (W/P_m =1.80, B/P_m = 3.00, α’ = 1.20 and W_{in}/W = 0.67) and A9 (W/P_m =1.80, B/P_m = 3.00, α’ = 1.45 and W_{in}/W = 0.81) are slightly more parabolic in shape. The only difference in these three models is the α’and in turn the W_{in}/W value and therefore the change is attributed to this. The reason that α’ affects the discharge could be because it changes the transversal length of the model, which gives the flow a longer length of spillway, increasing the L, which reducesthe total head (H_T).

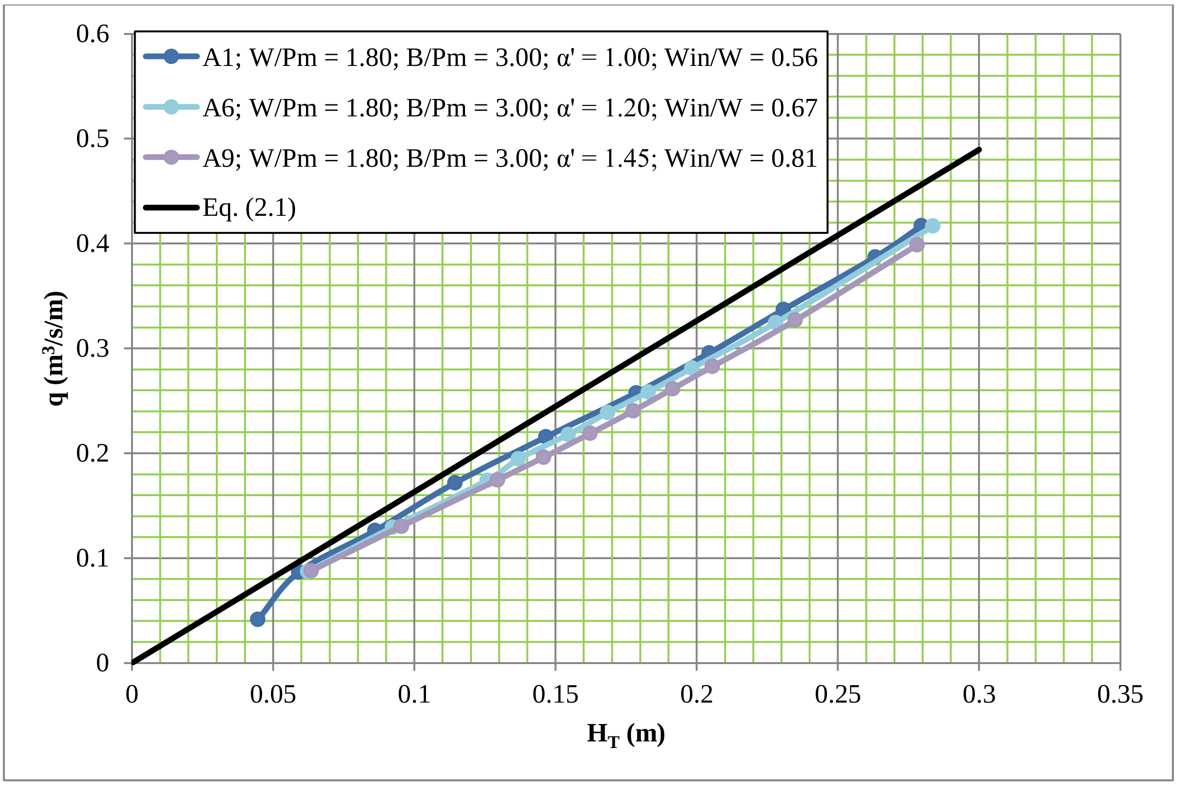

Figure 6.25: Measured and predicted (Eq. (2.1)) Head - Discharge curves for models A1, A6 and A9 with no roundings

Results for models A2, A3, A4, A7 and A10 are shown in Fig. 6.26. These models have constant W/P_m and B/P_m values with varying α' values. From Fig 6.26 it is evident that as the B/Pm value increases, the models with taper show higher discharge that the PKW designs. Figure 6.26 shows that model A7 has the most linear curve and is closest to that of Eq. (2.1). It is also evident that at low heads, the models all act the same having the same discharge rating as that of Eq. (2.1), however, at higher heads (H_T), there is a deviation.

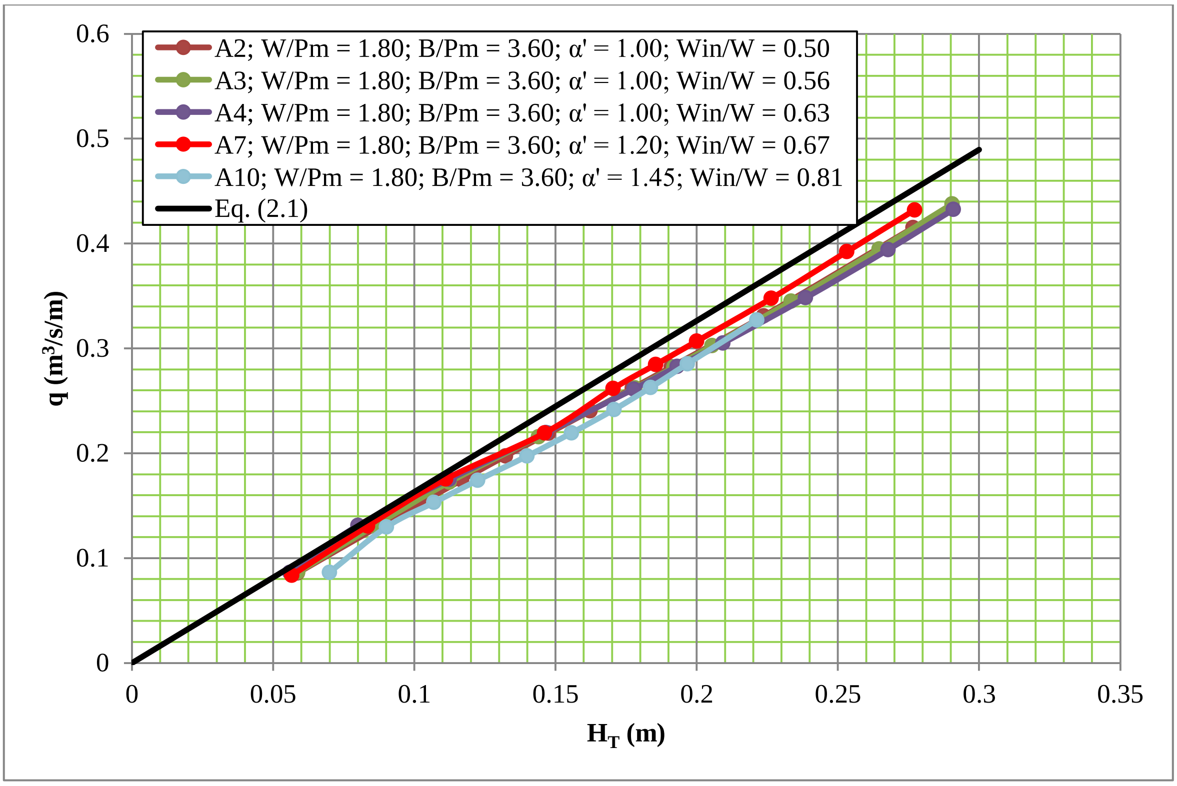

Figure 6.26: Measured and predicted (Eq. (2.1)) Head - Discharge curves for models A2, A3, A4, A7 and A10 with no roundings

The last set of data is shown in Fig. 6.27 and consists of models A5, A8 and A11. Figure 6.27 shows that model A11 has the highest rating curve and sits closest to Eq. (2.1). Model A11 is a combined design and has an α’ value of 1.45. This shows that models with a taper can behave linearly like the standard PKW design.

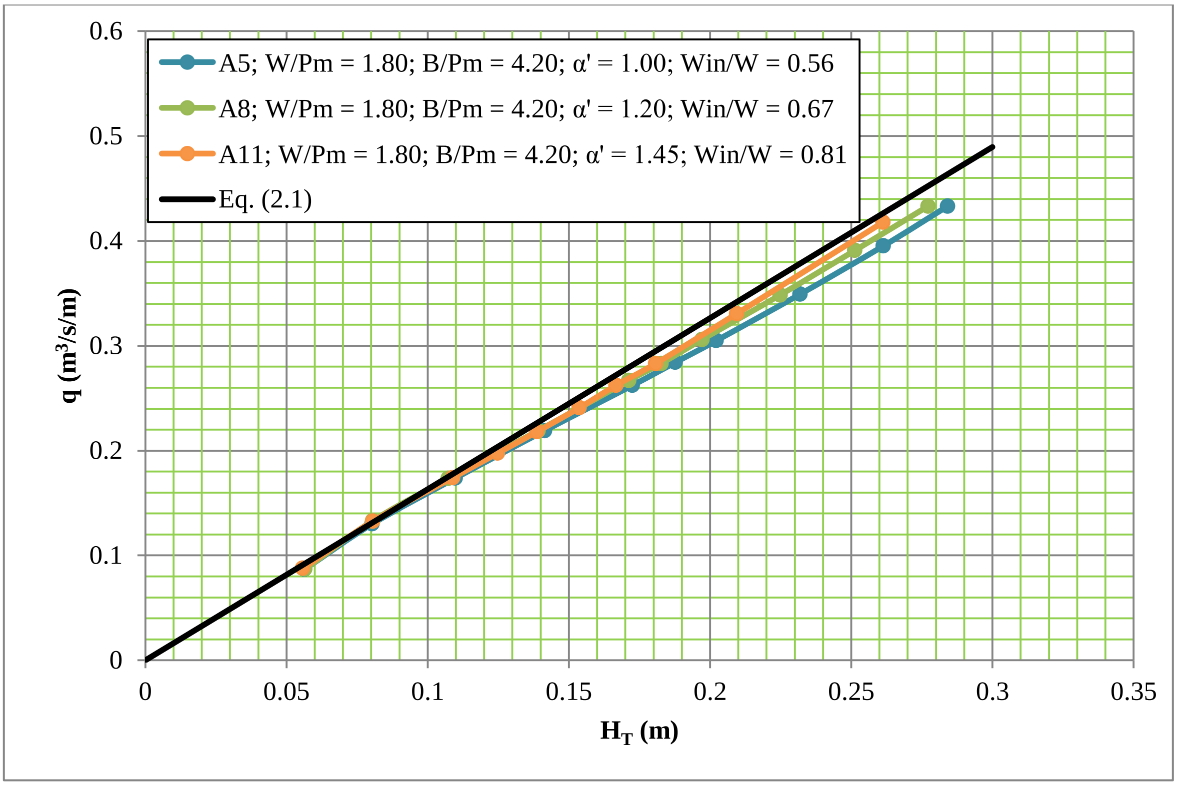

Figure 6.27: Measured and predicted (Eq. (2.1)) Head - Discharge curves for models A5, A8 and A11 with no roundings

6.3.2 Model set B

The rating curves for model set B are shown in Figs 6.28 – 6.30. These curves deviate more from the Eq. (2.1) curve than those shown in Figs 6.25 – 6.27. In this dataset W/P_m is constant at 2.4 with varying B/P_m, α' and Wi_n/W ratios. Figure 6.28 shows the data for models B1, B6 and B9, these models had constant W/P_m and B/P_m values with varying α' and W_{in}/W values. B1 (W/P_m =2.40, B/P_m = 3.00, α' = 1.00 and W_{in}/W = 0.55) is the closest fit to Eq. (2.1). Model B9 (W/P_m =2.40, B/P_m = 3.00, α' = 1.55 and W_{in}/W = 0.86) sits the furthest from Eq. (2.1). The difference in these models is the α' as well as the W_{in}/W ratios. The change in these results is therefore attributed to an entire change in flow area between B1 and B9 based on the variation in geometric parameters.

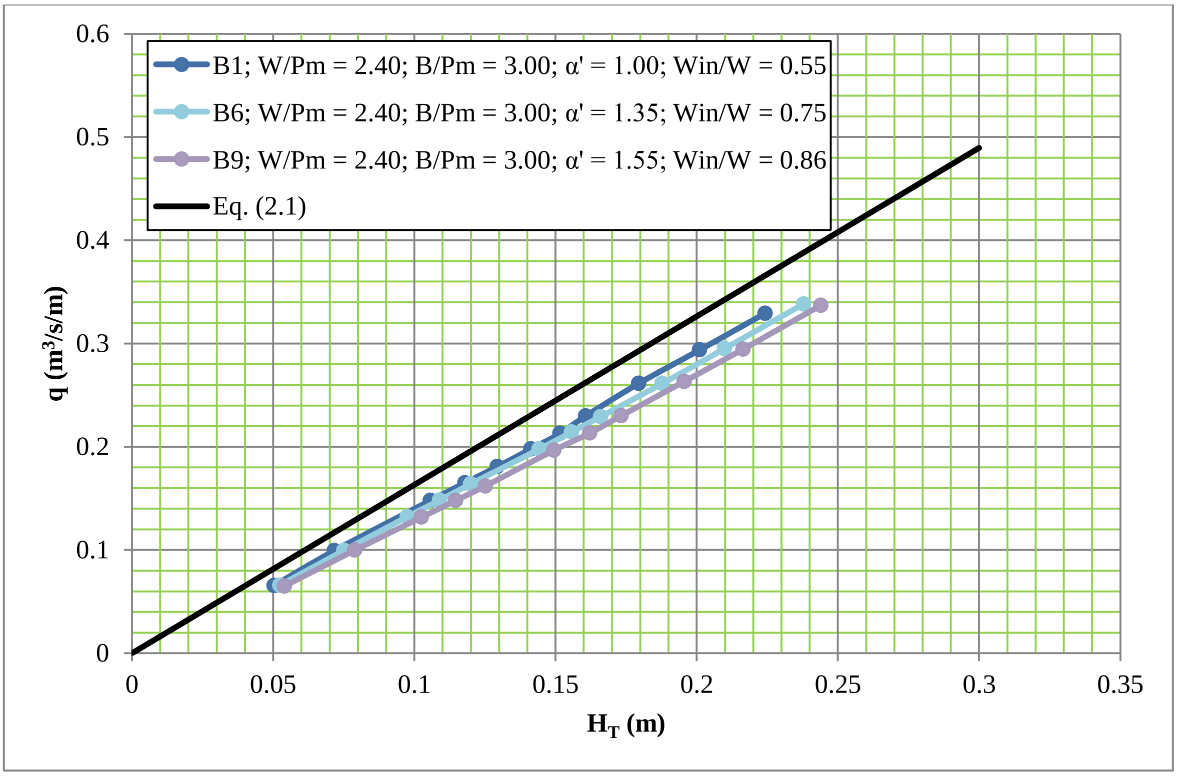

Figure 6.28: Measured and predicted (Eq. (2.1)) Head - Discharge curves for models B1, B6 and B9 with no roundings

The second dataset contains data for models B2, B3, B4, B7 and B10 and is shown in Fig. 6.29. The W/P_m and B/P_m values are constant with only α' and W_{in}/W varying. Figure 6.29 shows that model B4 has the best rating curve and sits closest to Eq. (2.1.). Model B4 is a PKW design and has parallel walls (i.e. α' = 1.00). In Fig. 6.26 it was model A7 that had the best discharge curve, this is due to the change in the increase in the W/P_m value and increase in α'. Model A7 had a B/P_m = 3.00 and α' = 1.20 whilst model B7 has a B/P_m = 3.60 and α' = 1.35. It is evident that with increasing B/P_m and α' values, the PKW designs have more idea discharge curves than the combined designs.

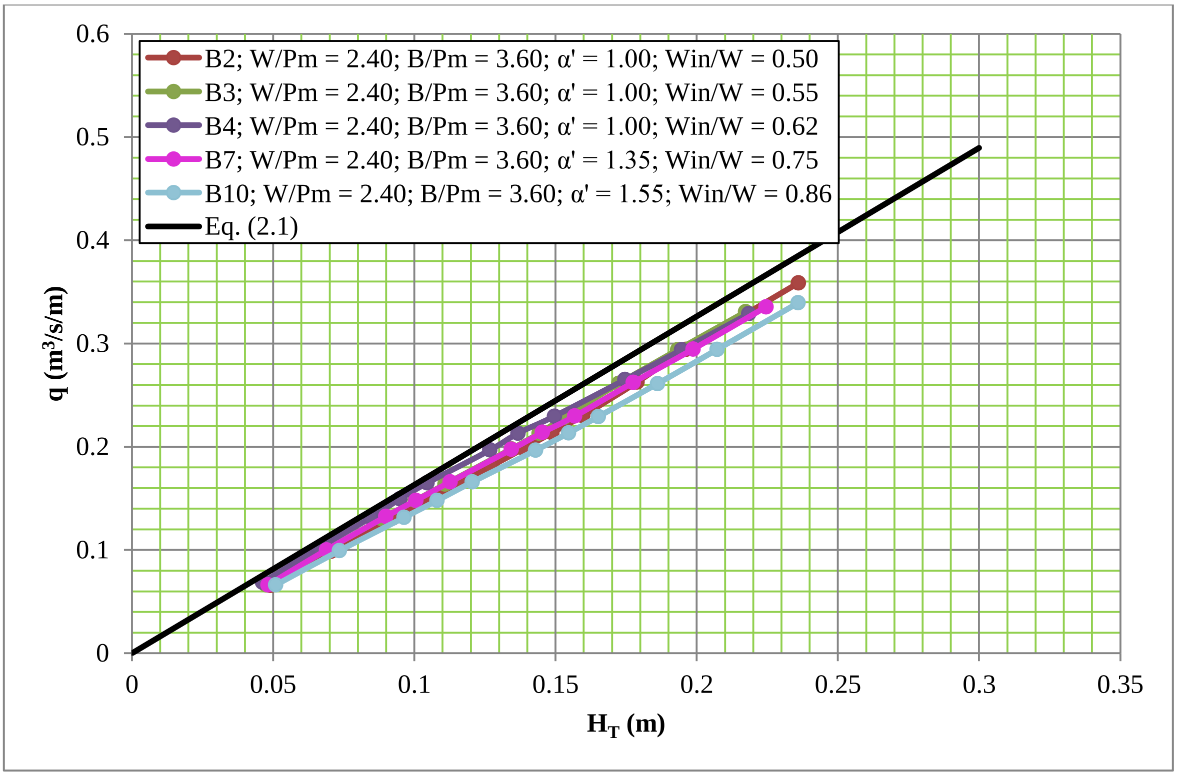

Figure 6.29: Measured and predicted (Eq. (2.1)) Head - Discharge curves for models B2, B3, B4, B7 and B10 with no roundings

The last dataset for model set B contains models B5, B8 and B11. This data is shown in Fig 6.30. Similar to the conclusions drawn for Fig. 6.29, the same can be said for Fig. 6.30. It can be seen that model B5 sits closest to Eq. (2.1). Although, model B8 is not very far away and the difference between model B8 and B5 is so small it could be regarded as negligible. Therefore, for higher B/P_m ratios and the same taper (α' = 1.35), the combined designs can give results the same as the PKW designs.

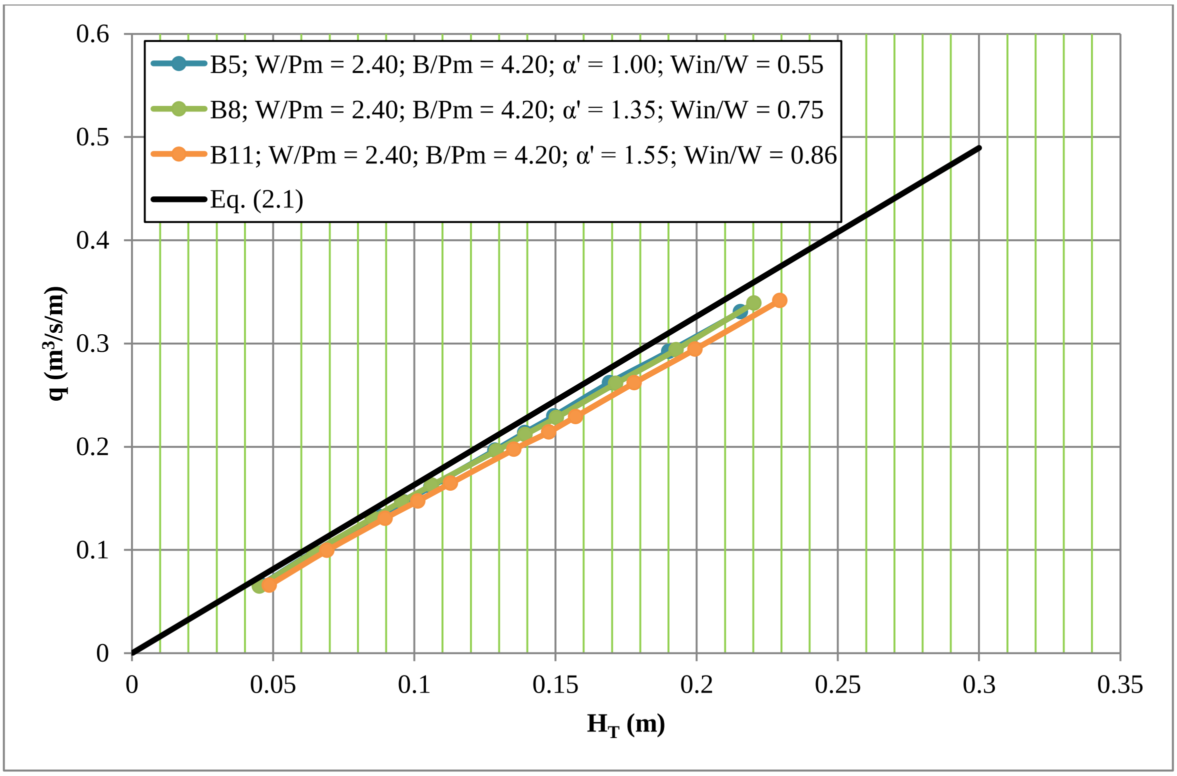

Figure 6.30: Measured and predicted (Eq. (2.1)) Head - Discharge curves for models B5, B8, and B11 with no roundings

6.3.3 Model set C

The rating curves shown in Figs 6.31- 6.33 have a bigger deviation from the predicted data of Eq. (2.1) than that of model set A and B. This shows that for larger W – values, the rating curves are less likely to follow the linear trend of the PKW design. These models also don't start of linear and following the trend of Eq. (2.1) like model set A and B.

In Fig. 6.31, model C1 (W/P_m = 3.00, B/P_m = 3.00 α' = 1.00 and W_{in}/W = 0.56) is the closest to Eq. (2.1) whereas C9 (W/P_m = 3.00, B/P_m = 3.00, α' = 1.60 and W_{in}/W = 0.89) is the furthest from Eq. (2.1). Similar to model set B, these models have different α' and W_{in}/W values which could result in changes of H_T and q based on the changing flow area.

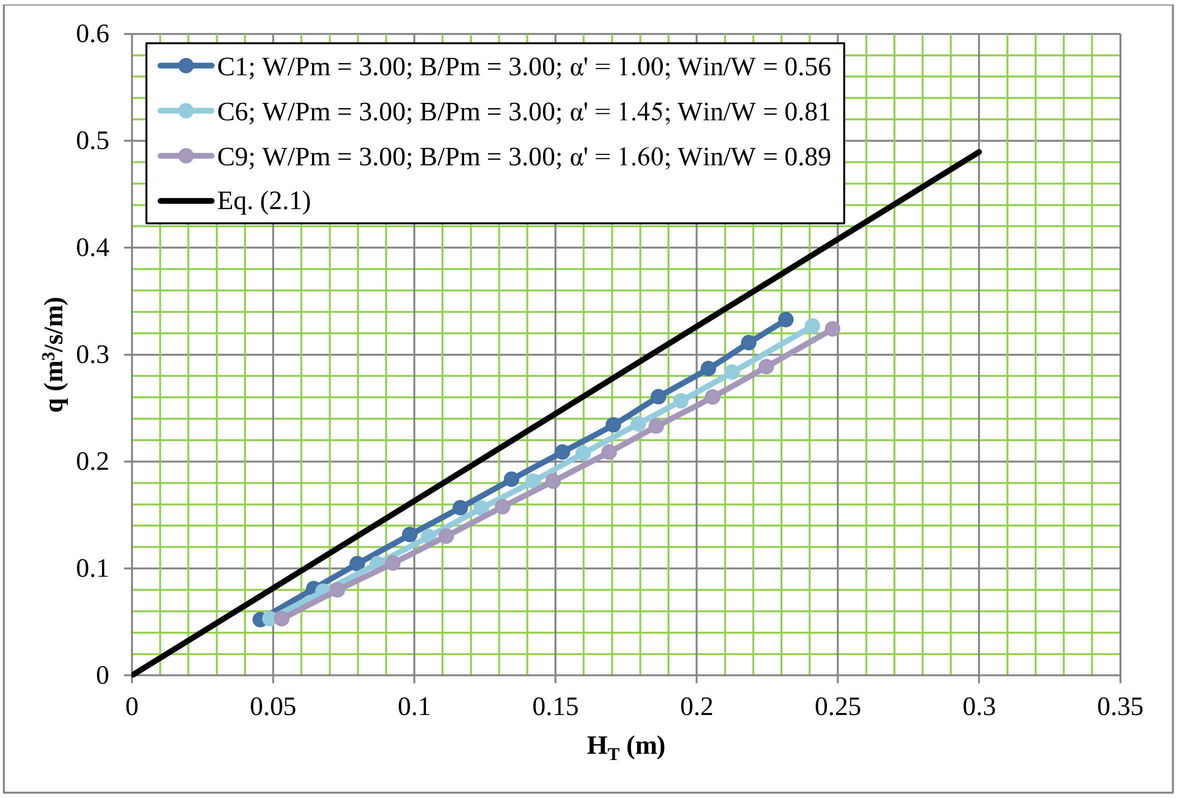

Figure 6.31: Measured and predicted (Eq. (2.1)) Head - Discharge curves for models C1, C6 and C9 with no roundings

The nest set of results is for models C2, C3, C4, C7 and C10. These results are shown in Fig. 6.32 and depict similar results to that of Fig. 6.28. In these results it also shows model C4 as having the best discharge curve however, it sits further away from Eq. (2.1) than models A7 and B4. This is due to the higher W/P_m value of model set C.

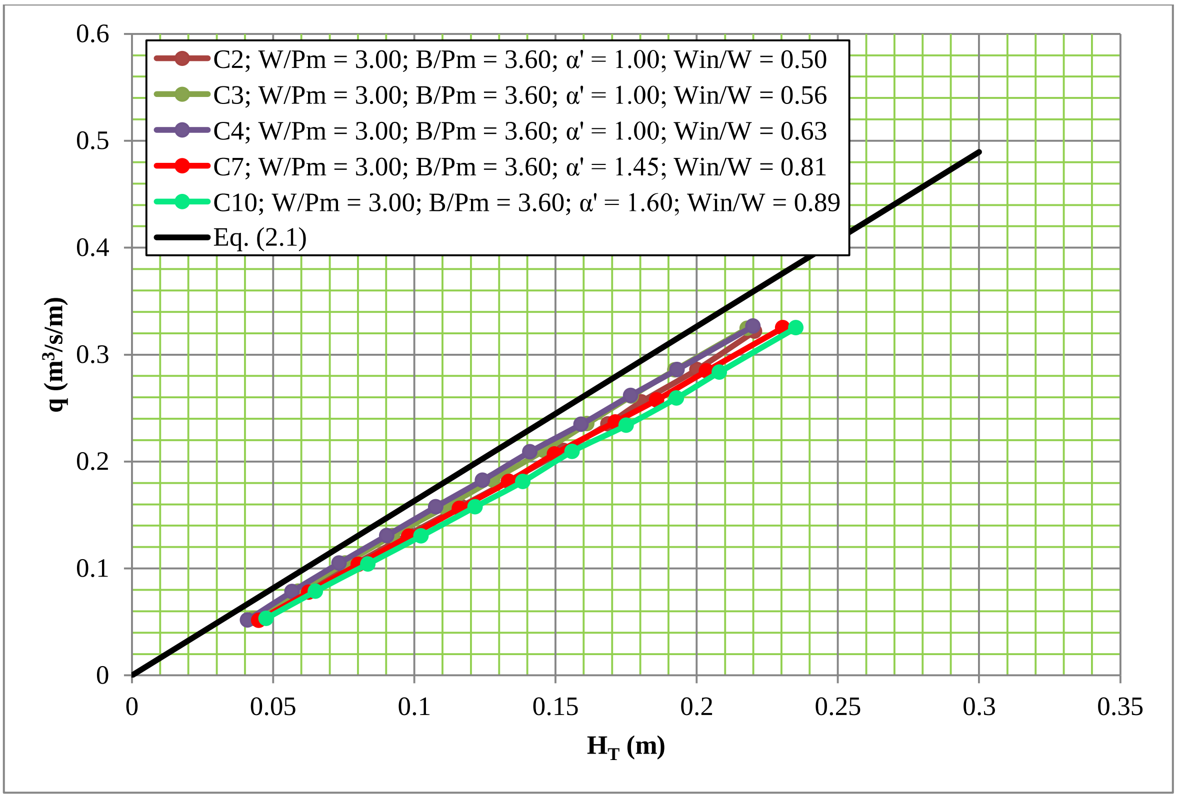

Figure 6.32: Measured and predicted (Eq. (2.1)) Head - Discharge curves for models C2, C3, C4, C7 and C10 with no roundings

The final dataset for model set C is shown in Fig. 6.33 and contains data for models C5, C8 and C11. These models all have the same W/P_m and B/P_m values with varying α' values. Model C5 exhibits the best discharge curve and sits closest to Eq. (2.1). This is a standard PKW design with a higher W/P_m value that models B5 and A5. It is clear from these results that wider channels result in PKW designs delivering the greatest discharge.

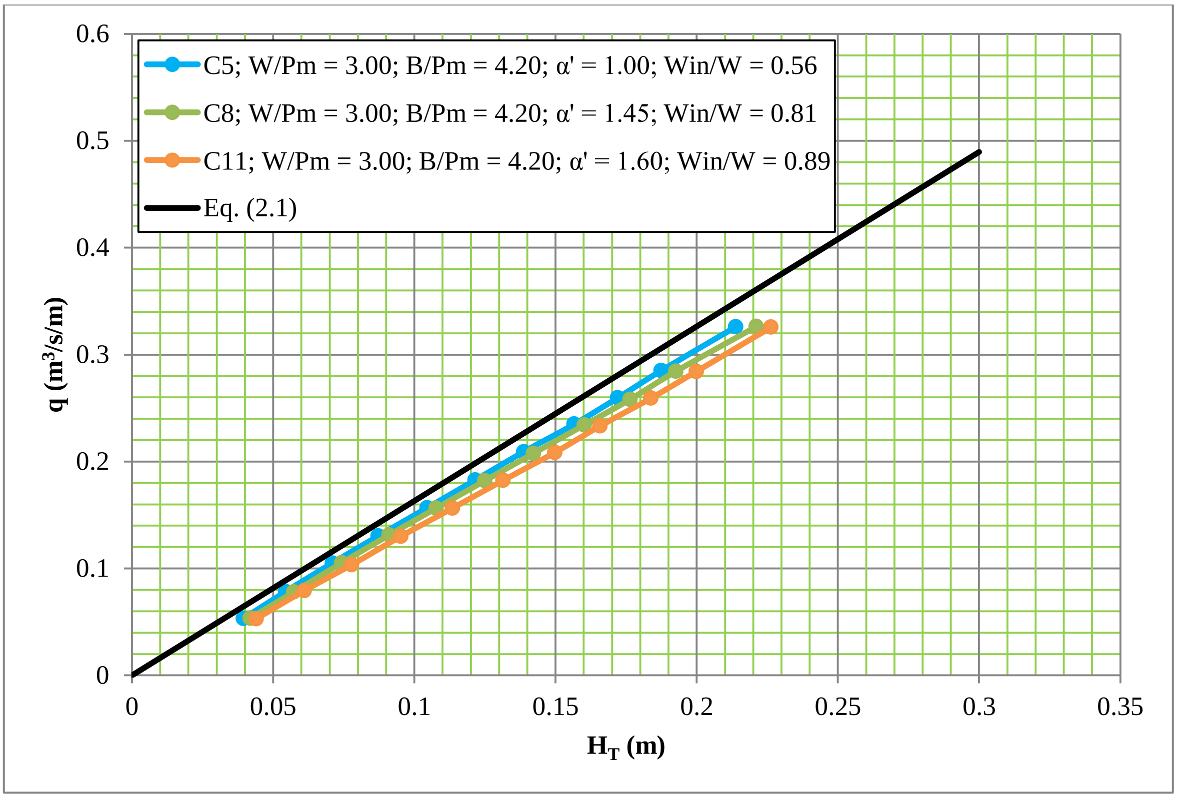

Figure 6.33: Measured and predicted (Eq. (2.1)) Head - Discharge curves for models C5, C8, and C11 with no roundings

The results from the rating curves show the hydraulic efficiency of the different spillway variations. These indicate how a lower total head (H_T) can be achieved through the various geometric changes (having roundings on the crest, W/P_m, B/P_m, W_{in}/W, α’). For different models, lower heads (H_T) are achieved at the same unit flow rate (q) for example, in Fig 6.31, looking at a unit flow rate of 0.3 m^3/s/m, different H_T – values are found for the different models with model C9 (W/P_m = 3.00, B/P_m = 3.00, α’ = 1.60 and W_{in}/W = 0.89) exhibiting the highest total head (H_T) and model C1(W/P_m = 3.00, B/P_m = 3.00 α’ = 1.00 and W_{in}/W = 0.56) exhibiting the lowest total head (H_T). For each model set, as W/P_m increases, H_T decreases. W/P_m increases the channel width and therefore increases the flow area, reducing H_T.

6.4 C_d’ vs.L/W (Length magnification factor)

Previous studies have claimed that a growth in the length magnification factor (L/W) increases the discharge capacity of weirs. From the model tests conducted, a basic trend line was developed for the discharge coefficient (C_d’), in terms of the length magnification factor (L/W). Increasing this ratio may result in increased discharge capacity but reducing it can lower the cost due to the reduced wall length. Figures 6.34- 6.35 show the results for all three model sets with and without roundings under the upstream overhang.

Since the C_d' value proved to be relatively constant for $0.5<H_T/P_m<1.0$, the results in this section are representative of a H_T/P_m ratio between 0.5 and 1 as these are minimum and maximum of the range that was tested.

Figures 6.34- 6.35 show a logarithmic relationship between C_d' and L/W with a variety of values for B/P_m, α' and W_{in}/W. For these models the L/W ratio was in the range of 2.4 and 6 with the C_d' value ranging from 0.6 to 1.0. Certain geometric features like the roundings of the inlet walls under the upstream overhang and the crest shape are helpful in reducing the required head and improving C_d'. Models with such geometries have C_d' values that sit above the fitted curve (e.g. y = 0.25ln(L/W) + 0.52).

The results from the combined design show some data that have higher C_d' values than others. This is due to the inlet channel width proportion (α') as well as the transversal length (B) used.

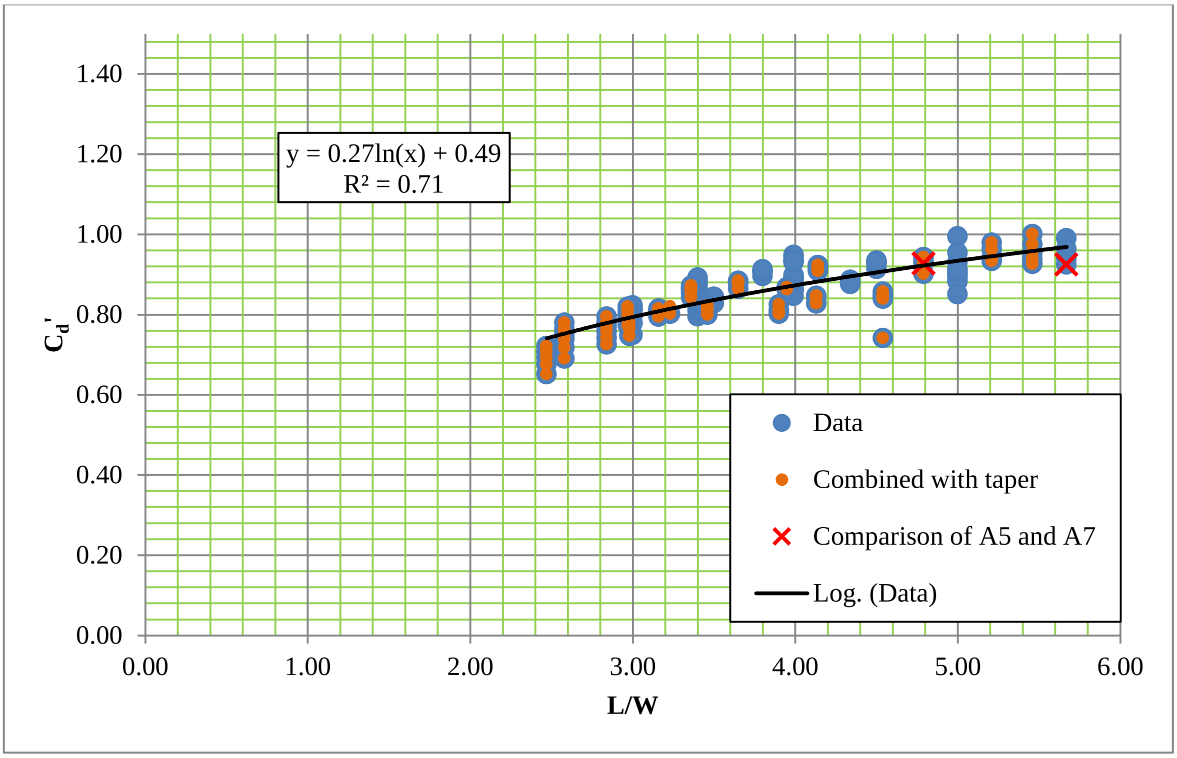

Figure 6.34: Results showing logarithmic relationship between C_d' and L/W for 0 .5<H_T/P_m<1.0 with roundings

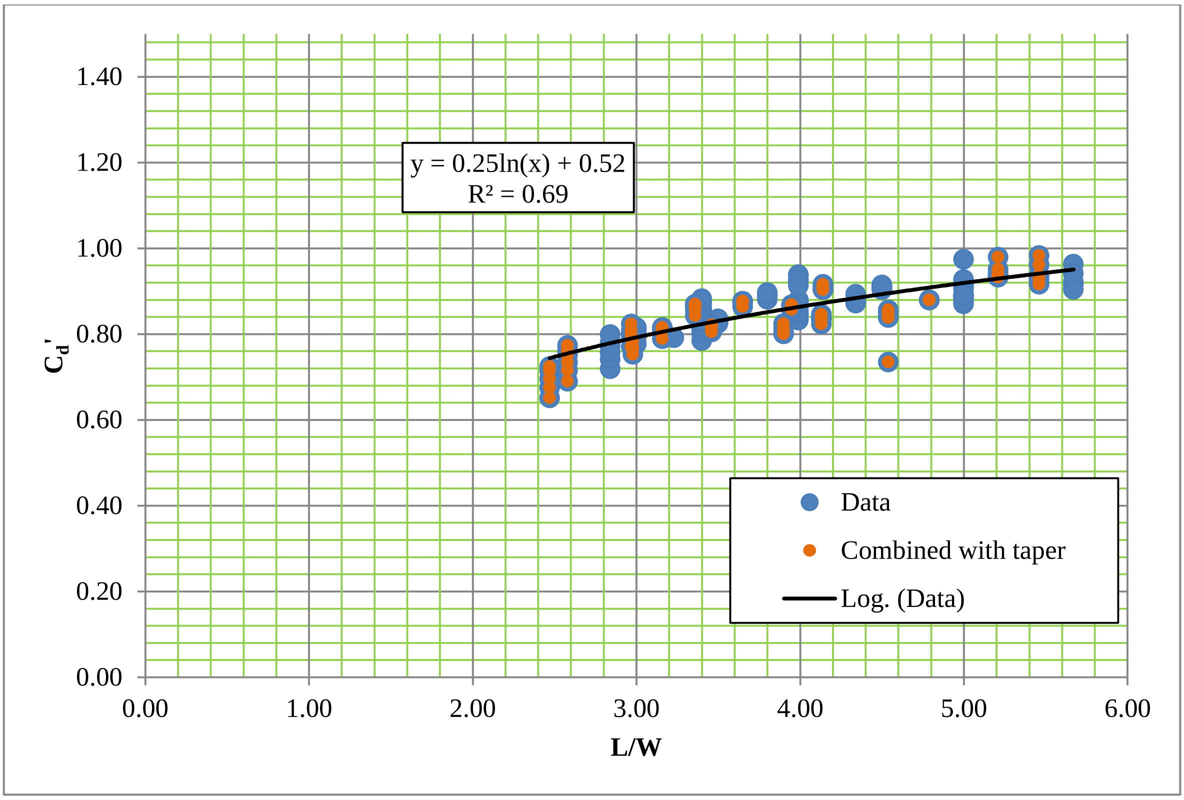

Figure 6.35: Results showing logarithmic relationship between C_d' and L/W for $0.5<H_T/P_m<1.0$ with no roundings

6.4.1 Overall effect of L/W

From the results shown in the previous section, it can be seen that as the L/W ratio increases so does the C_d' value. Having a combined design with tapered walls can help reduce the wall length required for construction. This in turn reduces the amount of concrete that will be used and helps to improve the design economically. In Figs 6.34 – 6.35 the results indicated in orange show the data captured for the combined and tapered designs, this shows that in certain instances having a combined design can result in lowered L/W ratios with the same or higher C_d' values as the standard PKW designs. Figure 6.34 shows the comparison of two models (A5 and A7), where Model A5 is a standard PKW design with a C_d' value of 0.92 and L/W = 5.67 whereas model A7 is a combined design with a C_d' value of 0.93 and L/W = 4.79.

These results indicate that increasing the total width together with the tapered walls of the combined design can have a large impact on the wall length (L/W) which in turn can affect the costs aswell asC_d'. In certain cases it is such that the models with the combined design and no roundings have higher C_d' values at reduced L/W ratios, eliminating the need for roundings altogether. This can be seen with model A7 where C_d' is 0.93 without roundings and 0.89 with roundings.

Figure 6.36 shows that as the inlet channel width proportion (α') is increased, the L/W ratio is reduced. This indicates that having the combined designs does definitely reduce the wall length and concrete used. In Fig. 6.36 each inlet channel width proportion (α') has a number of L/W ratios associated with it. This shift in L/W ratios is due to the various geometric parameters associated with each value. These parameters are B/P_m, W_{in}/W and α'. Models with higher L/W ratios generally have higher B/P_m, W_{in}/W and α' values.

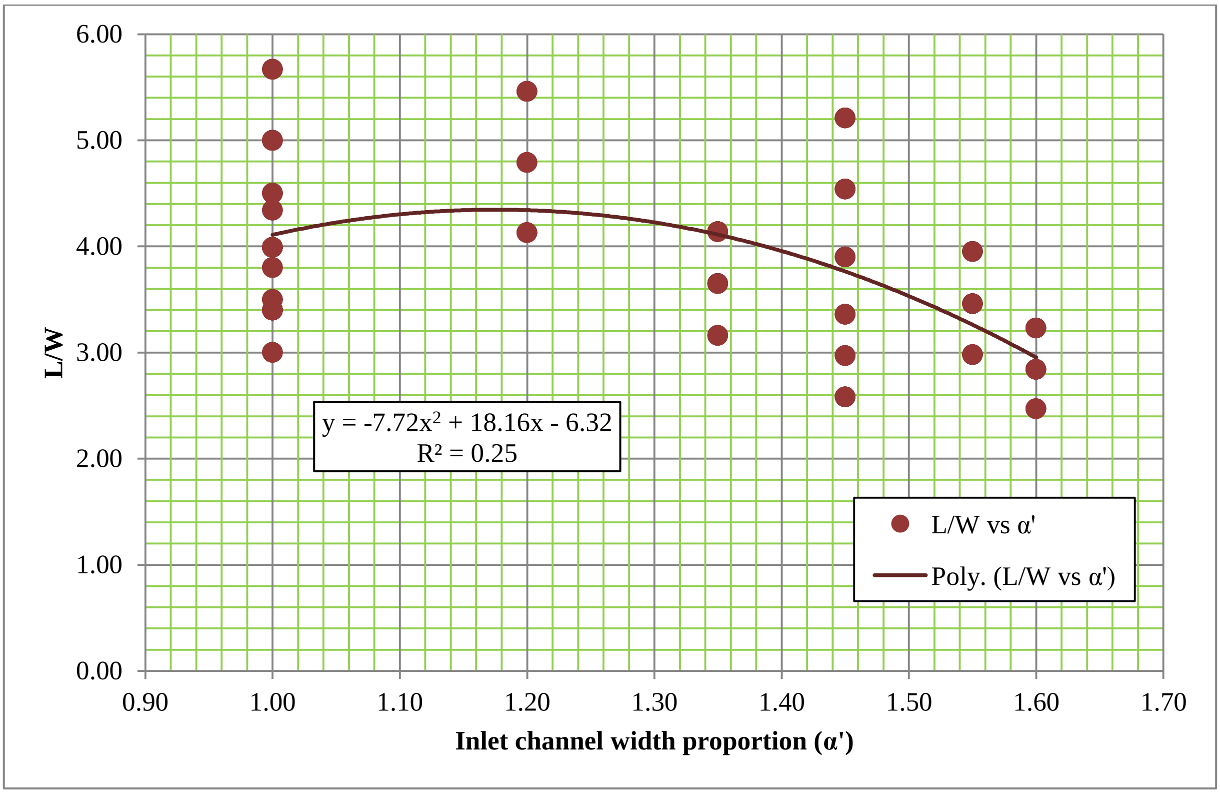

Figure 6.36: L/W vs. Inlet channel width proportion (α') for different model sets

6.5 C_d' vs. W/P_m

The overall width (W) of the weir is an important part of its design. For the purpose of this study, only three varying widths were chosen to determine how this affected the C_d' value. The vertical aspect ratio (W/P_m) is important for the design of PKW's and labyrinth spillways as it determines the number of cycles in a spillway which ultimately affects the C_d' value. Figures 6.37 and 6.38 show the results for the relationship between C_d' and W/P_m for the models with the same B/P_m values, with and without roundings and for $0.5<H_T/P_m<1.0$. Each data set consists of three models (e.g. A1 B1 C1), each model has the same B/P_m ratio with different α' and H_T/P_m values. Table 6.1 shows the B/P_m ratio for each dataset.

Table 6.1: B/P_m ratios for each dataset

Dataset	**B/P_m**
A1 B1 C1	3.00
A2 B2 C2	3.60
A3 B3 C3	3.60
A4 B4 C4	3.60
A5 B5 C5	4.20
A6 B6 C6	3.00
A7 B7 C7	3.60
A8 B8 C8	4.20
A9 B9 C9	3.00
A10 B10 C10	3.60
A11 B11 C11	4.20

Figures 6.37 and 6.38 show C_d' vs. W/P_m for models with and without roundings. The equation for each dataset is highlighted on the left side with the border colour corresponding to the trend line of each dataset.

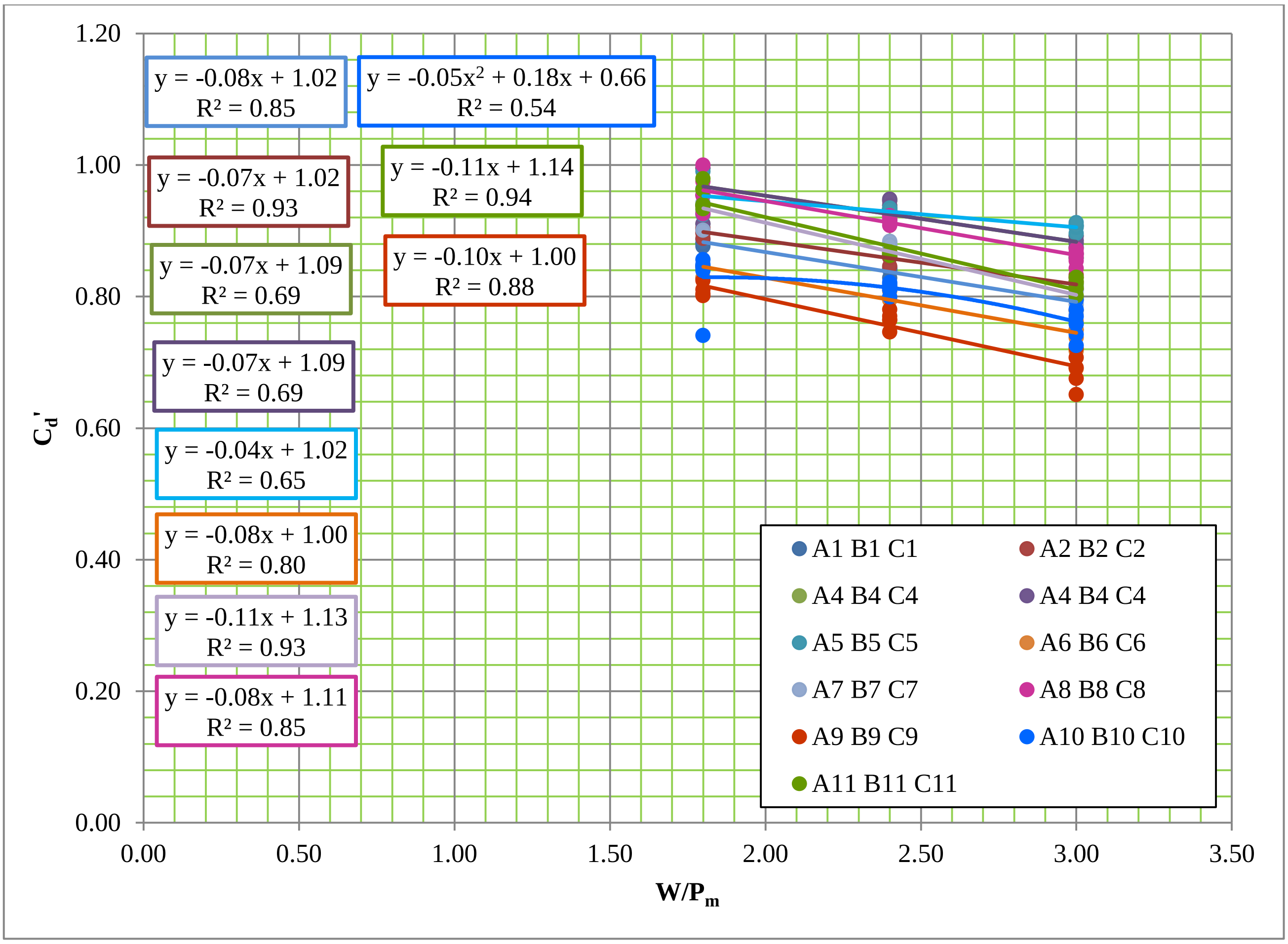

Figure 6.37: C_d' vs. W/P_m for $0.5<H_T/P_m<1.0$with roundings

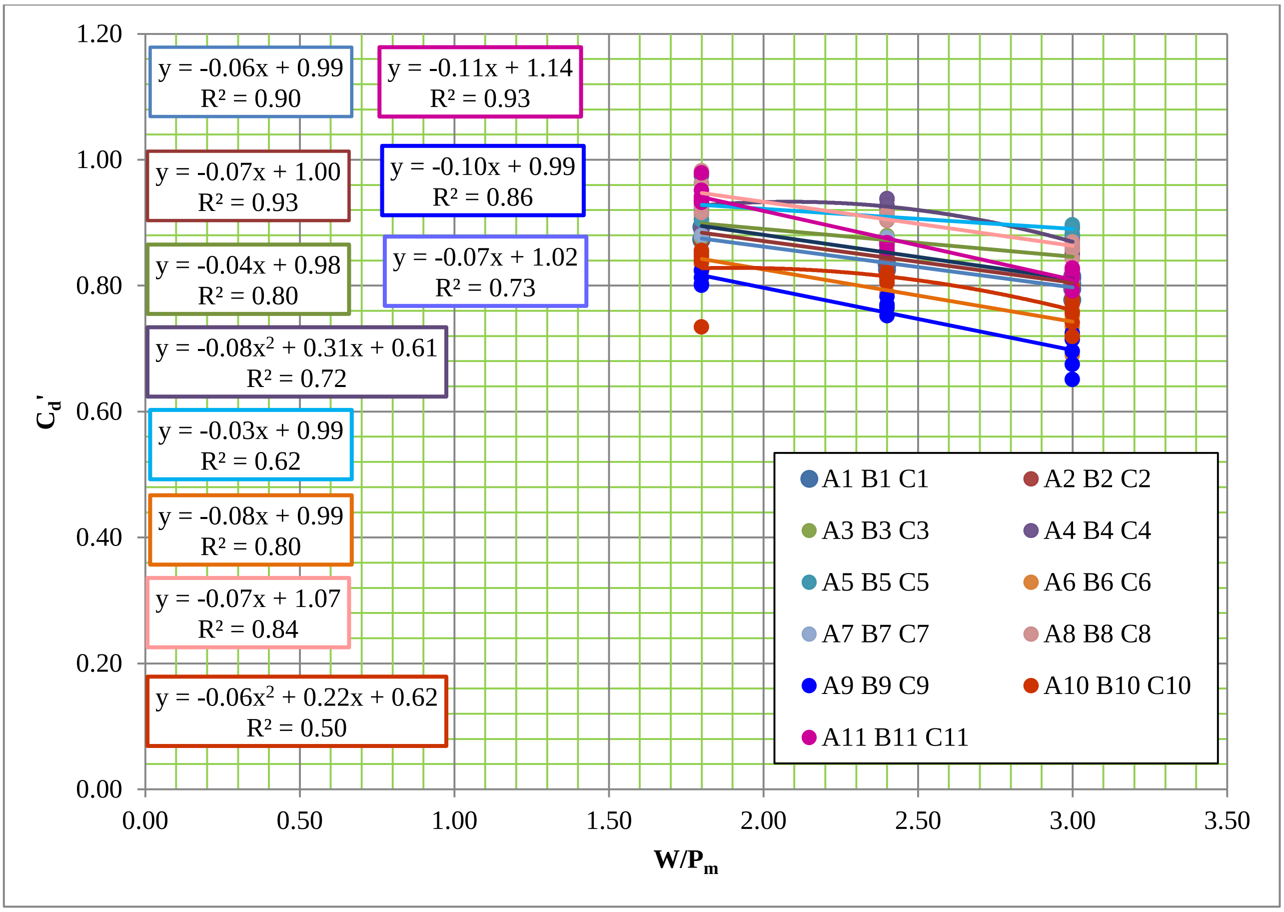

Figure 6.38: C_d' vs. W/P_m for $0.5<H_T/ P_m<1.0$with no roundings

6.5.1 Overall effect of W/P_m

From Figs 6.39 and 6.40 it can be seen that there is a downward trend in the C_d' value as W/P_m increases. The C_d' values are highest when W/P_m is 1.80. In Lempérière's (2011) design, the value of W/P_m was also defined as 1.80. This shows that the vertical aspect (W/P_m) ratio proposed by Lempérière (2011) is the most efficient in terms of C_d'. The coefficient of determination (R^2) for the models with and without roundings lies in the region of 0.50 - 0.94. Most models have a linear relationship between C_d' and W/P_m, with the excepton of models A4 B4 C4 and A10 B10 C10 that have polynomial relationships.

6.6 C_d' vs α' (Inlet channel width proportion)

One of the main objectives of this study was to develop a type of non – linear spillway that combined attributes from both the PKW and the labyrinth spillway. In trying to achieve this, a new layout was proposed. This layout consisted of a trapezoidal shape in plan view with sloped inlet and outlet channels. These combined designs all had an inlet channel width ratio (α') which, as explained in Chapter 3, refers to the opening of the inlet channel (W_{in}). In this section the results from the different combined designs are shown in terms of C_d'. Data were plotted for the three model with $0.5<H_T/Pm<1.0$. Each model set had three varying transversal lengths (B), Figs.6.39 and 6.40 show the C_d' vs. α' (inlet channel width proportion) for models with and without roundings.

The results reflected in Figs 6.39 and6.40, are not as expected. In the initial theory of this new proposed design, it was assumed that having a combined design will prove to have higher discharge capacities and improve hydraulic capacity than either PKW or labyrinth design on their own. It was expected that C_d' would increase based on the increased inlet width (W_{in}). The results from the thirty three model tests show differently. In these results it shows that as the model becomes a combined design (i.e. inlet channel width proportion (α') moves past 1), C_d' becomes lower. This indicates that the combined design with tapered walls and sloping channel floors does not improve C_d'.

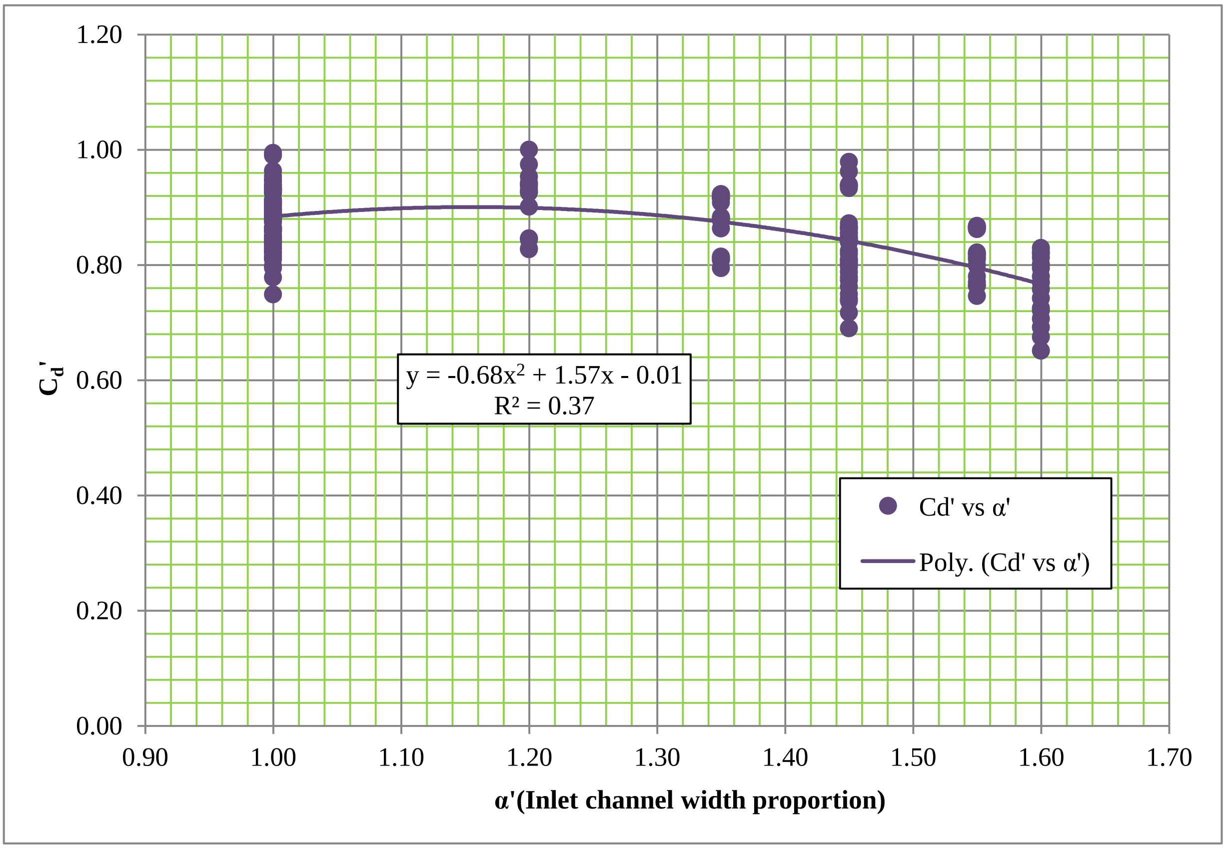

Figure 6.39: C_d' vs. α' (Inlet channel width proportion) for $0.5<H_T/P_m<1.0$ with roundings

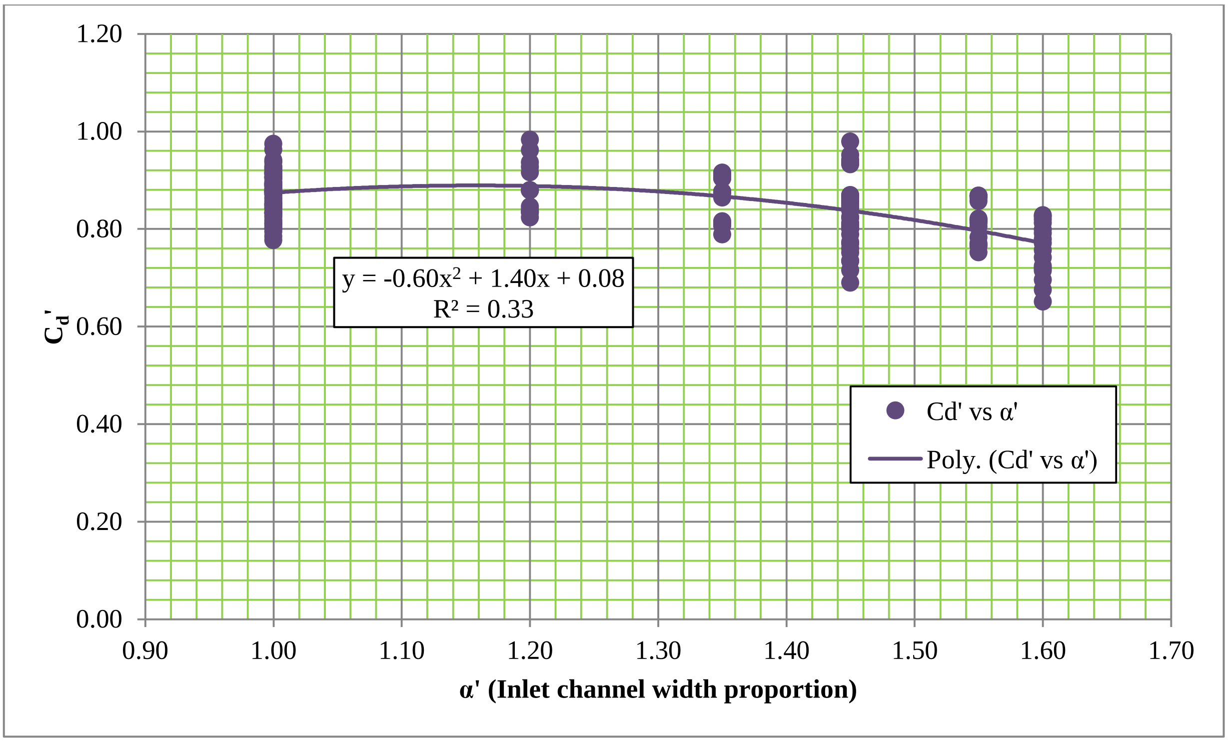

Figure 6.40: C_d' vs. α' (Inlet channel width proportion) for $0.5<H_T/P_m<1.0$ with no roundings

Figures 6.39and6.40show a descending trend for C_d' in terms of the inlet channel width proportion (α'). As the models inlet width (W_{in}) is increased,C_d' is decreased. These results proved different to the hypothesised results. In the inception of this study it was assumed that increasing the inlet channel width proportion from 1.00 would result in an increase in C_d' up to a certain extent.

After deliberating on what could be changed to improve the performance it was decided to adjust the floor orientation of the incoming and outgoing channels. Since the feasibility study of Tzaneen Dam raising was the stimulus for conducting this study, it was scrutinized to find out how the discharge coefficient could be further improved. From this study it was found that combining the PKW and labyrinth spillways result in a reduced flow area on the outlet channel due to the sloping floors. This was overcome by having a combined horizontal and sloping floor in the Tzaneen Dam study creating a chance for a parapet wall at the edge of the incoming channel crest based on the change in floor slope (see Fig. 6.42).

For this additional exercise, only three models were considered. These were models B3, B7 and B10. In order to calculate how the new orientation of the floors should look, the slopes of the floors were plotted for each of these models based on a constant velocity with respect to head over the spillway (Fig. 6.41). This was done since the overall idea for the labyrinths and PKW designs is to have a constant flow velocity over the spillway, having the combined design with tapered walls defied this ideal. With the taper in the walls, there is less flow area, which results in increased velocity over the weir and less flow depth. In order to keep this velocity constant, even with the taper in the sidewalls, the floor needed to be changed. Once it was known how the floors should be sloped in order to achieve a constant velocity over the spillway, a new design was attained. This design consisted of a horizontal section in the floors for the inlet and outlet channels. Fig 6.42 shows the side view of the new design with combined horizontal and sloped floors.

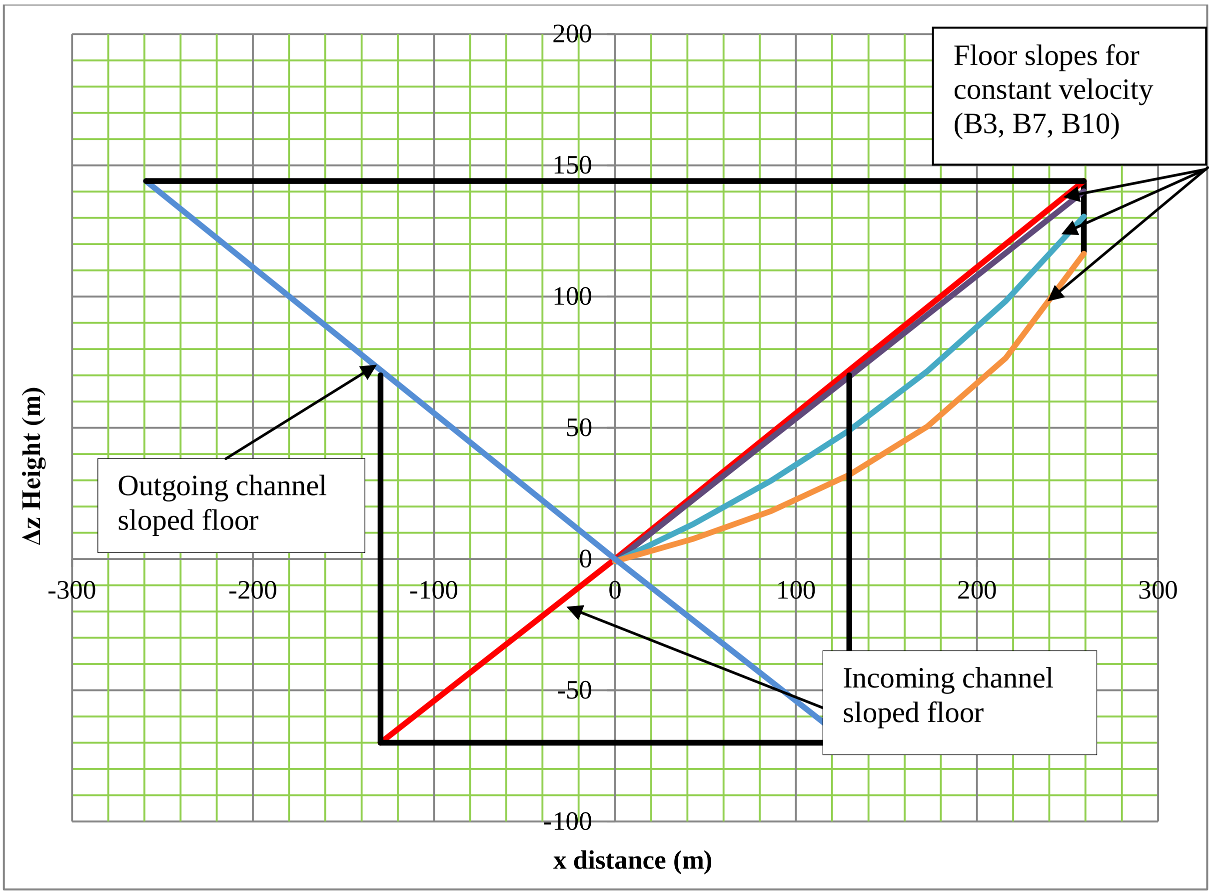

Figure 6.41: Slopes of floors showing the orientation for models B3, B7 and B10 based on a constant velocity over the spillway

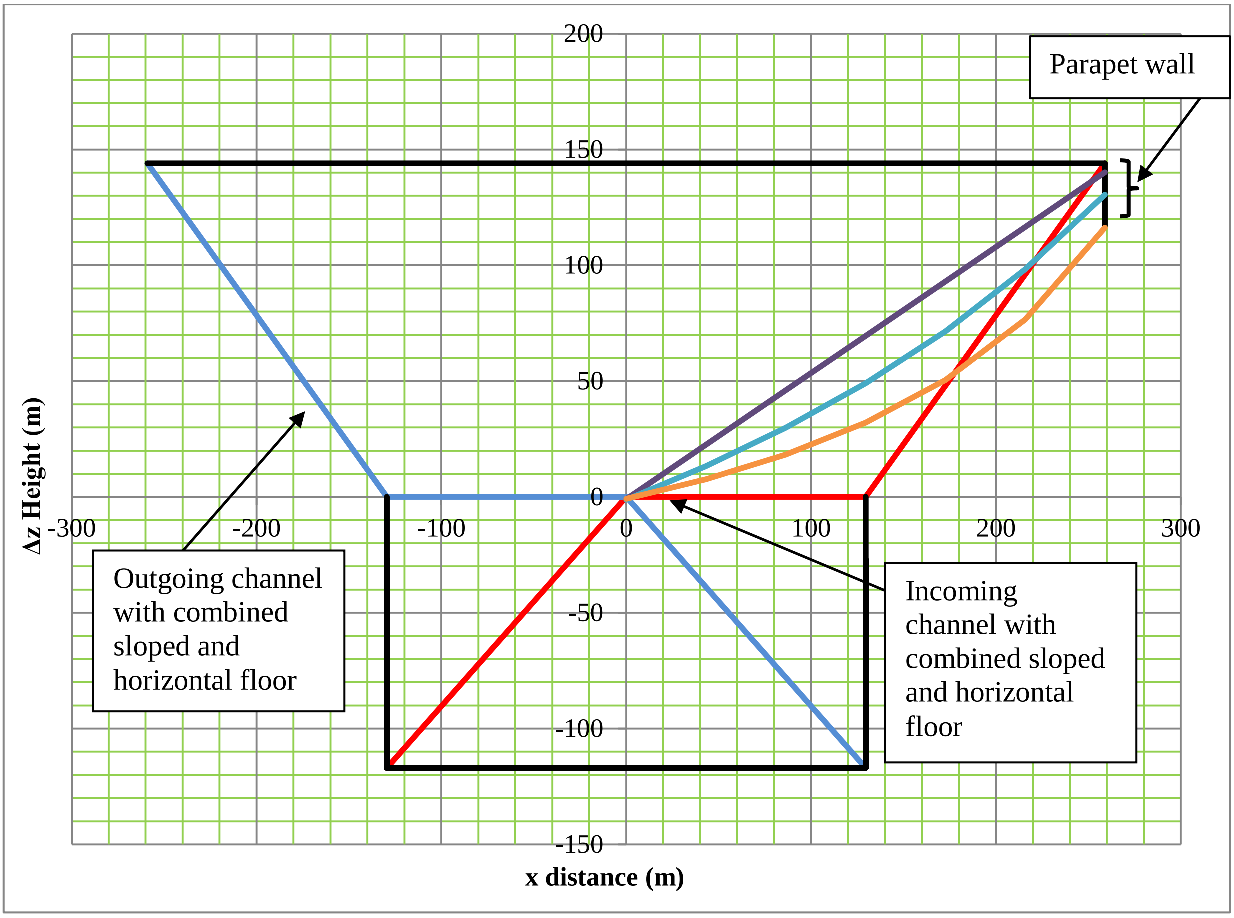

Figure 6.42: New design accommodating floor slopes by combining horizontal and sloping floors orientation

The results for this new design for H_T/P_m = 0.5 and H_T/P_m = 1.0are shown in Fig. 6.43. Since H_T/P_m = 0.5 and H_T/P_m = 1.0 are the minimum and maximum of the range that was investigated; only these were considered for this case.

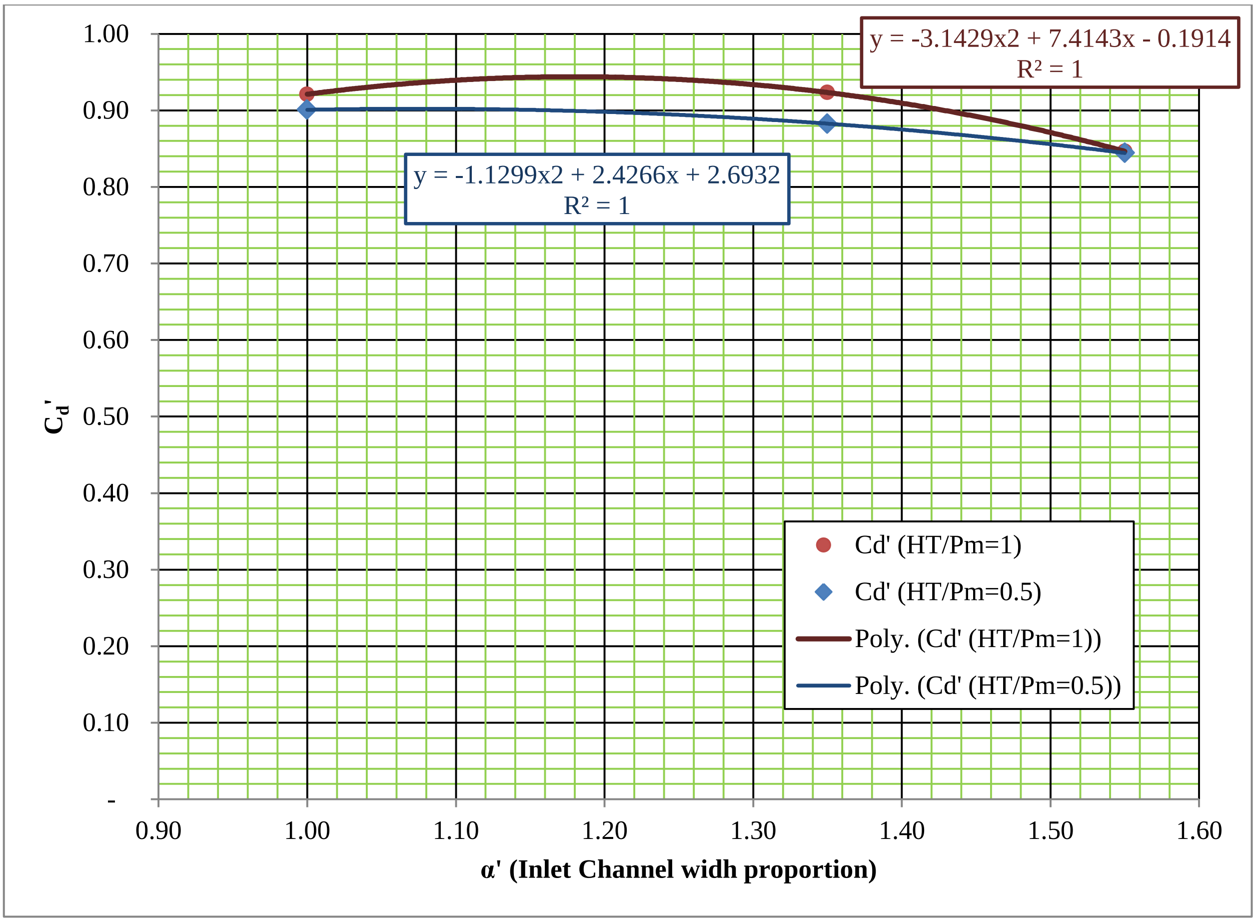

Figure 6.43: C_d’ vs. α’ (Inlet channel width proportion) for new floor design

The results from this new design are not much different from those previously noted. The main difference is shown for the inlet channel width between 1.00 and 1.35. Here it can be seen that there is possibility for an increase in C_d’. After this, C_d’ drops again as the channel width proportion is increased to 1.55. However, since only 5 changes altogether (i.e. for all models considered and not just the adjusted ones in Fig. 6.43)in the inlet channel width proportion (α’)were considered for this study, it is possible that more variations could result in the desired output.

Since this new design was only applied to three models the data are a bit sparse. If more data points were taken, this would have given more accurate results particularly in the section between the inlet channel width proportion of 1.00 and 1.35. Therefore, no conclusions can be drawn in this regard as there are not enough data between the inlet channel width proportion of 1.00 and 1.35. Themain conclusion that can be drawn presently is that the C_d’ value certainly gets lower as soon as the inlet channel width proportion has passed 1.35.

6.7 C_d' vs W_{in}/W

In section 6.6, the effect of the inlet channel width proportion (α') was discussed; this proportion results in changes of the inlet width therefore resulting in changes in the W_{in}/W ratio. Since the inlet channel width proportion (α') together with other parameters affects the discharge coefficient C_d', W_{in}/W also affects C_d'. There is a constant change in the L/W ratio and W_{in}/W based on the changing inlet channel width proportion (α') as well as the B/P_m and W/P_mratios. The results for C_d' vs. W_{in}/ W for models with and without roundings and for $0.5<H_T/P_m<1.0$ is shown in Figs. 6.44 and 6.45.

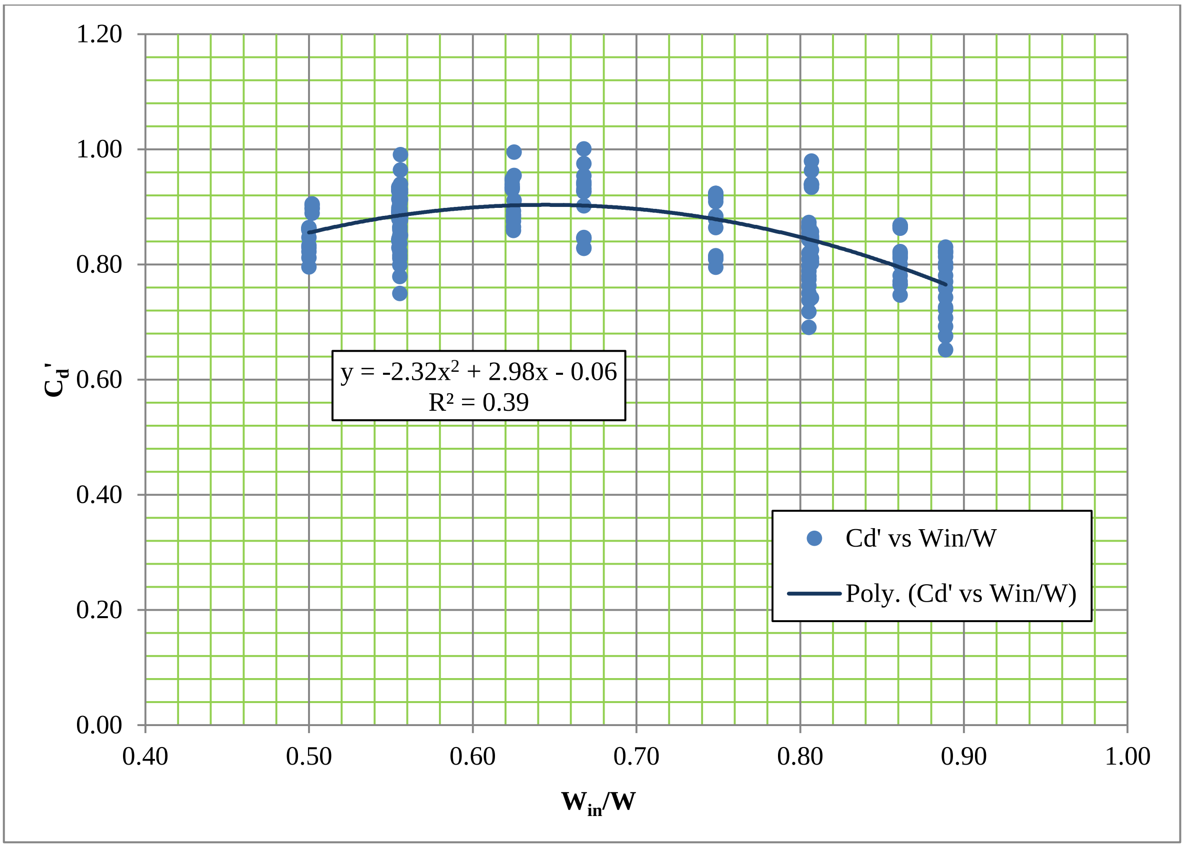

Figure 6.44: C_d' vs. W_{in}/W for $0.5<H_T/P_m<1.0$ with roundings

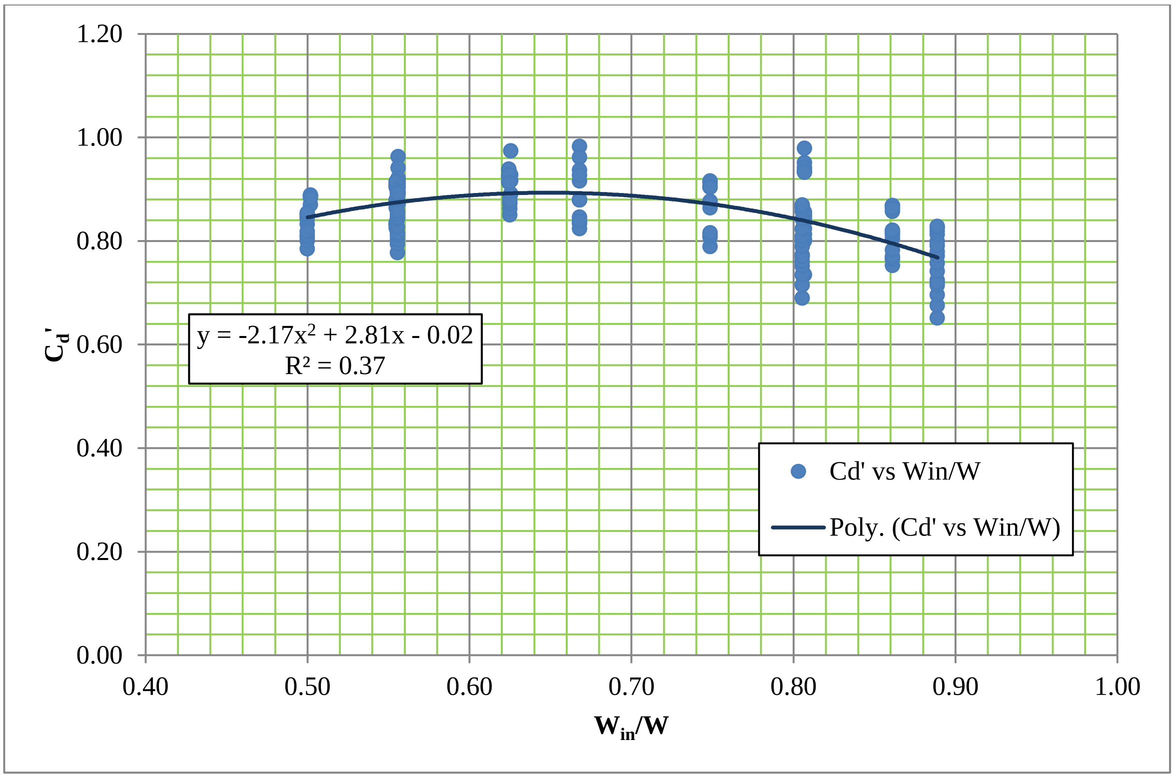

Figure 6.45: C_d' vs. W_{in}/W for $0.5<H_T/P_m<1.0$ with no roundings

From Figs 6.44 and 6.45 it can be seen that as W_{in}/W increases, C_d' also increases until it reaches a W_{in}/W of 0.67 after which it decreases. Therefore, having a high W_{in}/W ratio can result in lowered C_d' values. Models with a W_{in}/W ratio of 0.67 are the combined design models with an inlet channel width proportion (α')of 1.20. Models with higher inlet channel width proportions have a lower C_d'. Models with a PKW design and an inlet channel width proportion of 1 have increasing C_d' values. The vertical shift in the data points for each W_{in}/W ratio is due to the changing B/P_m, W/P_m and α' values.

6.8 C_d'vs. B/P_m

Another geometric parameter that was varied for each model dataset was the B/P_m ratio. B/P_m had three values for each model dataset (i.e. B/P_m = 3.0, 3.6 and 4.2). For each set the W/P_m ratio was kept constant and B/P_m and α' varied. The B/P_m ratio has a greater effect on the L/W ratio, the longer the transversal length (B), the larger the L/W ratio. This is an important part of the design of a PKW or labyrinth spillway as it determines the overhang of the spillway as well as the volume of concrete that will be used.

The results for C_d' vs. B/P_m are shown in Figs. 6.46 and 6.47. These results are for $0.5<H_T/P_m<1.0$ and for models with and without roundings.

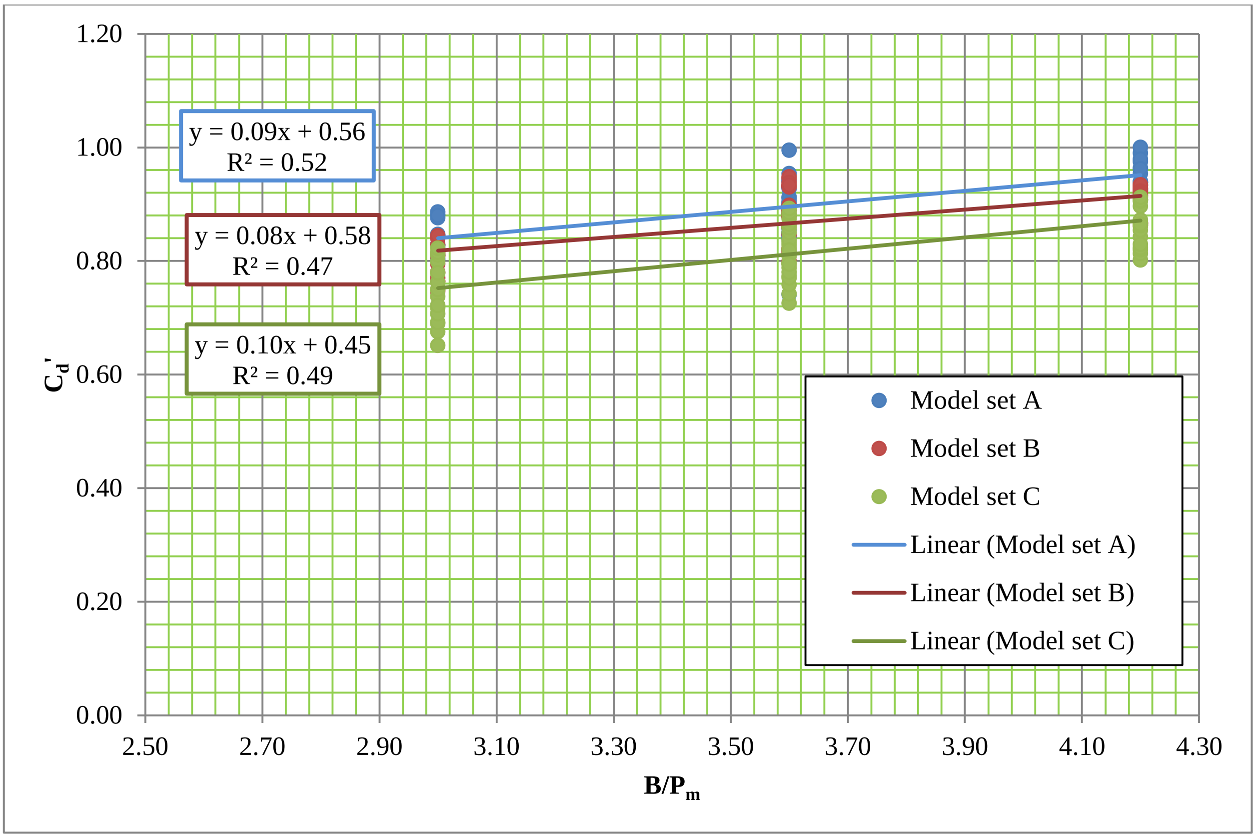

Figure 6.46: C_d' vs. B/P_m for $0.5<H_T/P_m<1.0$ with roundings

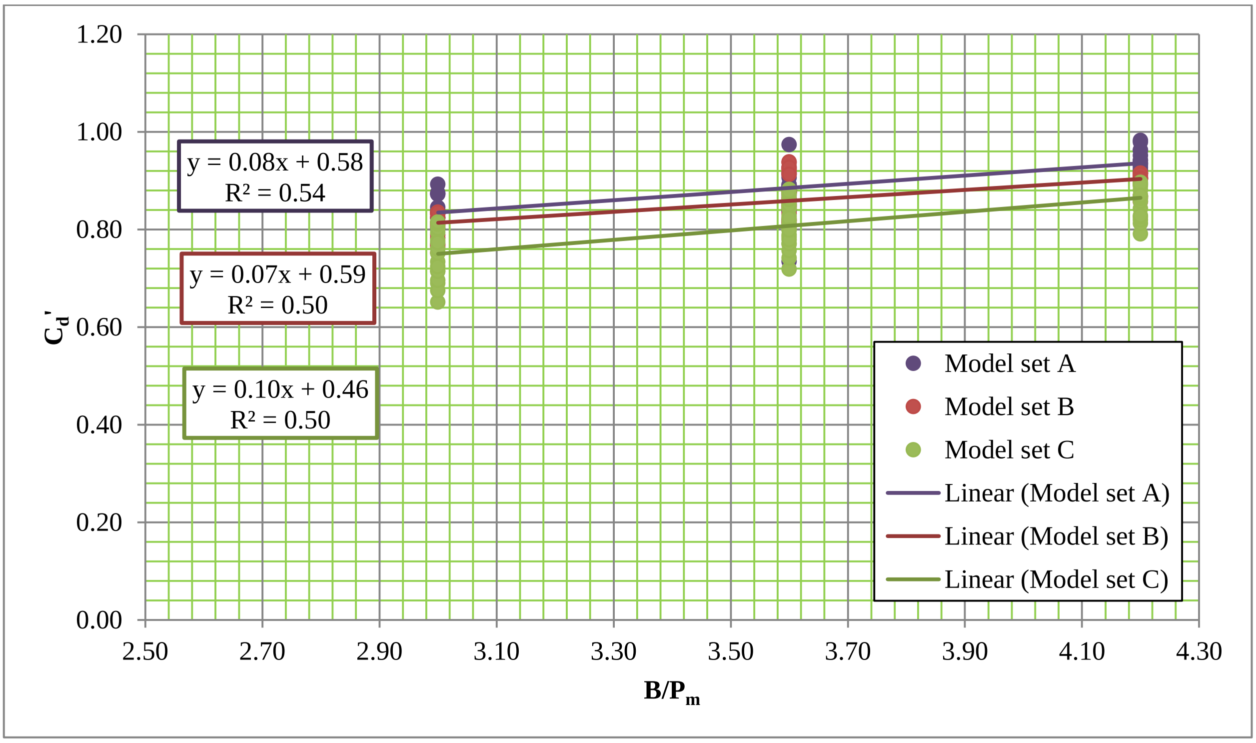

Figure 6.47: C_d' vs. B/P_m for $0.5<H_T/P_m<1.0$ with no roundings

Figures 6.46 and 6.47 show that as B/P_m increases, C_d' increases. Since B/Pm is directly linked to the L/W ratio, as previously mentioned, this matches with the data from section 6.4 where Figs. 6.34 and 6.35 showed that C_d' increases with increasing L/W ratios. It is also evident that as the W/P_m value increases for each model dataset (i.e. Model sets A, B and C), C_d' gets lower. Model sets with a higher α' value (i.e. Model sets B and C) also had lower C_d' values with respect to B/P_m. The vertical shift in data points is due to the changing inlet channel width proportion (α').

6.9 Predictive equations for C and C_d'

In order to quantify the discharge coefficient (C_d') as well as the coefficient representative of discharge (C), the parameters that were discussed in the previous sections were combined to provide and propose an analytical formulation for C and C_d'. As seen in sections 6.2 – 6.8, the factors that affect the C_d' value according to this study are H_T/P_m, L/W, W/P_m, α' (inlet channel width proportion), W_{in}/W and B/P_m.

Since C_d' and C are dependent on these six geometric parameters, an extension of linear regression, known as multiple regression was used to predict the values of C_d' and C based on the values of H_T/P_m, L/W, W/P_m, α' (inlet channel width proportion), W_{in}/W and B/P_m for models with and without roundings.

The comparison of the final analytical formulation for C and C_d' with the experimental results obtained in the 33 models that were considered in this study is shown in section 6.9.1 and 6.9.2.For most configurations, the error does not exceed 10 %.

6.9.1 $C_d'_{predicted}$ vs. $C_d'_{measured}$

Figs 6.48 – 6.49 show the comparison of the formulation for C_d' with the experimental results. The formulation for the prediction of C_d' proposed in this study for $0.5<H_T/P_m<1.0$ for models with and without roundings are shown in Eq.'s 6.1 – 6.2respectively.

$$C_d' \; (with\; roundings) = e^{-0.84}\left(\frac{B}{P_m}\right)^{-0.03}\left(\frac{W}{P_m}\right)^{0.25}\left(\frac{L}{W}\right)^{0.53}\left(\frac{H_T}{P_m}\right)^{0.03}\left(\frac{W_{in}}{W}\right)^{0.33}(\alpha')^{-0.35} \tag{6.1}$$

$$C_d' \; (no\; roundings) = e^{-0.96}\left(\frac{B}{P_m}\right)^{-0.16}\left(\frac{W}{P_m}\right)^{0.36}\left(\frac{L}{W}\right)^{0.66}\left(\frac{H_T}{P_m}\right)^{0.03}\left(\frac{W_{in}}{W}\right)^{0.34}(\alpha')^{-0.28} \tag{6.2}$$

The coefficient of determination (R^2) between the measured and predicted data for the whole data setis 0.85 and 0.84 for models with and without roundings respectively. For most configurations the error does not exceed 10%. The results for models with and without roundings are shown in Figs 6.48and 6.49.

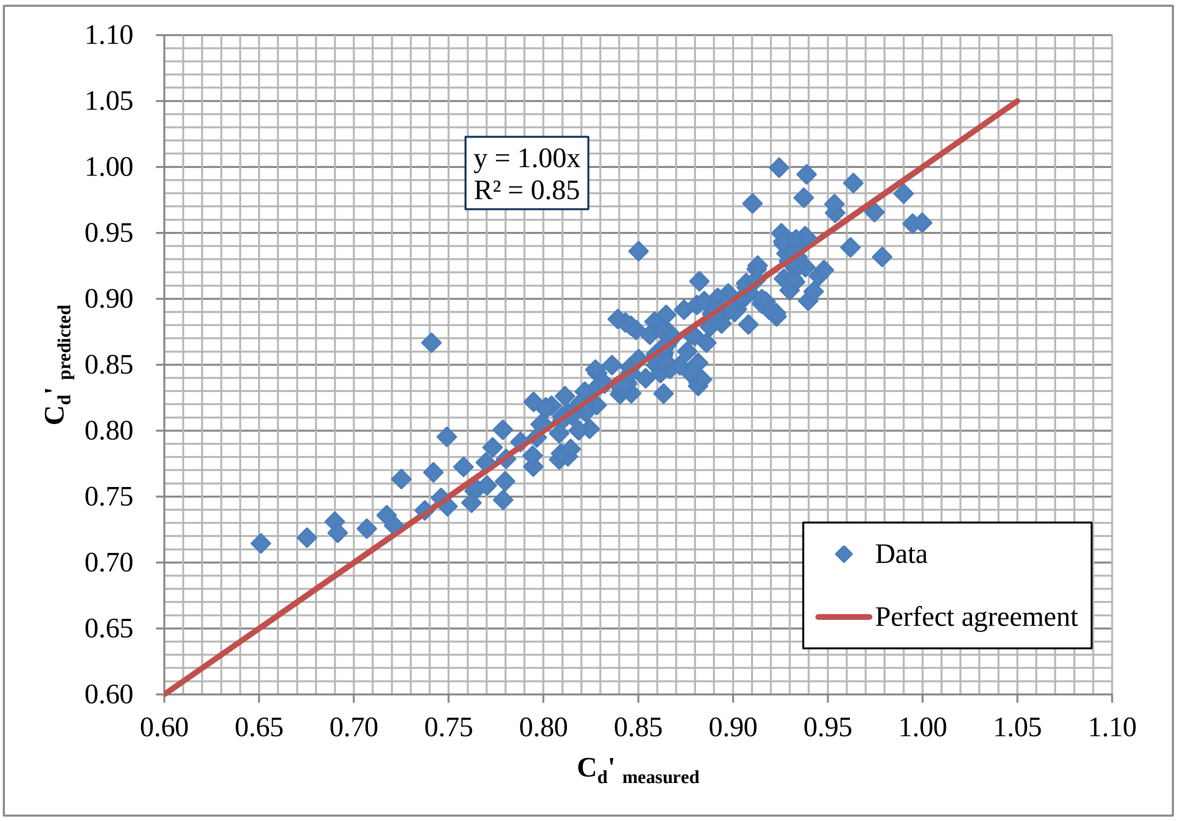

Figure 6.48: Comparison of C_d' values computed with the analytical formulation proposed in this study and the experimental results obtained for models with roundings

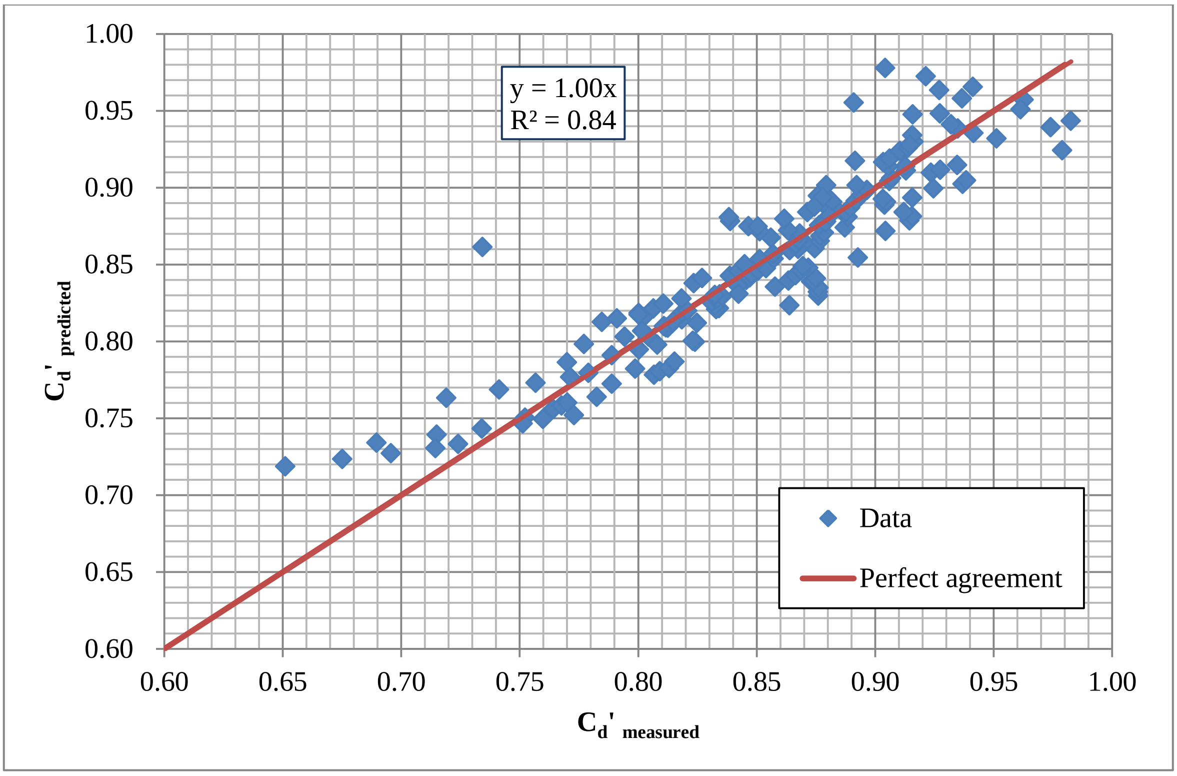

Figure 6.49: Comparison of C_d' values computed with the analytical formulation proposed in this study and the experimental results obtained for models with no roundings

From Figs 6.48 and 6.49 it can be seen that the results for models with roundings show better correlation with a higher coefficient of determination (R^2 =0.85). There is also less scatter in the data with roundings.

6.9.2 $C_{predicted}$ vs. $C_{measured}$

Since the relationship between C and C_d' has already been defined in Chapter 5 as Eq. 5.4, the formulation for the prediction of C is developed the same way. Therefore, the formulations proposed in this study for the prediction of C are as follows:

$$C\ (with\ roundings) = (\sqrt{2g})e^{-0.84}\left(\frac{B}{P_m}\right)^{-0.03}\left(\frac{W}{P_m}\right)^{0.25}\left(\frac{L}{W}\right)^{0.53}\left(\frac{H_T}{P_m}\right)^{0.03}\left(\frac{W_{in}}{W}\right)^{0.33}(\alpha')^{-0.35} \quad (6.3)$$

$$C\ (no\ roundings) = (\sqrt{2g})e^{0.96}\left(\frac{B}{P_m}\right)^{-0.16}\left(\frac{W}{P_m}\right)^{0.36}\left(\frac{L}{W}\right)^{0.66}\left(\frac{H_T}{P_m}\right)^{0.03}\left(\frac{W_{in}}{W}\right)^{0.34}(\alpha')^{-0.28} \quad (6.4)$$

The coefficient of determination (R^2) between the measured and predicted data for the whole data set is 0.85 and 0.83 for models with and without roundings respectively. For most configurations the error does not exceed 10%. The results for models with and without roundings are shown in Figs 6.50 and 6.51.

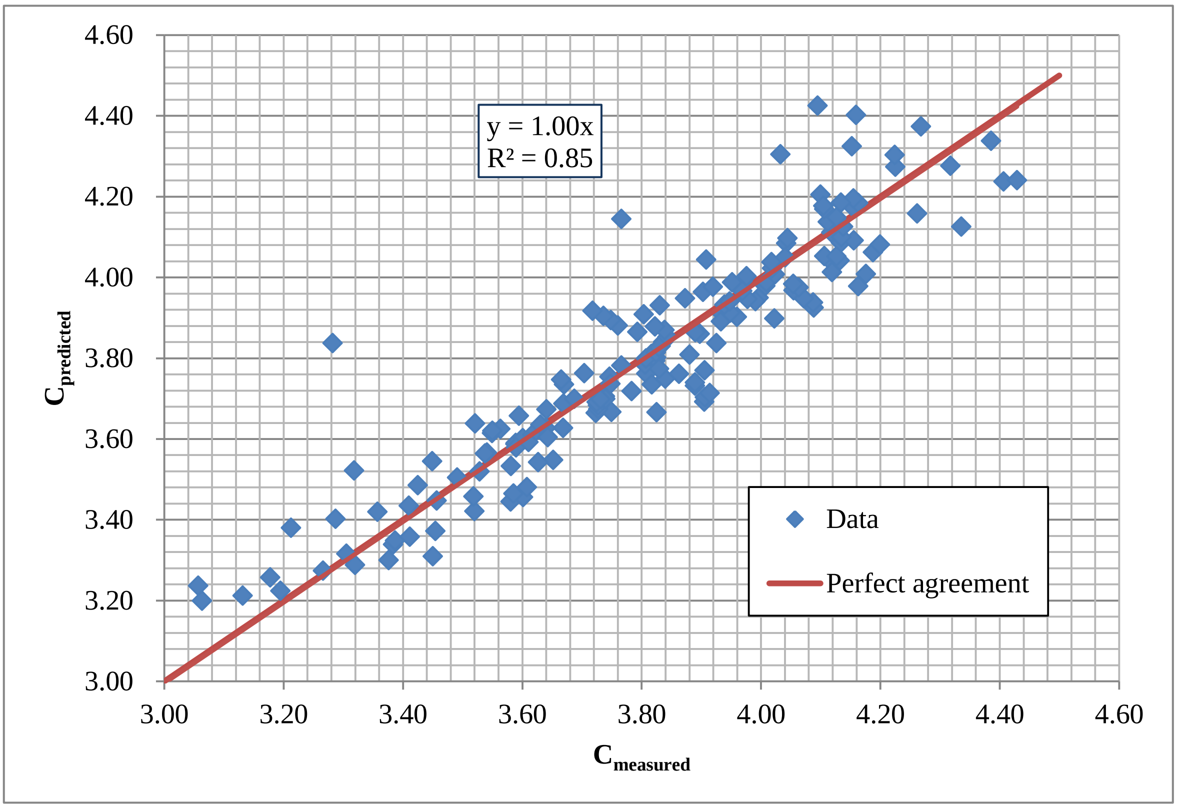

Figure 6.50: Comparison of C values computed with the analytical formulation proposed in this study and the experimental results obtained for models with roundings

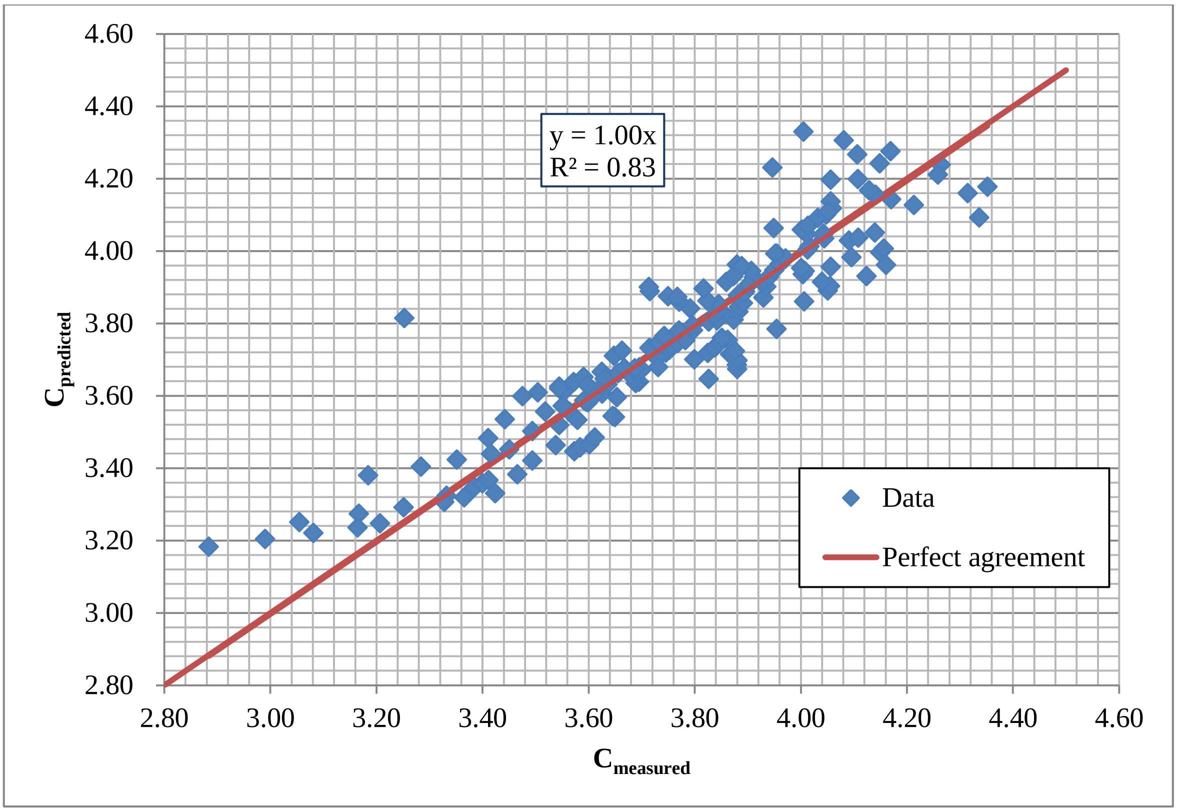

Figure 6.51: Comparison of C values computed with the analytical formulation proposed in this study and the experimental results obtained for model with no roundings

From Figs 6.50and 6.51 it can be seen that for the models with and without roundings, the coefficient of determination is the same for C and C_d'.The scatter of the data is also similar. In the case with roundings, the coefficient of determination (R^2) is higher indicating better correlation for this dataset compared to the dataset with no roundings.

It must be noted that the proposed formulations for the prediction of C and C_d' in this study are based only on the variability of H_T/P_m, L/W, W/P_m, α' (inlet channel width proportion), W_{in}/W and $B/P_{m.}$ The thickness of the walls was not included as it was kept constant for all thirty three models.

7 ECONOMIC SUITABILITY

One of the objectives of this study was to look at the economic viability of both designs used in the study. From the models that were built, the designs consisted of those with standard PKW designs and those with combined labyrinth and PKW designs. Each design had different geometric features that were adjusted iteratively to compare the differences. From these designs, three were chosen to do a cost comparison.

For the purpose of this study, cost was related to volume of concrete required for construction. Table 7.1 contains the volume requirement based on the walls and floors of each model.

Table 7.1: Volume requirement based on floors and walls for models A3, A7 and A10

Model	**Inlet channel width proportion**	**Volume requirement (x10^{-3} m^3)**
A3 (standard PKW)	1.00	4.16
A7 (combined design)	1.20	4.07
A10 (combined design)	1.45	3.96

From the data in Table7.1, it can be seen that having a combined design can reduce the concrete volume requirement which in turn will reduce the concrete costs. It can also be seen that as the inlet channel width requirement increases, the concrete volume requirement gets less. Therefore tapering the model to a large extent can prove to be quite economically favourable.

Using this together with the data acquired in Chapter 6 for the C_d' value and L/W ratios can help in selecting an optimal design.

For example, looking at model A7, it has its highest C_d' value of 0.94 with roundings under the upstream overhang at an H_T/P_m ratio of 0.77 (Fig. 7.2 (red arrows)). When looking at an H_T/P_m = 1.00, it has a C_d' of0.93 and an L/W ratio of 4.79 (see Fig. 7.1). This can work as an optimal solution since the discharge coefficient is favourable, the L/W ratio is not too high and the concrete volume is lower than that of a standard PKW. The hydraulic efficiency is also indicated by the discharge rating curve and shows how close the results (in terms of reduced total head (H_T)) come to that of Lempérière's (2011) optimal design (Eq. (2.1)) for PKW's (see Fig. 7.3).

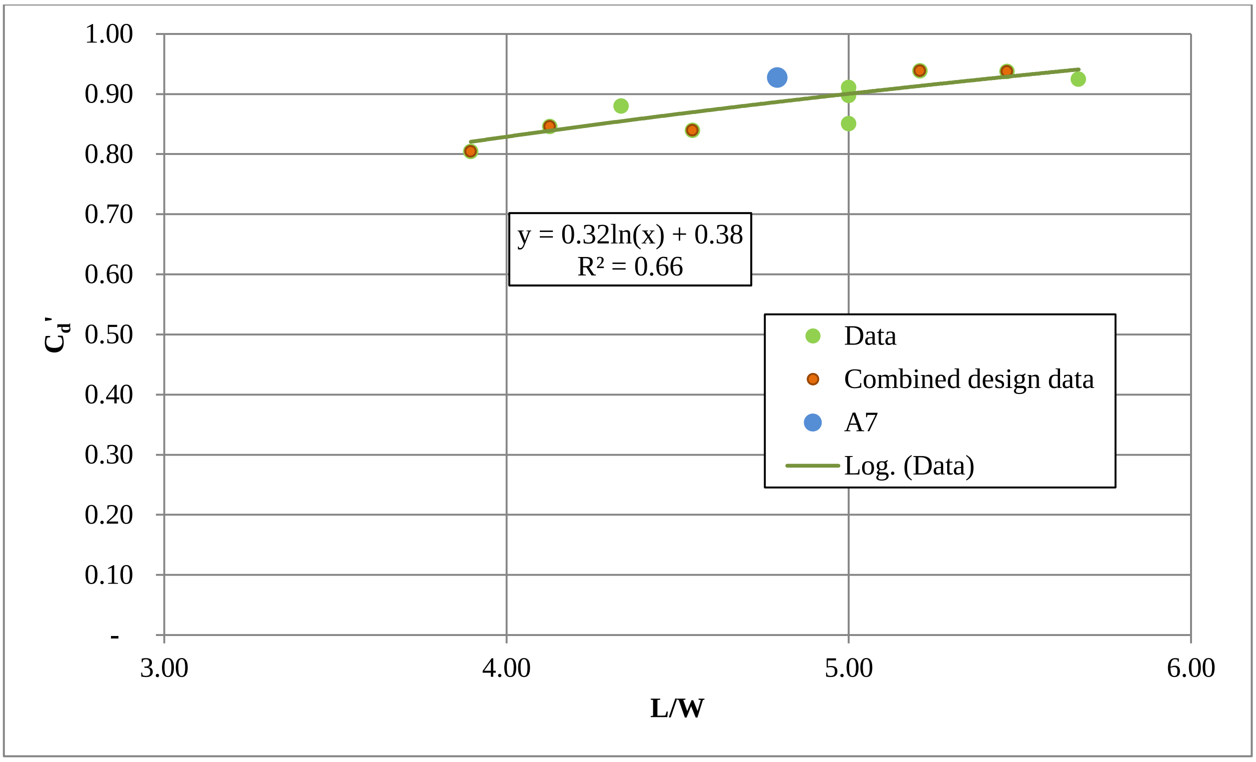

Figure 7.1: C_d' vs L/W for model A7 of model set A with roundings and H_T/P_m =1.00

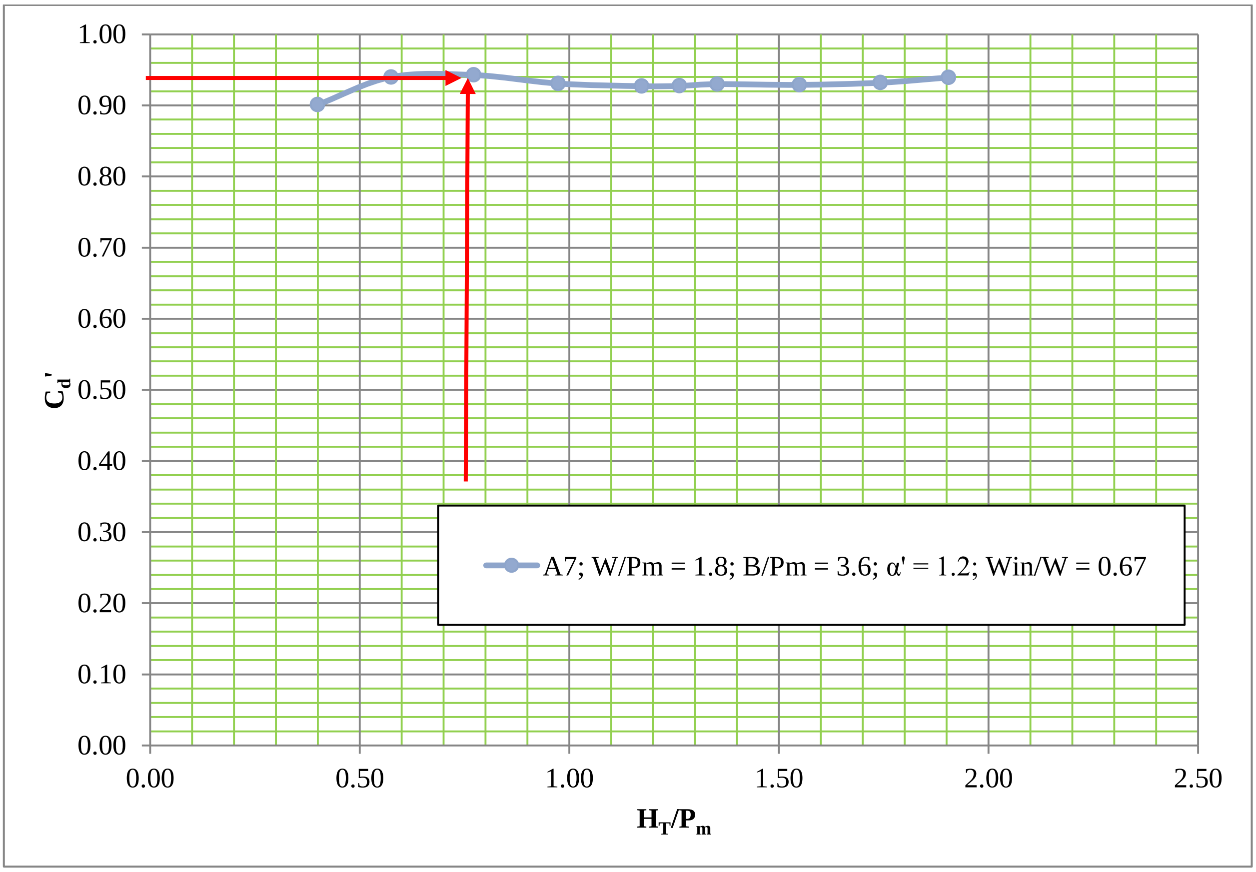

Figure 7.2: C_d' vs H_T/P_m for model A7 with roundings

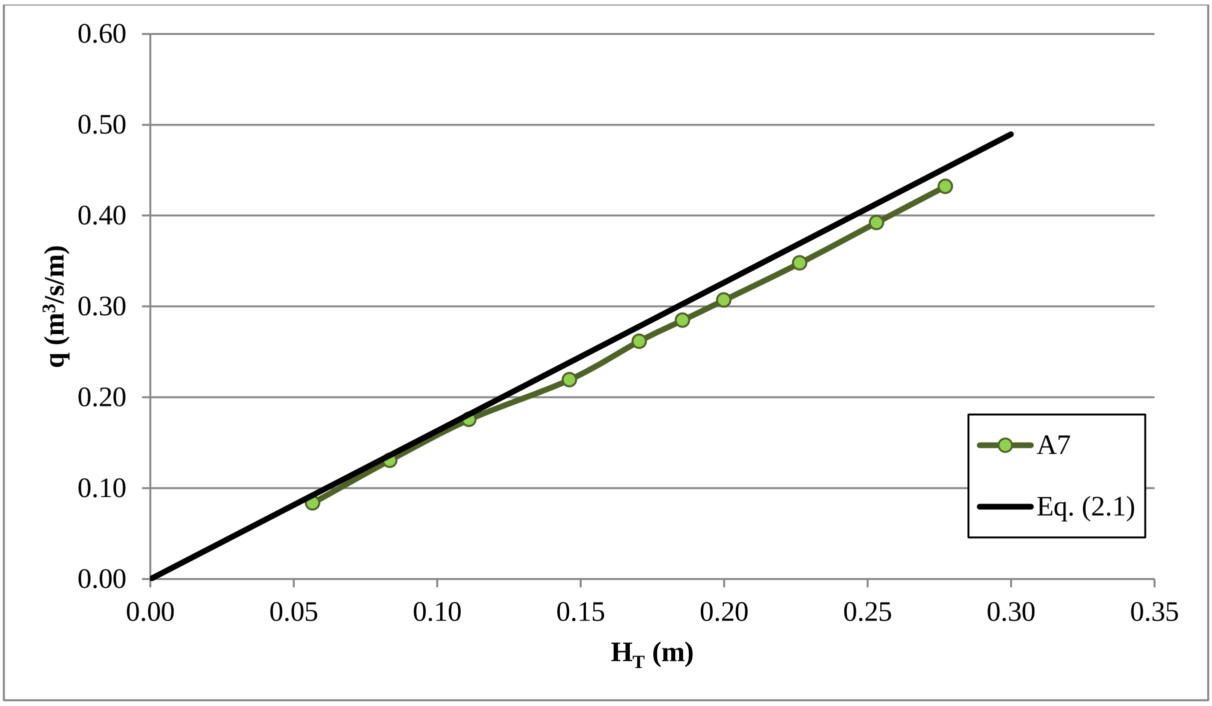

Figure 7.3: Head - discharge curve for model A7

These new combined designs give the options to choose differently based on the requirements of a project. If a project is cost driven, a lower L/W ratio can be used with a reduced C_d' that is still hydraulically acceptable. If the hydraulics is a driving force, C_d' can be chosen and matched to a required L/W ratio that lies within an acceptable region or alternatively a standard PKW design can be applied.

Using the graphs given in Chapter 6 for the L/W and C_d' values together with the designs developed in Chapter 3 can help any designer choose appropriately for new or rehabilitation projects. The main design decisions being the choice of spillway (either standard PKW or combined design); the W/P_m and B/P_m ratios; the thickness of the walls (t_w) (which will in turn help determine the P_m value); the inlet channel width proportion (α'); the discharge coefficient (C_d') or coefficient representative of discharge (C) based on the flow requirements and geometric features; and the L/W and H_T/P_m values that will result from the other parameters chosen.

8 CASE STUDY

8.1 Tzaneen Dam

A model study undertaken during the feasibility study for the raising of Tzaneen Dam explored both labyrinth and PKW spillways. This study also looked into the option of a combined labyrinth and PKW spillway. Details of this dam are as follows:

- Location: Limpopo province, 3km outside of Tzaneen
- Current ogee level (FSL): 723.97 masl
- Crest length : 1140 m
- Catchment size: 652 km^2
- Spillway length : 91.44 m
- Current spillway configuration is an uncontrolled Ogee

Different options were considered for this raising. The most favoured option from the model tests conducted was the combined design. This combined design had a combination of tapered/trapezoidal walls together with horizontal and sloping floors (Figs. 8.3 & 8.4).

Various physical models helped establish a basic trend line for the coefficient representative of discharge (C) in terms of the length-to-width ratio (L/W). This logarithmic relationship was developed($y = 0.95\ln(x) + 2.5$) to achieve a coefficient of determination $R^2 = 1$ and is shown in Fig. 8.1.

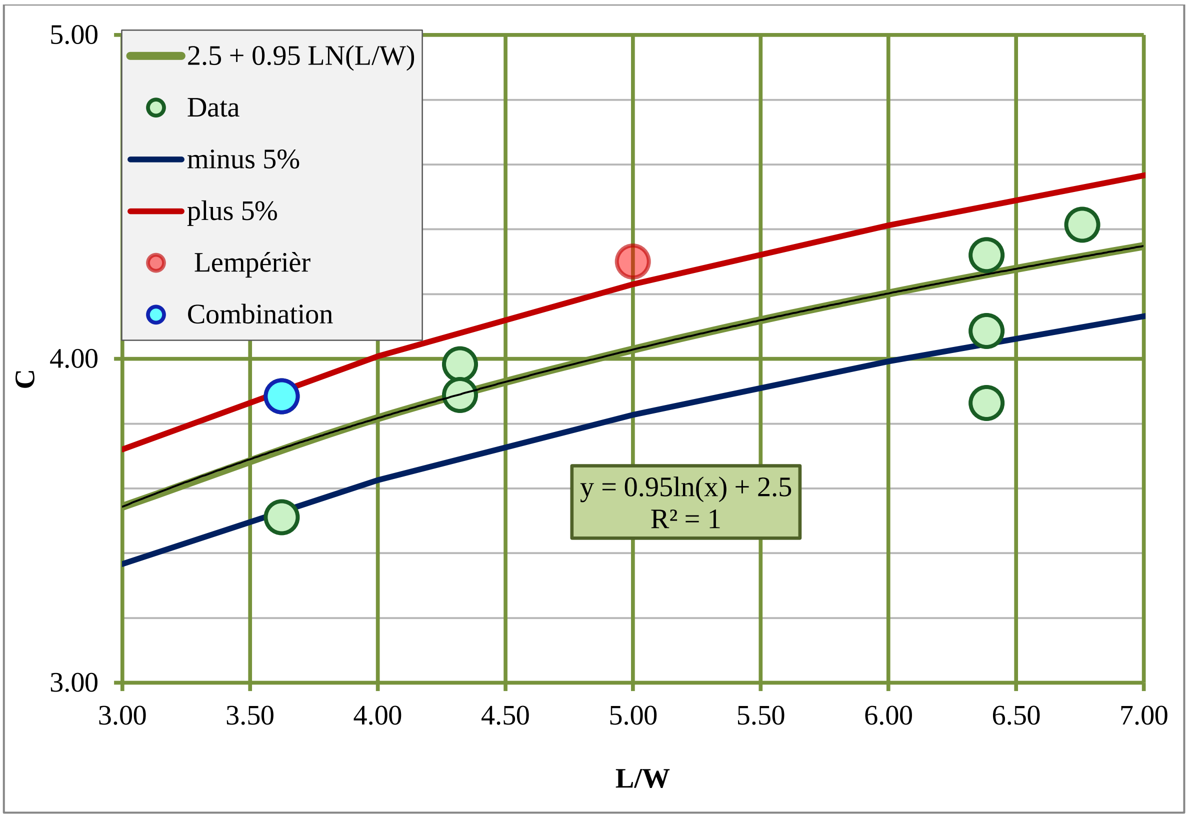

Figure 8.1: Results for models tests showing logarithmic relationship between L/W and C

This relationship was developed from the model tests in order to show how the Cvalues were obtained using the head (H_T) for q = 40 m^3/s/m for all layouts.

The data in Fig. 8.1 shows some scatter. This is based on the various geometries of the models tested. The variations in geometry were the addition of roundings at the inlet under the upstream overhang, roundings of the crest, floor orientation, standard PKW designs as well as the combined PKW and labyrinth design. The red and blue curves indicate a plus and minus 5 % region respectively. Certain geometric features like rounding of the crest and inlet walls are useful in reducing the required head but remain in the ±5 % range.

This ±5 %envelope shows the tolerance for well-constructed and poorly constructed models.

In this case study it was found that the advocated L/W ratio of 5.00 according to Lempérièr (2011) was too elaborate to be the optimum layout for this project. This was due to the cost, with an L/W ratio of 5, the wall length required was high resulting in higher concrete costs. It was found that an L/W of 3.6 was most appropriate for the raising of Tzaneen Dam, and that a labyrinth (trapezoidal) type plan layout can be utilised effectively to avoid the intricate roundings associated with the standard PKW layout. The results from the models tests are shown in Fig. 8.2.

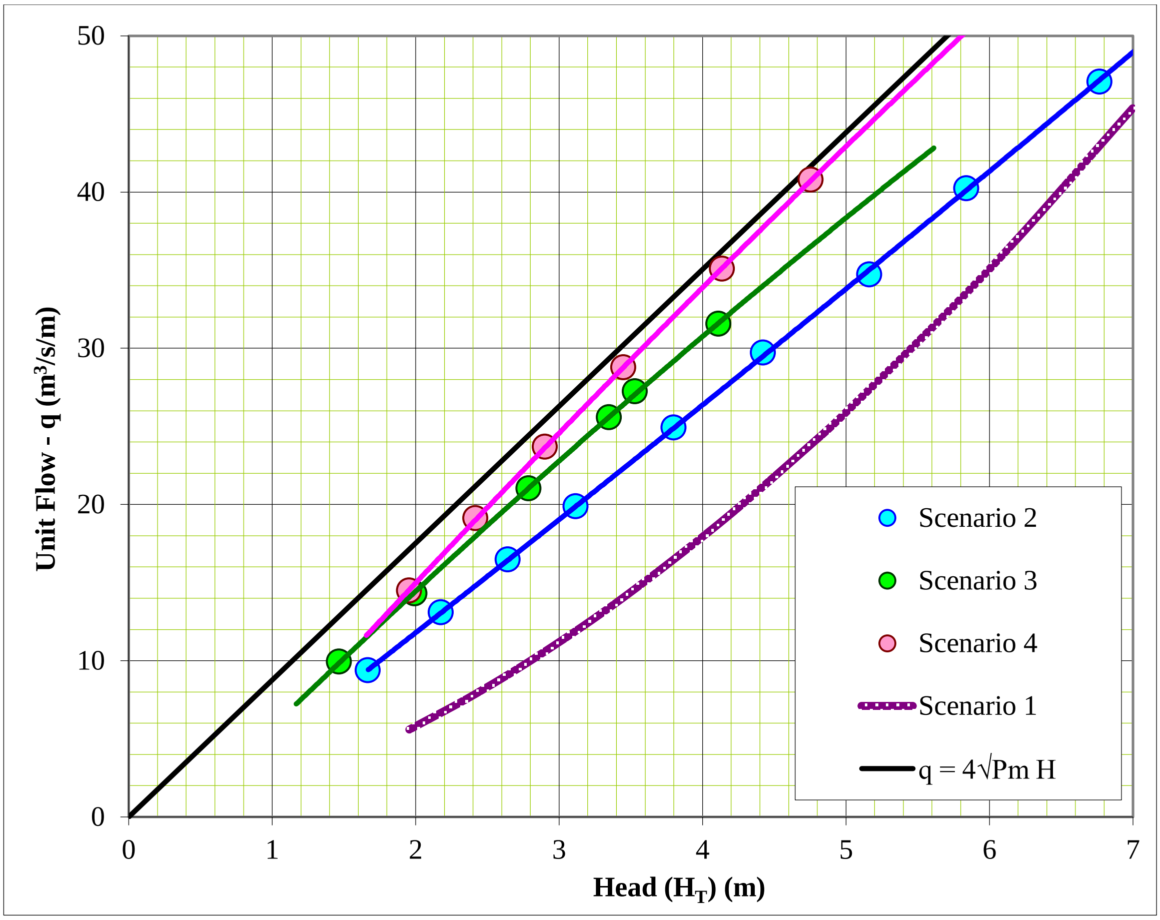

Figure 8.2: Discharge rating curves from model studies for Tzaneen Dam raising options

Different scenarios were analysed based on the different raising options and changes in geometric features.

Initially, the raising was done using an Ogee spillway (Scenario 1) (Fig. 8.2). This option proved least favourable as it required a much larger head for higher flows and this would result in a higher raising of the NOC (non-overspill crest). The design head (H_o) used was 5m.

The second option explored was the labyrinth spillway (Scenario 2). This proved to be a much better option than the Ogee spillway in terms of discharge efficiency and getting a higher flow at a required head (see Fig. 8.2). This is due to its increased wall length. The parameters used for this design are shown in Table 8.1.

The third option was the use of the standard PKW (Scenario 3) for the raising of Tzaneen Dam. This option resulted in a higher efficiency than the labyrinth due to its sloped floors (see Fig. 8.2). The parameters for this model are also indicated in Table 8.1.

The next test during the model study was the combination of Labyrinth and PKW (Scenario 4). These results proved most efficient from all the models built (see Fig.8.2). This is due to the combination of tapered walls and sloped floors (see Figs.8.3 and 8.4). This combined design used sloping as well as horizontal floors to accentuate the combined effect from the PKW and labyrinth spillway designs. This combination can be called the "broken back" concept due to its appearance as indicated by the red and blue lines in Fig. 8.4.The parameters are shown in Table 8.1.

Table 8.1: Parameter for different raising options

Scenario	W (m)	P_m (m)	B (m)
Scenario 1	91.4	N/A	N/A
Scenario 2	15	19	4.8
Scenario 3	15	20	4.8
Scenario 4	15	20	4.8

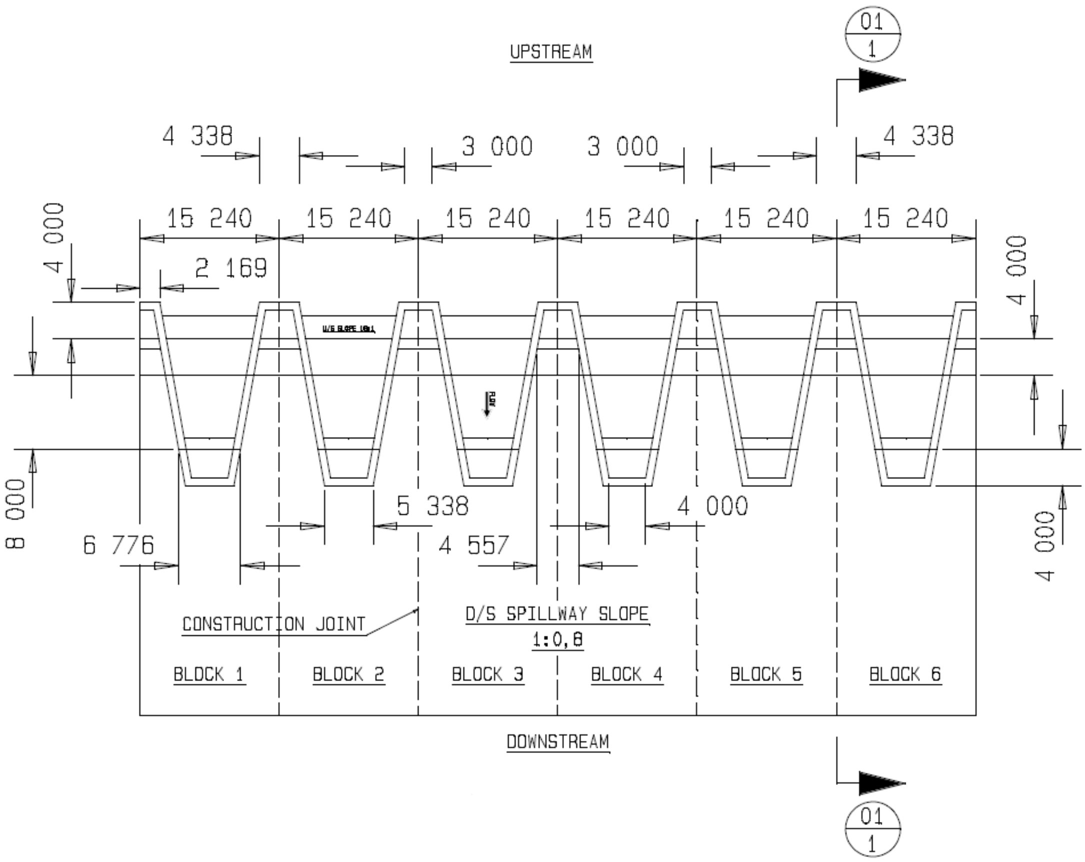

Figure 8.3: Plan view for combined design

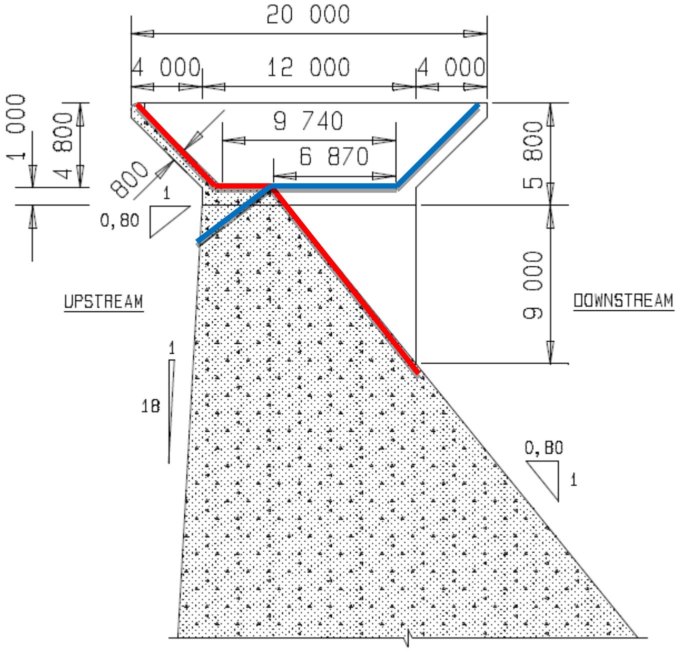

Figure 8.4: Section view of combined design

For the purposes of the model study and limited space at the hydraulics laboratory of the DWS (Department of Water and Sanitation), only half of the spillway was modelled for Tzaneen Dam. Some pictures of the physical model are shown in Fig. 8.5.

Figure 8.5: Model built for Tzaneen Dam raising options

9 CONCLUSIONS AND RECOMMENDATIONS

9.1 Summary and conclusions

The main goal of this study was to investigate the combined attributes of PKW's and labyrinth spillways to achieve an increased discharge capacity. This study looked at ways to provide a more innovative arrangement with a combined design that would assist in reducing the amount of concrete used and lower the length ratio (L/W). Crest length and discharge capacity can both be increased by making use of non-linear spillways (i.e. Labyrinths and PKW's).

Labyrinth weirs supply an increase in crest length for a given spillway width, therefore increasing the flow capacity for a given head. Piano key weirs (PKW's) were developed as an alternative to the traditional labyrinth spillways. Similarly, they increase discharge capacity with their increased crest lengths. The PKW was developed to imitate the functions of the labyrinth weir on dams with smaller foundation footprints.

Thirty five models were built and tested to determine the hydraulic efficiency and behaviour of the discharge coefficient (C_d')using Lempérière's (2011) proposed discharge equation (Eq. 5.3). Other tests included a sensitivity of the wall thickness and its effects on the discharge capacity, as well as sensitivity on the taper of the walls for the combined design in terms of an inlet channel width proportion (α'). The influence of variations in specific geometric parameters on the discharge capacity and hydraulic efficiency were also evaluated (i.e. roundings under the upstream overhang, W_{in}/W_{out}, B and W).

Additional to these tests, three models were retested with a change in the channel floor orientation. This was done in order to get a better understanding of how the combined design with the change in the inlet channel width proportion affected the C and C_d' values.

Based on the results from this study, the following conclusions were reached:

- Standard PKW's are effective in improving the discharge capacity of a spillway.
- The combined design (combination of PKW and labyrinth spillway) is also effective in improving the discharge capacity of a spillway.
- Using Lempérière's (2011) proposed discharge equation gives a more constant C_d' value with less variation compared to previous studies that use the standard linear discharge equation.
- Figures 6.7 and 6.8 show models A4 and A7 with higher efficiencies than model A3, which is based on Lempérière's (2011) optimal design. This shows that more efficient designs exist with the correct percentage of taper and inlet channel width.

- Roundings under the upstream overhang have an impact on the standard PKW design but have a reduced impact on the combined design. The trapezoidal plan layout of the combined design helps avoid using intricate roundings associated with the standard PKW design.
- Standard PKW designs are more efficient with wider inlet channel width proportions.
- The W and B values play an important role in the discharge efficiencies of the various models. From the results of sections 6.2 and 6.3, it can be seen that as B increases (keeping W constant), the standard PKW designs have higher discharge coefficients and more efficient discharge curves. The same conclusions can be made for the models with the combined design. When keeping both W and B constant while only varying the inlet channel width proportion, it appears that the models with combined designs are sometimes more efficient than the standard PKW design based on the amount of tapering. It must be noted that the W and B values are important as these can be limiting dimensions when designing non-linear spillways. Table 9.1 shows the various models built during this study with the varying W and B values for each model as well as different inlet channel width proportions that can be chosen based on the limits of either W or B. In order to use Table 9.1 effectively, a designer must know the P_m value and either B or W, with this a designer can then determine if they want to use a standard PKW design (α' = 1.00) or a combined design (α' = 1.20) based on the costs of each design and the efficiencies required. For example, if a designer has a limited W value and W/P_m = 1.8, he/she can then choose a B/P_m of 3.00, 3.60 or 4.20 and decide on α' of 1.00, 1.20 or 1.45.

Table 9.1: Variations of models built during this study displaying different W, B and α' values that can be used in different designs

Model Number		$\frac{W}{P_m}$ **= 1.80**			$\frac{W}{P_m}$ **= 2.4**			$\frac{W}{P_m}$ **= 3.00**		
		α'=1.00	**α'=1.20**	**α'=1.45**	**α'=1.00**	**α'=1.35**	**α'=1.55**	**α'=1.00**	**α'=1.45**	**α'=1.60**
$\frac{B}{P_m}$ **= 3.00**	SI	A1	A6	A9	B1	B6	B9	C1	C6	C9
$\frac{B}{P_m}$ **= 3.60**	NI	A2			B2			C2		
	SI	A3	A7	A10	B3	B7	B10	C3	C7	C10
	WI	A4			B4			C4		
$\frac{B}{P_m}$ **= 4.20**	SI	A5	A8	A11	B5	B8	B11	C5	C8	C11
Notes: SI – Standard inlet width; NI – Narrow inlet width; WI – Wide inlet width α' – inlet channel width proportion (percentage of taper)										

- Head – discharge curves showed how a lower total head (H_T) can be achieved through various geometric changes like roundings and the different combined designs with various inlet channel width proportions.
- Different geometric changes also showed reduced variation in C_d'. Increased B and W values resulted in flatter curves for C_d' vs H_T/P_m showing less variation. These graphs showed that for smaller W values, the highest C_d' value resides in the region where $H_T/P_m$is between 0.5 and 1.0. As the W value increases, the C_d' value gets higher at an H_T/P_m closer to 1 and the variation in C_d' decreases.
- The length magnification factor (L/W) shows how the wall length can be reduced by making use of a combined design. This also indicates how the roundings can assist in increasing the C_d' value for certain models (particularly the standard PKW designs). This L/W ratio assists in choosing an optimal design that meets the hydraulic and economic requirements of a project.
- The sensitivity with the inlet channel width proportion indicated that having a combined design with a trapezoidal plan layout and sloping floors resulted in a reduced C_d' value as the inlet channel width proportion was increased.
- The combined designs with a trapezoidal plan layout as well as combined sloping and horizontal floors showed that there is potential for an increase in the C_d' valuefor an inlet channel width proportion that lies between 1.00 and 1.35. However, there was not enough data in this study to confirm this.
- The inlet width (W_{in}/W) proportion and the transversal length ratio (B/P_m) also play a role in defining the C_d' value. The W_{in}/W ratio results in increases in C_d' up until a value of 0.67 after which C_d' decreases. The B/P_m value assists in the determination of L/W and has the same effect as L/W, as B/P_m increases so does the C_d' value.
- Due to the combined design of the PKW and labyrinth spillway, the volume of concrete used for the walls and floors of the spillway are reduced. This makes the new design more economically suitable since concrete volume is related to cost. Models with higher discharge coefficients that meet the hydraulic requirements for the project can be chosen using a combined design at a lower cost due to a reduced wall length.
- In the formulations proposed for the determination of C and C_d', only six geometric variations were considered. These were H_T/P_m, L/W, W/P_m, α' (inlet channel width proportion), W_{in}/W and B/P_m. from the comparison of the predicted and measured data for C and C_d', it is evident that these variables can help in determining and improving the efficiency of PKW's and labyrinth spillways in terms of C and C_d'.

The main thing to understand about the labyrinth and PKW is that they are both non-linear spillways. The PKW and labyrinth weir are essentially family and cannot be separated. The benefits from both of these spillway types should be considered, it is important to know how to use the best of both. A PKW has the benefit of a reduced base area and with wider inlets can achieve a much higher discharge, labyrinth weirs have the advantage of tapered walls which reduce the wall length required as well as the need for intricate roundings to achieve a higher discharge. Together, these models can improve a spillways discharge while also remaining economical.

From the results of Figs. 6.7, 7.1 and 7.2, it is clear that there is potential for taper. The aim for this study was to see PKW's and labyrinth weirs as partners and not as two separate entities, not to use each of these designs separately but using the best attributes from each design and combining it to get something better. There is potential for higher efficiency and economic suitability with a combined design.

Table 9.1 serves as a starting point for a designer looking to refine a PKW/labyrinth design. This data will help a designer choose whether to use a standard PKW design or determine if there is room for tapering the design based on the limitations of the W, B and P_m values as well as the cost.

9.2 Recommendations

Further studies can be done to investigate the use of different orientations and more combinations for the combined design. A larger number of inlet channel width proportions (α') can be investigated to get a better idea of the influence it has on the C and C_d' value. More geometric attributes from the labyrinth and PKW designs can be added to the combined design to see the influence on discharge capacity.

One of the main parameters tested in this study was the potential for tapering (α') a standard PKW. The hypothesis that a PKW that has a taper could result in better discharge efficiencies is still unclear. In this study only 5 taper options were tested and these results showed that the potential for tapering does exist. Therefore further studies should explore this parameter and look at a larger spectrum of these values (i.e. α' – inlet channel width proportion).

When planning to build a large number of physical models, ensure that a schedule is drawn up for testing and that building as well as testing can happen simultaneously so as to reduce the time spent in the laboratory. Another recommendation for physical modelling is the accuracy required for a study that already has so many inaccuracies. Human error plays a large role in physical modelling and the testing of physical models. Therefore it is important to always be alert when taking readings and to take readings more than once. It is also always beneficial to analyse the data acquired without delay, this will save time and make it easier and quicker to pick up mistakes made during testing.

Numerical modelling may also be conducted and compared to the physical model results to gain a broader and more accurate analysis spectrum.

An in-depth cost analysis with actual present concrete costs can be done to gain a better idea of the exact costs for the different designs.

10 REFERENCES

Anderson, R.M.(2011), 'Piano Key Weir Head Discharge Relationships', Masters Thesis, Utah State University, DigitalCommons@USU.

Anderson, R.M & Tullis, B.P.(2012), 'Comparison of Piano Key and Rectangular Labyrinth Weir Hydraulics', *Journal of Hydraulic Engineering*, vol 138, no. 4, pp. 358-361.

Anderson, R.M & Tullis, B.P.(2012), 'Piano Key Weir: Reservoir versus Channel Application', *Journal of Irrigation and Drainage Engineering*, vol 138, no. 8, pp. 773-776.

Anderson, R.M & Tullis, B.P.(2013), 'Piano Key Weir Hydraulics and Labyrinth Weir Comparison', *Journal of Irrigation and Drainage Engineering*, vol 139, no. 3, pp. 246-253.

Anon., 2016. *Labyrinth and Piano key weirs*. [Online] Available at: http://www.pk-weirs.ulg.ac.be/content/provisionalprogramworkshop [Accessed August 2016].

Anon., n.d. *Barrage de Gloriettes Dans Les Pyrenees francais*. [Online] Available at: https://fr.dreamstime.com/photo-stock-barrage-de-gloriettes-dans-les-pyrnes-franais-image64307150 [Accessed August 2016].

Anon., n.d. *Parsiab*. [Online] Available at: http://www.parsiab.com/files/uploads/1351895914.Untitled.png [Accessed August 2016].

Crookston, B.M.(2010), 'Labyrinth Weirs', PhD Thesis, Utah State University, DigitalCommons@USU, Logan, Utah.

Crookston, B.M & Tullis, B.P.(2013), 'Hydraulic Design and Analysis of Labyrinth Weirs. I: Discharge Relationships', *Journal of Irrigation and Drainage Engineering*, vol 139, no. 5, pp. 363-370.

Erpicum, S., Archambeau, P., Pirotton, M. and Dewals, B.J. (2014) 'Geometric parameters influence on Piano Key Weir hydraulic performances', 5th International Symposium on Hydraulic Structures, Brisbane, Australia, pp. 1-8.

Horton, R.E.(1907), 'Weir Experiments, Coefficients and Formulas', Department of the Interior United States Geological Survey, Government Printing Office, Washington.

Kabiri-Samani, A.& Javaheri, A.(2012), 'Discharge coefficients for free and submerged flow over Piano Key weirs', *Journal of Hydraulic Research*, vol 50, no. 1, pp. 114-120.

Karaeren, D.(2014), 'Comparison of linear, labyrinth and piano key weirs to increase discharge capacity of existing spillways for a give head_edited', Master of Science Thesis, Middle East Technical University, Middle East Technical University.

Khassaf, S.I.& Al-Baghdadi, M.B.(2015), 'Experimental study of non-rectangular piano key weir discharge coefficient', *International Journal of Energy and Environment*, vol 6, no. 5, pp. 425-436.

Lade, A., Jaltade, A., Kulkarni, J., Kokate, M., Lavate, A.& Harihar, R.(2015), 'Experimental Study of Different Sill Geometries in Piano Key Weirs', *International Journal of Civil Engineering and Technology*, vol 6, no. 2, pp. 30-37.

Leite Ribeiro, M., Bieri, M. and Boillat, J.L. (2009) 'Hydraulic capacity improvement of existing spillways - design of a piano key weirs', 23 Congress of the Int. Commission on Large Dams CIGB - ICOLD , Brasilia, pp. 100-118.

Leite Ribeiro, M., Bieri, M., Boillat, J.L., Schleiss, A.J., Singhal, G.& Sharma, N.(2012a), 'Discharge Capacity of Piano Key Weirs', *Journal of Hydraulic Engineering*, vol 138, no. 2, pp. 199-203.

Leite Ribeiro, M., Pfister, M., Schleiss, A.J.& Boillat, J.L.(2012b), 'Hydraulic design of A-type Piano Key Weirs', *Journal of Hydraulic Research*, vol 50, no. 4, pp. 400-408.

Lempérière, F.(2011), *New Labyrinth Weirs triple the spillways discharge*, Hydrocorp, viewed 2016.

Lempérière, F.& Ouamane, A.(2003), 'The Piano Keys weir: a new cost effective solution for spillways', *Hydropower and Dams*, no. 5, pp. 1-12.

Lempérière, F., Ouamane, A.& Vigny, J.P.(2013), *HydroCoop*, viewed April 2016.

Machiels, O., Erpicum, S., Archambeau, P., Dewals, B.J.& Pirotton, M.(2012a), 'Method for the preliminary design of Piano Key Weirs', *La Houille Blanche*, pp. 14-18.

Machiels, O., Erpicum, S., Archambeau, P., Dewals, B.& Pirotton, M.(2013), 'Parapet Wall Effect on Piano Key Weir Efficiency', *Journal of Irrigation and Drainage Engineering*, vol 139, no. 6, pp. 506-511.

Machiels, O., Erpicum, S., Dewals, B.J., Archambeau, P.& Pirroton, M.(2011), 'Experimental observation of flow characteristics over a Piano Key Weir', *Journal of Hydraulic Research*, vol 49, no. 3, pp. 359-366.

Machiels, O., Erpicum, S., Pirroton, M., Dewals, B. and Archambeau, P. (2009) 'Large scale experimental study of piano key weirs', Proceedings of 33rd IAHR Congress: Water Engineering for a Sustainable Environment, Vancouver, pp. 1030-1037.

Machiels, O., Erpicum, S., Pirroton, M., Dewals, B. and Archambeau, P. (2012b) 'Experimental analysis of PKW hydraulic performance and geometric parameters optimum', Proceedings of International Workshop on Piano Key Weir for In-stream Storage and Dam Safety (PKWISD-2012, 97-114.

Machiels, O., Pirotton, M., Archambeau, P., Dewals, B.& Erpicum, S.(2014), 'Experimental parametric study and design of Piano Key Weirs', *Journal Journal of Hydraulic Research*, vol 52, no. 3, pp. 326-335.

Oertel, M. (2015) 'Discharge Coefficients of Piano Key Weirs From Experimental and Numerical Models', 36th IAHR World Congress, The Hague, pp. 1-7.

Ouamane, A. and Lempérière, F. (2006) 'Design of a new economic shape of weir', International symposium on dams in the societies of the 21st century; Dams and reservoirs, societies and environment in the 21st century ICOLD-SPANCOLD, Barcelona, pp. 463-470.

Paxson, G., Tullis, B.P. and Campbell, D.B. (2012) 'Potential applications for piano key weirs at dams in the United States', 32nd Annual USSD Conference, New Orleans, Louisiana, pp. 1303-1315.

Pfister, M., Boillat, J.L., Schleiss, A.J., Laugier, F. and Leite Ribeiro, M. (2012) 'Piano Key Weirs as efficient spillway structure', 24th Congress of CIGB - ICOLD, Kyoto, pp. 176-186.

Pfister, M. and Schleiss, A.J. (2013a) 'Comparison of hydraulic design equations for A-type Piano Key weirs', Intl. Conf. Water Storage and Hydropower Development for Africa (Africa 2013), Addis Ababa, pp. 1-8.

Pfister, M. and Schleiss, A.J. (2013b) 'Estimation of A-type Piano key Weir PKW', Labyrinth and Piano Key Weirs II-PKW2013, Boca Raton, pp. 139-147.

Schleiss, A.J. (2011) 'From Labyrinth to Piano Key Weirs - A historical review', Proc. of International Conference on Labyrinth and Piano Key Weirs (PKW 2011), Belgium, pp. 3-15.

Tullis, J.P., Amanian, N. and Waldron, D. (1995) 'Design of labyrinth spillways', *Journal of Hydraulic Engineering*, vol. 121, no. 3, pp. 247-255.

Tullis, B.P., Young, J.C. and Chandler, M.A. (2007) 'Head-Discharge Relationships for Submerged Labyrinth Weirs', *Journal of Hydraulic Engineering*, vol. 133, no. 3, pp. 248-254.

Villemonte, J.R. (1974) 'Submerged weir discharge studies', *Eng. News-Rec*, vol. 139, no. 26, pp. 54-56.

11 APPENDIX A - HEAD DISCHARGE RELATIONSHIPS FOR MODELS WITH ROUNDINGS

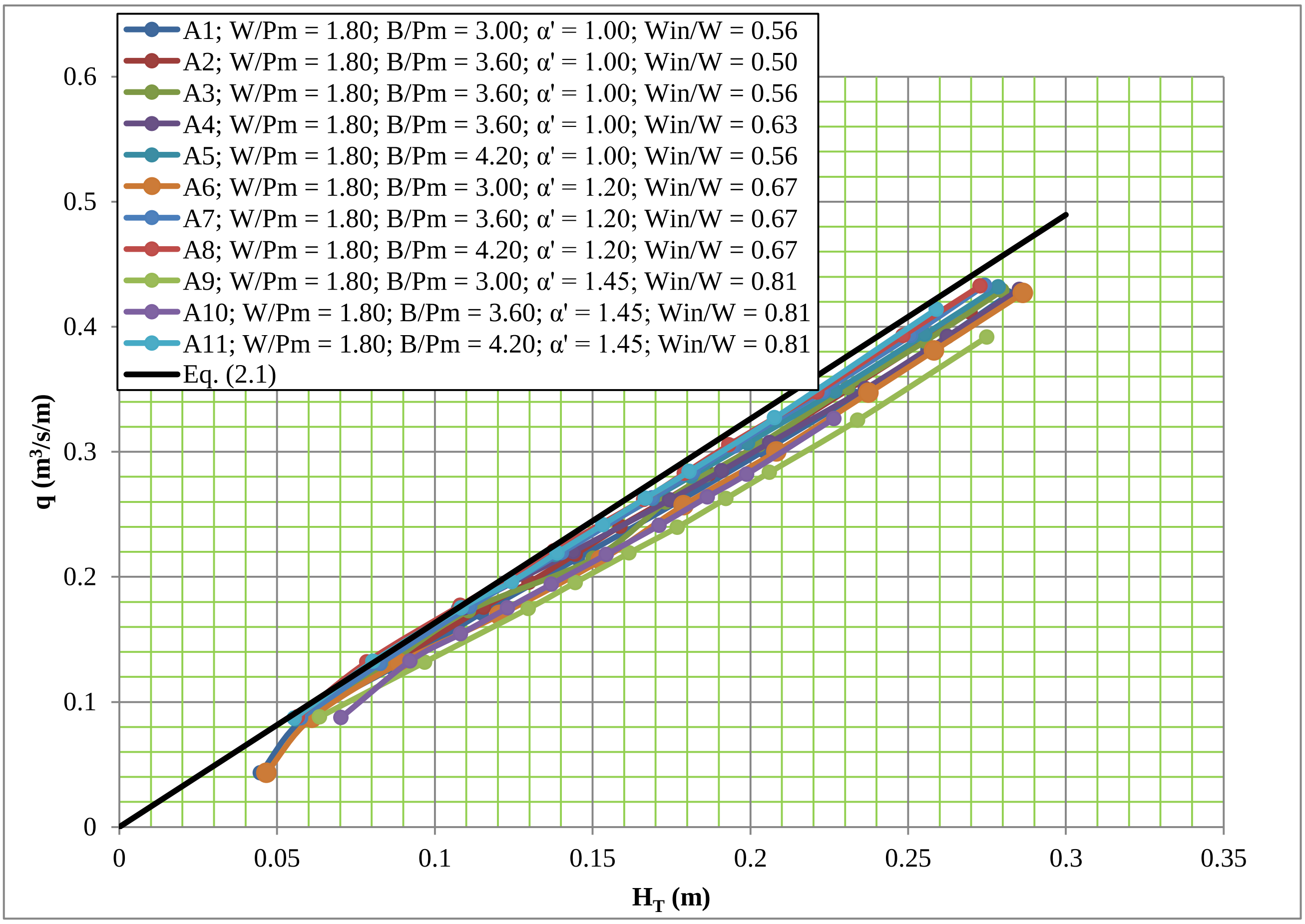

Figure 11.1: Measured and predicted (Eq. (2.1)) Head - Discharge curves for model set A with roundings

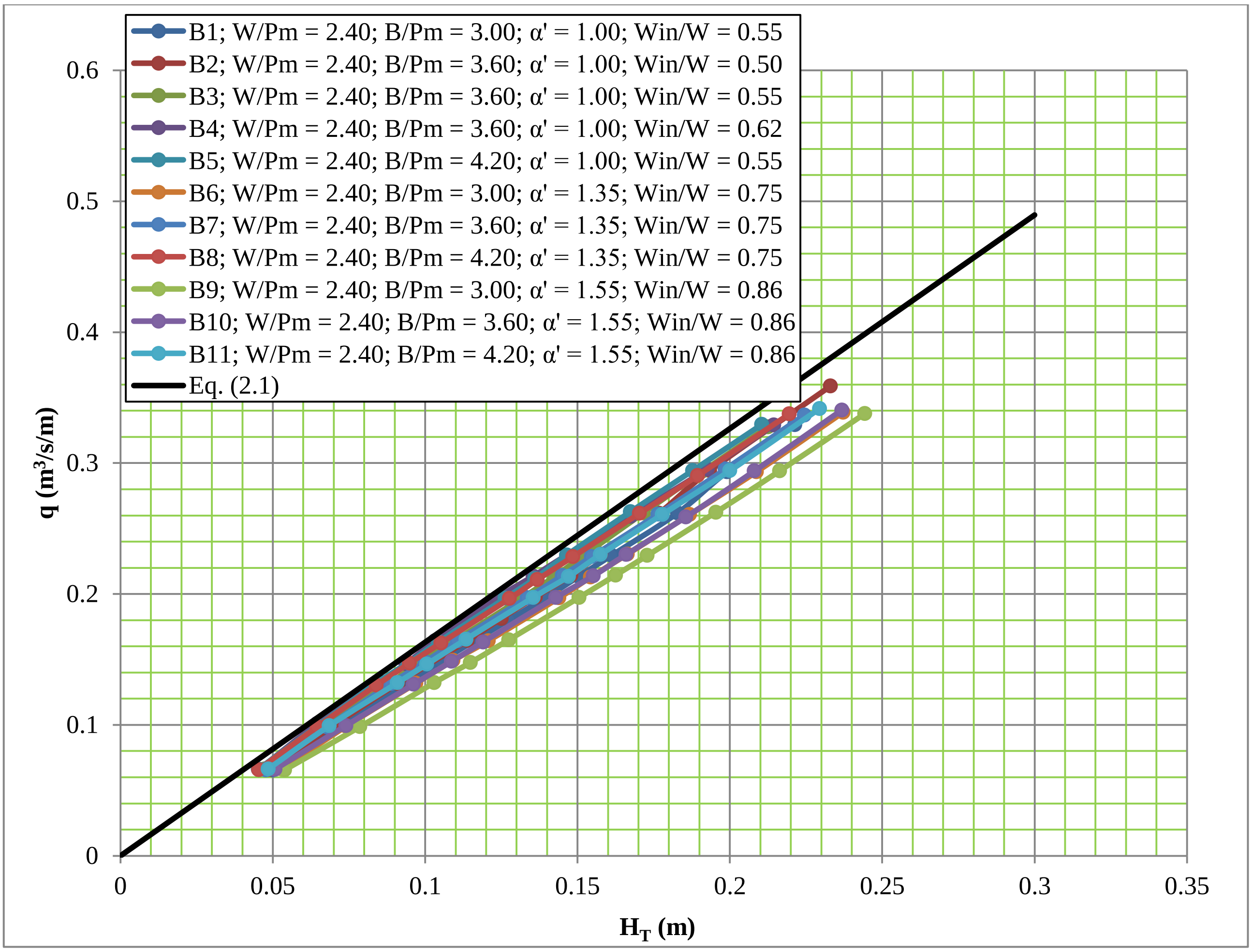

Figure 11.2: Measured and predicted (Eq. (2.1)) Head - Discharge curves for model set B with roundings

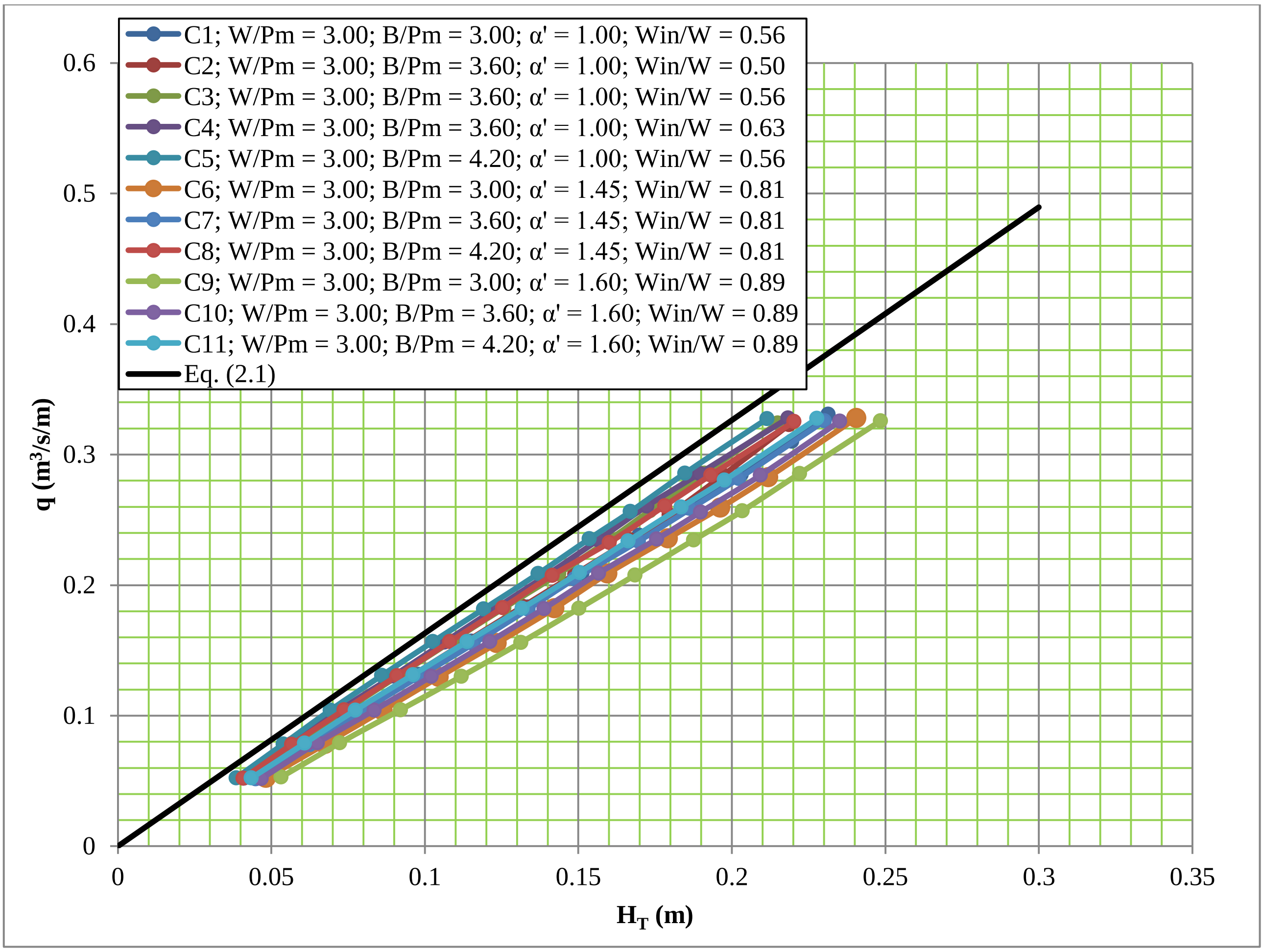

Figure 11.3: Measured and predicted (Eq. (2.1)) Head - Discharge curves for model set C with roundings

12 APPENDIX B – PICTURES OF PHYSICAL MODELS



Figure 12.1: Models installed in testing facility and during testing

Figure 12.2: Model sets A, B and C

Figure 12.3: Large models tested for wall thickness sensitivity

Figure 12.4: Models B3, B7 and B10 with the adjusted design consisting of a combined horizontal and sloping floor

Figure 12.5: Model set A

Figure 12.6: Model set C

Figure 12.7: Model set B

13 APPENDIX C – DATA SETS WITH CALCULATED AND MEASURED DATA

13.1 Large scale models

Table 13.1: Measured and calculated results of Model L1 with no roundings

Model L1 (No roundings)											
$Q_{measured}$	H	P	v	Hv $(\frac{v^2}{2g})$	H_T	q	H_T/P_m	C(H)	$C(H^{1.5})$	$C_d(H^{1.5})$	$C_d'(H)$
0.17	0.22	1.16	0.37	0.01	0.23	0.43	1.05	4.09	4.00	1.35	0.92
0.16	0.21	1.15	0.36	0.01	0.22	0.42	1.01	4.09	4.06	1.37	0.92
0.16	0.20	1.14	0.35	0.01	0.21	0.40	0.97	4.11	4.18	1.42	0.93
0.14	0.19	1.13	0.33	0.01	0.19	0.37	0.89	4.14	4.38	1.48	0.93
0.13	0.18	1.11	0.31	0.00	0.18	0.34	0.84	4.11	4.49	1.52	0.93
0.13	0.17	1.11	0.30	0.00	0.17	0.33	0.80	4.11	4.59	1.55	0.93
0.12	0.16	1.10	0.29	0.00	0.17	0.32	0.77	4.12	4.71	1.59	0.93
0.11	0.15	1.09	0.27	0.00	0.15	0.29	0.71	4.08	4.85	1.64	0.92
0.10	0.13	1.07	0.24	0.00	0.14	0.26	0.63	4.09	5.14	1.74	0.92
0.09	0.12	1.06	0.22	0.00	0.12	0.23	0.56	4.12	5.48	1.86	0.93
0.08	0.10	1.04	0.19	0.00	0.11	0.20	0.49	4.13	5.91	2.00	0.93
0.07	0.10	1.03	0.18	0.00	0.10	0.19	0.46	4.12	6.11	2.07	0.93
0.07	0.09	1.03	0.17	0.00	0.09	0.17	0.42	4.16	6.43	2.18	0.94
0.06	0.07	1.01	0.14	0.00	0.08	0.14	0.35	4.11	6.95	2.35	0.93
0.04	0.06	1.00	0.11	0.00	0.06	0.11	0.27	4.03	7.73	2.62	0.91
0.02	0.03	0.97	0.06	0.00	0.04	0.06	0.16	3.59	8.85	3.00	0.81

Table 13.2: Measured and calculated results of Model L1 with roundings

Model L1 (With roundings)											
$Q_{measured}$	H	P	v	Hv $(\frac{v^2}{2g})$	H_T	q	H_T/P_m	C(H)	$C(H^{1.5})$	$C_d(H^{1.5})$	$C_d'(H)$
0.17	0.22	1.16	0.38	0.01	0.23	0.44	1.05	4.16	4.06	1.38	0.94
0.16	0.21	1.15	0.36	0.01	0.21	0.42	0.99	4.19	4.21	1.42	0.95
0.16	0.20	1.14	0.35	0.01	0.20	0.40	0.94	4.22	4.34	1.47	0.95
0.14	0.18	1.12	0.33	0.01	0.19	0.37	0.88	4.20	4.47	1.52	0.95
0.13	0.17	1.11	0.31	0.00	0.18	0.35	0.82	4.20	4.63	1.57	0.95
0.13	0.17	1.10	0.30	0.00	0.17	0.33	0.79	4.16	4.68	1.58	0.94
0.12	0.16	1.10	0.29	0.00	0.17	0.32	0.77	4.12	4.71	1.59	0.93

0.11	0.15	1.09	0.27	0.00	0.15	0.29	0.70	4.13	4.94	1.67	0.93
0.10	0.13	1.07	0.24	0.00	0.13	0.26	0.62	4.20	5.34	1.81	0.95
0.09	0.11	1.05	0.22	0.00	0.12	0.23	0.54	4.23	5.74	1.94	0.96
0.08	0.10	1.04	0.19	0.00	0.10	0.20	0.48	4.20	6.07	2.05	0.95
0.06	0.07	1.01	0.14	0.00	0.07	0.14	0.34	4.20	7.18	2.43	0.95

Table 13.3: Measured and calculated results of Model L2 with no roundings

Model L2 (No roundings)											
$Q_{measured}$	H	P	v	Hv $(\frac{v^2}{2g})$	H_T	q	H_T/P_m	C(H)	C($H^{1.5}$)	C_d($H^{1.5}$)	C_d'(H)
0.15	0.22	1.16	0.34	0.01	0.23	0.40	1.04	3.79	3.71	1.26	0.86
0.15	0.21	1.16	0.33	0.01	0.22	0.39	1.01	3.80	3.77	1.28	0.86
0.14	0.20	1.15	0.32	0.01	0.21	0.37	0.97	3.81	3.86	1.31	0.86
0.13	0.19	1.13	0.31	0.00	0.19	0.35	0.90	3.84	4.05	1.37	0.87
0.12	0.17	1.12	0.28	0.00	0.18	0.32	0.82	3.88	4.29	1.45	0.88
0.12	0.16	1.11	0.27	0.00	0.17	0.30	0.77	3.90	4.43	1.50	0.88
0.11	0.16	1.10	0.26	0.00	0.16	0.29	0.74	3.91	4.55	1.54	0.88
0.10	0.14	1.08	0.24	0.00	0.14	0.26	0.66	3.92	4.82	1.63	0.89
0.09	0.13	1.07	0.22	0.00	0.13	0.23	0.60	3.84	4.97	1.68	0.87
0.08	0.11	1.06	0.19	0.00	0.11	0.20	0.53	3.85	5.31	1.80	0.87
0.07	0.10	1.05	0.18	0.00	0.10	0.19	0.48	3.84	5.52	1.87	0.87
0.07	0.10	1.04	0.17	0.00	0.10	0.17	0.45	3.83	5.71	1.93	0.87
0.06	0.08	1.03	0.14	0.00	0.08	0.15	0.38	3.85	6.25	2.12	0.87
0.04	0.06	1.01	0.11	0.00	0.07	0.12	0.30	3.79	6.87	2.33	0.86
0.03	0.05	0.99	0.09	0.00	0.05	0.09	0.23	3.61	7.46	2.53	0.82
0.02	0.04	0.98	0.06	0.00	0.04	0.06	0.17	3.38	8.09	2.74	0.76

Table 13.4: Measured and calculated results of Model L2 with roundings

Model L2 (With roundings)											
$Q_{measured}$	H	P	v	Hv $(\frac{v^2}{2g})$	H_T	q	H_T/P_m	C(H)	C($H^{1.5}$)	C_d($H^{1.5}$)	C_d'(H)
0.16	0.22	1.16	0.35	0.01	0.22	0.41	1.04	3.89	3.81	1.29	0.88
0.15	0.21	1.15	0.34	0.01	0.21	0.39	0.99	3.90	3.92	1.33	0.88
0.14	0.20	1.14	0.33	0.01	0.20	0.37	0.95	3.92	4.02	1.36	0.88
0.13	0.18	1.13	0.31	0.00	0.19	0.35	0.87	3.95	4.22	1.43	0.89
0.12	0.17	1.11	0.29	0.00	0.17	0.32	0.79	3.98	4.46	1.51	0.90

0.12	0.16	1.10	0.27	0.00	0.16	0.30	0.76	3.98	4.58	1.55	0.90
0.11	0.15	1.09	0.26	0.00	0.15	0.29	0.70	4.08	4.87	1.65	0.92
0.10	0.14	1.08	0.24	0.00	0.14	0.26	0.66	3.94	4.86	1.65	0.89
0.09	0.12	1.07	0.22	0.00	0.13	0.23	0.58	3.95	5.17	1.75	0.89
0.08	0.11	1.05	0.19	0.00	0.11	0.20	0.51	3.96	5.53	1.87	0.89
0.07	0.10	1.04	0.18	0.00	0.10	0.19	0.47	3.95	5.75	1.95	0.89
0.07	0.09	1.04	0.17	0.00	0.09	0.17	0.44	3.95	5.97	2.02	0.89
0.06	0.08	1.02	0.14	0.00	0.08	0.14	0.37	3.92	6.49	2.20	0.89
0.04	0.06	1.01	0.11	0.00	0.06	0.11	0.30	3.85	7.08	2.40	0.87
0.03	0.05	0.99	0.09	0.00	0.05	0.09	0.23	3.72	7.68	2.60	0.84
0.02	0.04	0.98	0.06	0.00	0.04	0.06	0.17	3.40	8.27	2.80	0.77

13.2 Model set A

Table 13.5: Measured and calculated results of Model A1 with no roundings

Model A1 (No roundings)											
$Q_{measured}$	**H**	**P**	**v**	**Hv** $(\frac{v^2}{2g})$	H_T	**q**	H_T/P_m	**C(H)**	$C(H^{1.5})$	$C_d(H^{1.5})$	$C_d'(H)$
0.11	0.27	1.07	0.39	0.01	0.28	0.42	1.94	3.93	2.82	0.95	0.89
0.10	0.26	1.05	0.37	0.01	0.26	0.39	1.83	3.88	2.87	0.97	0.88
0.09	0.22	1.02	0.33	0.01	0.23	0.34	1.60	3.85	3.04	1.03	0.87
0.08	0.20	1.00	0.30	0.00	0.20	0.30	1.42	3.81	3.20	1.08	0.86
0.07	0.17	0.97	0.27	0.00	0.18	0.26	1.24	3.80	3.41	1.16	0.86
0.06	0.14	0.94	0.23	0.00	0.15	0.22	1.02	3.87	3.84	1.30	0.87
0.04	0.11	0.91	0.19	0.00	0.11	0.17	0.79	3.95	4.44	1.50	0.89
0.03	0.08	0.88	0.14	0.00	0.09	0.13	0.60	3.86	4.99	1.69	0.87
0.02	0.06	0.86	0.10	0.00	0.06	0.09	0.41	3.87	6.04	2.04	0.87
0.01	0.04	0.84	0.05	0.00	0.04	0.04	0.31	2.45	4.40	1.49	0.55

Table 13.6: Measured and calculated results of Model A1 with roundings

Model A1 (with roundings)											
$Q_{measured}$	**H**	**P**	**v**	**Hv** $(\frac{v^2}{2g})$	H_T	**q**	H_T/P_m	**C(H)**	$C(H^{1.5})$	$C_d(H^{1.5})$	$C_d'(H)$
0.11	0.27	1.07	0.40	0.01	0.28	0.42	1.95	3.98	2.85	0.96	0.90
0.10	0.25	1.05	0.36	0.01	0.26	0.38	1.78	3.92	2.94	1.00	0.89
0.09	0.23	1.02	0.34	0.01	0.23	0.34	1.62	3.90	3.06	1.04	0.88

0.08	0.20	1.00	0.30	0.00	0.20	0.30	1.42	3.88	3.26	1.10	0.88
0.07	0.17	0.97	0.27	0.00	0.18	0.26	1.23	3.87	3.49	1.18	0.87
0.06	0.14	0.94	0.23	0.00	0.15	0.21	1.01	3.90	3.88	1.31	0.88
0.04	0.11	0.91	0.19	0.00	0.11	0.17	0.80	3.93	4.39	1.49	0.89
0.03	0.09	0.88	0.14	0.00	0.09	0.13	0.60	3.88	5.00	1.69	0.88
0.02	0.06	0.85	0.10	0.00	0.06	0.09	0.41	3.91	6.13	2.08	0.88
0.01	0.04	0.84	0.05	0.00	0.04	0.04	0.31	2.54	4.56	1.54	0.57

Table 13.7: Measured and calculated results of Model A2 with no roundings

Model A2 (No roundings)											
$Q_{measured}$	**H**	**P**	**v**	**Hv $(\frac{v^2}{2g})$**	**H_T**	**q**	**H_T/P_m**	**C(H)**	**$C(H^{1.5})$**	**$C_d(H^{1.5})$**	**$C_d'(H)$**
0.11	0.27	1.07	0.39	0.01	0.28	0.42	1.92	3.95	2.85	0.97	0.89
0.09	0.22	1.02	0.33	0.01	0.22	0.33	1.55	3.90	3.13	1.06	0.88
0.07	0.19	0.98	0.29	0.00	0.19	0.28	1.33	3.90	3.38	1.15	0.88
0.07	0.17	0.97	0.27	0.00	0.18	0.26	1.23	3.90	3.51	1.19	0.88
0.06	0.16	0.96	0.25	0.00	0.16	0.24	1.13	3.90	3.68	1.25	0.88
0.06	0.14	0.94	0.23	0.00	0.15	0.22	1.02	3.91	3.86	1.31	0.88
0.05	0.13	0.93	0.21	0.00	0.13	0.20	0.92	3.93	4.10	1.39	0.89
0.05	0.11	0.91	0.19	0.00	0.12	0.17	0.81	3.94	4.37	1.48	0.89
0.03	0.09	0.88	0.15	0.00	0.09	0.13	0.61	3.93	5.02	1.70	0.89
0.02	0.06	0.86	0.10	0.00	0.06	0.09	0.41	3.86	6.04	2.05	0.87

Table 13.8: Measured and calculated results of Model A2 with roundings

Model A2 (With roundings)											
$Q_{measured}$	**H**	**P**	**v**	**Hv $(\frac{v^2}{2g})$**	**H_T**	**q**	**H_T/P_m**	**C(H)**	**$C(H^{1.5})$**	**$C_d(H^{1.5})$**	**$C_d'(H)$**
0.11	0.26	1.06	0.39	0.01	0.27	0.41	1.87	4.02	2.94	1.00	0.91
0.08	0.21	1.01	0.32	0.01	0.22	0.33	1.50	3.98	3.24	1.10	0.90
0.07	0.18	0.98	0.29	0.00	0.19	0.28	1.30	3.98	3.50	1.18	0.90
0.07	0.17	0.97	0.27	0.00	0.17	0.26	1.20	3.98	3.63	1.23	0.90
0.06	0.16	0.95	0.25	0.00	0.16	0.24	1.10	3.99	3.80	1.29	0.90
0.06	0.14	0.94	0.23	0.00	0.14	0.22	1.00	3.98	3.97	1.34	0.90
0.05	0.13	0.92	0.21	0.00	0.13	0.20	0.90	3.97	4.18	1.42	0.90
0.05	0.11	0.91	0.19	0.00	0.12	0.18	0.80	4.01	4.48	1.52	0.90

0.03	0.09	0.88	0.15	0.00	0.09	0.13	0.61	4.00	5.14	1.74	0.90
0.02	0.06	0.85	0.10	0.00	0.06	0.09	0.41	3.94	6.17	2.09	0.89

Table 13.9: Measured and calculated results of Model A3 with no roundings

Model A3 (No roundings)											
$Q_{measured}$	**H**	**P**	**v**	**Hv $(\frac{v^2}{2g})$**	**H_T**	**q**	**H_T/P_m**	**C(H)**	**$C(H^{1.5})$**	**$C_d(H^{1.5})$**	**$C_d'(H)$**
0.11	0.28	1.08	0.41	0.01	0.29	0.44	2.02	3.97	2.80	0.95	0.90
0.10	0.26	1.05	0.37	0.01	0.26	0.39	1.84	3.93	2.90	0.98	0.89
0.09	0.23	1.02	0.34	0.01	0.23	0.34	1.62	3.89	3.06	1.04	0.88
0.08	0.20	1.00	0.30	0.00	0.21	0.30	1.43	3.88	3.25	1.10	0.88
0.07	0.19	0.98	0.29	0.00	0.19	0.28	1.33	3.87	3.35	1.14	0.87
0.07	0.17	0.97	0.27	0.00	0.18	0.26	1.24	3.88	3.49	1.18	0.88
0.06	0.14	0.94	0.23	0.00	0.14	0.22	1.00	3.95	3.95	1.34	0.89
0.04	0.11	0.91	0.19	0.00	0.11	0.17	0.78	4.04	4.58	1.55	0.91
0.03	0.08	0.88	0.15	0.00	0.09	0.13	0.60	4.01	5.20	1.76	0.91
0.02	0.06	0.85	0.10	0.00	0.06	0.09	0.41	3.88	6.07	2.06	0.88

Table 13.10: Measured and calculated results of Model A3 with roundings

Model A3 (With roundings)											
$Q_{measured}$	**H**	**P**	**v**	**Hv $(\frac{v^2}{2g})$**	**H_T**	**q**	**H_T/P_m**	**C(H)**	**$C(H^{1.5})$**	**$C_d(H^{1.5})$**	**$C_d'(H)$**
0.11	0.27	1.07	0.40	0.01	0.28	0.43	1.94	4.04	2.90	0.98	0.91
0.10	0.25	1.04	0.37	0.01	0.26	0.39	1.77	4.01	3.01	1.02	0.90
0.09	0.22	1.02	0.34	0.01	0.23	0.35	1.60	4.01	3.16	1.07	0.90
0.08	0.20	0.99	0.31	0.00	0.20	0.31	1.41	3.97	3.35	1.13	0.90
0.07	0.18	0.98	0.29	0.00	0.19	0.28	1.29	3.99	3.51	1.19	0.90
0.07	0.17	0.97	0.27	0.00	0.17	0.26	1.20	3.95	3.61	1.22	0.89
0.06	0.15	0.94	0.23	0.00	0.15	0.21	1.04	3.77	3.69	1.25	0.85
0.04	0.11	0.91	0.19	0.00	0.11	0.17	0.77	4.12	4.70	1.59	0.93
0.03	0.08	0.88	0.15	0.00	0.09	0.13	0.59	4.04	5.24	1.77	0.91
0.02	0.06	0.85	0.10	0.00	0.06	0.09	0.41	3.91	6.14	2.08	0.88

Table 13.11: Measured and calculated results of Model A4 with no roundings

Model A4 (No roundings)											
$Q_{measured}$	H	P	v	Hv ($\frac{v^2}{2g}$)	H_T	q	H_T/P_m	C(H)	C($H^{1.5}$)	C_d($H^{1.5}$)	C_d'(H)
0.11	0.28	1.08	0.40	0.01	0.29	0.43	2.02	3.92	2.76	0.93	0.88
0.10	0.26	1.06	0.37	0.01	0.27	0.39	1.86	3.88	2.84	0.96	0.88
0.09	0.23	1.03	0.34	0.01	0.24	0.35	1.66	3.85	2.99	1.01	0.87
0.08	0.20	1.00	0.30	0.00	0.21	0.30	1.45	3.84	3.19	1.08	0.87
0.07	0.19	0.99	0.29	0.00	0.19	0.28	1.34	3.86	3.33	1.13	0.87
0.07	0.17	0.97	0.27	0.00	0.18	0.26	1.23	3.87	3.49	1.18	0.87
0.06	0.14	0.94	0.23	0.00	0.15	0.22	1.02	3.95	3.91	1.32	0.89
0.05	0.11	0.91	0.19	0.00	0.11	0.18	0.78	4.11	4.65	1.57	0.93
0.03	0.08	0.88	0.15	0.00	0.08	0.13	0.56	4.32	5.79	1.96	0.97
0.02	0.05	0.85	0.10	0.00	0.06	0.09	0.39	4.06	6.51	2.20	0.92

Table 13.12: Measured and calculated results of Model A4 with roundings

Model A4 (with roundings)											
$Q_{measured}$	H	P	v	Hv ($\frac{v^2}{2g}$)	H_T	q	H_T/P_m	C(H)	C($H^{1.5}$)	C_d($H^{1.5}$)	C_d'(H)
0.11	0.28	1.07	0.40	0.01	0.29	0.43	1.98	3.97	2.82	0.96	0.90
0.10	0.25	1.05	0.37	0.01	0.26	0.39	1.82	3.94	2.92	0.99	0.89
0.09	0.23	1.03	0.34	0.01	0.24	0.35	1.64	3.91	3.05	1.03	0.88
0.08	0.20	1.00	0.31	0.00	0.21	0.31	1.43	3.93	3.28	1.11	0.89
0.07	0.19	0.98	0.29	0.00	0.19	0.28	1.33	3.93	3.41	1.16	0.89
0.07	0.17	0.97	0.27	0.00	0.17	0.26	1.21	3.95	3.59	1.22	0.89
0.06	0.14	0.94	0.23	0.00	0.14	0.22	1.00	4.03	4.03	1.37	0.91
0.05	0.11	0.90	0.19	0.00	0.11	0.18	0.76	4.23	4.85	1.64	0.95
0.03	0.08	0.87	0.15	0.00	0.08	0.13	0.55	4.41	5.97	2.02	0.99
0.02	0.05	0.85	0.10	0.00	0.06	0.09	0.39	4.10	6.58	2.23	0.93

Table 13.13: Measured and calculated results of Model A5 with no roundings

Model A5 (No roundings)											
$Q_{measured}$	H	P	v	Hv ($\frac{v^2}{2g}$)	H_T	q	H_T/P_m	C(H)	C($H^{1.5}$)	C_d($H^{1.5}$)	C_d'(H)
0.11	0.28	1.07	0.40	0.01	0.28	0.43	1.97	4.02	2.86	0.97	0.91
0.10	0.25	1.05	0.38	0.01	0.26	0.40	1.82	3.98	2.96	1.00	0.90

0.09	0.23	1.02	0.34	0.01	0.23	0.35	1.61	3.97	3.13	1.06	0.90
0.08	0.20	0.99	0.31	0.00	0.20	0.30	1.40	3.97	3.35	1.14	0.90
0.07	0.18	0.98	0.29	0.00	0.19	0.28	1.30	3.99	3.49	1.18	0.90
0.07	0.17	0.97	0.27	0.00	0.17	0.26	1.20	4.01	3.66	1.24	0.90
0.06	0.14	0.94	0.23	0.00	0.14	0.22	0.98	4.08	4.12	1.39	0.92
0.04	0.11	0.90	0.19	0.00	0.11	0.17	0.76	4.17	4.77	1.62	0.94
0.03	0.08	0.88	0.15	0.00	0.08	0.13	0.56	4.26	5.71	1.93	0.96
0.02	0.06	0.85	0.10	0.00	0.06	0.09	0.39	4.06	6.48	2.19	0.92

Table 13.14: Measured and calculated results of Model A5 with roundings

Model A5 (With roundings)											
$Q_{measured}$	**H**	**P**	**v**	**Hv $(\frac{v^2}{2g})$**	**H_T**	**q**	**H_T/P_m**	**C(H)**	**$C(H^{1.5})$**	**$C_d(H^{1.5})$**	**C_d'(H)**
0.11	0.27	1.07	0.40	0.01	0.28	0.43	1.93	4.08	2.94	0.99	0.92
0.10	0.25	1.05	0.38	0.01	0.26	0.39	1.77	4.07	3.05	1.03	0.92
0.09	0.22	1.02	0.34	0.01	0.23	0.35	1.58	4.05	3.23	1.09	0.91
0.08	0.19	0.99	0.31	0.00	0.20	0.31	1.38	4.06	3.45	1.17	0.92
0.07	0.18	0.97	0.29	0.00	0.18	0.28	1.26	4.08	3.64	1.23	0.92
0.07	0.16	0.96	0.27	0.00	0.17	0.26	1.17	4.09	3.78	1.28	0.92
0.06	0.13	0.93	0.23	0.00	0.14	0.22	0.96	4.16	4.25	1.44	0.94
0.04	0.11	0.90	0.19	0.00	0.11	0.17	0.75	4.27	4.94	1.67	0.96
0.03	0.08	0.87	0.15	0.00	0.08	0.13	0.55	4.39	5.93	2.01	0.99
0.02	0.05	0.85	0.10	0.00	0.06	0.09	0.39	4.07	6.53	2.21	0.92

Table 13.15: Measured and calculated results of Model A6 with no roundings

Model A6 (No roundings)											
$Q_{measured}$	**H**	**P**	**v**	**Hv $(\frac{v^2}{2g})$**	**H_T**	**q**	**H_T/P_m**	**C(H)**	**$C(H^{1.5})$**	**$C_d(H^{1.5})$**	**C_d'(H)**
0.11	0.27	1.07	0.39	0.01	0.28	0.42	1.97	3.87	2.76	0.93	0.87
0.08	0.22	1.02	0.32	0.01	0.23	0.32	1.58	3.75	2.98	1.01	0.85
0.07	0.19	0.99	0.28	0.00	0.20	0.28	1.38	3.74	3.18	1.08	0.84
0.07	0.18	0.97	0.27	0.00	0.18	0.26	1.27	3.72	3.30	1.12	0.84
0.06	0.16	0.96	0.25	0.00	0.17	0.24	1.17	3.74	3.45	1.17	0.84
0.06	0.15	0.95	0.23	0.00	0.15	0.22	1.07	3.72	3.59	1.21	0.84
0.05	0.13	0.93	0.21	0.00	0.14	0.19	0.95	3.75	3.84	1.30	0.85
0.05	0.12	0.92	0.19	0.00	0.13	0.17	0.87	3.65	3.90	1.32	0.82

0.03	0.09	0.89	0.15	0.00	0.09	0.13	0.64	3.70	4.62	1.56	0.83
0.02	0.06	0.86	0.10	0.00	0.06	0.09	0.43	3.70	5.62	1.90	0.83

Table 13.16: Measured and calculated results of Model A6 with roundings

Model A6 (With roundings)											
$Q_{measured}$	**H**	**P**	**v**	**Hv ($\frac{v^2}{2g}$)**	**H_T**	**q**	**H_T/P_m**	**C(H)**	**C($H^{1.5}$)**	**C_d($H^{1.5}$)**	**C_d'(H)**
0.11	0.27	1.07	0.39	0.01	0.28	0.41	1.96	3.87	2.77	0.94	0.87
0.08	0.22	1.02	0.32	0.01	0.23	0.32	1.57	3.76	3.00	1.02	0.85
0.07	0.19	0.99	0.28	0.00	0.20	0.28	1.37	3.77	3.22	1.09	0.85
0.07	0.18	0.97	0.27	0.00	0.18	0.26	1.27	3.76	3.35	1.13	0.85
0.06	0.16	0.96	0.25	0.00	0.17	0.24	1.16	3.76	3.50	1.18	0.85
0.06	0.15	0.94	0.23	0.00	0.15	0.22	1.05	3.75	3.65	1.24	0.85
0.05	0.14	0.93	0.21	0.00	0.14	0.20	0.98	3.67	3.71	1.26	0.83
0.05	0.12	0.92	0.19	0.00	0.12	0.17	0.87	3.67	3.94	1.34	0.83
0.03	0.09	0.88	0.15	0.00	0.09	0.13	0.64	3.74	4.68	1.59	0.84
0.02	0.06	0.86	0.10	0.00	0.06	0.09	0.43	3.75	5.73	1.94	0.85

Table 13.17: Measured and calculated results of Model A7 with no roundings

Model A7 (No roundings)											
$Q_{measured}$	**H**	**P**	**v**	**Hv ($\frac{v^2}{2g}$)**	**H_T**	**q**	**H_T/P_m**	**C(H)**	**C($H^{1.5}$)**	**C_d($H^{1.5}$)**	**C_d'(H)**
0.11	0.27	1.06	0.41	0.01	0.28	0.43	1.93	4.11	2.96	1.00	0.93
0.10	0.25	1.04	0.38	0.01	0.25	0.39	1.76	4.08	3.08	1.04	0.92
0.09	0.22	1.02	0.34	0.01	0.23	0.35	1.57	4.05	3.23	1.09	0.91
0.08	0.19	0.99	0.31	0.00	0.20	0.31	1.39	4.04	3.43	1.16	0.91
0.07	0.18	0.98	0.29	0.00	0.19	0.28	1.29	4.04	3.56	1.21	0.91
0.07	0.17	0.96	0.27	0.00	0.17	0.26	1.18	4.05	3.72	1.26	0.91
0.06	0.14	0.94	0.23	0.00	0.15	0.22	1.01	3.96	3.93	1.33	0.89
0.05	0.11	0.91	0.19	0.00	0.11	0.18	0.77	4.16	4.74	1.60	0.94
0.03	0.08	0.88	0.15	0.00	0.08	0.13	0.58	4.12	5.42	1.83	0.93
0.02	0.06	0.85	0.10	0.00	0.06	0.08	0.39	3.90	6.21	2.10	0.88

Table 13.18: Measured and calculated results of Model A7 with roundings

Model A7 (With roundings)											
$Q_{measured}$	H	P	v	Hv $(\frac{v^2}{2g})$	H_T	q	H_T/P_m	C(H)	$C(H^{1.5})$	$C_d(H^{1.5})$	C_d'(H)
0.11	0.27	1.06	0.41	0.01	0.27	0.43	1.90	4.16	3.01	1.02	0.94
0.10	0.24	1.04	0.38	0.01	0.25	0.39	1.74	4.13	3.13	1.06	0.93
0.09	0.22	1.01	0.34	0.01	0.22	0.35	1.55	4.11	3.31	1.12	0.93
0.08	0.19	0.99	0.31	0.00	0.19	0.30	1.35	4.12	3.54	1.20	0.93
0.07	0.18	0.97	0.29	0.00	0.18	0.28	1.26	4.11	3.66	1.24	0.93
0.07	0.16	0.96	0.27	0.00	0.17	0.26	1.17	4.11	3.79	1.28	0.93
0.06	0.14	0.93	0.24	0.00	0.14	0.22	0.97	4.12	4.18	1.41	0.93
0.05	0.11	0.91	0.19	0.00	0.11	0.18	0.77	4.18	4.75	1.61	0.94
0.03	0.08	0.88	0.15	0.00	0.08	0.13	0.57	4.16	5.49	1.86	0.94
0.02	0.06	0.85	0.10	0.00	0.06	0.09	0.40	3.99	6.31	2.14	0.90

Table 13.19: Measured and calculated results of Model A8 with no roundings

Model A8 (No roundings)											
$Q_{measured}$	H	P	v	Hv $(\frac{v^2}{2g})$	H_T	q	H_T/P_m	C(H)	$C(H^{1.5})$	$C_d(H^{1.5})$	C_d'(H)
0.11	0.27	1.06	0.41	0.01	0.28	0.43	1.93	4.12	2.97	1.00	0.93
0.10	0.24	1.04	0.38	0.01	0.25	0.39	1.74	4.10	3.10	1.05	0.93
0.09	0.22	1.01	0.34	0.01	0.22	0.35	1.56	4.08	3.27	1.11	0.92
0.08	0.19	0.99	0.31	0.00	0.20	0.31	1.37	4.09	3.49	1.18	0.92
0.07	0.18	0.97	0.29	0.00	0.18	0.28	1.27	4.08	3.63	1.23	0.92
0.07	0.17	0.96	0.28	0.00	0.17	0.27	1.19	4.11	3.77	1.28	0.93
0.06	0.14	0.93	0.24	0.00	0.14	0.22	0.97	4.15	4.22	1.43	0.94
0.04	0.10	0.90	0.19	0.00	0.11	0.17	0.75	4.26	4.93	1.67	0.96
0.03	0.08	0.87	0.15	0.00	0.08	0.13	0.56	4.35	5.82	1.97	0.98
0.02	0.06	0.85	0.10	0.00	0.06	0.09	0.39	4.06	6.47	2.19	0.92

Table 13.20: Measured and calculated results of Model A8 with roundings

Model A8 (With roundings)											
$Q_{measured}$	H	P	v	Hv $(\frac{v^2}{2g})$	H_T	q	H_T/P_m	C(H)	$C(H^{1.5})$	$C_d(H^{1.5})$	C_d'(H)
0.11	0.26	1.06	0.41	0.01	0.27	0.43	1.89	4.18	3.04	1.03	0.94
0.10	0.24	1.04	0.38	0.01	0.25	0.39	1.73	4.17	3.17	1.07	0.94

0.09	0.21	1.01	0.34	0.01	0.22	0.35	1.54	4.14	3.34	1.13	0.94
0.08	0.19	0.98	0.31	0.00	0.19	0.31	1.34	4.17	3.60	1.22	0.94
0.07	0.17	0.97	0.29	0.00	0.18	0.28	1.24	4.16	3.73	1.26	0.94
0.07	0.16	0.96	0.27	0.00	0.17	0.26	1.15	4.15	3.86	1.31	0.94
0.06	0.13	0.93	0.24	0.00	0.14	0.22	0.96	4.22	4.32	1.46	0.95
0.05	0.11	0.90	0.20	0.00	0.11	0.18	0.75	4.32	4.98	1.69	0.97
0.03	0.08	0.87	0.15	0.00	0.08	0.13	0.55	4.43	6.00	2.03	1.00
0.02	0.06	0.85	0.10	0.00	0.06	0.09	0.39	4.10	6.55	2.22	0.93

Table 13.21: Measured and calculated results of Model A9 with no roundings

Model A9 (No roundings)											
$Q_{measured}$	H	P	v	Hv $(\frac{v^2}{2g})$	H_T	q	H_T/P_m	C(H)	C($H^{1.5}$)	$C_d(H^{1.5})$	$C_d'(H)$
0.10	0.27	1.07	0.37	0.01	0.28	0.40	1.93	3.78	2.72	0.92	0.85
0.08	0.23	1.03	0.32	0.01	0.23	0.33	1.63	3.67	2.87	0.97	0.83
0.07	0.20	1.00	0.28	0.00	0.21	0.28	1.43	3.62	3.03	1.03	0.82
0.07	0.19	0.99	0.27	0.00	0.19	0.26	1.33	3.60	3.12	1.06	0.81
0.06	0.17	0.97	0.25	0.00	0.18	0.24	1.23	3.57	3.21	1.09	0.81
0.06	0.16	0.96	0.23	0.00	0.16	0.22	1.13	3.55	3.35	1.13	0.80
0.05	0.14	0.94	0.21	0.00	0.15	0.20	1.01	3.54	3.52	1.19	0.80
0.05	0.13	0.92	0.19	0.00	0.13	0.17	0.90	3.55	3.75	1.27	0.80
0.03	0.09	0.89	0.15	0.00	0.10	0.13	0.66	3.60	4.42	1.50	0.81
0.02	0.06	0.86	0.10	0.00	0.06	0.09	0.44	3.65	5.49	1.86	0.82

Table 13.22: Measured and calculated results of Model A9 with roundings

Model A9 (With roundings)											
$Q_{measured}$	H	P	v	Hv $(\frac{v^2}{2g})$	H_T	q	H_T/P_m	C(H)	C($H^{1.5}$)	$C_d(H^{1.5})$	$C_d'(H)$
0.10	0.27	1.07	0.37	0.01	0.27	0.39	1.91	3.75	2.72	0.92	0.85
0.08	0.23	1.03	0.32	0.01	0.23	0.33	1.63	3.66	2.87	0.97	0.83
0.07	0.20	1.00	0.28	0.00	0.21	0.28	1.43	3.63	3.03	1.03	0.82
0.07	0.19	0.99	0.27	0.00	0.19	0.26	1.34	3.60	3.12	1.05	0.81
0.06	0.17	0.97	0.25	0.00	0.18	0.24	1.23	3.57	3.22	1.09	0.81
0.06	0.16	0.96	0.23	0.00	0.16	0.22	1.12	3.57	3.37	1.14	0.81
0.05	0.14	0.94	0.21	0.00	0.14	0.20	1.00	3.56	3.56	1.20	0.80
0.05	0.13	0.92	0.19	0.00	0.13	0.17	0.90	3.55	3.74	1.27	0.80

0.03	0.10	0.89	0.15	0.00	0.10	0.13	0.67	3.59	4.38	1.48	0.81
0.02	0.06	0.86	0.10	0.00	0.06	0.09	0.44	3.65	5.50	1.86	0.82

Table 13.23: Measured and calculated results of Model A10 with no roundings

Model A10 (No roundings)											
$Q_{measured}$	**H**	**P**	**v**	**Hv ($\frac{v^2}{2g}$)**	**H_T**	**q**	**H_T/P_m**	**C(H)**	**C($H^{1.5}$)**	**C_d($H^{1.5}$)**	**C_d'(H)**
0.08	0.22	0.99	0.33	0.01	0.22	0.33	1.54	3.90	3.14	1.06	0.88
0.07	0.19	0.97	0.30	0.00	0.20	0.29	1.37	3.82	3.27	1.11	0.86
0.07	0.18	0.95	0.28	0.00	0.18	0.26	1.28	3.77	3.34	1.13	0.85
0.06	0.17	0.94	0.26	0.00	0.17	0.24	1.19	3.73	3.43	1.16	0.84
0.06	0.15	0.93	0.24	0.00	0.16	0.22	1.08	3.71	3.57	1.21	0.84
0.05	0.14	0.91	0.22	0.00	0.14	0.20	0.97	3.72	3.77	1.28	0.84
0.04	0.12	0.89	0.19	0.00	0.12	0.17	0.85	3.75	4.07	1.38	0.85
0.04	0.10	0.88	0.17	0.00	0.11	0.15	0.74	3.77	4.38	1.48	0.85
0.03	0.09	0.86	0.15	0.00	0.09	0.13	0.63	3.79	4.79	1.62	0.86
0.02	0.07	0.84	0.10	0.00	0.07	0.09	0.49	3.25	4.67	1.58	0.73

Table 13.24: Measured and calculated results of Model A10 with roundings

Model A10 (With roundings)											
$Q_{measured}$	**H**	**P**	**v**	**Hv ($\frac{v^2}{2g}$)**	**H_T**	**q**	**H_T/P_m**	**C(H)**	**C($H^{1.5}$)**	**C_d($H^{1.5}$)**	**C_d'(H)**
0.08	0.22	1.00	0.33	0.01	0.23	0.33	1.57	3.80	3.03	1.03	0.86
0.07	0.19	0.97	0.29	0.00	0.20	0.28	1.38	3.74	3.18	1.08	0.84
0.07	0.18	0.96	0.28	0.00	0.19	0.26	1.29	3.73	3.28	1.11	0.84
0.06	0.17	0.94	0.26	0.00	0.17	0.24	1.19	3.71	3.41	1.15	0.84
0.06	0.15	0.93	0.24	0.00	0.15	0.22	1.07	3.72	3.59	1.22	0.84
0.05	0.13	0.91	0.21	0.00	0.14	0.19	0.95	3.74	3.83	1.30	0.84
0.05	0.12	0.90	0.20	0.00	0.12	0.18	0.85	3.75	4.05	1.37	0.85
0.04	0.11	0.88	0.18	0.00	0.11	0.15	0.75	3.76	4.34	1.47	0.85
0.03	0.09	0.87	0.15	0.00	0.09	0.13	0.64	3.79	4.74	1.61	0.86
0.02	0.07	0.84	0.10	0.00	0.07	0.09	0.49	3.28	4.70	1.59	0.74

Table 13.25: Measured and calculated results of Model A11 with no roundings

Model A11 (No roundings)											
$Q_{measured}$	H	P	v	Hv ($\frac{v^2}{2g}$)	H_T	q	H_T/P_m	C(H)	C($H^{1.5}$)	C_d($H^{1.5}$)	C_d'(H)
0.11	0.25	1.05	0.40	0.01	0.26	0.42	1.81	4.21	3.13	1.06	0.95
0.09	0.20	1.00	0.33	0.01	0.21	0.33	1.45	4.16	3.45	1.17	0.94
0.07	0.18	0.97	0.29	0.00	0.18	0.28	1.26	4.13	3.68	1.25	0.93
0.07	0.16	0.96	0.27	0.00	0.17	0.26	1.16	4.15	3.85	1.30	0.94
0.06	0.15	0.95	0.25	0.00	0.15	0.24	1.07	4.13	4.00	1.35	0.93
0.06	0.14	0.93	0.23	0.00	0.14	0.22	0.96	4.14	4.22	1.43	0.93
0.05	0.12	0.92	0.21	0.00	0.12	0.20	0.87	4.17	4.48	1.52	0.94
0.04	0.11	0.91	0.19	0.00	0.11	0.17	0.76	4.21	4.85	1.64	0.95
0.03	0.08	0.88	0.15	0.00	0.08	0.13	0.56	4.34	5.80	1.96	0.98
0.02	0.05	0.85	0.10	0.00	0.06	0.09	0.39	4.14	6.65	2.25	0.93

Table 13.26: Measured and calculated results of Model A11 with roundings

Model A11 (With roundings)											
$Q_{measured}$	H	P	v	Hv ($\frac{v^2}{2g}$)	H_T	q	H_T/P_m	C(H)	C($H^{1.5}$)	C_d($H^{1.5}$)	C_d'(H)
0.11	0.25	1.05	0.39	0.01	0.26	0.41	1.80	4.21	3.14	1.06	0.95
0.08	0.20	1.00	0.33	0.01	0.21	0.33	1.44	4.15	3.45	1.17	0.94
0.07	0.18	0.97	0.29	0.00	0.18	0.28	1.25	4.15	3.70	1.25	0.94
0.07	0.16	0.96	0.27	0.00	0.17	0.26	1.16	4.15	3.86	1.31	0.94
0.06	0.15	0.95	0.25	0.00	0.15	0.24	1.06	4.16	4.03	1.36	0.94
0.06	0.14	0.93	0.23	0.00	0.14	0.22	0.96	4.16	4.24	1.44	0.94
0.05	0.12	0.92	0.21	0.00	0.12	0.20	0.86	4.16	4.47	1.51	0.94
0.05	0.11	0.90	0.19	0.00	0.11	0.18	0.75	4.26	4.91	1.66	0.96
0.03	0.08	0.88	0.15	0.00	0.08	0.13	0.56	4.34	5.80	1.96	0.98
0.02	0.05	0.85	0.10	0.00	0.06	0.09	0.39	4.13	6.66	2.26	0.93

13.3 Model set B

Table 13.27: Measured and calculated results of Model B1 with no roundings

Model B1 (No roundings)											
$Q_{measured}$	H	P	v	Hv ($\frac{v^2}{2g}$)	H_T	q	H_T/P_m	C(H)	C($H^{1.5}$)	C_d($H^{1.5}$)	C_d'(H)
0.11	0.22	1.03	0.32	0.01	0.22	0.33	1.56	3.87	3.10	1.05	0.87
0.10	0.20	1.01	0.29	0.00	0.20	0.29	1.40	3.85	3.26	1.10	0.87
0.09	0.18	0.99	0.26	0.00	0.18	0.26	1.25	3.84	3.44	1.16	0.87
0.08	0.16	0.97	0.24	0.00	0.16	0.23	1.12	3.77	3.57	1.21	0.85
0.07	0.15	0.96	0.22	0.00	0.15	0.21	1.05	3.70	3.61	1.22	0.84
0.07	0.14	0.95	0.21	0.00	0.14	0.20	0.98	3.69	3.73	1.26	0.83
0.06	0.13	0.94	0.19	0.00	0.13	0.18	0.90	3.68	3.88	1.32	0.83
0.06	0.12	0.93	0.18	0.00	0.12	0.17	0.82	3.69	4.07	1.38	0.83
0.05	0.10	0.92	0.16	0.00	0.11	0.15	0.73	3.69	4.31	1.46	0.83
0.03	0.07	0.89	0.11	0.00	0.07	0.10	0.50	3.65	5.18	1.75	0.82
0.02	0.05	0.87	0.08	0.00	0.05	0.07	0.35	3.44	5.82	1.97	0.78

Table 13.28: Measured and calculated results of Model B1 with roundings

Model B1 (With roundings)											
$Q_{measured}$	H	P	v	Hv ($\frac{v^2}{2g}$)	H_T	q	H_T/P_m	C(H)	C($H^{1.5}$)	C_d($H^{1.5}$)	C_d'(H)
0.11	0.22	1.03	0.32	0.01	0.22	0.33	1.54	3.92	3.16	1.07	0.89
0.10	0.19	1.01	0.29	0.00	0.20	0.29	1.38	3.88	3.30	1.12	0.88
0.09	0.18	1.00	0.26	0.00	0.18	0.26	1.27	3.77	3.35	1.13	0.85
0.08	0.16	0.97	0.24	0.00	0.16	0.23	1.12	3.75	3.55	1.20	0.85
0.07	0.15	0.96	0.22	0.00	0.15	0.21	1.04	3.74	3.66	1.24	0.84
0.07	0.14	0.95	0.21	0.00	0.14	0.20	0.97	3.72	3.78	1.28	0.84
0.06	0.13	0.94	0.19	0.00	0.13	0.18	0.89	3.73	3.96	1.34	0.84
0.06	0.11	0.93	0.18	0.00	0.12	0.16	0.80	3.73	4.16	1.41	0.84
0.05	0.10	0.92	0.16	0.00	0.10	0.15	0.73	3.72	4.36	1.48	0.84
0.03	0.07	0.89	0.11	0.00	0.07	0.10	0.49	3.67	5.23	1.77	0.83
0.02	0.05	0.87	0.08	0.00	0.05	0.07	0.35	3.45	5.85	1.98	0.78

Table 13.29: Measured and calculated results of Model B2 with no roundings

Model B2 (No roundings)											
$Q_{measured}$	H	P	v	Hv ($\frac{v^2}{2g}$)	H_T	q	H_T/P_m	C(H)	C($H^{1.5}$)	C_d($H^{1.5}$)	C_d'(H)
0.12	0.23	1.04	0.34	0.01	0.24	0.36	1.64	4.01	3.13	1.06	0.90
0.10	0.19	1.01	0.29	0.00	0.20	0.29	1.36	3.95	3.38	1.15	0.89
0.09	0.17	0.99	0.27	0.00	0.18	0.26	1.24	3.87	3.47	1.18	0.87
0.08	0.16	0.97	0.24	0.00	0.16	0.23	1.11	3.80	3.61	1.22	0.86
0.07	0.15	0.96	0.22	0.00	0.15	0.21	1.03	3.78	3.72	1.26	0.85
0.07	0.14	0.95	0.21	0.00	0.14	0.20	0.96	3.77	3.84	1.30	0.85
0.06	0.12	0.94	0.19	0.00	0.13	0.18	0.88	3.76	4.00	1.35	0.85
0.06	0.11	0.93	0.18	0.00	0.12	0.17	0.81	3.75	4.18	1.42	0.85
0.05	0.09	0.91	0.14	0.00	0.09	0.13	0.64	3.73	4.65	1.58	0.84
0.03	0.07	0.88	0.11	0.00	0.07	0.10	0.49	3.69	5.27	1.78	0.83
0.02	0.05	0.86	0.08	0.00	0.05	0.07	0.34	3.52	6.04	2.04	0.80

Table 13.30: Measured and calculated results of Model B2 with roundings

Model B2 (With roundings)											
$Q_{measured}$	H	P	v	Hv ($\frac{v^2}{2g}$)	H_T	q	H_T/P_m	C(H)	C($H^{1.5}$)	C_d($H^{1.5}$)	C_d'(H)
0.12	0.23	1.04	0.34	0.01	0.23	0.36	1.62	4.06	3.19	1.08	0.92
0.10	0.19	1.00	0.29	0.00	0.19	0.29	1.34	4.01	3.46	1.17	0.90
0.09	0.17	0.99	0.26	0.00	0.18	0.26	1.23	3.90	3.52	1.19	0.88
0.08	0.15	0.97	0.24	0.00	0.16	0.23	1.09	3.85	3.68	1.25	0.87
0.07	0.14	0.96	0.22	0.00	0.15	0.21	1.03	3.82	3.77	1.28	0.86
0.07	0.13	0.95	0.21	0.00	0.14	0.20	0.95	3.82	3.93	1.33	0.86
0.06	0.12	0.94	0.19	0.00	0.12	0.18	0.87	3.82	4.10	1.39	0.86
0.06	0.11	0.93	0.18	0.00	0.11	0.16	0.79	3.81	4.28	1.45	0.86
0.05	0.09	0.90	0.15	0.00	0.09	0.13	0.63	3.81	4.79	1.62	0.86
0.03	0.07	0.88	0.11	0.00	0.07	0.10	0.48	3.75	5.39	1.82	0.85
0.02	0.05	0.86	0.08	0.00	0.05	0.07	0.34	3.58	6.16	2.09	0.81

Table 13.31: Measured and calculated results of Model B3 with no roundings

Model B3 (No roundings)											
$Q_{measured}$	H	P	v	Hv $(\frac{v^2}{2g})$	H_T	q	H_T/P_m	C(H)	C($H^{1.5}$)	C_d($H^{1.5}$)	C_d'(H)
0.11	0.21	1.03	0.32	0.01	0.22	0.33	1.51	4.01	3.26	1.11	0.91
0.10	0.19	1.00	0.29	0.00	0.19	0.29	1.34	4.01	3.46	1.17	0.90
0.09	0.17	0.98	0.27	0.00	0.17	0.26	1.20	3.99	3.65	1.24	0.90
0.08	0.15	0.96	0.24	0.00	0.15	0.23	1.06	3.93	3.82	1.29	0.89
0.07	0.14	0.96	0.22	0.00	0.14	0.21	1.00	3.89	3.89	1.32	0.88
0.07	0.13	0.95	0.21	0.00	0.13	0.20	0.93	3.88	4.02	1.36	0.88
0.06	0.11	0.92	0.18	0.00	0.11	0.16	0.77	3.89	4.43	1.50	0.88
0.05	0.10	0.91	0.16	0.00	0.10	0.15	0.70	3.88	4.65	1.58	0.88
0.04	0.09	0.90	0.14	0.00	0.09	0.13	0.61	3.88	4.95	1.68	0.88
0.03	0.07	0.88	0.11	0.00	0.07	0.10	0.48	3.83	5.54	1.87	0.86
0.02	0.05	0.86	0.08	0.00	0.05	0.07	0.33	3.67	6.38	2.16	0.83

Table 13.32: Measured and calculated results of Model B3 with roundings

Model B3 (With roundings)											
$Q_{measured}$	H	P	v	Hv $(\frac{v^2}{2g})$	H_T	q	H_T/P_m	C(H)	C($H^{1.5}$)	C_d($H^{1.5}$)	C_d'(H)
0.11	0.21	1.02	0.32	0.01	0.21	0.33	1.48	4.06	3.34	1.13	0.92
0.10	0.19	1.00	0.29	0.00	0.19	0.29	1.33	4.05	3.51	1.19	0.91
0.09	0.17	0.98	0.27	0.00	0.17	0.26	1.19	4.02	3.68	1.25	0.91
0.08	0.15	0.96	0.24	0.00	0.15	0.23	1.06	3.98	3.87	1.31	0.90
0.07	0.14	0.95	0.22	0.00	0.14	0.21	0.99	3.95	3.97	1.34	0.89
0.07	0.13	0.94	0.21	0.00	0.13	0.20	0.92	3.94	4.11	1.39	0.89
0.06	0.11	0.92	0.18	0.00	0.11	0.16	0.76	3.95	4.54	1.54	0.89
0.05	0.10	0.91	0.16	0.00	0.10	0.15	0.68	3.96	4.79	1.62	0.89
0.05	0.09	0.90	0.15	0.00	0.09	0.13	0.61	3.93	5.03	1.70	0.89
0.03	0.07	0.88	0.11	0.00	0.07	0.10	0.47	3.89	5.68	1.92	0.88
0.02	0.05	0.86	0.08	0.00	0.05	0.07	0.33	3.69	6.43	2.18	0.83

Table 13.33: Measured and calculated results of Model B4 with no roundings

Model B4 (No roundings)											
$Q_{measured}$	H	P	v	Hv $(\frac{v^2}{2g})$	H_T	q	H_T/P_m	C(H)	C($H^{1.5}$)	C_d($H^{1.5}$)	C_d'(H)
0.11	0.21	1.03	0.32	0.01	0.22	0.33	1.52	3.97	3.22	1.09	0.90
0.10	0.19	1.01	0.29	0.00	0.19	0.29	1.35	3.98	3.42	1.16	0.90
0.09	0.17	0.99	0.27	0.00	0.17	0.27	1.21	4.00	3.63	1.23	0.90
0.08	0.15	0.96	0.24	0.00	0.15	0.23	1.04	4.04	3.97	1.34	0.91
0.07	0.13	0.95	0.22	0.00	0.14	0.21	0.95	4.11	4.22	1.43	0.93
0.07	0.12	0.94	0.21	0.00	0.13	0.20	0.88	4.09	4.36	1.48	0.92
0.06	0.10	0.92	0.18	0.00	0.10	0.16	0.73	4.16	4.88	1.65	0.94
0.05	0.09	0.91	0.16	0.00	0.09	0.15	0.66	4.15	5.11	1.73	0.94
0.05	0.08	0.90	0.15	0.00	0.08	0.13	0.59	4.10	5.34	1.81	0.92
0.04	0.07	0.88	0.12	0.00	0.07	0.10	0.46	4.06	5.97	2.02	0.92
0.02	0.05	0.86	0.08	0.00	0.05	0.07	0.32	3.91	6.90	2.34	0.88

Table 13.34: Measured and calculated results of Model B4 with roundings

Model B4 (With roundings)											
$Q_{measured}$	H	P	v	Hv $(\frac{v^2}{2g})$	H_T	q	H_T/P_m	C(H)	C($H^{1.5}$)	C_d($H^{1.5}$)	C_d'(H)
0.11	0.20	1.02	0.32	0.01	0.21	0.33	1.49	4.04	3.31	1.12	0.91
0.10	0.19	1.00	0.29	0.00	0.19	0.30	1.34	4.04	3.49	1.18	0.91
0.09	0.16	0.98	0.27	0.00	0.17	0.26	1.16	4.08	3.79	1.28	0.92
0.08	0.14	0.96	0.24	0.00	0.15	0.23	1.02	4.13	4.10	1.39	0.93
0.07	0.13	0.95	0.23	0.00	0.14	0.21	0.94	4.16	4.28	1.45	0.94
0.07	0.12	0.94	0.21	0.00	0.12	0.20	0.86	4.20	4.53	1.53	0.95
0.06	0.10	0.92	0.18	0.00	0.10	0.16	0.72	4.19	4.94	1.67	0.95
0.05	0.09	0.91	0.16	0.00	0.09	0.15	0.65	4.13	5.11	1.73	0.93
0.05	0.08	0.90	0.15	0.00	0.08	0.13	0.59	4.13	5.38	1.82	0.93
0.03	0.06	0.88	0.12	0.00	0.06	0.10	0.45	4.12	6.15	2.08	0.93
0.02	0.04	0.86	0.08	0.00	0.05	0.07	0.32	3.82	6.80	2.30	0.86

Table 13.35: Measured and calculated results of Model B5 with no roundings

Model B5 (No roundings)											
$Q_{measured}$	H	P	v	Hv ($\frac{v^2}{2g}$)	H_T	q	H_T/P_m	C(H)	C($H^{1.5}$)	C_d($H^{1.5}$)	C_d'(H)
0.11	0.21	1.02	0.32	0.01	0.22	0.33	1.50	4.04	3.31	1.12	0.91
0.10	0.19	1.00	0.29	0.00	0.19	0.29	1.32	4.05	3.53	1.19	0.91
0.09	0.17	0.98	0.27	0.00	0.17	0.26	1.17	4.08	3.77	1.28	0.92
0.08	0.15	0.96	0.24	0.00	0.15	0.23	1.04	4.05	3.98	1.35	0.91
0.07	0.14	0.95	0.22	0.00	0.14	0.21	0.97	4.05	4.12	1.39	0.91
0.07	0.13	0.94	0.21	0.00	0.13	0.20	0.89	4.03	4.27	1.45	0.91
0.06	0.10	0.92	0.18	0.00	0.11	0.16	0.74	4.01	4.68	1.58	0.91
0.05	0.09	0.91	0.16	0.00	0.10	0.15	0.67	4.00	4.89	1.66	0.90
0.05	0.09	0.90	0.15	0.00	0.09	0.13	0.61	4.01	5.15	1.75	0.91
0.03	0.06	0.88	0.11	0.00	0.06	0.10	0.45	4.02	6.01	2.03	0.91
0.02	0.04	0.86	0.08	0.00	0.05	0.07	0.32	3.82	6.78	2.30	0.86

Table 13.36: Measured and calculated results of Model B5 with roundings

Model B5 (With roundings)											
$Q_{measured}$	H	P	v	Hv ($\frac{v^2}{2g}$)	H_T	q	H_T/P_m	C(H)	C($H^{1.5}$)	C_d($H^{1.5}$)	C_d'(H)
0.11	0.20	1.02	0.32	0.01	0.21	0.33	1.46	4.13	3.41	1.16	0.93
0.10	0.18	1.00	0.30	0.00	0.19	0.29	1.30	4.13	3.62	1.22	0.93
0.09	0.16	0.98	0.27	0.00	0.17	0.26	1.16	4.14	3.84	1.30	0.93
0.08	0.14	0.96	0.24	0.00	0.15	0.23	1.02	4.13	4.10	1.39	0.93
0.07	0.13	0.95	0.22	0.00	0.14	0.21	0.94	4.10	4.22	1.43	0.93
0.07	0.12	0.94	0.21	0.00	0.13	0.20	0.88	4.11	4.38	1.48	0.93
0.06	0.10	0.92	0.18	0.00	0.10	0.16	0.73	4.13	4.85	1.64	0.93
0.05	0.09	0.91	0.16	0.00	0.09	0.15	0.66	4.11	5.08	1.72	0.93
0.05	0.08	0.90	0.15	0.00	0.08	0.13	0.59	4.14	5.40	1.83	0.93
0.03	0.06	0.88	0.11	0.00	0.06	0.10	0.45	4.04	6.04	2.05	0.91
0.02	0.04	0.86	0.08	0.00	0.05	0.07	0.31	3.85	6.87	2.33	0.87

Table 13.37: Measured and calculated results of Model B6 with no roundings

Model B6 (No roundings)											
$Q_{measured}$	H	P	v	Hv $(\frac{v^2}{2g})$	H_T	q	H_T/P_m	C(H)	C($H^{1.5}$)	$C_d(H^{1.5})$	C_d'(H)
0.12	0.23	1.05	0.32	0.01	0.24	0.34	1.65	3.75	2.92	0.99	0.85
0.10	0.20	1.02	0.29	0.00	0.21	0.30	1.46	3.71	3.07	1.04	0.84
0.09	0.18	1.00	0.26	0.00	0.19	0.26	1.30	3.67	3.21	1.09	0.83
0.08	0.16	0.98	0.23	0.00	0.17	0.23	1.15	3.64	3.39	1.15	0.82
0.07	0.15	0.97	0.22	0.00	0.16	0.21	1.08	3.63	3.49	1.18	0.82
0.07	0.14	0.96	0.21	0.00	0.14	0.20	1.00	3.61	3.61	1.22	0.82
0.06	0.12	0.93	0.18	0.00	0.12	0.16	0.83	3.60	3.95	1.34	0.81
0.05	0.11	0.92	0.16	0.00	0.11	0.15	0.76	3.58	4.12	1.39	0.81
0.05	0.10	0.91	0.14	0.00	0.10	0.13	0.68	3.57	4.34	1.47	0.81
0.03	0.07	0.89	0.11	0.00	0.08	0.10	0.52	3.49	4.84	1.64	0.79
0.02	0.05	0.87	0.08	0.00	0.05	0.07	0.36	3.32	5.50	1.86	0.75

Table 13.38: Measured and calculated results of Model B6 with roundings

Model B6 (With roundings)											
$Q_{measured}$	H	P	v	Hv $(\frac{v^2}{2g})$	H_T	q	H_T/P_m	C(H)	C($H^{1.5}$)	$C_d(H^{1.5})$	C_d'(H)
0.12	0.23	1.05	0.32	0.01	0.24	0.34	1.65	3.76	2.93	0.99	0.85
0.10	0.20	1.02	0.29	0.00	0.21	0.29	1.45	3.70	3.08	1.04	0.84
0.09	0.18	1.00	0.26	0.00	0.19	0.26	1.30	3.68	3.23	1.09	0.83
0.08	0.16	0.98	0.24	0.00	0.17	0.23	1.16	3.65	3.40	1.15	0.82
0.07	0.15	0.97	0.22	0.00	0.15	0.21	1.07	3.64	3.51	1.19	0.82
0.07	0.14	0.96	0.21	0.00	0.14	0.20	1.00	3.61	3.61	1.22	0.81
0.06	0.12	0.93	0.18	0.00	0.12	0.16	0.84	3.59	3.92	1.33	0.81
0.05	0.11	0.92	0.16	0.00	0.11	0.15	0.76	3.60	4.14	1.40	0.81
0.05	0.10	0.91	0.14	0.00	0.10	0.13	0.67	3.58	4.36	1.48	0.81
0.03	0.07	0.89	0.11	0.00	0.07	0.10	0.51	3.52	4.91	1.66	0.79
0.02	0.05	0.87	0.08	0.00	0.05	0.07	0.37	3.30	5.44	1.84	0.75

Table 13.39: Measured and calculated results of Model B7 with no roundings

Model B7 (No roundings)											
$Q_{measured}$	H	P	v	Hv $(\frac{v^2}{2g})$	H_T	q	H_T/P_m	C(H)	C($H^{1.5}$)	C_d($H^{1.5}$)	C_d'(H)
0.12	0.22	1.03	0.32	0.01	0.22	0.34	1.56	3.94	3.15	1.07	0.89
0.10	0.19	1.01	0.29	0.00	0.20	0.29	1.38	3.91	3.32	1.13	0.88
0.09	0.17	0.99	0.27	0.00	0.18	0.26	1.23	3.89	3.51	1.19	0.88
0.08	0.15	0.97	0.24	0.00	0.16	0.23	1.09	3.86	3.70	1.25	0.87
0.07	0.14	0.96	0.22	0.00	0.15	0.21	1.01	3.88	3.86	1.31	0.88
0.07	0.13	0.95	0.21	0.00	0.13	0.20	0.93	3.87	4.01	1.36	0.87
0.06	0.11	0.92	0.18	0.00	0.11	0.17	0.78	3.88	4.39	1.49	0.88
0.05	0.10	0.91	0.16	0.00	0.10	0.15	0.70	3.88	4.64	1.57	0.88
0.05	0.09	0.90	0.15	0.00	0.09	0.13	0.62	3.88	4.91	1.66	0.88
0.03	0.07	0.88	0.11	0.00	0.07	0.10	0.48	3.83	5.53	1.87	0.86
0.02	0.05	0.86	0.08	0.00	0.05	0.07	0.33	3.62	6.26	2.12	0.82

Table 13.40: Measured and calculated results of Model B7 with roundings

Model B7 (With roundings)											
$Q_{measured}$	H	P	v	Hv $(\frac{v^2}{2g})$	H_T	q	H_T/P_m	C(H)	C($H^{1.5}$)	C_d($H^{1.5}$)	C_d'(H)
0.12	0.22	1.03	0.33	0.01	0.22	0.34	1.56	3.95	3.17	1.07	0.89
0.10	0.19	1.01	0.29	0.00	0.20	0.30	1.38	3.92	3.34	1.13	0.89
0.09	0.17	0.99	0.26	0.00	0.18	0.26	1.23	3.90	3.52	1.19	0.88
0.08	0.15	0.96	0.24	0.00	0.15	0.23	1.07	3.89	3.76	1.27	0.88
0.07	0.14	0.96	0.22	0.00	0.15	0.21	1.01	3.89	3.88	1.31	0.88
0.07	0.13	0.94	0.21	0.00	0.13	0.20	0.93	3.89	4.04	1.37	0.88
0.06	0.11	0.92	0.18	0.00	0.11	0.16	0.77	3.91	4.47	1.51	0.88
0.05	0.10	0.91	0.16	0.00	0.10	0.15	0.69	3.91	4.69	1.59	0.88
0.05	0.09	0.90	0.15	0.00	0.09	0.13	0.62	3.91	4.97	1.68	0.88
0.03	0.07	0.88	0.11	0.00	0.07	0.10	0.47	3.83	5.58	1.89	0.86
0.02	0.05	0.86	0.08	0.00	0.05	0.07	0.33	3.62	6.29	2.13	0.82

Table 13.41: Measured and calculated results of Model B8 with no roundings

Model B8 (No roundings)											
$Q_{measured}$	H	P	v	Hv $(\frac{v^2}{2g})$	H_T	q	H_T/P_m	C(H)	$C(H^{1.5})$	$C_d(H^{1.5})$	$C_d'(H)$
0.12	0.21	1.03	0.33	0.01	0.22	0.34	1.53	4.06	3.28	1.11	0.92
0.10	0.19	1.00	0.29	0.00	0.19	0.29	1.34	4.02	3.48	1.18	0.91
0.09	0.17	0.98	0.27	0.00	0.17	0.26	1.19	4.02	3.68	1.25	0.91
0.08	0.15	0.96	0.24	0.00	0.15	0.23	1.04	4.00	3.91	1.33	0.90
0.07	0.14	0.95	0.22	0.00	0.14	0.21	0.97	4.01	4.08	1.38	0.90
0.07	0.13	0.94	0.21	0.00	0.13	0.20	0.90	4.00	4.23	1.43	0.90
0.06	0.10	0.92	0.18	0.00	0.11	0.16	0.74	4.04	4.70	1.59	0.91
0.05	0.09	0.91	0.16	0.00	0.10	0.15	0.66	4.06	4.98	1.69	0.92
0.05	0.08	0.90	0.15	0.00	0.09	0.13	0.59	4.05	5.27	1.78	0.91
0.03	0.06	0.88	0.11	0.00	0.06	0.10	0.45	4.01	5.98	2.03	0.90
0.02	0.04	0.86	0.08	0.00	0.05	0.06	0.31	3.79	6.76	2.29	0.86

Table 13.42: Measured and calculated results of Model B8 with roundings

Model B8 (With roundings)											
$Q_{measured}$	H	P	v	Hv $(\frac{v^2}{2g})$	H_T	q	H_T/P_m	C(H)	$C(H^{1.5})$	$C_d(H^{1.5})$	$C_d'(H)$
0.12	0.21	1.03	0.33	0.01	0.22	0.34	1.52	4.05	3.28	1.11	0.91
0.10	0.18	1.00	0.29	0.00	0.19	0.29	1.32	4.04	3.52	1.19	0.91
0.09	0.17	0.98	0.27	0.00	0.17	0.26	1.18	4.05	3.72	1.26	0.91
0.08	0.15	0.96	0.24	0.00	0.15	0.23	1.03	4.05	3.99	1.35	0.92
0.07	0.13	0.95	0.22	0.00	0.14	0.21	0.95	4.06	4.17	1.41	0.92
0.07	0.13	0.94	0.21	0.00	0.13	0.20	0.89	4.05	4.31	1.46	0.92
0.06	0.10	0.92	0.18	0.00	0.11	0.16	0.73	4.07	4.76	1.61	0.92
0.05	0.09	0.91	0.16	0.00	0.09	0.15	0.66	4.09	5.04	1.71	0.92
0.04	0.08	0.90	0.15	0.00	0.08	0.13	0.58	4.09	5.35	1.81	0.92
0.03	0.06	0.88	0.11	0.00	0.06	0.10	0.45	4.02	6.01	2.03	0.91
0.02	0.04	0.86	0.08	0.00	0.05	0.07	0.31	3.83	6.82	2.31	0.86

Table 13.43: Measured and calculated results of Model B9 with no roundings

Model B9 (No roundings)											
$Q_{measured}$	H	P	v	Hv ($\frac{v^2}{2g}$)	H_T	q	H_T/P_m	C(H)	C($H^{1.5}$)	C_d($H^{1.5}$)	C_d'(H)
0.12	0.24	1.06	0.32	0.01	0.24	0.34	1.69	3.64	2.80	0.95	0.82
0.10	0.21	1.03	0.29	0.00	0.22	0.29	1.50	3.59	2.92	0.99	0.81
0.09	0.19	1.01	0.26	0.00	0.20	0.26	1.36	3.55	3.04	1.03	0.80
0.08	0.17	0.99	0.23	0.00	0.17	0.23	1.20	3.50	3.19	1.08	0.79
0.07	0.16	0.98	0.22	0.00	0.16	0.21	1.13	3.47	3.27	1.11	0.78
0.07	0.15	0.97	0.20	0.00	0.15	0.20	1.04	3.47	3.40	1.15	0.78
0.06	0.12	0.94	0.17	0.00	0.13	0.16	0.87	3.41	3.66	1.24	0.77
0.05	0.11	0.93	0.16	0.00	0.11	0.15	0.80	3.40	3.81	1.29	0.77
0.05	0.10	0.92	0.14	0.00	0.10	0.13	0.71	3.39	4.01	1.36	0.76
0.03	0.08	0.90	0.11	0.00	0.08	0.10	0.55	3.33	4.50	1.52	0.75
0.02	0.05	0.87	0.07	0.00	0.05	0.07	0.38	3.17	5.18	1.75	0.72

Table 13.44: Measured and calculated results of Model B9 with roundings

Model B9 (With roundings)											
$Q_{measured}$	H	P	v	Hv ($\frac{v^2}{2g}$)	H_T	q	H_T/P_m	C(H)	C($H^{1.5}$)	C_d($H^{1.5}$)	C_d'(H)
0.12	0.24	1.06	0.32	0.01	0.24	0.34	1.70	3.64	2.80	0.95	0.82
0.10	0.21	1.03	0.29	0.00	0.22	0.29	1.50	3.58	2.92	0.99	0.81
0.09	0.19	1.01	0.26	0.00	0.20	0.26	1.36	3.54	3.04	1.03	0.80
0.08	0.17	0.99	0.23	0.00	0.17	0.23	1.20	3.50	3.19	1.08	0.79
0.07	0.16	0.98	0.22	0.00	0.16	0.21	1.13	3.48	3.27	1.11	0.78
0.07	0.15	0.97	0.20	0.00	0.15	0.20	1.05	3.45	3.38	1.14	0.78
0.06	0.13	0.94	0.17	0.00	0.13	0.16	0.89	3.41	3.63	1.23	0.77
0.05	0.11	0.93	0.16	0.00	0.11	0.15	0.80	3.39	3.79	1.28	0.76
0.05	0.10	0.92	0.14	0.00	0.10	0.13	0.72	3.38	4.00	1.36	0.76
0.03	0.08	0.90	0.11	0.00	0.08	0.10	0.55	3.31	4.47	1.51	0.75
0.02	0.05	0.87	0.08	0.00	0.05	0.07	0.37	3.21	5.25	1.78	0.72

Table 13.45: Measured and calculated results of Model B10 with no roundings

Model B10 (No roundings)											
$Q_{measured}$	H	P	v	Hv $(\frac{v^2}{2g})$	H_T	q	H_T/P_m	C(H)	C($H^{1.5}$)	$C_d(H^{1.5})$	$C_d'(H)$
0.12	0.23	1.05	0.32	0.01	0.24	0.34	1.64	3.79	2.96	1.00	0.86
0.10	0.20	1.02	0.29	0.00	0.21	0.29	1.44	3.74	3.12	1.06	0.84
0.09	0.18	1.00	0.26	0.00	0.19	0.26	1.29	3.70	3.25	1.10	0.83
0.08	0.16	0.98	0.23	0.00	0.17	0.23	1.15	3.66	3.41	1.16	0.83
0.07	0.15	0.97	0.22	0.00	0.15	0.21	1.07	3.64	3.51	1.19	0.82
0.07	0.14	0.96	0.21	0.00	0.14	0.20	0.99	3.62	3.64	1.23	0.82
0.06	0.12	0.93	0.18	0.00	0.12	0.17	0.84	3.63	3.96	1.34	0.82
0.05	0.11	0.92	0.16	0.00	0.11	0.15	0.75	3.61	4.16	1.41	0.81
0.05	0.09	0.91	0.14	0.00	0.10	0.13	0.67	3.60	4.40	1.49	0.81
0.03	0.07	0.89	0.11	0.00	0.07	0.10	0.51	3.56	4.99	1.69	0.80
0.02	0.05	0.87	0.08	0.00	0.05	0.07	0.35	3.42	5.75	1.95	0.77

Table 13.46: Measured and calculated results of Model B10 with roundings

Model B10 (With roundings)											
$Q_{measured}$	H	P	v	Hv $(\frac{v^2}{2g})$	H_T	q	H_T/P_m	C(H)	C($H^{1.5}$)	$C_d(H^{1.5})$	$C_d'(H)$
0.12	0.23	1.05	0.33	0.01	0.24	0.34	1.64	3.79	2.96	1.00	0.86
0.10	0.20	1.02	0.29	0.00	0.21	0.29	1.44	3.72	3.10	1.05	0.84
0.09	0.18	1.00	0.26	0.00	0.19	0.26	1.29	3.68	3.24	1.10	0.83
0.08	0.16	0.98	0.24	0.00	0.17	0.23	1.15	3.65	3.40	1.15	0.83
0.07	0.15	0.97	0.22	0.00	0.16	0.21	1.08	3.63	3.50	1.18	0.82
0.07	0.14	0.96	0.21	0.00	0.14	0.20	0.99	3.64	3.65	1.24	0.82
0.06	0.12	0.93	0.18	0.00	0.12	0.16	0.83	3.62	3.98	1.35	0.82
0.05	0.11	0.92	0.16	0.00	0.11	0.15	0.76	3.60	4.14	1.40	0.81
0.05	0.09	0.91	0.14	0.00	0.10	0.13	0.67	3.59	4.39	1.49	0.81
0.03	0.07	0.89	0.11	0.00	0.07	0.10	0.51	3.54	4.94	1.67	0.80
0.02	0.05	0.87	0.08	0.00	0.05	0.07	0.35	3.43	5.79	1.96	0.78

Table 13.47: Measured and calculated results of Model B11 with no roundings

Model B11 (No roundings)											
$Q_{measured}$	H	P	v	Hv $(\frac{v^2}{2g})$	H_T	q	H_T/P_m	C(H)	$C(H^{1.5})$	$C_d(H^{1.5})$	$C_d'(H)$
0.12	0.22	1.04	0.33	0.01	0.23	0.34	1.59	3.92	3.11	1.05	0.89
0.10	0.19	1.01	0.29	0.00	0.20	0.29	1.39	3.89	3.31	1.12	0.88
0.09	0.17	0.99	0.26	0.00	0.18	0.26	1.24	3.88	3.49	1.18	0.88
0.08	0.15	0.97	0.24	0.00	0.16	0.23	1.09	3.84	3.68	1.25	0.87
0.07	0.14	0.96	0.22	0.00	0.15	0.21	1.03	3.82	3.78	1.28	0.86
0.07	0.13	0.95	0.21	0.00	0.14	0.20	0.94	3.85	3.97	1.34	0.87
0.06	0.11	0.93	0.18	0.00	0.11	0.16	0.78	3.84	4.34	1.47	0.87
0.05	0.10	0.92	0.16	0.00	0.10	0.15	0.70	3.84	4.58	1.55	0.87
0.04	0.09	0.90	0.14	0.00	0.09	0.13	0.62	3.84	4.87	1.65	0.87
0.03	0.07	0.88	0.11	0.00	0.07	0.10	0.48	3.80	5.48	1.86	0.86
0.02	0.05	0.86	0.08	0.00	0.05	0.07	0.34	3.57	6.13	2.08	0.81

Table 13.48: Measured and calculated results of Model B11 with roundings

Model B11 (With roundings)											
$Q_{measured}$	H	P	v	Hv $(\frac{v^2}{2g})$	H_T	q	H_T/P_m	C(H)	$C(H^{1.5})$	$C_d(H^{1.5})$	$C_d'(H)$
0.12	0.22	1.04	0.33	0.01	0.23	0.34	1.59	3.92	3.11	1.05	0.89
0.10	0.20	1.01	0.29	0.00	0.20	0.29	1.39	3.88	3.29	1.11	0.88
0.09	0.17	0.99	0.26	0.00	0.18	0.26	1.24	3.86	3.48	1.18	0.87
0.08	0.15	0.97	0.24	0.00	0.16	0.23	1.09	3.85	3.68	1.25	0.87
0.07	0.14	0.96	0.22	0.00	0.15	0.21	1.02	3.82	3.78	1.28	0.86
0.07	0.13	0.95	0.21	0.00	0.14	0.20	0.94	3.84	3.96	1.34	0.87
0.06	0.11	0.93	0.18	0.00	0.11	0.17	0.79	3.84	4.33	1.47	0.87
0.05	0.10	0.91	0.16	0.00	0.10	0.15	0.70	3.84	4.59	1.55	0.87
0.05	0.09	0.91	0.15	0.00	0.09	0.13	0.63	3.83	4.82	1.63	0.87
0.03	0.07	0.88	0.11	0.00	0.07	0.10	0.48	3.82	5.54	1.87	0.86
0.02	0.05	0.86	0.08	0.00	0.05	0.07	0.34	3.61	6.21	2.10	0.81

13.4 Model set C

Table 13.49: Measured and calculated results of Model C1 with no roundings

Model C1 (No roundings)											
$Q_{measured}$	H	P	v	Hv $(\frac{v^2}{2g})$	H_T	q	H_T/P_m	C(H)	C($H^{1.5}$)	$C_d(H^{1.5})$	$C_d'(H)$
0.14	0.23	1.04	0.32	0.01	0.23	0.33	1.61	3.78	2.98	1.01	0.85
0.13	0.21	1.03	0.30	0.00	0.22	0.31	1.52	3.75	3.05	1.03	0.85
0.12	0.20	1.02	0.28	0.00	0.20	0.29	1.42	3.70	3.11	1.05	0.84
0.11	0.18	1.00	0.26	0.00	0.19	0.26	1.30	3.68	3.23	1.10	0.83
0.10	0.17	0.98	0.24	0.00	0.17	0.23	1.18	3.62	3.33	1.13	0.82
0.09	0.15	0.97	0.22	0.00	0.15	0.21	1.06	3.61	3.51	1.19	0.81
0.08	0.13	0.95	0.19	0.00	0.13	0.18	0.93	3.59	3.72	1.26	0.81
0.07	0.11	0.93	0.17	0.00	0.12	0.16	0.81	3.55	3.95	1.34	0.80
0.06	0.10	0.91	0.14	0.00	0.10	0.13	0.68	3.52	4.25	1.44	0.79
0.05	0.08	0.89	0.12	0.00	0.08	0.10	0.55	3.44	4.62	1.57	0.78
0.04	0.06	0.88	0.09	0.00	0.06	0.08	0.45	3.32	4.96	1.68	0.75
0.02	0.04	0.86	0.06	0.00	0.05	0.05	0.32	3.02	5.38	1.82	0.68

Table 13.50: Measured and calculated results of Model C1 with roundings

Model C1 (With roundings)											
$Q_{measured}$	H	P	v	Hv $(\frac{v^2}{2g})$	H_T	q	H_T/P_m	C(H)	C($H^{1.5}$)	$C_d(H^{1.5})$	$C_d'(H)$
0.14	0.23	1.04	0.32	0.01	0.23	0.33	1.61	3.77	2.97	1.01	0.85
0.13	0.21	1.03	0.30	0.00	0.22	0.31	1.52	3.72	3.02	1.02	0.84
0.12	0.20	1.01	0.28	0.00	0.20	0.28	1.41	3.70	3.11	1.05	0.83
0.11	0.18	1.00	0.26	0.00	0.19	0.26	1.29	3.67	3.23	1.10	0.83
0.10	0.17	0.98	0.24	0.00	0.17	0.24	1.18	3.70	3.40	1.15	0.83
0.09	0.15	0.96	0.22	0.00	0.15	0.21	1.05	3.64	3.56	1.20	0.82
0.08	0.13	0.95	0.19	0.00	0.13	0.18	0.93	3.61	3.75	1.27	0.82
0.07	0.11	0.93	0.17	0.00	0.12	0.16	0.80	3.59	4.01	1.36	0.81
0.06	0.10	0.91	0.14	0.00	0.10	0.13	0.68	3.54	4.29	1.45	0.80
0.05	0.08	0.90	0.12	0.00	0.08	0.10	0.56	3.45	4.62	1.57	0.78
0.03	0.06	0.88	0.09	0.00	0.06	0.08	0.43	3.32	5.05	1.71	0.75
0.02	0.04	0.86	0.06	0.00	0.05	0.05	0.32	3.06	5.44	1.84	0.69

Table 13.51: Measured and calculated results of Model C2 with no roundings

Model C2 (No roundings)											
$Q_{measured}$	H	P	v	Hv $(\frac{v^2}{2g})$	H_T	q	H_T/P_m	C(H)	C($H^{1.5}$)	C_d($H^{1.5}$)	C_d'(H)
0.14	0.22	1.03	0.31	0.00	0.22	0.32	1.53	3.84	3.11	1.05	0.87
0.12	0.20	1.01	0.28	0.00	0.20	0.29	1.39	3.77	3.20	1.08	0.85
0.11	0.18	0.99	0.26	0.00	0.18	0.26	1.25	3.74	3.34	1.13	0.84
0.10	0.17	0.98	0.24	0.00	0.17	0.24	1.17	3.67	3.39	1.15	0.83
0.09	0.15	0.96	0.22	0.00	0.15	0.21	1.06	3.63	3.52	1.19	0.82
0.08	0.13	0.94	0.19	0.00	0.13	0.18	0.93	3.59	3.73	1.26	0.81
0.07	0.11	0.93	0.17	0.00	0.12	0.16	0.81	3.57	3.97	1.34	0.81
0.06	0.10	0.91	0.14	0.00	0.10	0.13	0.68	3.54	4.30	1.46	0.80
0.05	0.08	0.89	0.12	0.00	0.08	0.10	0.55	3.48	4.69	1.59	0.78
0.03	0.06	0.87	0.09	0.00	0.06	0.08	0.43	3.36	5.14	1.74	0.76
0.02	0.04	0.86	0.06	0.00	0.04	0.05	0.31	3.11	5.57	1.89	0.70

Table 13.52: Measured and calculated results of Model C2 with roundings

Model C2 (With roundings)											
$Q_{measured}$	H	P	v	Hv $(\frac{v^2}{2g})$	H_T	q	H_T/P_m	C(H)	C($H^{1.5}$)	C_d($H^{1.5}$)	C_d'(H)
0.14	0.21	1.03	0.31	0.01	0.22	0.32	1.52	3.89	3.16	1.07	0.88
0.12	0.19	1.01	0.28	0.00	0.20	0.28	1.37	3.80	3.25	1.10	0.86
0.11	0.18	0.99	0.26	0.00	0.18	0.25	1.25	3.73	3.34	1.13	0.84
0.10	0.16	0.98	0.24	0.00	0.17	0.23	1.16	3.70	3.44	1.17	0.84
0.09	0.15	0.96	0.22	0.00	0.15	0.21	1.03	3.69	3.63	1.23	0.83
0.08	0.13	0.94	0.19	0.00	0.13	0.18	0.92	3.67	3.83	1.30	0.83
0.07	0.11	0.92	0.17	0.00	0.11	0.16	0.79	3.64	4.10	1.39	0.82
0.06	0.09	0.91	0.14	0.00	0.10	0.13	0.67	3.59	4.40	1.49	0.81
0.05	0.08	0.89	0.12	0.00	0.08	0.10	0.54	3.52	4.77	1.62	0.79
0.04	0.06	0.87	0.09	0.00	0.06	0.08	0.42	3.58	5.50	1.86	0.81
0.02	0.04	0.86	0.06	0.00	0.04	0.05	0.31	3.12	5.60	1.90	0.70

Table 13.53: Measured and calculated results of Model C3 with no roundings

Model C3 (No roundings)											
$Q_{measured}$	H	P	v	Hv $(\frac{v^2}{2g})$	H_T	q	H_T/P_m	C(H)	C($H^{1.5}$)	C_d($H^{1.5}$)	C_d'(H)
0.14	0.21	1.03	0.32	0.01	0.22	0.32	1.51	3.92	3.19	1.08	0.89
0.12	0.19	1.00	0.28	0.00	0.19	0.29	1.34	3.91	3.39	1.15	0.88
0.11	0.17	0.99	0.26	0.00	0.18	0.26	1.23	3.89	3.51	1.19	0.88
0.10	0.16	0.97	0.24	0.00	0.16	0.24	1.12	3.85	3.64	1.23	0.87
0.09	0.14	0.96	0.22	0.00	0.15	0.21	1.01	3.80	3.77	1.28	0.86
0.08	0.13	0.94	0.19	0.00	0.13	0.18	0.89	3.77	4.00	1.36	0.85
0.07	0.11	0.92	0.17	0.00	0.11	0.16	0.77	3.74	4.27	1.45	0.84
0.06	0.09	0.91	0.14	0.00	0.09	0.13	0.64	3.73	4.66	1.58	0.84
0.05	0.07	0.89	0.12	0.00	0.08	0.11	0.52	3.66	5.06	1.71	0.83
0.03	0.06	0.87	0.09	0.00	0.06	0.08	0.41	3.52	5.51	1.87	0.80
0.02	0.04	0.86	0.06	0.00	0.04	0.05	0.30	3.25	5.95	2.01	0.73

Table 13.54: Measured and calculated results of Model C3 with roundings

Model C3 (With roundings)											
$Q_{measured}$	H	P	v	Hv $(\frac{v^2}{2g})$	H_T	q	H_T/P_m	C(H)	C($H^{1.5}$)	C_d($H^{1.5}$)	C_d'(H)
0.14	0.21	1.02	0.32	0.01	0.21	0.32	1.49	3.97	3.25	1.10	0.90
0.12	0.19	1.00	0.29	0.00	0.19	0.29	1.33	3.94	3.42	1.16	0.89
0.11	0.17	0.98	0.26	0.00	0.17	0.26	1.20	3.91	3.56	1.21	0.88
0.10	0.16	0.97	0.24	0.00	0.16	0.24	1.11	3.87	3.66	1.24	0.87
0.09	0.14	0.96	0.22	0.00	0.14	0.21	1.00	3.83	3.83	1.30	0.86
0.08	0.12	0.94	0.19	0.00	0.13	0.18	0.87	3.82	4.09	1.39	0.86
0.07	0.11	0.92	0.17	0.00	0.11	0.16	0.76	3.81	4.38	1.48	0.86
0.06	0.09	0.90	0.14	0.00	0.09	0.13	0.63	3.77	4.73	1.60	0.85
0.05	0.07	0.89	0.12	0.00	0.07	0.10	0.52	3.70	5.15	1.74	0.84
0.03	0.06	0.87	0.09	0.00	0.06	0.08	0.41	3.56	5.58	1.89	0.80
0.02	0.04	0.86	0.06	0.00	0.04	0.05	0.30	3.26	5.99	2.03	0.74

Table 13.55: Measured and calculated results of Model C4 with no roundings

Model C4 (No roundings)											
$Q_{measured}$	H	P	v	Hv $(\frac{v^2}{2g})$	H_T	q	H_T/P_m	C(H)	$C(H^{1.5})$	$C_d(H^{1.5})$	$C_d'(H)$
0.14	0.21	1.03	0.32	0.01	0.22	0.33	1.53	3.91	3.16	1.07	0.88
0.12	0.19	1.01	0.28	0.00	0.19	0.29	1.34	3.90	3.37	1.14	0.88
0.11	0.17	0.99	0.26	0.00	0.18	0.26	1.23	3.91	3.53	1.19	0.88
0.10	0.16	0.97	0.24	0.00	0.16	0.23	1.10	3.89	3.70	1.25	0.88
0.09	0.14	0.96	0.22	0.00	0.14	0.21	0.98	3.91	3.95	1.34	0.88
0.08	0.12	0.94	0.19	0.00	0.12	0.18	0.86	3.87	4.17	1.41	0.87
0.07	0.11	0.92	0.17	0.00	0.11	0.16	0.75	3.86	4.46	1.51	0.87
0.06	0.09	0.91	0.14	0.00	0.09	0.13	0.63	3.82	4.82	1.63	0.86
0.05	0.07	0.89	0.12	0.00	0.07	0.10	0.51	3.77	5.28	1.79	0.85
0.03	0.06	0.88	0.09	0.00	0.06	0.08	0.39	3.64	5.80	1.96	0.82
0.02	0.04	0.86	0.06	0.00	0.04	0.05	0.28	3.33	6.23	2.11	0.75

Table 13.56: Measured and calculated results of Model C4 with roundings

Model C4 (With roundings)											
$Q_{measured}$	H	P	v	Hv $(\frac{v^2}{2g})$	H_T	q	H_T/P_m	C(H)	$C(H^{1.5})$	$C_d(H^{1.5})$	$C_d'(H)$
0.14	0.21	1.03	0.32	0.01	0.22	0.33	1.52	3.96	3.22	1.09	0.89
0.12	0.18	1.00	0.28	0.00	0.19	0.29	1.32	3.97	3.46	1.17	0.90
0.11	0.17	0.99	0.26	0.00	0.17	0.26	1.20	3.98	3.64	1.23	0.90
0.10	0.15	0.97	0.24	0.00	0.16	0.23	1.09	3.95	3.79	1.28	0.89
0.09	0.14	0.96	0.22	0.00	0.14	0.21	0.97	3.92	3.97	1.35	0.88
0.08	0.12	0.94	0.20	0.00	0.12	0.18	0.86	3.90	4.21	1.42	0.88
0.07	0.10	0.92	0.17	0.00	0.11	0.16	0.74	3.87	4.51	1.53	0.87
0.06	0.09	0.91	0.14	0.00	0.09	0.13	0.62	3.83	4.86	1.64	0.86
0.04	0.07	0.89	0.12	0.00	0.07	0.10	0.50	3.80	5.38	1.82	0.86
0.03	0.06	0.88	0.09	0.00	0.06	0.08	0.39	3.65	5.82	1.97	0.82
0.02	0.04	0.86	0.06	0.00	0.04	0.05	0.28	3.34	6.26	2.12	0.75

Table 13.57: Measured and calculated results of Model C5 with no roundings

Model C5 (No roundings)											
$Q_{measured}$	H	P	v	Hv $(\frac{v^2}{2g})$	H_T	q	H_T/P_m	C(H)	$C(H^{1.5})$	$C_d(H^{1.5})$	C_d'(H)
0.14	0.21	1.03	0.32	0.01	0.21	0.33	1.48	4.02	3.30	1.12	0.91
0.12	0.18	1.00	0.28	0.00	0.19	0.29	1.30	4.01	3.51	1.19	0.90
0.11	0.17	0.99	0.26	0.00	0.17	0.26	1.19	3.98	3.64	1.23	0.90
0.10	0.15	0.97	0.24	0.00	0.16	0.23	1.09	3.95	3.79	1.28	0.89
0.09	0.14	0.95	0.22	0.00	0.14	0.21	0.96	3.97	4.05	1.37	0.90
0.08	0.12	0.94	0.19	0.00	0.12	0.18	0.84	3.96	4.31	1.46	0.89
0.07	0.10	0.92	0.17	0.00	0.10	0.16	0.73	3.95	4.64	1.57	0.89
0.06	0.09	0.90	0.14	0.00	0.09	0.13	0.61	3.94	5.06	1.71	0.89
0.05	0.07	0.89	0.12	0.00	0.07	0.11	0.49	3.90	5.56	1.88	0.88
0.03	0.05	0.87	0.09	0.00	0.05	0.08	0.38	3.80	6.17	2.09	0.86
0.02	0.04	0.86	0.06	0.00	0.04	0.05	0.27	3.55	6.78	2.29	0.80

Table 13.58: Measured and calculated results of Model C5 with roundings

Model C5 (With roundings)											
$Q_{measured}$	H	P	v	Hv $(\frac{v^2}{2g})$	H_T	q	H_T/P_m	C(H)	$C(H^{1.5})$	$C_d(H^{1.5})$	C_d'(H)
0.14	0.21	1.02	0.32	0.01	0.21	0.33	1.47	4.08	3.37	1.14	0.92
0.12	0.18	1.00	0.29	0.00	0.18	0.29	1.28	4.08	3.60	1.22	0.92
0.11	0.16	0.98	0.26	0.00	0.17	0.26	1.16	4.05	3.76	1.27	0.91
0.10	0.15	0.97	0.24	0.00	0.15	0.24	1.07	4.04	3.91	1.32	0.91
0.09	0.13	0.95	0.22	0.00	0.14	0.21	0.95	4.02	4.12	1.40	0.91
0.08	0.12	0.93	0.19	0.00	0.12	0.18	0.83	4.02	4.42	1.50	0.91
0.07	0.10	0.92	0.17	0.00	0.10	0.16	0.71	4.02	4.77	1.61	0.91
0.06	0.08	0.90	0.14	0.00	0.09	0.13	0.60	4.01	5.19	1.76	0.91
0.05	0.07	0.89	0.12	0.00	0.07	0.10	0.48	3.97	5.72	1.94	0.90
0.03	0.05	0.87	0.09	0.00	0.05	0.08	0.37	3.83	6.26	2.12	0.86
0.02	0.04	0.86	0.06	0.00	0.04	0.05	0.27	3.58	6.91	2.34	0.81

Table 13.59: Measured and calculated results of Model C6 with no roundings

Model C6 (No roundings)											
$Q_{measured}$	H	P	v	Hv ($\frac{v^2}{2g}$)	H_T	q	H_T/P_m	C(H)	C($H^{1.5}$)	C_d($H^{1.5}$)	C_d'(H)
0.14	0.24	1.05	0.31	0.00	0.24	0.33	1.67	3.57	2.76	0.93	0.81
0.12	0.21	1.02	0.28	0.00	0.21	0.28	1.48	3.51	2.89	0.98	0.79
0.11	0.19	1.01	0.26	0.00	0.19	0.26	1.35	3.48	2.99	1.01	0.79
0.10	0.18	0.99	0.24	0.00	0.18	0.24	1.25	3.46	3.10	1.05	0.78
0.09	0.16	0.97	0.21	0.00	0.16	0.21	1.11	3.42	3.25	1.10	0.77
0.08	0.14	0.95	0.19	0.00	0.14	0.18	0.99	3.37	3.39	1.15	0.76
0.07	0.12	0.94	0.17	0.00	0.12	0.16	0.86	3.33	3.59	1.22	0.75
0.06	0.10	0.92	0.14	0.00	0.11	0.13	0.73	3.25	3.81	1.29	0.73
0.05	0.09	0.90	0.12	0.00	0.09	0.10	0.60	3.17	4.08	1.38	0.71
0.03	0.07	0.88	0.09	0.00	0.07	0.08	0.47	3.05	4.45	1.51	0.69
0.02	0.05	0.86	0.06	0.00	0.05	0.05	0.34	2.85	4.90	1.66	0.64

Table 13.60: Measured and calculated results of Model C6 with roundings

Model C6 (With roundings)											
$Q_{measured}$	H	P	v	Hv ($\frac{v^2}{2g}$)	H_T	q	H_T/P_m	C(H)	C($H^{1.5}$)	C_d($H^{1.5}$)	C_d'(H)
0.14	0.24	1.05	0.31	0.00	0.24	0.33	1.67	3.59	2.78	0.94	0.81
0.12	0.21	1.02	0.28	0.00	0.21	0.28	1.47	3.51	2.90	0.98	0.79
0.11	0.19	1.01	0.26	0.00	0.20	0.26	1.36	3.48	2.98	1.01	0.79
0.10	0.18	0.99	0.24	0.00	0.18	0.24	1.24	3.47	3.11	1.05	0.78
0.09	0.16	0.97	0.21	0.00	0.16	0.21	1.11	3.45	3.28	1.11	0.78
0.08	0.14	0.95	0.19	0.00	0.14	0.18	0.99	3.38	3.40	1.15	0.76
0.07	0.12	0.94	0.17	0.00	0.12	0.16	0.86	3.32	3.59	1.21	0.75
0.06	0.10	0.92	0.14	0.00	0.10	0.13	0.73	3.27	3.83	1.30	0.74
0.05	0.09	0.90	0.12	0.00	0.09	0.10	0.60	3.18	4.10	1.39	0.72
0.03	0.07	0.88	0.09	0.00	0.07	0.08	0.47	3.06	4.47	1.51	0.69
0.02	0.05	0.86	0.06	0.00	0.05	0.05	0.34	2.85	4.92	1.67	0.64

Table 13.61: Measured and calculated results of Model C7 with no roundings

Model C7 (No roundings)											
$Q_{measured}$	H	P	v	Hv $(\frac{v^2}{2g})$	H_T	q	H_T/P_m	C(H)	C($H^{1.5}$)	C_d($H^{1.5}$)	C_d'(H)
0.14	0.23	1.04	0.31	0.00	0.23	0.33	1.60	3.72	2.94	0.99	0.84
0.12	0.20	1.01	0.28	0.00	0.20	0.28	1.41	3.69	3.10	1.05	0.83
0.11	0.18	1.00	0.26	0.00	0.19	0.26	1.29	3.65	3.22	1.09	0.82
0.10	0.17	0.98	0.24	0.00	0.17	0.24	1.19	3.65	3.35	1.13	0.82
0.09	0.15	0.96	0.22	0.00	0.15	0.21	1.04	3.65	3.58	1.21	0.82
0.08	0.13	0.95	0.19	0.00	0.13	0.18	0.93	3.58	3.72	1.26	0.81
0.07	0.11	0.93	0.17	0.00	0.12	0.16	0.81	3.55	3.95	1.34	0.80
0.06	0.10	0.91	0.14	0.00	0.10	0.13	0.68	3.49	4.23	1.43	0.79
0.05	0.08	0.89	0.12	0.00	0.08	0.10	0.56	3.41	4.57	1.55	0.77
0.03	0.06	0.88	0.09	0.00	0.06	0.08	0.44	3.27	4.96	1.68	0.74
0.02	0.04	0.86	0.06	0.00	0.04	0.05	0.31	3.02	5.41	1.83	0.68

Table 13.62: Measured and calculated results of Model C7 with roundings

Model C7 (With roundings)											
$Q_{measured}$	H	P	v	Hv $(\frac{v^2}{2g})$	H_T	q	H_T/P_m	C(H)	C($H^{1.5}$)	C_d($H^{1.5}$)	C_d'(H)
0.14	0.22	1.04	0.31	0.01	0.23	0.33	1.60	3.73	2.95	1.00	0.84
0.12	0.20	1.01	0.28	0.00	0.20	0.28	1.40	3.67	3.10	1.05	0.83
0.11	0.18	1.00	0.26	0.00	0.19	0.26	1.30	3.65	3.21	1.09	0.82
0.10	0.17	0.98	0.24	0.00	0.17	0.23	1.18	3.63	3.34	1.13	0.82
0.09	0.15	0.96	0.21	0.00	0.15	0.20	1.03	3.63	3.57	1.21	0.82
0.08	0.13	0.95	0.19	0.00	0.13	0.18	0.93	3.58	3.72	1.26	0.81
0.07	0.11	0.93	0.17	0.00	0.12	0.16	0.80	3.53	3.94	1.33	0.80
0.06	0.10	0.91	0.14	0.00	0.10	0.13	0.68	3.49	4.23	1.43	0.79
0.05	0.08	0.89	0.12	0.00	0.08	0.10	0.55	3.43	4.60	1.56	0.77
0.03	0.06	0.88	0.09	0.00	0.06	0.08	0.43	3.28	4.97	1.68	0.74
0.02	0.04	0.86	0.06	0.00	0.04	0.05	0.31	3.03	5.42	1.83	0.68

Table 13.63: Measured and calculated results of Model C8 with no roundings

Model C8 (No roundings)											
$Q_{measured}$	**H**	**P**	**v**	**Hv $(\frac{v^2}{2g})$**	**H_T**	**q**	**H_T/P_m**	**C(H)**	**$C(H^{1.5})$**	**$C_d(H^{1.5})$**	**$C_d'(H)$**
0.14	0.22	1.03	0.32	0.01	0.22	0.33	1.54	3.89	3.14	1.06	0.88
0.12	0.19	1.00	0.28	0.00	0.19	0.28	1.34	3.89	3.36	1.14	0.88
0.11	0.17	0.99	0.26	0.00	0.18	0.26	1.23	3.85	3.48	1.18	0.87
0.10	0.16	0.97	0.24	0.00	0.16	0.23	1.11	3.85	3.65	1.24	0.87
0.09	0.14	0.96	0.22	0.00	0.14	0.21	0.99	3.85	3.87	1.31	0.87
0.08	0.12	0.94	0.19	0.00	0.12	0.18	0.87	3.84	4.12	1.39	0.87
0.07	0.11	0.92	0.17	0.00	0.11	0.16	0.75	3.82	4.42	1.50	0.86
0.06	0.09	0.91	0.14	0.00	0.09	0.13	0.63	3.80	4.78	1.62	0.86
0.05	0.07	0.89	0.12	0.00	0.07	0.11	0.52	3.73	5.19	1.76	0.84
0.03	0.06	0.87	0.09	0.00	0.06	0.08	0.40	3.59	5.69	1.93	0.81
0.02	0.04	0.86	0.06	0.00	0.04	0.05	0.29	3.37	6.25	2.12	0.76

Table 13.64: Measured and calculated results of Model C8 with roundings

Model C8 (With roundings)											
$Q_{measured}$	**H**	**P**	**v**	**Hv $(\frac{v^2}{2g})$**	**H_T**	**q**	**H_T/P_m**	**C(H)**	**$C(H^{1.5})$**	**$C_d(H^{1.5})$**	**$C_d'(H)$**
0.14	0.21	1.03	0.32	0.01	0.22	0.33	1.53	3.89	3.15	1.07	0.88
0.12	0.19	1.01	0.28	0.00	0.19	0.28	1.34	3.88	3.35	1.13	0.88
0.11	0.17	0.99	0.26	0.00	0.18	0.26	1.24	3.86	3.47	1.17	0.87
0.10	0.16	0.97	0.24	0.00	0.16	0.23	1.11	3.83	3.63	1.23	0.86
0.09	0.14	0.96	0.22	0.00	0.14	0.21	0.98	3.86	3.90	1.32	0.87
0.08	0.12	0.94	0.19	0.00	0.13	0.18	0.87	3.84	4.12	1.39	0.87
0.07	0.11	0.92	0.17	0.00	0.11	0.16	0.75	3.82	4.40	1.49	0.86
0.06	0.09	0.91	0.14	0.00	0.09	0.13	0.63	3.78	4.76	1.61	0.85
0.05	0.07	0.89	0.12	0.00	0.07	0.10	0.51	3.73	5.21	1.77	0.84
0.03	0.06	0.87	0.09	0.00	0.06	0.08	0.39	3.63	5.78	1.96	0.82
0.02	0.04	0.86	0.06	0.00	0.04	0.05	0.28	3.36	6.32	2.14	0.76

Table 13.65: Measured and calculated results of Model C9 with no roundings

Model C9 (No roundings)											
$Q_{measured}$	H	P	v	Hv $(\frac{v^2}{2g})$	H_T	q	H_T/P_m	C(H)	$C(H^{1.5})$	$C_d(H^{1.5})$	$C_d'(H)$
0.14	0.24	1.06	0.31	0.00	0.25	0.32	1.72	3.44	2.62	0.89	0.78
0.13	0.22	1.04	0.28	0.00	0.22	0.29	1.56	3.38	2.71	0.92	0.76
0.11	0.20	1.02	0.26	0.00	0.21	0.26	1.43	3.33	2.79	0.94	0.75
0.10	0.18	1.00	0.23	0.00	0.19	0.23	1.29	3.30	2.91	0.98	0.75
0.09	0.17	0.98	0.21	0.00	0.17	0.21	1.17	3.26	3.00	1.02	0.74
0.08	0.15	0.96	0.19	0.00	0.15	0.18	1.04	3.21	3.15	1.07	0.72
0.07	0.13	0.95	0.17	0.00	0.13	0.16	0.91	3.16	3.31	1.12	0.71
0.06	0.11	0.93	0.14	0.00	0.11	0.13	0.77	3.08	3.50	1.19	0.70
0.05	0.09	0.91	0.12	0.00	0.09	0.10	0.64	2.99	3.73	1.26	0.68
0.03	0.07	0.89	0.09	0.00	0.07	0.08	0.51	2.88	4.06	1.37	0.65
0.02	0.05	0.87	0.06	0.00	0.05	0.05	0.37	2.62	4.32	1.46	0.59

Table 13.66: Measured and calculated results of Model C9 with roundings

Model C9 (With roundings)											
$Q_{measured}$	H	P	v	Hv $(\frac{v^2}{2g})$	H_T	q	H_T/P_m	C(H)	$C(H^{1.5})$	$C_d(H^{1.5})$	$C_d'(H)$
0.14	0.24	1.06	0.31	0.00	0.25	0.33	1.73	3.46	2.63	0.89	0.78
0.12	0.22	1.03	0.28	0.00	0.22	0.29	1.54	3.39	2.73	0.92	0.76
0.11	0.20	1.02	0.25	0.00	0.20	0.26	1.41	3.33	2.80	0.95	0.75
0.10	0.18	1.00	0.23	0.00	0.19	0.23	1.30	3.30	2.89	0.98	0.74
0.09	0.17	0.98	0.21	0.00	0.17	0.21	1.17	3.25	3.00	1.02	0.73
0.08	0.15	0.97	0.19	0.00	0.15	0.18	1.04	3.20	3.13	1.06	0.72
0.07	0.13	0.95	0.16	0.00	0.13	0.16	0.91	3.13	3.28	1.11	0.71
0.06	0.11	0.93	0.14	0.00	0.11	0.13	0.78	3.06	3.47	1.18	0.69
0.05	0.09	0.91	0.12	0.00	0.09	0.10	0.64	2.99	3.74	1.27	0.68
0.03	0.07	0.89	0.09	0.00	0.07	0.08	0.50	2.88	4.07	1.38	0.65
0.02	0.05	0.87	0.06	0.00	0.05	0.05	0.37	2.62	4.32	1.46	0.59

Table 13.67: Measured and calculated results of Model C10 with no roundings

Model C10 (No roundings)											
$Q_{measured}$	H	P	v	Hv $(\frac{v^2}{2g})$	H_T	q	H_T/P_m	C(H)	C($H^{1.5}$)	$C_d(H^{1.5})$	C_d'(H)
0.14	0.23	1.05	0.31	0.00	0.24	0.33	1.63	3.64	2.85	0.97	0.82
0.12	0.20	1.02	0.28	0.00	0.21	0.28	1.44	3.59	2.99	1.01	0.81
0.11	0.19	1.01	0.26	0.00	0.19	0.26	1.34	3.54	3.06	1.04	0.80
0.10	0.17	0.99	0.24	0.00	0.18	0.23	1.22	3.52	3.19	1.08	0.79
0.09	0.15	0.97	0.22	0.00	0.16	0.21	1.08	3.54	3.40	1.15	0.80
0.08	0.14	0.95	0.19	0.00	0.14	0.18	0.96	3.45	3.52	1.19	0.78
0.07	0.12	0.94	0.17	0.00	0.12	0.16	0.84	3.42	3.72	1.26	0.77
0.06	0.10	0.92	0.14	0.00	0.10	0.13	0.71	3.35	3.97	1.35	0.76
0.05	0.08	0.90	0.12	0.00	0.08	0.10	0.58	3.28	4.31	1.46	0.74
0.03	0.06	0.88	0.09	0.00	0.07	0.08	0.45	3.18	4.74	1.61	0.72
0.02	0.05	0.86	0.06	0.00	0.05	0.05	0.33	2.95	5.14	1.74	0.67

Table 13.68: Measured and calculated results of Model C10 with roundings

Model C10 (With roundings)											
$Q_{measured}$	H	P	v	Hv $(\frac{v^2}{2g})$	H_T	q	H_T/P_m	C(H)	C($H^{1.5}$)	$C_d(H^{1.5})$	C_d'(H)
0.14	0.23	1.05	0.31	0.00	0.24	0.33	1.63	3.65	2.86	0.97	0.82
0.12	0.20	1.02	0.28	0.00	0.21	0.28	1.45	3.58	2.97	1.00	0.81
0.11	0.19	1.00	0.26	0.00	0.19	0.26	1.32	3.55	3.09	1.05	0.80
0.10	0.17	0.99	0.24	0.00	0.18	0.24	1.22	3.53	3.20	1.08	0.80
0.09	0.15	0.97	0.22	0.00	0.16	0.21	1.09	3.52	3.37	1.14	0.79
0.08	0.14	0.95	0.19	0.00	0.14	0.18	0.96	3.46	3.52	1.19	0.78
0.07	0.12	0.94	0.17	0.00	0.12	0.16	0.84	3.41	3.72	1.26	0.77
0.06	0.10	0.92	0.14	0.00	0.10	0.13	0.71	3.36	3.99	1.35	0.76
0.05	0.08	0.90	0.12	0.00	0.08	0.10	0.58	3.29	4.32	1.46	0.74
0.03	0.06	0.88	0.09	0.00	0.07	0.08	0.45	3.21	4.78	1.62	0.73
0.02	0.05	0.86	0.06	0.00	0.05	0.05	0.33	2.92	5.13	1.74	0.66

Table 13.69: Measured and calculated results of Model C11 with no roundings

Model C11 (No roundings)											
$Q_{measured}$	H	P	v	Hv $(\frac{v^2}{2g})$	H_T	q	H_T/P_m	C(H)	$C(H^{1.5})$	$C_d(H^{1.5})$	$C_d'(H)$
0.14	0.22	1.04	0.31	0.01	0.23	0.33	1.57	3.79	3.02	1.02	0.86
0.12	0.20	1.01	0.28	0.00	0.20	0.28	1.39	3.75	3.18	1.08	0.85
0.11	0.18	1.00	0.26	0.00	0.18	0.26	1.28	3.72	3.29	1.11	0.84
0.10	0.16	0.98	0.24	0.00	0.17	0.23	1.15	3.71	3.45	1.17	0.84
0.09	0.15	0.96	0.22	0.00	0.15	0.21	1.04	3.67	3.60	1.22	0.83
0.08	0.13	0.94	0.19	0.00	0.13	0.18	0.91	3.66	3.83	1.30	0.83
0.07	0.11	0.93	0.17	0.00	0.11	0.16	0.79	3.63	4.09	1.38	0.82
0.06	0.09	0.91	0.14	0.00	0.10	0.13	0.66	3.60	4.42	1.50	0.81
0.04	0.08	0.89	0.12	0.00	0.08	0.10	0.54	3.50	4.77	1.61	0.79
0.03	0.06	0.88	0.09	0.00	0.06	0.08	0.42	3.42	5.26	1.78	0.77
0.02	0.04	0.86	0.06	0.00	0.04	0.05	0.31	3.17	5.74	1.94	0.72

Table 13.70: Measured and calculated results of Model C11 with roundings

Model C11 (With roundings)											
$Q_{measured}$	H	P	v	Hv $(\frac{v^2}{2g})$	H_T	q	H_T/P_m	C(H)	$C(H^{1.5})$	$C_d(H^{1.5})$	$C_d'(H)$
0.14	0.22	1.04	0.32	0.01	0.23	0.33	1.58	3.79	3.01	1.02	0.86
0.12	0.19	1.01	0.28	0.00	0.20	0.28	1.37	3.74	3.19	1.08	0.84
0.11	0.18	1.00	0.26	0.00	0.18	0.26	1.27	3.73	3.30	1.12	0.84
0.10	0.16	0.98	0.24	0.00	0.17	0.23	1.15	3.71	3.45	1.17	0.84
0.09	0.15	0.96	0.22	0.00	0.15	0.21	1.04	3.67	3.59	1.22	0.83
0.08	0.13	0.95	0.19	0.00	0.13	0.18	0.91	3.65	3.81	1.29	0.82
0.07	0.11	0.93	0.17	0.00	0.11	0.16	0.79	3.63	4.09	1.38	0.82
0.06	0.09	0.91	0.14	0.00	0.10	0.13	0.67	3.60	4.41	1.49	0.81
0.05	0.08	0.89	0.12	0.00	0.08	0.10	0.54	3.55	4.84	1.64	0.80
0.03	0.06	0.88	0.09	0.00	0.06	0.08	0.42	3.42	5.25	1.78	0.77
0.02	0.04	0.86	0.06	0.00	0.04	0.05	0.30	3.17	5.76	1.95	0.71

13.5 Models with change in floor shape

Table 13.71: Measured and calculated results of Model B3 with no roundings and change in floor shape

Model B3 with change in floor (No roundings)											
$Q_{measured}$	H	P	v	Hv $(\frac{v^2}{2g})$	H_T	q	H_T/P_m	C(H)	$C(H^{1.5})$	$C_d(H^{1.5})$	C_d'(H)
0.11	0.20	1.02	0.31	0.01	0.21	0.32	1.44	4.08	3.40	1.15	0.92
0.10	0.19	1.00	0.29	0.00	0.19	0.29	1.32	4.08	3.55	1.20	0.92
0.09	0.16	0.98	0.27	0.00	0.17	0.26	1.17	4.09	3.78	1.28	0.92
0.08	0.14	0.96	0.24	0.00	0.15	0.23	1.03	4.08	4.02	1.36	0.92
0.07	0.13	0.95	0.22	0.00	0.14	0.21	0.96	4.10	4.19	1.42	0.93
0.07	0.12	0.94	0.21	0.00	0.13	0.20	0.88	4.11	4.39	1.49	0.93
0.06	0.10	0.92	0.18	0.00	0.11	0.16	0.73	4.10	4.79	1.62	0.92
0.05	0.09	0.91	0.16	0.00	0.10	0.15	0.66	4.07	4.99	1.69	0.92
0.05	0.09	0.90	0.15	0.00	0.09	0.13	0.60	4.07	5.25	1.78	0.92
0.03	0.06	0.88	0.11	0.00	0.07	0.10	0.46	3.98	5.89	1.99	0.90
0.02	0.05	0.86	0.08	0.00	0.05	0.07	0.33	3.70	6.47	2.19	0.83

Table 13.72: Measured and calculated results of Model B7 with no roundings and change in floor shape

Model B7 with change in floor (No roundings)											
$Q_{measured}$	H	P	v	Hv $(\frac{v^2}{2g})$	H_T	q	H_T/P_m	C(H)	$C(H^{1.5})$	$C_d(H^{1.5})$	C_d'(H)
0.11	0.21	1.03	0.00	0.00	0.21	0.33	1.44	4.13	3.44	1.16	0.93
0.10	0.19	1.01	0.00	0.00	0.19	0.29	1.31	4.10	3.58	1.21	0.93
0.09	0.17	0.99	0.00	0.00	0.17	0.26	1.15	4.10	3.81	1.29	0.92
0.08	0.15	0.97	0.00	0.00	0.15	0.23	1.03	4.09	4.03	1.36	0.92
0.07	0.14	0.96	0.00	0.00	0.14	0.21	0.95	4.08	4.17	1.41	0.92
0.07	0.13	0.95	0.00	0.00	0.13	0.20	0.89	4.08	4.33	1.47	0.92
0.06	0.11	0.93	0.00	0.00	0.11	0.16	0.74	4.05	4.73	1.60	0.91
0.05	0.10	0.92	0.00	0.00	0.10	0.15	0.67	4.04	4.94	1.67	0.91
0.05	0.09	0.91	0.00	0.00	0.09	0.13	0.60	4.02	5.19	1.76	0.91
0.03	0.07	0.89	0.00	0.00	0.07	0.10	0.46	3.90	5.73	1.94	0.88
0.02	0.05	0.87	0.00	0.00	0.05	0.07	0.33	3.68	6.40	2.17	0.83

Table 13.73: Measured and calculated results of Model B10 with no roundings and change in floor shape

Model B10 with change in floor (No roundings)											
$Q_{measured}$	H	P	v	Hv ($\frac{v^2}{2g}$)	H_T	q	H_T/P_m	C(H)	C($H^{1.5}$)	C_d($H^{1.5}$)	C_d'(H)
0.12	0.23	1.05	0.32	0.01	0.23	0.34	1.62	3.83	3.00	1.02	0.86
0.10	0.20	1.02	0.29	0.00	0.21	0.29	1.42	3.78	3.17	1.07	0.85
0.09	0.18	1.00	0.26	0.00	0.18	0.26	1.28	3.74	3.31	1.12	0.84
0.08	0.16	0.98	0.23	0.00	0.16	0.23	1.13	3.71	3.48	1.18	0.84
0.07	0.15	0.97	0.22	0.00	0.15	0.21	1.06	3.69	3.58	1.21	0.83
0.07	0.14	0.96	0.21	0.00	0.14	0.20	0.98	3.68	3.72	1.26	0.83
0.06	0.12	0.94	0.18	0.00	0.12	0.17	0.82	3.69	4.07	1.38	0.83
0.05	0.10	0.92	0.16	0.00	0.11	0.15	0.74	3.68	4.29	1.45	0.83
0.05	0.09	0.91	0.14	0.00	0.09	0.13	0.65	3.68	4.55	1.54	0.83
0.03	0.07	0.89	0.11	0.00	0.07	0.10	0.50	3.67	5.21	1.76	0.83
0.02	0.05	0.87	0.08	0.00	0.05	0.07	0.34	3.57	6.14	2.08	0.81

14 APPENDIX D – OVERALL RESULTS FOR ALL MODELS

Table 14.1: Results for the whole dataset where $0.5<H_T/P_m<1$ with no roundings

Model No.	B/P_m	W/P_m	L/W	Inlet width proportion (α')	H_T/P_m	W_{in}/W	C	C_d'
A1	3.00	1.80	4.34	1.00	0.41	0.56	3.87	0.87
	3.00	1.80	4.34	1.00	0.60	0.56	3.86	0.87
	3.00	1.80	4.34	1.00	0.79	0.56	3.95	0.89
	3.00	1.80	4.34	1.00	1.02	0.56	3.87	0.87
A2	3.60	1.80	5.00	1.00	0.41	0.50	3.86	0.87
	3.60	1.80	5.00	1.00	0.61	0.50	3.93	0.89
	3.60	1.80	5.00	1.00	0.81	0.50	3.94	0.89
	3.60	1.80	5.00	1.00	0.92	0.50	3.93	0.89
	3.60	1.80	5.00	1.00	1.02	0.50	3.91	0.88
A3	3.60	1.80	5.00	1.00	0.41	0.56	3.88	0.88
	3.60	1.80	5.00	1.00	0.60	0.56	4.01	0.91
	3.60	1.80	5.00	1.00	0.78	0.56	4.04	0.91
	3.60	1.80	5.00	1.00	1.00	0.56	3.95	0.89
A4	3.60	1.80	5.00	1.00	0.39	0.63	4.06	0.92
	3.60	1.80	5.00	1.00	0.56	0.63	4.32	0.97
	3.60	1.80	5.00	1.00	0.78	0.63	4.11	0.93
	3.60	1.80	5.00	1.00	1.02	0.63	3.95	0.89
A5	4.20	1.80	5.67	1.00	0.39	0.56	4.06	0.92
	4.20	1.80	5.67	1.00	0.56	0.56	4.26	0.96
	4.20	1.80	5.67	1.00	0.76	0.56	4.17	0.94
	4.20	1.80	5.67	1.00	0.98	0.56	4.08	0.92
	4.20	1.80	5.67	1.00	1.20	0.56	4.01	0.90
A6	3.00	1.80	4.13	1.20	0.43	0.67	3.70	0.83
	3.00	1.80	4.13	1.20	0.64	0.67	3.70	0.83
	3.00	1.80	4.13	1.20	0.87	0.67	3.65	0.82
	3.00	1.80	4.13	1.20	0.95	0.67	3.75	0.85
	3.00	1.80	4.13	1.20	1.07	0.67	3.72	0.84
A7	3.60	1.80	4.79	1.20	0.39	0.67	3.90	0.88
	3.60	1.80	4.79	1.20	0.58	0.67	4.12	0.88
	3.60	1.80	4.79	1.20	0.77	0.67	4.16	0.88
	3.60	1.80	4.79	1.20	1.01	0.67	3.96	0.88

A8	4.20	1.80	5.46	1.20	0.39	0.67	4.06	0.92
	4.20	1.80	5.46	1.20	0.56	0.67	4.35	0.98
	4.20	1.80	5.46	1.20	0.75	0.67	4.26	0.96
	4.20	1.80	5.46	1.20	0.97	0.67	4.15	0.94
	4.20	1.80	5.46	1.20	1.19	0.67	4.11	0.93
A9	3.00	1.80	3.90	1.45	0.44	0.81	3.65	0.82
	3.00	1.80	3.90	1.45	0.66	0.81	3.60	0.81
	3.00	1.80	3.90	1.45	0.90	0.81	3.55	0.80
	3.00	1.80	3.90	1.45	1.01	0.81	3.54	0.80
A10	3.60	1.80	4.54	1.45	0.49	0.81	3.25	0.73
	3.60	1.80	4.54	1.45	0.63	0.81	3.79	0.86
	3.60	1.80	4.54	1.45	0.74	0.81	3.77	0.85
	3.60	1.80	4.54	1.45	0.85	0.81	3.75	0.85
	3.60	1.80	4.54	1.45	0.97	0.81	3.72	0.84
	3.60	1.80	4.54	1.45	1.08	0.81	3.71	0.84
A11	4.20	1.80	5.21	1.45	0.39	0.81	4.14	0.93
	4.20	1.80	5.21	1.45	0.56	0.81	4.34	0.98
	4.20	1.80	5.21	1.45	0.76	0.81	4.21	0.95
	4.20	1.80	5.21	1.45	0.87	0.81	4.17	0.94
	4.20	1.80	5.21	1.45	0.96	0.81	4.14	0.93
	4.20	1.80	5.21	1.45	1.07	0.81	4.13	0.93
B1	3.00	2.40	3.50	1.00	0.50	0.55	3.65	0.82
	3.00	2.40	3.50	1.00	0.73	0.55	3.69	0.83
	3.00	2.40	3.50	1.00	0.82	0.55	3.69	0.83
	3.00	2.40	3.50	1.00	0.90	0.55	3.68	0.83
	3.00	2.40	3.50	1.00	0.98	0.55	3.69	0.83
	3.00	2.40	3.50	1.00	1.05	0.55	3.70	0.84
B2	3.60	2.40	3.99	1.00	0.49	0.50	3.69	0.83
	3.60	2.40	3.99	1.00	0.64	0.50	3.73	0.84
	3.60	2.40	3.99	1.00	0.81	0.50	3.75	0.85
	3.60	2.40	3.99	1.00	0.88	0.50	3.76	0.85
	3.60	2.40	3.99	1.00	0.96	0.50	3.77	0.85
	3.60	2.40	3.99	1.00	1.03	0.50	3.78	0.85
B3	3.60	2.40	3.99	1.00	0.48	0.55	3.83	0.86
	3.60	2.40	3.99	1.00	0.61	0.55	3.88	0.88

	3.60	2.40	3.99	1.00	0.70	0.55	3.88	0.88
	3.60	2.40	3.99	1.00	0.77	0.55	3.89	0.88
	3.60	2.40	3.99	1.00	0.93	0.55	3.88	0.88
	3.60	2.40	3.99	1.00	1.00	0.55	3.89	0.88
B4	3.60	2.40	3.99	1.00	0.46	0.62	4.06	0.92
	3.60	2.40	3.99	1.00	0.59	0.62	4.10	0.92
	3.60	2.40	3.99	1.00	0.66	0.62	4.15	0.94
	3.60	2.40	3.99	1.00	0.73	0.62	4.16	0.94
	3.6	2.40	3.99	1.00	0.88	0.62	4.09	0.92
	3.60	2.40	3.99	1.00	0.95	0.62	4.11	0.93
	3.60	2.40	3.99	1.00	1.04	0.62	4.04	0.91
B5	4.20	2.40	4.50	1.00	0.45	0.55	4.02	0.91
	4.20	2.40	4.50	1.00	0.61	0.55	4.01	0.91
	4.20	2.40	4.50	1.00	0.67	0.55	4.00	0.90
	4.20	2.40	4.50	1.00	0.74	0.55	4.01	0.91
	4.20	2.40	4.50	1.00	0.89	0.55	4.03	0.91
	4.20	2.40	4.50	1.00	0.97	0.55	4.05	0.91
	4.20	2.40	4.50	1.00	1.04	0.55	4.05	0.91
B6	3.00	2.40	3.16	1.35	0.52	0.75	3.49	0.79
	3.00	2.40	3.16	1.35	0.68	0.75	3.57	0.81
	3.00	2.40	3.16	1.35	0.76	0.75	3.58	0.81
	3.00	2.40	3.16	1.35	0.83	0.75	3.60	0.81
	3.00	2.40	3.16	1.35	1.00	0.75	3.61	0.82
B7	3.60	2.40	3.65	1.35	0.48	0.75	3.83	0.86
	3.60	2.40	3.65	1.35	0.62	0.75	3.88	0.88
	3.60	2.40	3.65	1.35	0.70	0.75	3.88	0.88
	3.60	2.40	3.65	1.35	0.78	0.75	3.88	0.88
	3.60	2.40	3.65	1.35	0.93	0.75	3.87	0.87
	3.60	2.40	3.65	1.35	1.01	0.75	3.88	0.88
B8	4.20	2.40	4.14	1.35	0.45	0.75	4.01	0.90
	4.20	2.40	4.14	1.35	0.59	0.75	4.05	0.91
	4.20	2.40	4.14	1.35	0.66	0.75	4.06	0.92
	4.20	2.40	4.14	1.35	0.74	0.75	4.04	0.91
	4.20	2.40	4.14	1.35	0.90	0.75	4.00	0.90
	4.20	2.40	4.14	1.35	0.97	0.75	4.01	0.90

	4.20	2.40	4.14	1.35	1.04	0.75	4.00	0.90
B9	3.00	2.40	2.98	1.55	0.55	0.86	3.33	0.75
	3.00	2.40	2.98	1.55	0.71	0.86	3.39	0.76
	3.00	2.40	2.98	1.55	0.80	0.86	3.40	0.77
	3.00	2.40	2.98	1.55	0.87	0.86	3.41	0.77
	3.00	2.40	2.98	1.55	1.04	0.86	3.47	0.78
B10	3.60	2.40	3.46	1.55	0.51	0.86	3.56	0.80
	3.60	2.40	3.46	1.55	0.67	0.86	3.60	0.81
	3.60	2.40	3.46	1.55	0.75	0.86	3.61	0.81
	3.60	2.40	3.46	1.55	0.84	0.86	3.63	0.82
	3.60	2.40	3.46	1.55	0.99	0.86	3.62	0.82
	3.60	2.40	3.46	1.55	1.07	0.86	3.64	0.82
B11	4.20	2.40	3.95	1.55	0.48	0.86	3.80	0.86
	4.20	2.40	3.95	1.55	0.62	0.86	3.84	0.87
	4.20	2.40	3.95	1.55	0.70	0.86	3.84	0.87
	4.20	2.40	3.95	1.55	0.78	0.86	3.84	0.87
	4.20	2.40	3.95	1.55	0.94	0.86	3.85	0.87
	4.20	2.40	3.95	1.55	1.03	0.86	3.82	0.86
C1	3.00	3.00	3.00	1.00	0.55	0.56	3.44	0.78
	3.00	3.00	3.00	1.00	0.68	0.56	3.52	0.79
	3.00	3.00	3.00	1.00	0.81	0.56	3.55	0.80
	3.00	3.00	3.00	1.00	0.93	0.56	3.59	0.81
	3.00	3.00	3.00	1.00	1.06	0.56	3.61	0.81
C2	3.60	3.00	3.40	1.00	0.55	0.50	3.48	0.78
	3.60	3.00	3.40	1.00	0.68	0.50	3.54	0.80
	3.60	3.00	3.40	1.00	0.81	0.50	3.57	0.81
	3.60	3.00	3.40	1.00	0.93	0.50	3.59	0.81
	3.60	3.00	3.40	1.00	1.06	0.50	3.63	0.82
C3	3.60	3.00	3.40	1.00	0.52	0.56	3.66	0.83
	3.60	3.00	3.40	1.00	0.64	0.56	3.73	0.84
	3.60	3.00	3.40	1.00	0.77	0.56	3.74	0.84
	3.60	3.00	3.40	1.00	0.89	0.56	3.77	0.85
	3.60	3.00	3.40	1.00	1.01	0.56	3.80	0.86
C4	3.60	3.00	3.40	1.00	0.51	0.63	3.77	0.85
	3.60	3.00	3.40	1.00	0.63	0.63	3.82	0.86

	3.60	3.00	3.40	1.00	0.75	0.63	3.86	0.87
	3.60	3.00	3.40	1.00	0.86	0.63	3.87	0.87
	3.60	3.00	3.40	1.00	0.98	0.63	3.91	0.88
	3.60	3.00	3.40	1.00	1.10	0.63	3.89	0.88
C5	4.20	3.00	3.80	1.00	0.49	0.56	3.90	0.88
	4.20	3.00	3.80	1.00	0.61	0.56	3.94	0.89
	4.20	3.00	3.80	1.00	0.73	0.56	3.95	0.89
	4.20	3.00	3.80	1.00	0.84	0.56	3.96	0.89
	4.20	3.00	3.80	1.00	0.96	0.56	3.97	0.90
	4.20	3.00	3.80	1.00	1.09	0.56	3.95	0.89
C6	3.00	3.00	2.58	1.45	0.47	0.81	3.05	0.69
	3.00	3.00	2.58	1.45	0.60	0.81	3.17	0.71
	3.00	3.00	2.58	1.45	0.73	0.81	3.25	0.73
	3.00	3.00	2.58	1.45	0.86	0.81	3.33	0.75
	3.00	3.00	2.58	1.45	0.99	0.81	3.37	0.76
	3.00	3.00	2.58	1.45	1.11	0.81	3.42	0.77
C7	3.60	3.00	2.97	1.45	0.56	0.81	3.41	0.77
	3.60	3.00	2.97	1.45	0.68	0.81	3.49	0.79
	3.60	3.00	2.97	1.45	0.81	0.81	3.55	0.80
	3.60	3.00	2.97	1.45	0.93	0.81	3.58	0.81
	3.60	3.00	2.97	1.45	1.04	0.81	3.65	0.82
C8	4.20	3.00	3.36	1.45	0.52	0.81	3.73	0.84
	4.20	3.00	3.36	1.45	0.63	0.81	3.80	0.86
	4.20	3.00	3.36	1.45	0.75	0.81	3.82	0.86
	4.20	3.00	3.36	1.45	0.87	0.81	3.84	0.87
	4.20	3.00	3.36	1.45	0.99	0.81	3.85	0.87
	4.20	3.00	3.36	1.45	1.11	0.81	3.85	0.87
C9	3.00	3.00	2.47	1.60	0.51	0.89	2.88	0.65
	3.00	3.00	2.47	1.60	0.64	0.89	2.99	0.68
	3.00	3.00	2.47	1.60	0.77	0.89	3.08	0.70
	3.00	3.00	2.47	1.60	0.91	0.89	3.16	0.71
	3.00	3.00	2.47	1.60	1.04	0.89	3.21	0.72
C10	3.60	3.00	2.84	1.60	0.45	0.89	3.18	0.72
	3.60	3.00	2.84	1.60	0.58	0.89	3.28	0.74
	3.60	3.00	2.84	1.60	0.71	0.89	3.35	0.76

	3.60	3.00	2.84	1.60	0.84	0.89	3.42	0.77
	3.60	3.00	2.84	1.60	0.96	0.89	3.45	0.78
	3.60	3.00	2.84	1.60	1.08	0.89	3.54	0.80
C11	4.20	3.00	3.23	1.60	0.54	0.89	3.50	0.79
	4.20	3.00	3.23	1.60	0.66	0.89	3.60	0.81
	4.20	3.00	3.23	1.60	0.79	0.89	3.63	0.82
	4.20	3.00	3.23	1.60	0.91	0.89	3.66	0.83
	4.20	3.00	3.23	1.60	1.04	0.89	3.67	0.83

Table 14.2: Results for the whole dataset where $0.5<H_T/P_m<1$ with roundings

Model No.	B/P_m	W/P_m	L/W	Inlet width proportion (α')	Ht/P_m	W_{in}/W	C	C_d'
A1	3.00	1.80	4.34	1.00	0.41	0.56	3.91	0.88
	3.00	1.80	4.34	1.00	0.60	0.56	3.88	0.88
	3.00	1.80	4.34	1.00	0.80	0.56	3.93	0.89
	3.00	1.80	4.34	1.00	1.01	0.56	3.90	0.88
A2	3.60	1.80	5.00	1.00	0.41	0.50	3.94	0.89
	3.60	1.80	5.00	1.00	0.61	0.50	4.00	0.90
	3.60	1.80	5.00	1.00	0.80	0.50	4.01	0.90
	3.60	1.80	5.00	1.00	0.90	0.50	3.97	0.90
	3.60	1.80	5.00	1.00	1.00	0.50	3.98	0.90
A3	3.60	1.80	5.00	1.00	0.41	0.56	3.91	0.88
	3.60	1.80	5.00	1.00	0.59	0.56	4.04	0.91
	3.60	1.80	5.00	1.00	0.77	0.56	4.12	0.93
	3.60	1.80	5.00	1.00	1.04	0.56	3.77	0.85
A4	3.60	1.80	5.00	1.00	0.55	0.63	4.41	0.99
	3.60	1.80	5.00	1.00	0.76	0.63	4.23	0.95
	3.60	1.80	5.00	1.00	1.00	0.63	4.03	0.91
A5	4.20	1.80	5.67	1.00	0.55	0.56	4.39	0.99
	4.20	1.80	5.67	1.00	0.75	0.56	4.27	0.96
	4.20	1.80	5.67	1.00	0.96	0.56	4.16	0.94
	4.20	1.80	5.67	1.00	1.17	0.56	4.09	0.92
A6	3.00	1.80	4.13	1.20	0.43	0.67	3.75	0.85
	3.00	1.80	4.13	1.20	0.64	0.67	3.74	0.84
	3.00	1.80	4.13	1.20	0.87	0.67	3.67	0.83

	3.00	1.80	4.13	1.20	0.98	0.67	3.67	0.83
	3.00	1.80	4.13	1.20	1.05	0.67	3.75	0.85
A7	3.60	1.80	4.79	1.20	0.40	0.67	3.99	0.90
	3.60	1.80	4.79	1.20	0.57	0.67	4.16	0.94
	3.60	1.80	4.79	1.20	0.77	0.67	4.18	0.94
	3.60	1.80	4.79	1.20	0.97	0.67	4.12	0.93
	3.60	1.80	4.79	1.20	1.17	0.67	4.11	0.93
A8	4.20	1.80	5.46	1.20	0.39	0.67	4.10	0.93
	4.20	1.80	5.46	1.20	0.55	0.67	4.43	1.00
	4.20	1.80	5.46	1.20	0.75	0.67	4.32	0.97
	4.20	1.80	5.46	1.20	0.96	0.67	4.22	0.95
	4.20	1.80	5.46	1.20	1.15	0.67	4.15	0.94
A9	3.00	1.80	3.90	1.45	0.44	0.81	3.65	0.82
	3.00	1.80	3.90	1.45	0.67	0.81	3.59	0.81
	3.00	1.80	3.90	1.45	0.90	0.81	3.55	0.80
	3.00	1.80	3.90	1.45	1.00	0.81	3.56	0.80
A10	3.60	1.80	4.54	1.45	0.49	0.81	3.28	0.74
	3.60	1.80	4.54	1.45	0.64	0.81	3.79	0.86
	3.60	1.80	4.54	1.45	0.75	0.81	3.76	0.85
	3.60	1.80	4.54	1.45	0.85	0.81	3.75	0.85
	3.60	1.80	4.54	1.45	0.95	0.81	3.74	0.84
	3.60	1.80	4.54	1.45	1.07	0.81	3.72	0.84
A11	4.20	1.80	5.21	1.45	0.39	0.81	4.13	0.93
	4.20	1.80	5.21	1.45	0.56	0.81	4.34	0.98
	4.20	1.80	5.21	1.45	0.75	0.81	4.26	0.96
	4.20	1.80	5.21	1.45	0.86	0.81	4.16	0.94
	4.20	1.80	5.21	1.45	0.96	0.81	4.16	0.94
	4.20	1.80	5.21	1.45	1.06	0.81	4.16	0.94
B1	3.00	2.40	3.50	1.00	0.49	0.55	3.67	0.83
	3.00	2.40	3.50	1.00	0.73	0.55	3.72	0.84
	3.00	2.40	3.50	1.00	0.80	0.55	3.73	0.84
	3.00	2.40	3.50	1.00	0.89	0.55	3.73	0.84
	3.00	2.40	3.50	1.00	0.97	0.55	3.72	0.84
	3.00	2.40	3.50	1.00	1.04	0.55	3.74	0.84

B2	3.60	2.40	3.99	1.00	0.48	0.50	3.75	0.85
	3.60	2.40	3.99	1.00	0.63	0.50	3.81	0.86
	3.60	2.40	3.99	1.00	0.79	0.50	3.81	0.86
	3.60	2.40	3.99	1.00	0.87	0.50	3.82	0.86
	3.60	2.40	3.99	1.00	0.95	0.50	3.82	0.86
	3.60	2.40	3.99	1.00	1.03	0.50	3.82	0.86
B3	3.60	2.40	3.99	1.00	0.47	0.55	3.89	0.88
	3.60	2.40	3.99	1.00	0.61	0.55	3.93	0.89
	3.60	2.40	3.99	1.00	0.68	0.55	3.96	0.89
	3.60	2.40	3.99	1.00	0.76	0.55	3.95	0.89
	3.60	2.40	3.99	1.00	0.92	0.55	3.94	0.89
	3.60	2.40	3.99	1.00	0.99	0.55	3.95	0.89
	3.60	2.40	3.99	1.00	1.06	0.55	3.98	0.90
B4	3.60	2.40	3.99	1.00	0.45	0.62	4.12	0.93
	3.60	2.40	3.99	1.00	0.59	0.62	4.13	0.93
	3.60	2.40	3.99	1.00	0.65	0.62	4.13	0.93
	3.60	2.40	3.99	1.00	0.72	0.62	4.19	0.95
	3.60	2.40	3.99	1.00	0.86	0.62	4.20	0.95
	3.60	2.40	3.99	1.00	0.94	0.62	4.16	0.94
	3.60	2.40	3.99	1.00	1.02	0.62	4.13	0.93
B5	4.20	2.40	4.50	1.00	0.45	0.55	4.04	0.91
	4.20	2.40	4.50	1.00	0.59	0.55	4.14	0.93
	4.20	2.40	4.50	1.00	0.66	0.55	4.11	0.93
	4.20	2.40	4.50	1.00	0.73	0.55	4.13	0.93
	4.20	2.40	4.50	1.00	0.88	0.55	4.11	0.93
	4.20	2.40	4.50	1.00	0.94	0.55	4.10	0.93
	4.20	2.40	4.50	1.00	1.02	0.55	4.13	0.93
B6	3.00	2.40	3.16	1.35	0.51	0.75	3.52	0.79
	3.00	2.40	3.16	1.35	0.67	0.75	3.58	0.81
	3.00	2.40	3.16	1.35	0.76	0.75	3.60	0.81
	3.00	2.40	3.16	1.35	0.84	0.75	3.59	0.81
	3.00	2.40	3.16	1.35	1.00	0.75	3.61	0.81
B7	3.60	2.40	3.65	1.35	0.47	0.75	3.83	0.86
	3.60	2.40	3.65	1.35	0.62	0.75	3.91	0.88

	3.60	2.40	3.65	1.35	0.69	0.75	3.91	0.88
	3.60	2.40	3.65	1.35	0.77	0.75	3.91	0.88
	3.60	2.40	3.65	1.35	0.93	0.75	3.89	0.88
	3.60	2.40	3.65	1.35	1.01	0.75	3.89	0.88
B8	4.20	2.40	4.14	1.35	0.45	0.75	4.02	0.91
	4.20	2.40	4.14	1.35	0.58	0.75	4.09	0.92
	4.20	2.40	4.14	1.35	0.66	0.75	4.09	0.92
	4.20	2.40	4.14	1.35	0.73	0.75	4.07	0.92
	4.20	2.40	4.14	1.35	0.89	0.75	4.05	0.92
	4.20	2.40	4.14	1.35	0.95	0.75	4.06	0.92
	4.20	2.40	4.14	1.35	1.03	0.75	4.05	0.92
B9	3.00	2.40	2.98	1.55	0.55	0.86	3.31	0.75
	3.00	2.40	2.98	1.55	0.72	0.86	3.38	0.76
	3.00	2.40	2.98	1.55	0.80	0.86	3.39	0.76
	3.00	2.40	2.98	1.55	0.89	0.86	3.41	0.77
	3.00	2.40	2.98	1.55	1.05	0.86	3.45	0.78
B10	3.60	2.40	3.46	1.55	0.51	0.86	3.54	0.80
	3.60	2.40	3.46	1.55	0.67	0.86	3.59	0.81
	3.60	2.40	3.46	1.55	0.76	0.86	3.60	0.81
	3.60	2.40	3.46	1.55	0.83	0.86	3.62	0.82
	3.60	2.40	3.46	1.55	0.99	0.86	3.64	0.82
	3.60	2.40	3.46	1.55	1.08	0.86	3.63	0.82
B11	4.20	2.40	3.95	1.55	0.48	0.86	3.82	0.86
	4.20	2.40	3.95	1.55	0.63	0.86	3.83	0.87
	4.20	2.40	3.95	1.55	0.70	0.86	3.84	0.87
	4.20	2.40	3.95	1.55	0.79	0.86	3.84	0.87
	4.20	2.40	3.95	1.55	0.94	0.86	3.84	0.87
	4.20	2.40	3.95	1.55	1.02	0.86	3.82	0.86
C1	3.00	3.00	3.00	1.00	0.43	0.56	3.32	0.75
	3.00	3.00	3.00	1.00	0.56	0.56	3.45	0.78
	3.00	3.00	3.00	1.00	0.68	0.56	3.54	0.80
	3.00	3.00	3.00	1.00	0.80	0.56	3.59	0.81
	3.00	3.00	3.00	1.00	0.93	0.56	3.61	0.82
	3.00	3.00	3.00	1.00	1.05	0.56	3.64	0.82

C2	3.60	3.00	3.40	1.00	0.54	0.50	3.52	0.79
	3.60	3.00	3.40	1.00	0.67	0.50	3.59	0.81
	3.60	3.00	3.40	1.00	0.79	0.50	3.64	0.82
	3.60	3.00	3.40	1.00	0.92	0.50	3.67	0.83
	3.60	3.00	3.40	1.00	1.03	0.50	3.69	0.83
C3	3.60	3.00	3.40	1.00	0.52	0.56	3.70	0.84
	3.60	3.00	3.40	1.00	0.63	0.56	3.77	0.85
	3.60	3.00	3.40	1.00	0.76	0.56	3.81	0.86
	3.60	3.00	3.40	1.00	0.87	0.56	3.82	0.86
	3.60	3.00	3.40	1.00	1.00	0.56	3.83	0.86
C4	3.60	3.00	3.40	1.00	0.50	0.63	3.80	0.86
	3.60	3.00	3.40	1.00	0.62	0.63	3.83	0.86
	3.60	3.00	3.40	1.00	0.74	0.63	3.87	0.87
	3.60	3.00	3.40	1.00	0.86	0.63	3.90	0.88
	3.60	3.00	3.40	1.00	0.97	0.63	3.92	0.88
	3.60	3.00	3.40	1.00	1.09	0.63	3.95	0.89
C5	4.20	3.00	3.80	1.00	0.48	0.56	3.97	0.90
	4.20	3.00	3.80	1.00	0.60	0.56	4.01	0.91
	4.20	3.00	3.80	1.00	0.71	0.56	4.02	0.91
	4.20	3.00	3.80	1.00	0.83	0.56	4.02	0.91
	4.20	3.00	3.80	1.00	0.95	0.56	4.02	0.91
	4.20	3.00	3.80	1.00	1.07	0.56	4.04	0.91
C6	3.00	3.00	2.58	1.45	0.47	0.81	3.06	0.69
	3.00	3.00	2.58	1.45	0.60	0.81	3.18	0.72
	3.00	3.00	2.58	1.45	0.73	0.81	3.27	0.74
	3.00	3.00	2.58	1.45	0.86	0.81	3.32	0.75
	3.00	3.00	2.58	1.45	0.99	0.81	3.38	0.76
	3.00	3.00	2.58	1.45	1.11	0.81	3.45	0.78
C7	3.60	3.00	2.97	1.45	0.55	0.81	3.43	0.77
	3.60	3.00	2.97	1.45	0.68	0.81	3.49	0.79
	3.60	3.00	2.97	1.45	0.80	0.81	3.53	0.80
	3.60	3.00	2.97	1.45	0.93	0.81	3.58	0.81
	3.60	3.00	2.97	1.45	1.03	0.81	3.63	0.82
C8	4.20	3.00	3.36	1.45	0.51	0.81	3.73	0.84

	4.20	3.00	3.36	1.45	0.63	0.81	3.78	0.85
	4.20	3.00	3.36	1.45	0.75	0.81	3.82	0.86
	4.20	3.00	3.36	1.45	0.87	0.81	3.84	0.87
	4.20	3.00	3.36	1.45	0.98	0.81	3.86	0.87
	4.20	3.00	3.36	1.45	1.11	0.81	3.83	0.86
C9	3.00	3.00	2.47	1.60	0.50	0.89	2.88	0.65
	3.00	3.00	2.47	1.60	0.64	0.89	2.99	0.68
	3.00	3.00	2.47	1.60	0.78	0.89	3.06	0.69
	3.00	3.00	2.47	1.60	0.91	0.89	3.13	0.71
	3.00	3.00	2.47	1.60	1.04	0.89	3.20	0.72
C10	3.60	3.00	2.84	1.60	0.45	0.89	3.21	0.73
	3.60	3.00	2.84	1.60	0.58	0.89	3.29	0.74
	3.60	3.00	2.84	1.60	0.71	0.89	3.36	0.76
	3.60	3.00	2.84	1.60	0.84	0.89	3.41	0.77
	3.60	3.00	2.84	1.60	0.96	0.89	3.46	0.78
	3.60	3.00	2.84	1.60	1.09	0.89	3.52	0.79
C11	4.20	3.00	3.23	1.60	0.54	0.89	3.55	0.80
	4.20	3.00	3.23	1.60	0.67	0.89	3.60	0.81
	4.20	3.00	3.23	1.60	0.79	0.89	3.63	0.82
	4.20	3.00	3.23	1.60	0.91	0.89	3.65	0.82
	4.20	3.00	3.23	1.60	1.04	0.89	3.67	0.83